

Materials Forming, Machining and Tribology

K. Palanikumar
Elango Natarajan
Ramesh Sengottuvelu
J. Paulo Davim *Editors*

Futuristic Trends in Intelligent Manufacturing

Optimization and Intelligence in
Manufacturing

 Springer

Materials Forming, Machining and Tribology

Series Editor

J. Paulo Davim, Department of Mechanical Engineering, University of Aveiro,
Aveiro, Portugal

This series fosters information exchange and discussion on all aspects of materials forming, machining and tribology. This series focuses on materials forming and machining processes, namely, metal casting, rolling, forging, extrusion, drawing, sheet metal forming, microforming, hydroforming, thermoforming, incremental forming, joining, powder metallurgy and ceramics processing, shaping processes for plastics/composites, traditional machining (turning, drilling, milling, broaching, etc.), non-traditional machining (EDM, ECM, USM, LAM, etc.), grinding and others abrasive processes, hard part machining, high speed machining, high efficiency machining, micro and nanomachining, among others. The formability and machinability of all materials will be considered, including metals, polymers, ceramics, composites, biomaterials, nanomaterials, special materials, etc. The series covers the full range of tribological aspects such as surface integrity, friction and wear, lubrication and multiscale tribology including biomedical systems and manufacturing processes. It also covers modelling and optimization techniques applied in materials forming, machining and tribology. Contributions to this book series are welcome on all subjects of “green” materials forming, machining and tribology. To submit a proposal or request further information, please contact Dr. Mayra Castro, Publishing Editor Applied Sciences, via mayra.castro@springer.com or Professor J. Paulo Davim, Book Series Editor, via pdavim@ua.pt

More information about this series at <http://www.springer.com/series/11181>


K. Palanikumar · Elango Natarajan ·
Ramesh Sengottuvelu · J. Paulo Davim
Editors


Futuristic Trends in Intelligent Manufacturing

Optimization and Intelligence
in Manufacturing


 Springer

Editors

K. Palanikumar 
Department of Mechanical Engineering
Sri Sai Ram Institute of Technology
Chennai, Tamil Nadu, India

Ramesh Sengottuvelu 
Mechanical Engineering Department
Presidency University
Bengaluru, Karnataka, India

Elango Natarajan 
Department of Mechanical
and Mechatronic Engineering
UCSI University
Kuala Lumpur, Malaysia

J. Paulo Davim 
Department of Mechanical Engineering
University of Aveiro
Aveiro, Portugal

ISSN 2195-0911

ISSN 2195-092X (electronic)

Materials Forming, Machining and Tribology

ISBN 978-3-030-70008-9

ISBN 978-3-030-70009-6 (eBook)

<https://doi.org/10.1007/978-3-030-70009-6>

© The Editor(s) (if applicable) and The Author(s), under exclusive license to Springer Nature Switzerland AG 2021

This work is subject to copyright. All rights are solely and exclusively licensed by the Publisher, whether the whole or part of the material is concerned, specifically the rights of translation, reprinting, reuse of illustrations, recitation, broadcasting, reproduction on microfilms or in any other physical way, and transmission or information storage and retrieval, electronic adaptation, computer software, or by similar or dissimilar methodology now known or hereafter developed.

The use of general descriptive names, registered names, trademarks, service marks, etc. in this publication does not imply, even in the absence of a specific statement, that such names are exempt from the relevant protective laws and regulations and therefore free for general use.

The publisher, the authors and the editors are safe to assume that the advice and information in this book are believed to be true and accurate at the date of publication. Neither the publisher nor the authors or the editors give a warranty, expressed or implied, with respect to the material contained herein or for any errors or omissions that may have been made. The publisher remains neutral with regard to jurisdictional claims in published maps and institutional affiliations.

This Springer imprint is published by the registered company Springer Nature Switzerland AG
The registered company address is: Gewerbestrasse 11, 6330 Cham, Switzerland

Preface

The world of today is wholly connected with the new trends of technology and updations. The seamless integration of technology is a part of our daily lives. Also, it is a known fact that web technology keeps changing and warrants for “smarter technology” to take decision-making on any unseen issues. Accordingly, this book deals on the use of smart technologies existing in the current era. It is designed as a source of information on the futuristic trends in Intelligent Manufacturing in order to meet the needs of the globe.

It has new insights on the Industrial 4.0 Technology, as it revolutionizes the use of technology in a smart way. The main goal of this book is to guide the readers with advanced trends in Intelligence Manufacturing. Besides, it grasps the attentions of the readers towards the increased level of production and profit in industries, particularly Intelligent Manufacturing industry with the use of smart Industrial 4.0 Technology. The authors of this book venture the key components on the use of smart technology in various applications for the benefit of the users.

The main characteristics of this book are:

It highlights on Industry 4.0, a strategic approach as it uses smart technology and real-time data to increase the productivity at reduced cost.

It focuses on the key aspects of futuristic trends in order to equip future production systems with smart sensors and smart actuators, communication and intelligent operation control, etc.

It includes cyber-physical systems, Internet of Things, Cloud computing, and Cognitive computing.

It emphasizes on the quality of the product in advance and also draws attention towards near-net shaped components to avoid wastages in the production.

It promotes the high advantages of the smart technology like minimal waste in production, high profit and sustainable manufacturing, etc.

It insists on the use of fault diagnosis during the production as well as it guides the production companies to avoid downtime.

It accentuates the users about the data-driven decision-making in each process because it is a smart way to increase the productivity with low cost.

It focuses on different articles related to advanced technologies as their integration with “Industry 4.0” will rule the world in the forthcoming years.

The articles in it help researchers as well as industrialists to utilize the information in production control.

Chennai, India
Kuala Lumpur, Malaysia
Bengaluru, India
Aveiro, Portugal

Dr. K. Palanikumar
Dr. Elango Natarajan
Dr. Ramesh Sengottuvelu
Dr. J. Paulo Davim

Contents

Smart Manufacturing—A Lead Way to Sustainable Manufacturing	1
Elango Natarajan, K. Palanikumar, and S. Ramesh	
Smart Machining of Titanium Alloy Using ANN Encompassed Prediction Model and GA Optimization	9
V. Kaviarasan, Sangeetha Elango, Ezra Morris Abraham Gnanamuthu, and R. Durairaj	
Fuzzy Interference System of Drilling Parameters for Delrin Parts	21
S. Parasuraman, Brian Cheong Tjun Yew, Sangeetha Elango, I. Elamvazuthi, and V. Kaviarasan	
Optimization and Effect Analysis of Sustainable Micro Electrochemical Machining Using Organic Electrolyte	33
V. Subburam, S. Ramesh, and Lidio Inacio Freitas	
Artificial Fish Swarm Algorithm Driven Optimization for Copper-Nano Particles Suspended Sodium Nitrate Electrolyte Enabled ECM on Die Tool Steel	47
T. Sekar, V. Sathiyamoorthy, K. Muthusamy, A. Sivakumar, and S. Balamurugan	
Comparative Analysis Between Conventional Method Versus Machine Learning Method for Pipeline Condition Prediction	61
Firdaus Basheer, Mohamed Saleem Nazmudeen, and Fadzliwati Mohiddin	
Application of Back Propagation Algorithm in Optimization of Weave Friction Stir Welding—A Study	91
M. Balasubramanian, D. Jayabalakrishnan, C. Hemadri, and B. Ashwin	
ANFIS and RSM Modelling Analysis on Surface Roughness of PB Composites in Drilling with HSS Drills	129
T. N. Valarmathi, K. Palanikumar, S. Sekar, and B. Latha	

Machine Learning for Smart Manufacturing for Healthcare Applications	145
Nivesh Gadipudi, I. Elamvazuthi, S. Parasuraman, and Alberto Borboni	
A Comparative Analysis of Two Soft Computing Methods for Sales Forecasting in Dairy Production: A Case Study	159
A. Fallahpour, E. U. Olugu, K. Y. Wong, and O. C. Aja	
AR and VR in Manufacturing	171
R. Dhanalakshmi, Cherukuri Dwaraka Mai, B. Latha, and N. Vijayaraghavan	
Industrial IoT and Intelligent Manufacturing	185
S. Rajarajan, S. Renukadevi, and N. Mohammed Abu Basim	
Cyber-Physical Systems: A Pilot Adoption in Manufacturing	205
Srivardhini Veeraragavan, Edwin Tong Jiann, Regina Leong, and Veera Ragavan Sampath Kumar	
Intelligent Machining of Abrasive Jet on Carbon Fiber and Glass Fiber Polymeric Composites Using Modified Nozzle	225
M. Balasubramanian, S. Madhu, and C. Hemadri	
Additive Manufacturing of Nylon Parts and Implication Study on Change in Infill Densities and Structures	245
J. Nagarjun, S. Manimaran, and M. Krishnaprakash	
Index	261

About the Editors

Dr. K. Palanikumar is presently Professor and Principal, Sri Sai Ram Institute of Technology, Chennai, India. He was conferred Ph.D. by Anna University, Chennai. He is serving in higher learning institutions for more than 25 years. ISTE has awarded him as a National Best Researcher. He has published around 400 papers in Journals/Conferences and his h-index is 40+. He is attached to professional bodies in the area of tribology, non-destructive testing, welding etc. He has become Fellow in Institution of Engineers (India). He is working on many research projects including on composite materials and processing.

Dr. Elango Natarajan is an Associate Professor in Mechanical and Mechatronic Engineering, UCSI University, Kuala Lumpur, Malaysia. He has obtained Chartered Engineer(CEng.) from Engineering Council, UK. He has been in higher learning education for more than 20 years. He has completed many funded projects and has published 66 research articles in refereed Scopus/WoS Journals as of today and his h-index is 12. His interests are Machining of composite materials and Optimization, Machine Learning in Manufacturing, Soft Robotics, Composite materials. He is associated with many professional bodies including IEEE, IET, Board of Engineers, Malaysia. He has been appointed as a Professional Review Interviewer by IET, UK. He is currently the Secretary of IEEE/Robotics and Automation Society, Malaysia.

Dr. Ramesh Sengottuvelu is currently Professor and Head of Mech. Engg. Department, Presidency University, Bengaluru, India. Though he was hailing from a rural village in southern part of India, he has obtained M.Tech. from IITM, and Ph.D. from Anna University, Chennai with his hard work, dedication, and sincerity. With his specialization in Mechanical and Production Engineering, he has served in higher learning institutions for about 25+ years. He has extended his teaching service in

Mekelle University, Ethiopia, Salalah College of Technology, Sultanate of Oman for some countable years. He has received some notable academic awards in his career. He has produced 10 Ph.D. scholars and contributed 100+ publications in refereed Scopus/WoS Journals. He is now supervising 7 Ph.D. scholars in Manufacturing interests. He has achieved more than 1000 citations and his h index is 14.

Dr. J. Paulo Davim is a Full Professor at the University of Aveiro, Portugal. He is also distinguished as honorary professor in several universities/colleges/institutes in China, India and Spain. He received his Ph.D. degree in Mechanical Engineering in 1997, M.Sc. degree in Mechanical Engineering (materials and manufacturing processes) in 1991, Mechanical Engineering degree (5 years) in 1986, from the University of Porto (FEUP), the Aggregate title (Full Habilitation) from the University of Coimbra in 2005 and the D.Sc. (Higher Doctorate) from London Metropolitan University in 2013. He is Senior Chartered Engineer by the Portuguese Institution of Engineers with an MBA and Specialist titles in Engineering and Industrial Management as well as in Metrology. He is also Eur Ing by FEANI-Brussels and Fellow (FIET) of IET-London. He has more than 30 years of teaching and research experience in Manufacturing, Materials, Mechanical and Industrial Engineering, with special emphasis in Machining & Tribology. He has also interest in Management, Engineering Education and Higher Education for Sustainability. He has guided large numbers of postdoc, Ph.D. and master's students as well as has coordinated and participated in several financed research projects. He has received several scientific awards and honors. He has worked as evaluator of projects for ERC-European Research Council and other international research agencies as well as examiner of Ph.D. thesis for many universities in different countries. He is the Editor in Chief of several international journals, Guest Editor of journals, books Editor, book Series Editor and Scientific Advisory for many international journals and conferences. Presently, he is an Editorial Board member of 30 international journals and acts as reviewer for more than 100 prestigious Web of Science journals. In addition, he has also published as editor (and co-editor) more than 200 books and as author (and co-author) more than 15 books, 100 book chapters and 500 articles in journals and conferences (more than 280 articles in journals indexed in Web of Science core collection/h-index 59+/11500+ citations, SCOPUS/h-index 63+/14000+ citations, Google Scholar/h-index 82+/23500+ citations). He has listed in World's Top 2% Scientists by Stanford University study.

Smart Manufacturing—A Lead Way to Sustainable Manufacturing



Elango Natarajan, K. Palanikumar, and S. Ramesh

1 Introduction

Sustainability is a world agenda. Success in global sustainability hinges strongly on the commitment of the entire world community, not just any individual country. Since the manufacturing sector can potentially negate sustainability, it is seen as a key player in making a success of global sustainability. A key factor which is working against sustainability in manufacturing is the rising number of wastages. Reducing wastages in manufacturing is therefore one of the ways to support the global drive for sustainability. These include wastages in energy, labour, material and the other critical resources of manufacturing, including water.

There is no denying that the prime aim of any business is to increase productivity and make the company profitable. The wastage of materials, labour, and machine time during production is a major contributor to low productivity and reduced profit. The big challenge in sustainable manufacturing is how best to reduce wastes from the production without undermining the effectiveness and efficiency of the process. The wastes in production include the excessive consumption of energy, high usage of materials and labour, rejection of products in the inspection, and operational failure

E. Natarajan (✉)

Department of Mechanical and Mechatronic Engineering, UCSI University, Kuala Lumpur, Malaysia

e-mail: cad.elango.n@gmail.com

K. Palanikumar

Department of Mechanical Engineering, Sri Sai Ram Institute of Technology, Chennai, Tamil Nadu, India

e-mail: palanikumar_k@yahoo.com

S. Ramesh

Mechanical Engineering Department, Presidency University, Bengaluru, Karnataka, India

e-mail: ramesh_1968in@yahoo.com

© The Author(s), under exclusive license to Springer Nature Switzerland AG 2021

K. Palanikumar et al. (eds.), *Futuristic Trends in Intelligent Manufacturing*,

Materials Forming, Machining and Tribology,

https://doi.org/10.1007/978-3-030-70009-6_1

during product use. The wastage, also known as ‘muda’ in lean manufacturing terminology includes over-production, long waiting time, non-optimized transportation, inappropriate processing, excess inventory, excess motion, and defects. The solution to these issues lies in understanding the production process well and designing the product accordingly. Industry 4.0 aims to utilize the digital transformation and knowledge base activities to serve the human community. It uses the cyber physical systems (CPS) and Internet of things (IOT) that are embedded with the decision models. The development of decision models is accomplished using Artificial intelligence (AI)

AI has been extensively used in gaming, banking, government and commercial sectors. It is slowly impending towards the manufacturing sector to build industrial automation. It is able to bring close interaction between machine and human involved in the manufacturing. This new way of incorporating AI and knowledge base in manufacturing sector will build stronger and superior digital economy.

2 Smart Manufacturing and Requirements for Implementation

Manufacturing essentially involves production of parts and assembly of parts. The production of parts involves the selection of machine tools, cutting tools, and optimal cutting condition. Industry 4.0 has been hailed by manufacturers as a valuable tool to achieve their overarching business goal of high productivity and lucrative profit. One of the core technologies driving IR 4.0 and this new wave of ultra-automation is Industrial AI and Machine Learning. The digital transformation of end-to-end processes are governed by CPS, IOT, knowledge-based decision making, integration of sensors, AR/VR technologies, autonomous robots, etc. But, these key attributes are required for the implementation of smart factory. In smart factory, production line in the same building and other buildings/places can be connected together through CPS. The data collected from one production center can be communicated to other production branches to automate material purchases, maintenance and other related operations that were previously done.

As far as smart manufacturing is concerned, we can limit ourselves to integration of smart sensors and knowledge-based decision making. These are key things for smart manufacturing in terms of maintaining the quality of the product and avoidance of downtime of machines. At this end, we propose the following three use cases that stand out in terms of their suitability for starting AI in any manufacturing company.

1. Fault diagnosis and Intelligent maintenance
2. Intelligent product quality control
3. Intelligent demand planning.

2.1 Smart Machining

The machining is known to be highly a nonlinear element. Distributed Process Planning (DPP) can be implemented to divide the machining process planning into supervisory planning, execution control and operation planning. In the supervisory planning, the generic processes are obtained based on machining features and machining knowledge. In execution control and operation planning, the resource-specific processes including machine tool selection, cutting tool selection, optimum machining parameters and machining conditions are carried out. Each of these processes involve precise decision making that leads to the success of production. In the consideration of these, we suggest prediction models for the following activities in machining.

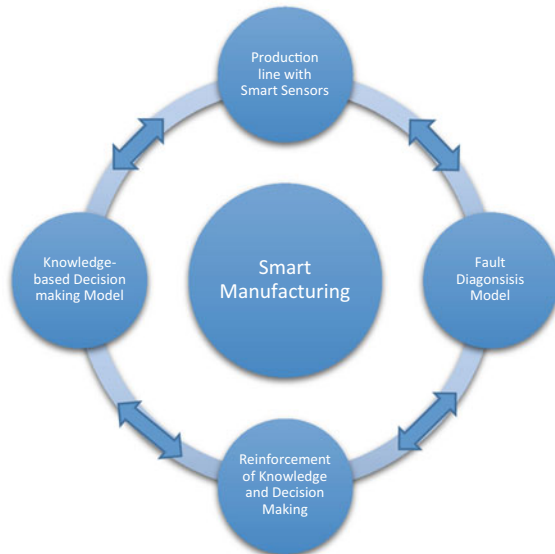
- (a) Prediction of optimum cutting tool
- (b) Prediction of optimum machining parameters
- (c) Prediction of machine tool based on the fault diagnosis.

Figure 1 depicts the key items needed for smart manufacturing.

Two key items are knowledge-based decision-making model for production and knowledge-based decision making model for fault diagnosis. The data driven production is used to ensure the quality of the part, while data driven fault diagnosis is used to avoid the downtime of the machine. For the easy understanding, these use cases are explained below;

Use case I: Digital Machining

Fig. 1 Key items of smart manufacturing



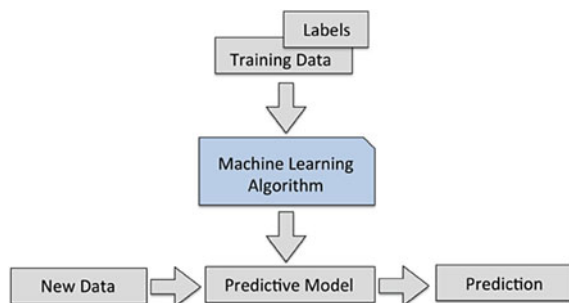
The parts are manufactured closest to the net shape through various manufacturing processes such as drilling, milling, turning, tapping and shaping. The operator decides the operating condition for any machining process based on his past experience or the data provided in the operations manual. The parameters include speed, feed, depth of cut, cutting tool selection, and coolant condition. They are decided and set beforehand at the start of production. These parameters play a vital role on the quality of the product finish. The machined part is accepted, when checked for quality, only it fulfills the limit of acceptance prescribed. Otherwise, it is rejected as a waste. The cutting conditions influence the energy consumption. The setting of the best cutting parameters will therefore assist the company to avoid the rejection of machined parts, as well as reduce energy consumption. There have been many researches on determining optimal cutting condition for various machining processes. Interested readers may refer [1–16] for understanding meta-heuristic algorithms used in optimization of machining parameters. In connection to prediction model development, readers may refer [17–31]. The prediction models are needed to predict the output response for any unseen input condition, while optimization algorithms help to get the best input condition to achieve the required output response. Figure 2 shows the development of predictive model.

Use case II: Digital Tooling

A digital decision making of tool selection is another use case where the knowledge-based model can be utilized. The model can be built by gathering the information of tools being in use. The optimum tool for cutting can be chosen from the predictive model based on the exactness of the required surface finish and the condition of the tool. Hence the waste in production can be avoided. The tool monitoring model gathers the condition of the tool and update its knowledge base. It tracks the condition of each tool in the industry and gives alarm to the management. So that the downtime of machine can be avoided.

Given a scenario: For machining of a part in CNC lathe, one has to select the appropriate tool, and set appropriate cutting condition (speed, feed, depth of cut, coolant etc.). We will build a model which can predict the cutting condition based on the requirement of the surface finish of the part. If there is a new task that is to be

Fig. 2 Predictive model development



carried out, the operator can take the predicted cutting condition with respect to his expected surface finish of the part. He can then use such optimum cutting condition to produce the part to the exact expectations. Meanwhile the machine model related to tool monitoring would suggest to the operator the condition of the tool and predict the right tool to be used for the operation. This step is important for any company as the use of precision tool for simple operation leads to waste.

The challenge in building the machine model is to collect enormous data set for training and validation. So, we may start the training with as much as possible data set, which must be experimentally determined. Once the model is built, we may validate the predicted data experimentally and input the new dataset into the model for tuning. This iterative way of tuning the model will prepare more effective ML model. Readers may refer [23, 24] for understanding prediction models for tool monitoring.

Use case III: Digital machine tool selection

The International Society of Automation says that \$647 billion is lost globally each year due to machine downtime. The machine tools in the production line must be networked either using intranet or cyber-physical system. Each machine tool must have unique ID and smart sensors integrated to sense the flow information. These flow information are periodical information that helps the fault diagnosis model to take decision. The prediction model in this way works in two aspects; firstly, it helps in identifying the faults in any machine tool and alarming the maintenance department to take the preventive maintenance. Secondly, it helps in selecting the right machine tool for the operation.

3 Conclusions

The avoidance of wastages in manufacturing stand in the way of making manufacturing more sustainable. Recent developments in the IR 4.0 technologies, especially machine learning and artificial intelligence, offer new opportunities to reduce such wastages. Research to develop such technologies is the way forward if we are to make manufacturing smarter and more sustainable. Smart manufacturing will contribute effectively to support the global agenda on sustainability.

References

1. Natarajan, E., Kaviarasan, V., Lim, W.H., Tiang, S.S., Parasuraman, S., & Elango, S. (2020). Non-dominated sorting modified teaching–learning-based optimization for multi-objective machining of polytetrafluoroethylene (PTFE). *Journal of Intelligent Manufacturing*. <https://doi.org/10.1007/s10845-019-01486-9>.
2. Kaviarasan, V., Venkatesan, R., & Natarajan, Elango. (2019). Prediction of surface quality and optimization of process parameters in drilling of Delrin using neural network. *Progress*

- in Rubber Plastics and Recycling Technology*, 35(3), 149–169. <https://doi.org/10.1177/1477760619855078>.
3. Suresh, S., Elango, N., Venkatesan, K., Lim, W. H., Palanikumar, K., & Rajesh, S. (2020). Sustainable friction stir spot welding of 6061-T6 aluminium alloy using improved non-dominated sorting teaching learning. *Journal of Materials Research and Technology*, 9(5), 11650–11674. <https://doi.org/10.1016/j.jmrt.2020.08.043>.
 4. Gaitonde, V. N., Karnik, S. R., Mata, Francisco, & Paulo Davim, J. (2018). Taguchi approach for achieving better machinability in unreinforced and reinforced polyamides. *Journal of Reinforced Plastics and Composites*, 27(9), 909–924.
 5. Natarajan, E., Kaviarasan, V., Lim, W. H., Tiang, S. S. & Tan, T. H. (2018). Enhanced multi-objective teaching-learning-based optimization for machining of Delrin. In *IEEE Access*, vol. 6, pp. 51528–51546. <https://doi.org/10.1109/access.2018.2869040>.
 6. Chabbi, A., Yallese, M. A., Nouioua, M., Meddour, I., Mabrouki, T., & Girardin, François. (2017). Modeling and optimization of process parameters during the cutting of polymer (POM C) based on RSM, ANN, and DF methods. *International Journal of Advanced Manufacturing Technology*, 91(5–8), 2267–2290.
 7. Hamlaoui, N., Azzouz, S., Chaoui, K., Azari, Z., & Yallese, M. A. (2017). Machining of tough polyethylene pipe material: Surface roughness and cutting temperature optimization. *International Journal of Advanced Manufacturing Technology*, 92(5–8), 2231–2245.
 8. Panda, M. R., Biswal, S. K., & Sharma, Y. K. (2016). Experimental analysis on the effect of process parameters during CNC turning on nylon-6/6 using tungsten carbide tool. *The International Journal of Engineering Science & Research and Technology*, 5(4), 79–84.
 9. Abdul Shukor, J., Said, S., Harun, R., Husin, S., & Kadir, Ab. (2016). Optimising of machining parameters of plastic material using Taguchi method. *Advanced Materials and Technologies*, 2(1), 50–56.
 10. Sathiyamoorthy, V., Sekar, T., & Elango, N. (2015). Optimization of Processing Parameters in ECM of Die Tool Steel Using Nanofluid by Multiobjective Genetic Algorithm, Volume 2015, Article ID 895696. <https://doi.org/10.1155/2015/895696>.
 11. Sathiyamoorthy, V., Sekar, T., Suresh, P., Vijayan, R., & Elango, N. (2015). Optimization of processing parameters in electrochemical machining of AISI 202 using response surface methodology. *Journal of Engineering Science and Technology*, 10(6), 780–789.
 12. Suresh, P., Venkatesan, R., Sekar, T., Elango, N., & Sathiyamoorthy, V. (2014). Optimization of Intervening Variables in MicroEDM of SS 316L using a Genetic Algorithm and Response-Surface Methodology. *Strojniški vestnik—Journal of Mechanical Engineering*, 60(10), 656–664. <https://doi.org/10.5545/sv-jme.2014.1665>.
 13. Kaddeche, M., Chaoui, K., & Yallese, M. A. (2012). Cutting parameters effects on the machining of two high density polyethylene pipes resins. *Mechanical Industry*, 13(14), 307–316.
 14. Lazarevića, D., Madića, M., Jankovića, P., & Lazarevičb, A. (2012). Cutting parameters optimization for surface roughness in turning operation of Polyethylene (PE) using Taguchi method. *Tribol. Industrial*, 34(2), 68–73.
 15. Madic, M., Marinkovic, V., & Radovanovic, M. (2012). Mathematical modeling and optimization of surface roughness in turning of polyamide based on artificial neural network. *MECHANIKA*, 18(5), 2029–6983.
 16. Lela, B., Bajić, D., & Jozić, S. (2008). Regression analysis, support vector machines, and Bayesian neural network approaches to modeling surface roughness in face milling. *International Journal Advanced Manufacturing Technology*, 42, 1082–1088.
 17. Li, Zhixiong, Zhang, Ziyang, Shi, Junchuan, & Dazhong, Wu. (2019). Prediction of surface roughness in extrusion-based additive manufacturing with machine learning. *Robotics and Computer Integrated Manufacturing*, 57, 488–495. <https://doi.org/10.1016/j.rcim.2019.01.004>.
 18. Cherukuri, Harish, Perez-Bernabeu, Elena, Selles, Miguel, Schmitz (2019). Machining chatter prediction using a data learning model. *Journal of Manufacturing and Materials Processing*, 3(45). <https://doi.org/10.3390/jmmp3020045>.

19. Frye, M., & Schmitt, R. H. (2019). Quality improvement of milling processes using machine learning-algorithms. In *16th IMEKO TC10 Conference “Testing, Diagnostics & Inspection as a comprehensive value chain for Quality & Safety*, Berlin, Germany.
20. Zurkovic, Z., Cukor, G., Brezocnik, M., et al. (2018). A comparison of machine learning methods for cutting parameters prediction in high speed turning process. *Journal of Intelligent Manufacturing*, 29, 1683–1693. <https://doi.org/10.1007/s10845-016-1206-1>.
21. Kim, Dong-Hyeon, Kim, Thomas J. Y., Wang, Xinlin, Kim, Mincheol, Quan, Ying-Jun, Jin Woo, Oh, et al. (2018). Smart machining process using machine learning: A review and perspective on machining industry. *International Journal of Precision Engineering and Manufacturing-Green Technology*, 5(4), 555–568.
22. Lu, X., Hu, X., Wang, H., Si, L., Liu, Y., & Gao, L. (2016). Research on the prediction model of micro-milling surface roughness of Inconel718 based on SVM. *Industrial Lubrication and Tribology*, 68(2), 206–211.
23. Benkedjough, T., Medjaher, K., Zerhouni, N., & Rechak, S. (2013). Health Assessment and Life Prediction of cutting tools based on support vector regression. *Journal of Intelligent Manufacturing, Springer Verlag (Germany)*, pp. 1–19. <https://doi.org/10.1007/s10845-013-0774-6.hal-00867582>.
24. Gupta, A. K., Guntuku, S. C., Desu, R. K., & Balu, A. (2015). Optimisation of turning parameters by integrating genetic algorithm with support vector regression and artificial neural networks. *International Journal of Advanced Manufacturing Technology*, 77, 331–339.
25. Çaydaş, Ulaş, & Ekici, Sami. (2012). Support vector machines models for surface roughness prediction in CNC turning of AISI 304 austenitic stainless steel. *Journal of Intelligent Manufacturing—J INTELL MANUF*, 21, 1–12. <https://doi.org/10.1007/s10845-010-0415-2>.
26. Gupta, Amit Kumar. (2010). Predictive modelling of turning operations using response surface methodology, artificial neural networks and support vector regression. *International Journal of Production Research*, 48(3), 763–778. <https://doi.org/10.1080/00207540802452132>.
27. Palanikumar, Kayaroganam. (2009). Surface roughness model for machining glass fiber reinforced plastics by PCD tool using fuzzy logics. *Journal of Reinforced Plastics and Composites*, 28, 2273–2286. <https://doi.org/10.1177/0731684408092009>.
28. Yilmaz, Oguzhan, Eyercioglu, Omer, & Gindy, Nabil. (2006). A user-friendly fuzzy-based system for the selection of electro discharge machining process parameters. *Journal of Materials Processing Technology*, 172, 363–371. <https://doi.org/10.1016/j.jmatprotec.2005.09.023>.
29. Yang, H., Xuesong, M., Gedong, J., Tao, T., Changyu, P., & Ziwei, M. (2019). Milling tool wear state recognition by vibration signal using a stacked generalization ensemble model. *Shock and Vibration*. pp. 1–16. <https://doi.org/10.1155/2019/7386523>.
30. Sun, Shixu, Xiaofeng, Hu, Cai, Weili, & Zhong, Jin. (2019). Tool breakage detection of milling cutter insert based on SVM, IFAC-PapersOnLine. 52, 1549–1554(13), 2405–8963. <https://doi.org/10.1016/j.ifacol.2019.11.420>. ISSN 2405-8963.
31. Krishnakumar, P., Krishnaswamy, Rameshkumar, K. I., Ramachandran. (2015). Tool wear condition prediction using vibration signals in high speed machining (HSM) of Titanium (Ti-6Al-4 V) Alloy. *Procedia Computer Science*, 50. <https://doi.org/10.1016/j.procs.2015.04.049>.

Smart Machining of Titanium Alloy Using ANN Encompassed Prediction Model and GA Optimization



V. Kaviarasan, Sangeetha Elango, Ezra Morris Abraham Gnanamuthu, and R. Durairaj

1 Introduction

Titanium alloys are greatly utilized in industries including biomedical application and aerospace application because of their high strength-to-weight ratio. In general, milling or turning operations are carried out to produce the final part. The machining of titanium alloys, especially turning, is a challenging task to acquire good quality of machining. The reasons are:

- (a) The titanium alloys have a low elastic modulus, which causes chatter during the machining.
- (b) They have a high work hardening that results long continuous chips during turning, and drilling. These chips entangle the machine tool and delay the machining. And moreover, these chips leave marks over the machined surface.

The above two reasons make it difficult for machinists to get a good surface quality in the final product. One of the solutions to achieve smooth surface is to use the optimum cutting parameters during machining.

V. Kaviarasan

Department of Mechanical Engineering, Sona College of Technology, Salem, India

e-mail: vkavi.cim@gmail.com

S. Elango (✉) · E. M. A. Gnanamuthu · R. Durairaj

Lee Kong Chian Faculty of Engineering and Science, Universiti Tunku Abdul Rahman (UTAR),
Sungai Long, Malaysia

e-mail: csgeetha80@gmail.com

E. M. A. Gnanamuthu

e-mail: ezram@utar.edu.my

R. Durairaj

e-mail: rajkumar@utar.edu.my

There has been some research on optimization of cutting condition for machining of titanium alloys. Sangwan et al. [1] conducted research on finding the optimal parameters for turning Titanium alloy (Ti-6Al-4 V). They formulated a feed forward ANN and used Genetic algorithm (GA) to obtain the results. Paulo Davim et al. [2] developed ANN prediction model to analyse the impact of cutting condition during turning of 9SMnPb28k(DIN). They used L_{27} orthogonal array for experiments and applied experimental results in error back-propagation training algorithm to create the knowledge base. Ramesh et al. [3–6] investigated to determine optimum control parameters for machining Titanium alloys. They RSM and fuzzy logic to study the influence of cutting variables on turning of titanium alloy (gr5), while Suresh et al. [7] used RSM for analysis of parameters involved in machining of mild steel. Thirumalai et al. [8] evaluated optimum machining parameters for machining of Titanium material against various cutting insert. The authors observed from the ANOVA that the cutting speed is that the most influencing parameter Zhong et al. [9] conducted experiments on carbide and diamond turning tools and developed ANN model to predict the surface roughness. They adopted a systemic approach to identify optimum number of neurons in the hidden layers.

The current research differs from all these researches by adopting ANN model to generate the optimal predicted parameters which can be used to develop RSM model. The hypothesis is to have more accurate RSM equation which can be applied in optimization of turning condition for achieving minimum R_a .

2 Experimental Design

Titanium grade Ti-6Al-4 V alloy rod of $\phi 30$ mm was used as material. CNC turning center (Sprint 16TC Fanuc 0i T Mate Model C) with CNMG cutting tool and servo super cut coolant 32 was used in the turning operation. The reasons for selecting the diamond tip carbide tool is that it can resist the stickiness of the alloy and break up the long chips. It also assists to manage the heat produced during machining. The application of high-pressure servo super cut coolant 32 also assists to reduce heat and damage to the tool.

Figure 1 shows a titanium sample being turned in CNC machine. The three levels of cutting speed (V_c), feed rate (f) and depth of cut (ap) were selected as recommended in the cutting tool manufacturer catalogue as shown in Table 1. L_{27} matrix was formulated with the selected three levels using design of experiments (DOE). The turning of titanium samples was conducted with these twenty-seven cutting conditions and the surface roughness (R_a) in each experiment was rapidly measured using Mitutoyo make Surf tester. Each measurement was carried out in four different places and the average was recorded. Table 2 shows the cutting parameters and the respective R_a measured during the experiments.

3 Methodology

3.1 Response Surface Model

The regression response model of the current problem was formulated using RSM. The RSM model was developed as a second order full quadratic regression model using Box Benkhan’s uncoded units. It represents the correlation between turning parameters and the response variable.

The general second order RSM model is given by

$$Y = \alpha_0 + \sum_{i=1}^k \beta_i X_i + \sum_{i=j}^k \beta_{ij} X_i X_j + \sum_{i=1}^k \beta_{ii} X_i^2 \tag{1}$$

where α_0 represents the constant term of the regression equation, X_1, X_2, \dots, X_n are independent parameters involved in the model, $\beta_1, \beta_2, \dots, \beta_n$ are linear coefficient terms, $\beta_{11}, \beta_{22}, \dots, \beta_{kk}$ are quadratic coefficient terms, and $\beta_{12}, \beta_{13}, \dots, \beta_{k-1}$ are the interacting coefficient terms.

The surface roughness can be represented as

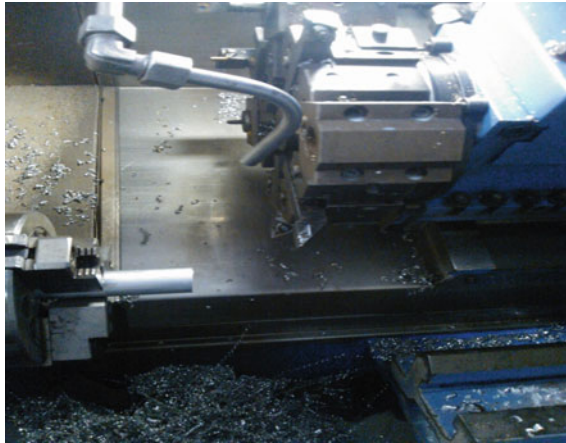


Fig. 1 Turning experiments on titanium alloy in CNC machine

Table 1 Machining parameter and selected levels

Machining parameter	Levels		
	I	II	III
Cutting speed V_c (m.min ⁻¹)	50	100	150
Feed rate f (mm.rev ⁻¹)	0.1	0.3	0.5
Depth of cut ap (mm)	0.5	0.75	1.0

Table 2 L27 matrix along with measured surface roughness

Expt. no	Vc m.min ⁻¹	F mm.rev ⁻¹	ap mm	Surface Roughness (Ra) μm
1	50	0.1	0.5	1.19
2	50	0.1	0.75	2.28
3	50	0.1	1	3.15
4	50	0.3	0.5	3.85
5	50	0.3	0.75	4.27
6	50	0.3	1	4.86
7	50	0.5	0.5	4.98
8	50	0.5	0.75	5.26
9	50	0.5	1	5.73
10	100	0.1	0.5	1.18
11	100	0.1	0.75	1.36
12	100	0.1	1	2.62
13	100	0.3	0.5	4.21
14	100	0.3	0.75	4.74
15	100	0.3	1	4.97
16	100	0.5	0.5	5.26
17	100	0.5	0.75	5.59
18	100	0.5	1	5.98
19	150	0.1	0.5	1.12
20	150	0.1	0.75	1.94
21	150	0.1	1	2.12
22	150	0.3	0.5	3.58
23	150	0.3	0.75	3.64
24	150	0.3	1	3.98
25	150	0.5	0.5	5.21
26	150	0.5	0.75	5.39
27	150	0.5	1	5.68

$$R_a = Y(V_c, f, ap) \quad (2)$$

The regression coefficients α_0 and β_i of RSM model were calculated with the experimental data. Table 3 shows the computed coefficients, while Eq. 3 shows RSM equation.

$$R_a = -2.55 + 0.0176V_c + 19.01f + 3.38ap - 0.00008V_c \times V_c - 14.11f \times f + 0.65ap \times ap + 0.01458V_c \times f - 0.01233V_c \times ap - 4.1f \times ap \quad (3)$$

Table 3 The calculated uncoded β_i coefficients for regression model

Box Benkhan's coefficient Term	Computed value
α_0	-2.55
β_1	0.0176
β_2	19.01
β_3	3.38
β_{11}	-0.000080
β_{22}	-14.11
β_{33}	0.65
β_{12}	0.01458
β_{13}	-0.01233
β_{23}	-4.10

The regression Eq. (3) was further used to find the optimum turning parameters with regard to the minimization of R_a of the titanium part.

3.2 Genetic Algorithm (GA)

Numerous metaheuristic optimization algorithm and solution techniques have been attempted to solve the constrained and unconstrained minimization problems [10–20]. GA has been used in a broad range of problem domains because of their simplicity, ease of operations, minimum requirements and global perspective. The minimization of R_a was attempted with the minimization problem formulated as;

$$\text{minimize } R_a(V_c, f, ap)$$

Subject to.

$$50 \text{ m/min} \leq V_c \leq 150 \frac{\text{m}}{\text{minute}}$$

$$0.1 \text{ mm/rev} \leq f \leq 0.5 \text{ mm/rev}$$

$$0.5 \text{ mm} \leq ap \leq 1 \text{ mm}$$

The initial parameters of GA were set, and the numerical simulation was conducted to determine the optimum turning parameters for resulting minimum R_a . From GA optimization, it was found that the best turning parameters are $V_c = 116 \text{ m/minute}$, $f = 0.1 \text{ mm/rev}$, $ap = 0.5 \text{ mm}$, which could result the minimum surface roughness of $R_a = 1.79 \mu\text{m}$.

Table 4 Initial setting, GA predicted result, result from validation experiment and the error rate

Optimum parameter setting			Surface roughness (R_a)		Error rate %
V_c m.min ⁻¹	f mm.rev ⁻¹	ap mm	Predicted result from GA μm	Result from validation experiment μm	
116	0.1	0.5	1.79	1.87	4.27

Initial setting: Population size = 100, Fitness scaling function = Rank, Selection function = Stochastic uniform, Reproduction elite count = 2, Crossover probability = 0.8, Cross over function = scattered, Mutation probability = 0.05, Initial penalty = 10, Number of generations = 300, Stopping criteria and plot = Best fitness

To validate the optimization results, the same turning parameters were used in validation experiment and the surface roughness respective to the settings was measured. The initial setting used in GA optimization, predicted result, result from the validation experiment and the error rate are shown in Table 4. It is found from the validation result that the current minimization function deviates from the experimental result by 4.27%. Having found high error rate between the predicted result and the validation experiment, ANN model was attempted to improve the accuracy of the RSM model and to obtain a more accurate prediction model.

3.3 ANN Prediction Model

ANN is the computation method to develop prediction model for any real-world problem. It is based on neurons. Neural networks are one of the techniques to train the knowledge base for the prediction of responses. ANN has the ability of learning the knowledge through experimental information set to express the linear or nonlinear relationship as well as interaction effects between input and output parameters. It consists of input, output and hidden layer. An input layer provides information to the network, while the output layer generates prediction. There are one or many hidden layers between input layer(s) and output layer(s). In the current research, ANN was attempted to improve the previous formulated RSM model that resulted high error rate.

The current ANN model comprises three input layer variables, each representing a control parameter of the turning operation (V_c , f , ap) and one output layer that representing the response variable (R_a). 60% of the experimental data was used for training, while 20% for testing and another 20% for validation. The back propagation-gradient descent method and training function as adaptive learning (TRAINGDX) were chosen. The learning function called LEARNGDM was used in learning of knowledge and mean squared error (MSE) was used for performance evaluation. Mean Square Error values (MSE) was used to evaluate the number of hidden neurons. The optimal ANN model was finalized which resulted minimum MSE. The final

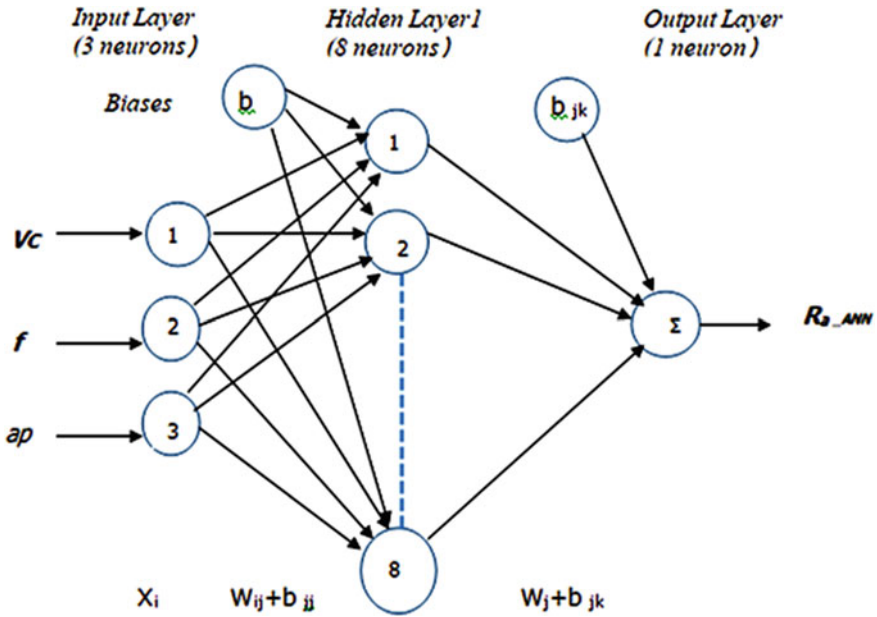


Fig. 2 ANN network (3-8-1) model for prediction of R_a

formulated ANN model as shown in Fig. 2 was a (3-8-1) model, in which eight hidden layers were involved to predict the optimum results.

3.4 Results and Discussions

The formulated ANN model was firstly trained with 60% of the experimental data, tested with 20% of the experimental data and finally validated with the remaining 20% of experimental data. Table 5 shows the ANN predicted results. The ANN predicted values were then used to build a new RSM model. Table 6 shows the newly computed uncoded β_i Coefficients from the ANN predicted dataset. The new RSM equation with the newly computed coefficients is;

$$\begin{aligned}
 R_{a_ANN} = & -3.58 + 0.02055V_c + 18.6f + 6.28ap - 0.000093V_c \times V_c - 13.09f \times f \\
 & - 1.42ap \times ap + 0.01214V_c \times f - 0.01186V_c \times ap - 3.97f \times ap \quad (4)
 \end{aligned}$$

After arriving at the new minimization function (R_{a_ANN}), GA algorithm was used to determine the optimum turning parameters. The same initial setting was used, as discussed in Sect. 3.2, in the numerical simulation. The newly predicted surface roughness R_a , by using GA, was found to be $1.42\mu\text{m}$ for the optimum turning condition of $V_c = 148\text{m/min}$, $f = 0.1\text{mm/rev}$, $ap = 0.5\text{mm}$. The predicted

Table 5 ANN predicted surface roughness R_a

Expt. no	Vc m.min ⁻¹	f mm.rev ⁻¹	ap mm	Surface roughness R_a	
				Value measured in experiment μm	ANN Predicted value μm
1	50	0.1	0.5	1.19	1.1601
2	50	0.1	0.75	2.28	2.1919
3	50	0.1	1	3.15	3.1575
4	50	0.3	0.5	3.85	3.8718
5	50	0.3	0.75	4.27	4.2566
6	50	0.3	1	4.86	4.9207
7	50	0.5	0.5	4.98	4.9924
8	50	0.5	0.75	5.26	5.4084
9	50	0.5	1	5.73	5.7422
10	100	0.1	0.5	1.18	1.1958
11	100	0.1	0.75	1.36	2.0536
12	100	0.1	1	2.62	2.3681
13	100	0.3	0.5	4.21	4.1329
14	100	0.3	0.75	4.74	5.7910
15	100	0.3	1	4.97	4.8022
16	100	0.5	0.5	5.26	5.4847
17	100	0.5	0.75	5.59	5.8523
18	100	0.5	1	5.98	5.4862
19	150	0.1	0.5	1.12	1.1314
20	150	0.1	0.75	1.94	2.9827
21	150	0.1	1	2.12	3.0610
22	150	0.3	0.5	3.58	3.5988
23	150	0.3	0.75	3.64	4.7125
24	150	0.3	1	3.98	4.0178
25	150	0.5	0.5	5.21	5.1190
26	150	0.5	0.75	5.39	5.3597
27	150	0.5	1	5.68	5.7869

result from GA was further validated experimentally. The error rate between predicted results from ANN encompassed RSM model and the validation experiment is 2.73%. Table 7 shows the comparison of the results. Figure 3 shows the regression analysis on the output and target from the ANN. It is observed from the analysis that the training data best fits with $R=0.99401$, testing data best fits with 0.9708 and validation data best fits with 0.99629.

Figure 3 Regression analysis on output and target from ANN

Table 6 The newly calculated uncoded β_i coefficients for RSM model

Box Benkhan's coefficient term	Updated coefficient value from ANN predicted dataset
α_0	-3.58
β_1	0.02055
β_2	18.60
β_3	6.28
β_{11}	-0.000093
β_{22}	-13.09
β_{33}	-1.42
β_{12}	0.01214
β_{13}	-0.01186
β_{23}	-3.97

Table 7 Comparison results

Model	Optimum Parameter Setting			Surface rroughness		Error %
	V_c m/min	f mm/rev	A_p Mm	Predicted R_a from GA μm	R_a measured from validation Experiment μm	
ANN encompassed RSM	148	0.1	0.5	1.42	1.46	2.73
RSM (initial)	116	0.1	0.5	1.79	1.87	4.27

4 Conclusions

The research was attempted to decide the optimum turning parameters to achieve the minimum R_a , which is regarded as one of the important quality of any machined part. The titanium (Ti-6Al-4 V) grade5 was machined in CNC machine with diamond tip insert with servo coolant according to the L_{27} orthogonal array. The experimental results were used to develop the RSM model. The minimization of R_a was carried out using GA. The predicted result from GA had 4.27% of error, which could be the measurement error and computation model error. In order to develop a more accurate RSM model and achieve the best turning parameters, ANN methodology was applied. A systematic approach was used to develop a more accurate ANN model. The new RSM model was developed with ANN predicted results, which was further applied in GA. The newly predicted results deviate from the validation results by only 2.73%. This is considered as a new method of encompassing the ANN model in the development of RSM model and the optimization of cutting parameters to achieve the minimum surface roughness of the titanium alloy. The newly predicted surface roughness R_a , by using GA, was found to be $1.42\mu\text{m}$ for the optimum turning condition of $V_c = 148\text{m/min}$, $f = 0.1\text{mm/rev}$, $a_p = 0.5\text{mm}$.

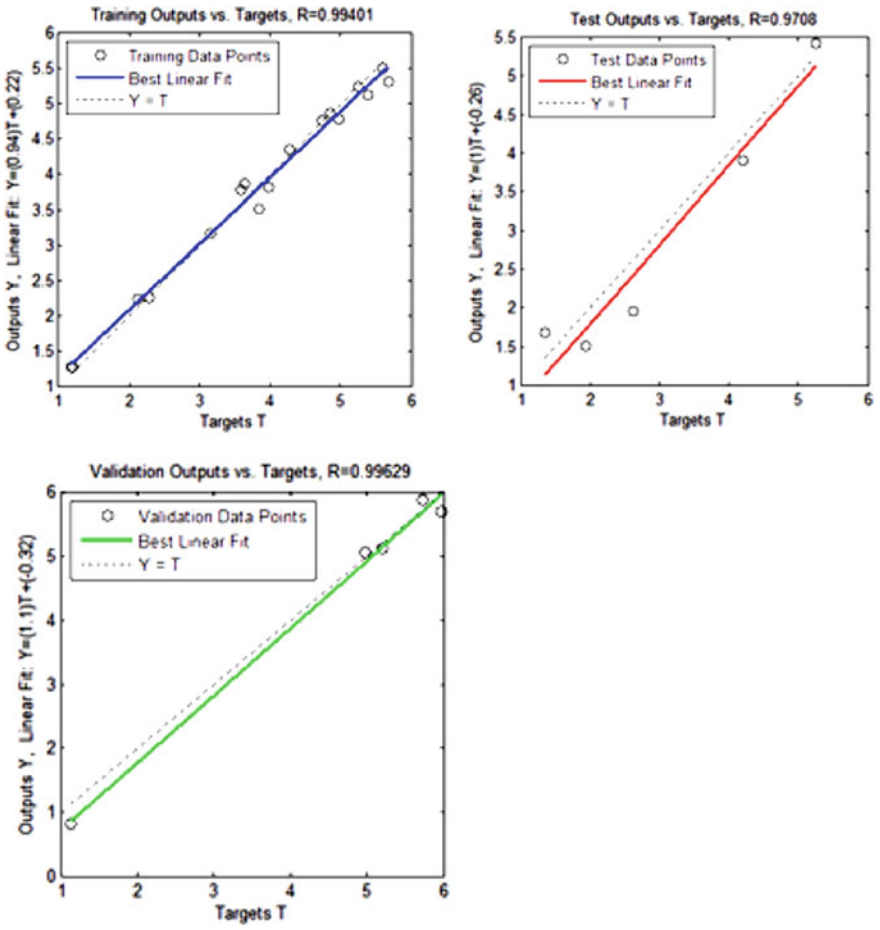


Fig. 3 Regression analysis on output and target from ANN

Conflict of Interest: Authors do not have any conflict of interest.

References

1. Sangwan, K. S., Saxena, S. & Kant, G. (2015). Optimization of machining parameters to minimize surface roughness using integrated ANN-GA approach. *Procedia CIRP*, 29, 305–310. <https://doi.org/10.1016/j.procir.2015.02.002>.
2. Paulo Davim, J., Gaitonde, V. N., & Karnik, S. R. (2008). Investigations into the effect of cutting conditions on surface roughness in turning of free machining steel by ANN models. *Journal of Materials Processing Technology*, 205(1–3), 16–23. <https://doi.org/10.1016/j.jmptotec.2007.11.082>.

3. Ramesh, S., Karunamoorthy, L., & Palanikumar, K. (2012). Measurement and analysis of surface roughness in turning of aerospace titanium alloy (gr5). *Measurement*, 45(5), 1266–1276. <https://doi.org/10.1016/j.measurement.2012.01.010>.
4. Ramesh, S., Karunamoorthy, L., Senthilkumar, V. S., & Palanikumar, K. (2009). Experimental study on machining of titanium alloy (Ti64) by CVD and PVD coated carbide inserts. *International Journal of Manufacturing Technology and Management*, 17(4), 373–385.
5. Ramesh, S., & Karunamoorthy, L. (2013). Turning investigations on machining of Ti64 alloy with different cutting tool inserts. *Materials Science Forum*, 763, 1–27. <https://doi.org/10.4028/www.scientific.net/msf.763.1>.
6. Ramesh, S., Karunamoorthy, L., & Palanikumar, K. (2008). Fuzzy modeling and analysis of machining parameters in machining titanium alloy. *Materials and Manufacturing Processes*, 23(4), 439–447. <https://doi.org/10.1080/10426910801976676>.
7. Suresh, P. V. S., Venkateswara Rao, P., & Deshmukh, S. G. (2002). A genetic algorithmic approach for optimization of surface roughness prediction model. *International Journal of Machine Tools and Manufacture*, 42(6), 675–680. [https://doi.org/10.1016/S0890-6955\(02\)00005-6](https://doi.org/10.1016/S0890-6955(02)00005-6).
8. Thirumalai, R., Techato, K., Chandrasekaran, M., Venkatapathy, K., & Seenivasan, M. (2020). Experimental investigation during turning process of titanium material for surface roughness. *Materials Today: Proceedings*. <https://doi.org/10.1016/j.matpr.2020.07.213>.
9. Zhong, Z. W., Khoo, L. P., & Han, S. T.(2007). Neural-network predicting of surface finish or cutting parameters for carbide and diamond turning processes. *Materials and Manufacturing Processes*, 23(1), 92–97. <https://doi.org/10.1080/10426910701524667>.
10. Natarajan, E., Kaviarasan, V., Lim, W. H., Tiang, S. S., & Tan, T. H. (2018). Enhanced multi-objective teaching-learning-based optimization for machining of Delrin. *IEEE Access*, 6(1), 1–19.
11. Kaviarasan, V., Venkatesan, R., & Natarajan, E. (2019). Prediction of surface quality and optimization of process parameters in drilling of Delrin using neural network. *Progress in Rubber, Plastics and Recycling Technology*, 35(3).
12. Natarajan, E., Kaviarasan, V., Lim, W. H., Tiang, S. S., Parasuraman, S., & Elango, S. (2020). Non-dominated sorting modified teaching-learning-based optimization for multi-objective machining of polytetrafluoroethylene (PTFE). *Journal of Intelligent Manufacturing*, 31(4), 911–935. <https://doi.org/10.1007/s10845-019-01486-9>.
13. Suresh, S., Elango, N., Venkatesan, K., Lim, W. H., Palanikumar, K., & Rajesh, S. (2020). Sustainable friction stir spot welding of 6061-T6 aluminum alloy using improved non-dominated sorting teaching learning algorithm. *Journal of Materials Research and Technology*, 9(5), 11650–11674. <https://doi.org/10.1016/j.jmrt.2020.08.043>.
14. Ramesh, S., Viswanathan, R., & Elango, N. (2017). Temperature measurement and optimization in machining magnesium alloy using RSM and ANOVA. *Pertanika J Sci Technol*, 25(1), 255–262.
15. Sathiyamoorthy, V., Sekar, T., & Elango, N. (2015). Optimization of processing parameters in ECM of Die tool steel using Nanofluid by Multiobjective genetic algorithm. *Scientific World Journal*. <https://doi.org/10.1155/2015/895696>.
16. Ang, K. M., Lim, W. H., Isa, N. A. M., Tiang, S. S., Ang, C. K., Natarajan, E., & Solihin, M. I. (2020). A constrained teaching-learning-based optimization with modified learning phases for constrained optimization. *Journal of Advanced Research in Dynamical and Control Systems*, 12(4 Special Issue), 1442–1456. <https://doi.org/10.5373/jardcs/v12sp4/20201623>.
17. Nagarajan, P., Murugesan, P. K., & Natarajan, E. (2019). Optimum control parameters during machining of LM13 aluminum alloy under dry electrical discharge machining (EDM) with a modified tool design. *Medziagotyra*, 25(3), 270–275. <https://doi.org/10.5755/j01.ms.25.3.20899>.
18. Chabbi, A., Yaltese, M. A., Nouioua, M., Meddour, I., Mabrouki, T., & Girardin, F. (2017). Modeling and optimization of turning process parameters during the cutting of polymer (POM C) based on RSM, ANN, and DF methods. *The International Journal of Advanced Manufacturing Technology*, 91(5), 2267–2290. <https://doi.org/10.1007/s00170-016-9858-8>.

19. Karnik, S. R., Gaitonde, V. N., & Campos Rubio, J., et al (2008). Delamination analysis in high speed drilling of carbon fibre reinforced plastics (CFRP) using artificial neural network model. *Mater Design*, 29, 1768–1776.
20. Suresh, P., Venkatesan, R., Sekar, T., Elango, N., & Sathiyamoorthy, V. (2014). Optimization of intervening variables in MicroEDM of SS 316L using a genetic algorithm and response-surface methodology. *Strojniski Vestnik/Journal of Mechanical Engineering*, 60(10), 656–664. <https://doi.org/10.5545/sv-jme.2014.1665>.

Fuzzy Interference System of Drilling Parameters for Delrin Parts



S. Parasuraman, Brian Cheong Tjun Yew, Sangeetha Elango,
I. Elamvazuthi, and V. Kaviarasan

1 Introduction

Delrin is a brand of Polyoxymethylene (POM) used in many industrial applications. It is a semi-crystalline thermoplastic, biomaterial, which can be used in food industries. The material is attributed with good stiffness, mechanical strength, elastic properties, toughness, hardness, frictional coefficient [1]. This combination of properties makes POM a versatile material, hence its widespread used. Traditionally, machining parameters have been chosen through human judgments or handbook. If these parameters are low conservative, the machining process will be led to poor accuracy and loss of productivity. It will significantly increase the production cost. The optimal solution should meet the desired target smoothness while maximizing productivity as required by the customers. Kaviarasan et al. [2] used Artificial neural

S. Parasuraman (✉)

School of Engineering, Monash University Malaysia, 46150 Bandar Sunway, Malaysia

e-mail: s.parasuraman@monash.edu

B. C. T. Yew

Monash University Malaysia, 46150 Bandar Sunway, Malaysia

e-mail: bche001@student.edu

S. Elango

Lee Kong Chian Faculty of Engineering and Science, Universiti Tunku Abdul Rahman (UTAR),
Sungai Long, Malaysia

e-mail: csgeetha80@gmail.com

I. Elamvazuthi

Department of Electrical and Electronic Engineering, Universiti Teknologi PETRONAS, 32610
Bandar Seri Iskandar, Malaysia

e-mail: irraivan_elamvazuthi@utp.edu.my

V. Kaviarasan

Department of Mechanical Engineering, Sona College of Technology, Salem, India

e-mail: vkavi.cim@gmail.com

© The Author(s), under exclusive license to Springer Nature Switzerland AG 2021

21

K. Palanikumar et al. (eds.), *Futuristic Trends in Intelligent Manufacturing*,

Materials Forming, Machining and Tribology,

https://doi.org/10.1007/978-3-030-70009-6_3

network (ANN) to develop the prediction model for drilling of POM. They used feed rate, spindle speed and tool point angle as independent parameters and evaluated the effect of parameters on drilling tool made of high strength steel and carbide tool.

Knowledge based Fuzzy inference can be applied in the production, when there is intrinsic fuzziness in tangible manufacturing systems such as drilling, where knowledge or understanding is incomplete or vague [3]. For example, fuzzy inference was used together with sensor fusion, in a study by Barai et al. [4] to predict the smoothness of the parts from turning process. Similarly, a fuzzy inference system was also used to predict the roughness during turning process [5]. Meanwhile, many optimization algorithms have also been used in prediction of parameters in production. Natarajan et al. applied modified TLBO algorithm for finding the optimal turning parameters for POM [6] and PTFE [7]. Suresh et al. applied enhanced TLBO algorithm [8] and GRA [9] for finding the optimal welding parameters for welding aluminum alloys. Sathyamoorthy et al. [10, 11] used GA to obtain optimal process parameters for ECM of aluminum alloy, while Wang et al. [12] used GA for turning process. Ramesh et al. [13] used RSM to optimize the process parameters of machining of magnesium alloy, while Nagarajan et al. [14] used response surface methodology to model the process parameters of machining of aluminium alloy. Abbas et al. [15] solved multiobjective optimization problem(MOP) of abrasive jet machining, while Rao et al. [16] solved MOP of many modern machining processes using TLBO. Abhishek et al. [17, 18] solved the problem of machining of CFRP material. Hazza et al. [19] attempted optimization of end milling process. While many research articles cover machining optimization with traditional metallic materials, a few deals with thermoplastics. Moreover, the application of AI along with optimization is seldom existing in the literature.

2 Material and Experimental Data

Experimental data were sourced from the research article published by Kaviarasan et al. [3]. Table 1 shows the experimental data published in the article. The experimental data has 3 independent variables such as spindle speed, feed rate and tool point angle. These are parameters used to set the drilling condition. Surface roughness is the dependent variable measured with respect to the drilling condition. These 27 sets of experimental data were used to determine the basis for rules and membership of fuzzy inference system. A simple analysis was conducted to identify the dominance of the drilling parameters. One of the input parameters was held constant, while the remaining variables were varied to reveal the effect of each input parameter on surface roughness. It is observed from Fig. 1 that lower the feed rate, the lower the surface roughness. The similar pattern is observed in other parameters such as tool point angle and spindle speed as well from Figs. 2 and 3, respectively. Also observed that feed rate is found to be the most influencing parameter followed by tool point angle and spindle speed.

Table 1 Raw data for delrin drilling

Spindle speed (rpm)	Feed rate (mm/min)	Tool point angle (°)	Surface roughness (μm)
1000	0.1	118	0.76
1000	0.15	118	1.22
1000	0.2	118	1.56
1500	0.1	118	0.81
1500	0.15	118	1.29
1500	0.2	118	1.42
2000	0.1	118	0.94
2000	0.15	118	1.65
2000	0.2	118	1.6
1000	0.1	125	0.84
1000	0.15	125	1.35
1000	0.2	125	1.68
1500	0.1	125	0.89
1500	0.15	125	1.5
1500	0.2	125	1.62
2000	0.1	125	0.95
2000	0.15	125	1.52
2000	0.2	125	1.79
1000	0.1	135	0.82
1000	0.15	135	1.59
1000	0.2	135	1.95
1500	0.1	135	0.79
1500	0.15	135	1.6
1500	0.2	135	1.86
2000	0.1	135	0.88
2000	0.15	135	1.74
2000	0.2	135	1.78

The data clustering was carried out to determine the best number of membership to divide the output data for a Mamdani fuzzy inference system. Theoretically, the range of each membership function would be the range of values of the member within each group. k-means clustering based data partitioning method was proposed which treats each observation in data set as an object that has a location in space. The function finds a partition in which objects within each cluster are possible. Each cluster partition consists of member objects and a centroid (or center). In each cluster, this method reduces the sum of the distances between the centroid and all member objects in the cluster.

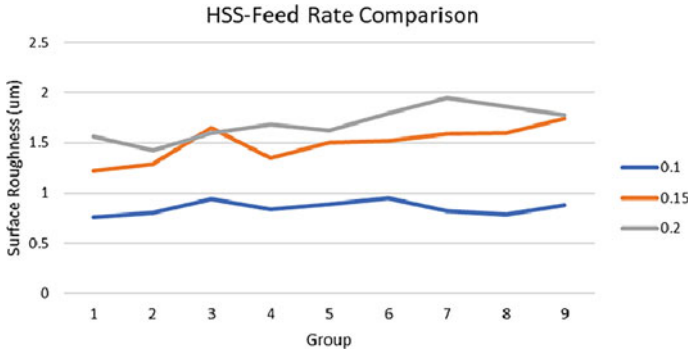


Fig. 1 The influence of feed rate on surface roughness

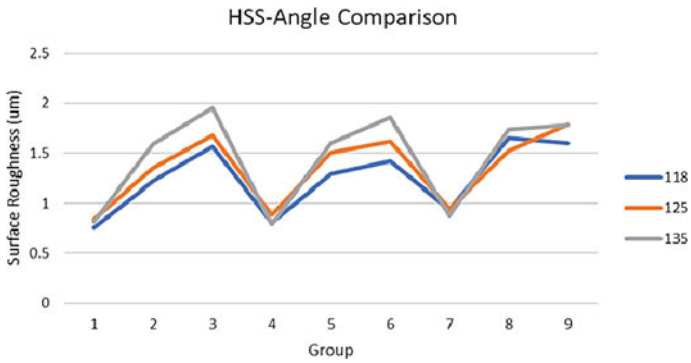


Fig. 2 The influence of tool point angle on surface roughness

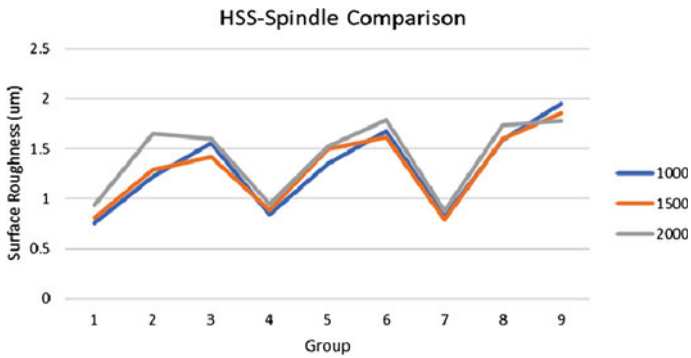


Fig. 3 The influence of spindle speed on surface roughness

The data of surface roughness was separated into several clusters, ranging from 2 to 10 clusters, to see which would fit the data best. For each cluster setting, the experiment was run 10 times to get a good mean value. Silhouette plot was used to demonstrate the fitness of each data point in their respective cluster. The fitness value ranges from -1 to 1 , where 1 indicates the point is very distant from neighboring clusters. 0 represents the data point is not distinct in one cluster or another. -1 means the data point is probably assigned to the wrong cluster. The fitness value of each data point in 2, 4, 7 and 10 clusters is shown in Figs. 4, 5, 6 and 7, respectively.

Fig. 4 Fitness value of each point in 2 Clusters

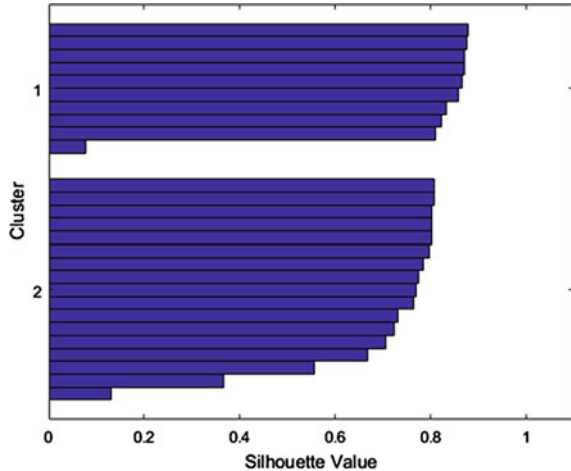


Fig. 5 Fitness value of each point in 4 Clusters

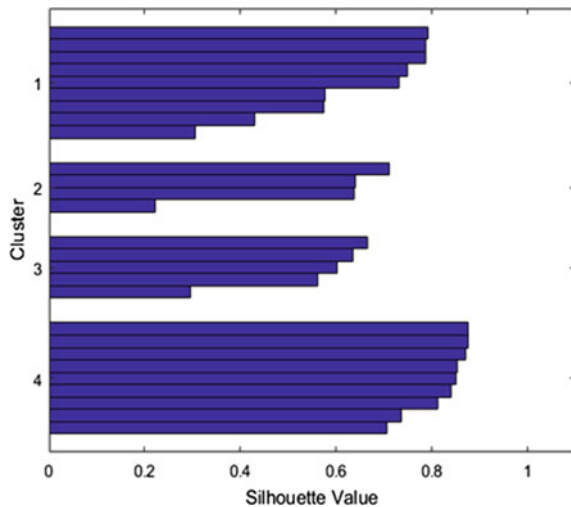


Fig. 6 Fitness value of each point in 7 Clusters

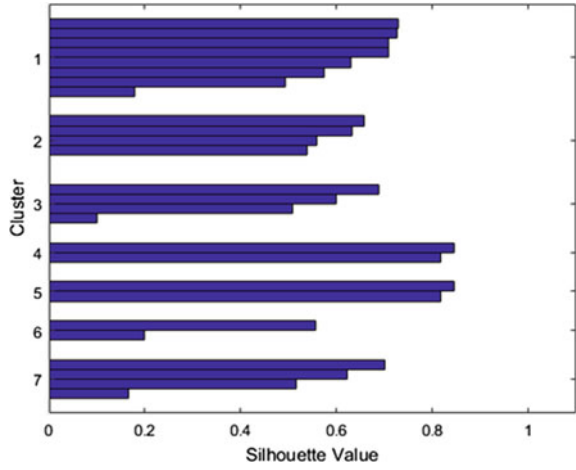
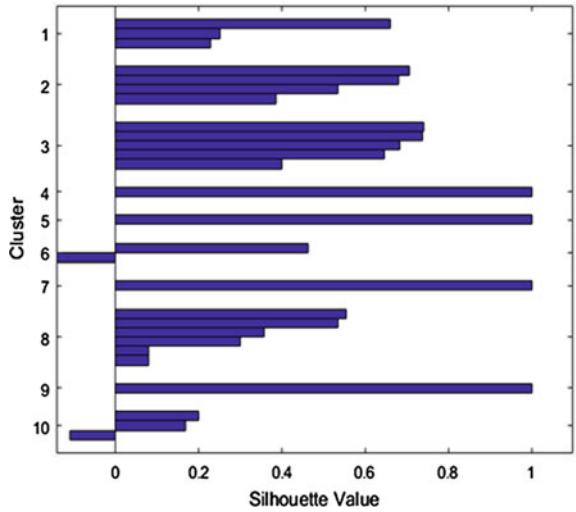


Fig. 7 Fitness value of 10 clusters



As the number of cluster increases, the average fitness of data in their respective group has decreased as shown in Table 2. The best fit value was achieved when data was separated into 2 clusters. However, a Mamdani fuzzy inference system (FIS)

Table 2 K-means clustering fitness value

Number of clusters	2	3	4	5	6	7	8	9	10
Mean fitness value	0.7272	0.5958	0.6492	0.5922	0.5447	0.5305	0.5310	0.5173	0.5223

Table 3 Fuzzy membership of Input variables

<i>Linguistic variable/Membership: feed rate-input</i>			
Group name	Lower limit	Upper limit	Peak
Low_F	0.1	0.15	0.1
Medium_F	0.1	0.2	0.15
High_F	0.15	0.20	0.2
<i>Linguistic variable/Membership spindle speed-input</i>			
Group name	Lower limit	Upper limit	Midpoint
Slow spindle	1000	1500	1000
Medium spindle	1000	2000	1500
Fast spindle	1500	2000	2000
<i>Linguistic variable/Membership tool point angle-input</i>			
Group name	Lower limit	Upper limit	Midpoint
Low	118	125	118
Moderate	118	135	125
High	125	135	135

with so few output memberships cannot accurately estimate the surface roughness of drilled hole. Hence, a Sugeno fuzzy inference system was chosen instead. Sugeno fuzzy inference uses singleton output membership functions that are either constant or a linear function of the input values [20].

3 Fuzzy Inference System (FIS)

A fuzzy inference system (FIS) takes in crisp (definitive) inputs and applies the rules to produce a crisp output. The decision-making unit decides what rules to apply. The degree to which rules are applied is based on weightage. The rules and weightages are based on data trends within the database and are usually set by the user beforehand. The current fuzzy inference system of has 3 inputs and 1 output as shown in Fig. 8. Feed rate, tool point angle and spindle speed are the inputs for FIS. Each input has

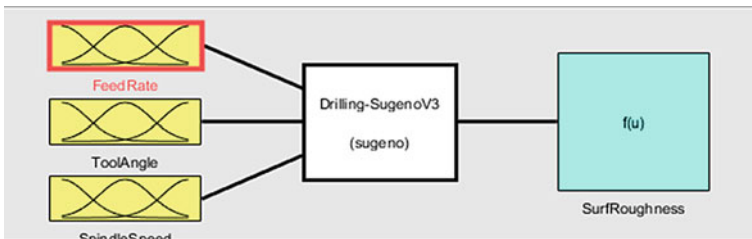


Fig. 8 Overview of FIS

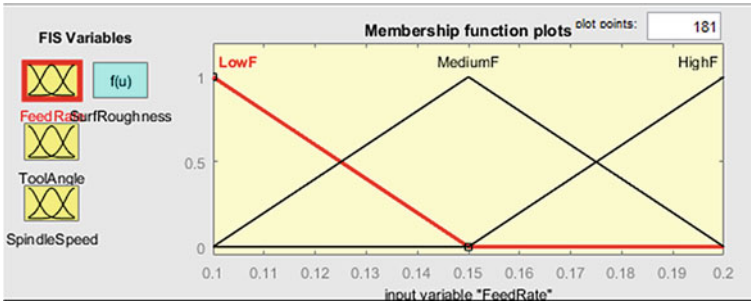


Fig. 9 Feed rate memberships

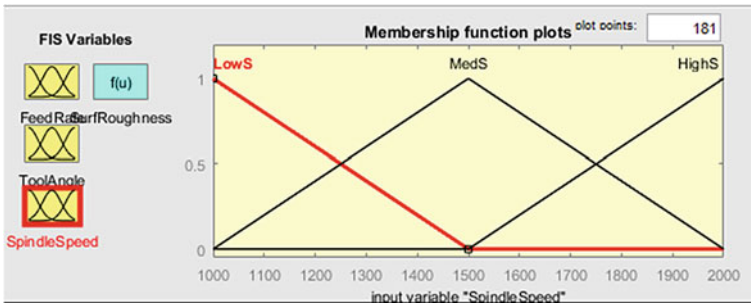


Fig. 10 Spindle speed membership

3 triangle memberships. Each of these memberships overlaps with their neighbor, extending until the midpoint of their adjacent membership as shown in Figs. 9, 10 and 11. Surface roughness is the FIS output. The output has 26 membership functions to represent the 26 unique output data points. Analysis of raw data indicated that surface roughness mainly depends on feed rate, in such a way that the other inputs only play a minor role in determining the output. Feed rate value can determine a

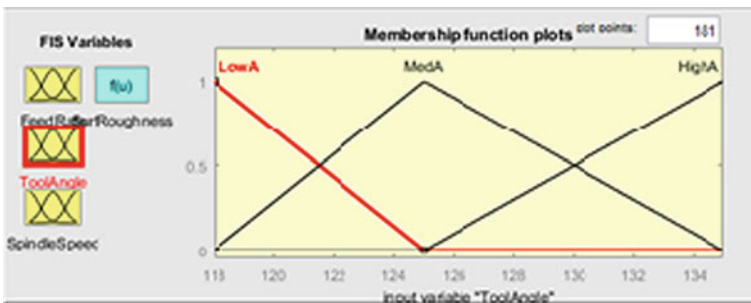


Fig. 11 Tool angle membership

large extent the possible range of value for surface roughness. To model this system, the fuzzy inference system has a rule for every possible combination of inputs. In this case, each rule has 3 criteria (matching the 3 inputs of the system), use the “and” condition, and an equal weightage of 1. The total number of rules matches the number of experimental data points, which in this case is 27.

The fuzzy rule is shown in Fig. 12. The comparison of FIS predicted data and the experimental data is shown in Fig. 13. It is observed that FIS has mean error of 7.59% with the correlation coefficient of 0.98. The regression equation of the experimental

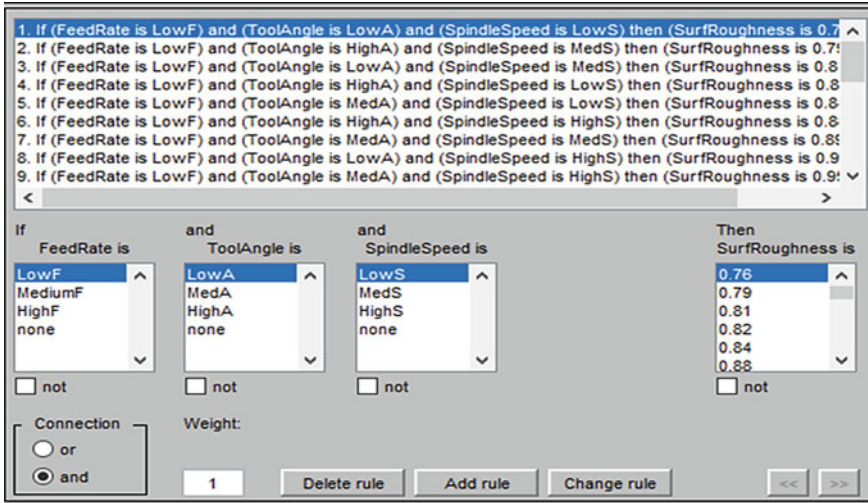


Fig. 12 Fuzzy rules

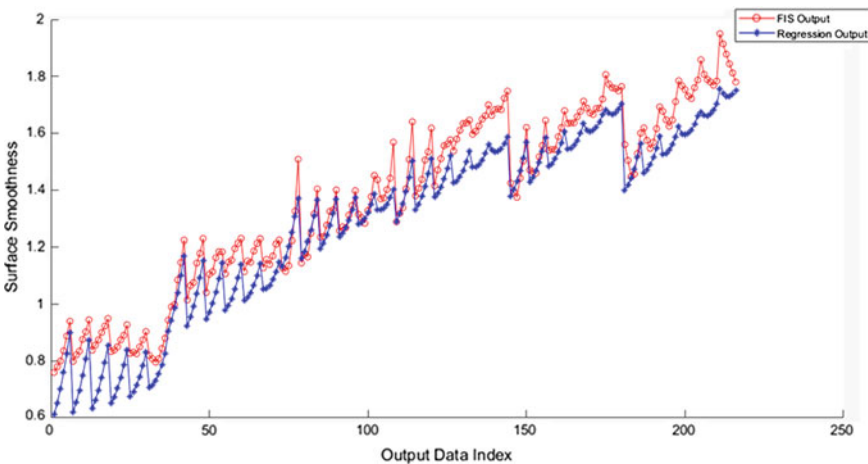


Fig. 13 comparison of FIS predicted data and experimental data

data is given in Eq. 1, which can be further used in optimization of independent variables for getting the maximum surface roughness (Table 3).

$$R_a = 1.527 + 0.00128N + 16.7422f - 0.058\theta + 9,9677e - 8 * N * N - 85.582*f*f + 0.00023*\theta * \theta - 0.001251*N*f - 9.87512e - 6*N*\theta + 0.153165*f*\theta \quad (1)$$

4 Conclusions

This research attempts to model the drilling data of POM material. The experimental data were sourced from the existing literature where RSM model was applied. The experimental data was analyzed and found that feed rate is a dominant independent parameter. Sugeno fuzzy inference system was developed with three input member functions and 26 output membership functions. The regression output of FIS and the experimental data were computed and seen that FIS has mean error of 7.59% with the correlation coefficient of 0.98.

References

1. Campos Rubio, J. C., Panzera, H. T., & Scarpa, F. (2015). Machining behaviour of three high-performance engineering plastics. *Proceedings of the Institution of Mechanical Engineers*, 229(1), 28–37.
2. Kaviarasan, V., & Venkatesan, R. (2019). Prediction of surface quality and optimization of process parameters in drilling of delrin using neural network, progress in rubber. *Plastics and Recycling Technology*, 35(3), 149–169.
3. Sugeno, M. (1985). *Industrial applications of fuzzy control*. Elsevier Science Pub. Co.
4. Barai, R. K., Tjahjowidodo, T., & Pappachan, B. K. (2015). Fuzzy inference system based intelligent sensor fusion for estimation of surface roughness in machining process. in *9th International Conference on Sensing Technology (ICST)* (Auckland), pp. 799–802. <https://doi.org/10.1109/icsenst.2015.7438506>.
5. Tóth-Laufer, E., & Horváth, R. (2019). A MIMO fuzzy model to predict turning metrics. in *2019 IEEE 17th International Symposium on Intelligent Systems and Informatics (SISY)* (Subotica, Serbia), pp. 000109–000114. <https://doi.org/10.1109/SISY47553.2019.9111531>.
6. Natarajan, E., Kaviarasan, V., Lim, W. H., Tiang, S. S., & Tan, T. H. (2018). Enhanced multi-objective teaching-learning-based optimization for machining of delrin. *IEEE Access*, 6, 51528–51546. <https://doi.org/10.1109/ACCESS.2018.2869040>.
7. Natarajan, E., Kaviarasan, V., Lim, W. H., et al. (2020). Non-dominated sorting modified teaching-learning-based optimization for multi-objective machining of polytetrafluoroethylene (PTFE). *Journal of Intelligent Manufacturing*, 31, 911–935. <https://doi.org/10.1007/s10845-019-01486-9>.
8. Suresh, S., Elango, N., Venkatesan, K., Lim, W. H., Palanikumar, K., & Rajesh, S. (2020). Sustainable friction stir spot welding of 6061-T6 aluminium alloy using improved non-dominated sorting teaching learning algorithm. *Journal of Materials Research and Technology*, 9(5), 11650–11674.

9. Suresh, S., Venkatesan, K., Natarajan, E., et al. (2020). Performance analysis of nano silicon carbide reinforced swept friction stir spot weld joint in AA6061-T6 Alloy. Silicon. <https://doi.org/10.1007/s12633-020-00751-4>.
10. Sathiyamoorthy, V., Sekar, T., & Elango, N. (2015). Optimization of processing parameters in ECM of die tool steel using nanofluid by multiobjective genetic algorithm. *The Scientific World Journal*, 2015(895696). <https://doi.org/10.1155/2015/895696>.
11. Sathiyamoorthy, V., Sekar, T., Suresh, P., Vijayan, R., & Elango, N. (2015). Optimization of processing parameters in electrochemical machining of AISI 202 using response surface methodology. *Journal of Engineering Science and Technology*, 10(6), 780–789.
12. Wang, Z. H., Yuan, J. T., Hu, X. Q., & Deng, W. (2009). Surface roughness prediction and cutting parameters optimization in high-speed milling AlMn1Cu using regression and genetic algorithm. in *2009 International Conference on Measuring Technology and Mechatronics Automation* (Zhangjiajie, Hunan), pp. 334–337. <https://doi.org/10.1109/icmtma.2009.599>.
13. Viswanathan, R., Ramesh, S., Elango, N., & Kamesh Kumar, D. (2017). Temperature measurement and optimisation in machining magnesium alloy using RSM and ANOVA. *Pertanika Journal of Science & Technology*, 25(1), 255–262.
14. Nagarajan, P., Murugesan, P. K., & Natarajan, E. (2019). Optimum control parameters during machining of LM13 aluminum alloy under dry electrical discharge machining (EDM) with a modified tool design. *Materials Science*, 25(4).
15. Abbas, A. T., Aly, M., & Hamza, K. (2016). Multiobjective optimization under uncertainty in advanced abrasive machining processes via a fuzzy-evolutionary approach. *Journal of Manufacturing Science and Engineering*, 138(7), 071003-1–071003-9.
16. Rao, R., Rai, D., & Balic, J. (2017). A multi-objective algorithm for optimization of modern machining processes. *Engineering Applications of Artificial Intelligence*, 61, 103–125. <https://doi.org/10.1016/j.engappai.2017.03.001>.
17. Abhishek, K., Kumar, V., Datta, S., & Mahapatra, S. (2017). Application of JAYA algorithm for the optimization of machining performance characteristics during the turning of CFRP (epoxy) composites: comparison with TLBO. *GA, and ICA, Engineering with Computers*, 33(3), 457–475.
18. Abhishek, K., Rakesh Kumar, V., Datta, S., & Mahapatra, S. (2015). Parametric appraisal and optimization in machining of CFRP composites by using TLBO (teaching–learning based optimization algorithm). *Journal of Intelligent Manufacturing*, 28(8), 1769–1785. <https://doi.org/10.1007/s10845-015-1050-8>.
19. Al Hazza, M., Adesta, E., Riza, M., & Suprianto, M. (2012). Surface roughness optimization in end milling using the multi objective genetic algorithm approach. *Advanced Materials Research*, 576, 103–106. <https://doi.org/10.4028/www.scientific.net/amr.576.103>.
20. Mamdani, E. H., & Assilian, S. (1975). An experiment in linguistic synthesis with a fuzzy logic controller. *International Journal of Man-Machine Studies*, 7(1), 1–13.

Optimization and Effect Analysis of Sustainable Micro Electrochemical Machining Using Organic Electrolyte



V. Subburam, S. Ramesh, and Lidio Inacio Freitas

1 Introduction

Electrochemical micromachining is emerging as one of the capable techniques among the non-conventional machining methods that are preferred for its accuracy, surface finish along with other favorable outcomes. EMM is considered as a complex process because the parameters that are not significant at macro level become very sensitive at micro level [1]. The effect of scale on electrochemical machining (ECM) applied in the micro level was investigated by Mouliprasanth et al. and stated that operating parameters require down scaling for similarity between macro and micro ECM [2]. As the process requires research for numerous combination of materials and other input variations, this technique is under constant investigation to overcome the challenges and improve its capability. The electrochemical machining has been brought into micromachining domain because of the continuous works of the researchers world-wide. Reducing the inter-electrode-gap (IEG) without distracting the performance of EMM was a great challenge encountered by the researchers. By employing ultra-short pulses, the machining gap was considerably reduced by Schuster et al.

V. Subburam (✉)

Department of Mechanical Engineering, Paavai Engineering College, Namakkal 637018, India

e-mail: subburam1903@gmail.com

S. Ramesh

Department of Mechanical Engineering, School of Engineering, Presidency University, Bangalore 560064, India

e-mail: ramesh_1968in@yahoo.com

L. I. Freitas

Research Scholar, Faculty of Engineering, UCSI University, Kuala Lumpur, Malaysia

Dili Institute of Technology, Dili, Timor-Leste

L. I. Freitas

e-mail: lidiofreitas00@gmail.com

to realize the potential utilization of EMM in the micro-fabrication domain. The research used a mixed electrolyte of $\text{CuSO}_4 + \text{HClO}_4$ to machine copper [3]. Also the EMM experimental setups are being developed by different organizations, laboratories, educational institutions and individual researchers all over the world to enhance the capability and refine the various sub-systems and components involved in the process. An EMM setup with pulsed power was designed in which experiments were carried out successfully with precision by Bhattacharyya et al. The IEG was reduced to the lowest possible micrometer range to achieve better accuracy. The inter electrode gap was monitored by detecting the value of current at the gap through a sensor. The experiments also revealed the impact of various input parameters on performance parameters and emphasized the need for optimization of process parameters [4]. Mithu et al. designed and developed an EMM setup having three co-ordinate movements of tool and automation of tool-feed system with computer monitoring [5]. To avoid deposition of sludge on micro-tool, it was made to vibrate during machining by Ghoshal et al. and obtained improved performance [6].

Micro tools with different shapes and aspect ratios have been experimented in EMM to find their influence on the performance [1]. Thanigaivelan et al. conducted EMM experiments with micro tools having different tip shapes to investigate their effect on the process and found the conical shaped tools to provide better performance [7]. To avoid stray machining and as well the taper effect on the workpieces having higher depths, the side surface of the tool requires insulation [8, 9]. The surface quality of the work materials have been improved by using masks in the EMM process [10]. Kumar et al. have utilized reusable masked tool to produce micro square pattern on SS-304 material through EMM [11]. An electrolyte flushing technique for continuous flushing of passive layer and sludge from the electrode interface was utilized for improving the circularity of the micro-hole fabricated through EMM by Pooranachandran et al. [12]. A sensor arrangement was used to maintain constant flow velocity in the electrode gap to cause improvement in the performance of the EMM process by Geethapriyan [13]. Apart from metals, materials such as alloys and electrically conducting composites of different types have also been machined for micro-features using EMM and the input parameters optimized [14, 15].

Using appropriate electrolyte for a particular materials is very important in EMM process. It is the electrolyte which carries the ionic charges and causes dissolution of the anode work material. With every experimental research, electrolytes for different materials are identified and data base made available. Aluminium metal matrix composites have been machined through EMM using NaNO_3 (sodium nitrate) and NaCl (sodium chloride), considered as neutral solutions to investigate the variation in performance by Hackert et al. [16]. For machining very hard alloys, a small fraction of acid is added in the neutral electrolytes which otherwise becomes very difficult to machine through EMM process [17]. Some alloy compositions having multiple elements require mixed electrolytes for machining through EMM. A composite solution containing NaNO_3 and NaCl was used for machining $\text{Cr}_{12}\text{Ni}_9\text{Mo}_4\text{Cu}_2$ and the input parameters were optimized by Tang et al. [18]. A material called ‘Gamma-Titanium—Aluminium-Intermetallic’ used in engine applications in aero industry which has poor machinability was machined through EMM

using NaCl solution successfully by Liu et al. [19]. Eco-friendly electrolytic solution like citric acid solution has also been attempted to machine steel under EMM and found to give excellent performance by Ryu [20]. Even pure water as electrolyte was used with an ion-exchange catalyst to machine stainless steel work-material under EMM process successfully by Huaiqian et al. [21]. The performance of the EMM process is affected mainly by the contaminants. The various contaminants such as conductive/non-conductive particles, chemical by-products, sludge, gas bubbles that hinder the machining gap and lower the performance of the process were investigated by Schulze et al. [22].

Due to complex nature and interaction between input factors, EMM process requires multi-objective optimization to get optimal parametric combination to maximize the performance. Researchers have been applying many different optimization techniques and their combinations to enhance the predictions. In the optimization of micro-EDM process variables for SS-316L material, the response function modeled through RSM was utilized in GA (genetic algorithm) to get optimal set for maximum MRR (material removal rate) and minimum TWR (tool wear rate) by Suresh et al. [23]. In the ECM of die-tool-steel (containing high carbon & high chromium), copper nano-particles mixed NaNO_3 solution (nano-fluid) was utilized as electrolyte to reduce spike formation. Also MOGA (multiobjective genetic-algorithm) was applied for achieving enhanced MRR and surface quality through optimization of voltage and tool-feed levels by Sathiyamoorthy et al. [24]. The ECM process parameters such as voltage and electrolyte feeding rate were optimized in the machining of AISI-202 austenitic SS material to attain improved MRR and surface texture by making use of RSM [25]. Researchers have also optimized EMM operating parameters using Taguchi technique, GRA (Grey relational analysis) and other techniques [26, 27]. The current research involves electrochemical micromachining of SS304 steel work-material using citric acid to generate micro-holes and multi objective optimization of the input parameters through GRA.

2 Materials and Experimental Details

The details of experimental setup used and the materials used for experimentation along with input parameters are discussed below.

2.1 *Experimental Device for EMM Process*

An experimental setup built in-house was utilized to perform electrochemical micromachining experiments. The experimental arrangement is presented in Fig. 1. The setup is an assembly of all the essential sub-units required for EMM operation like mechanical support elements, micro-tool feeding system with stepper motor and lead-screw provision, micro-controller kit to monitor tool-feed and a pulse rectifier

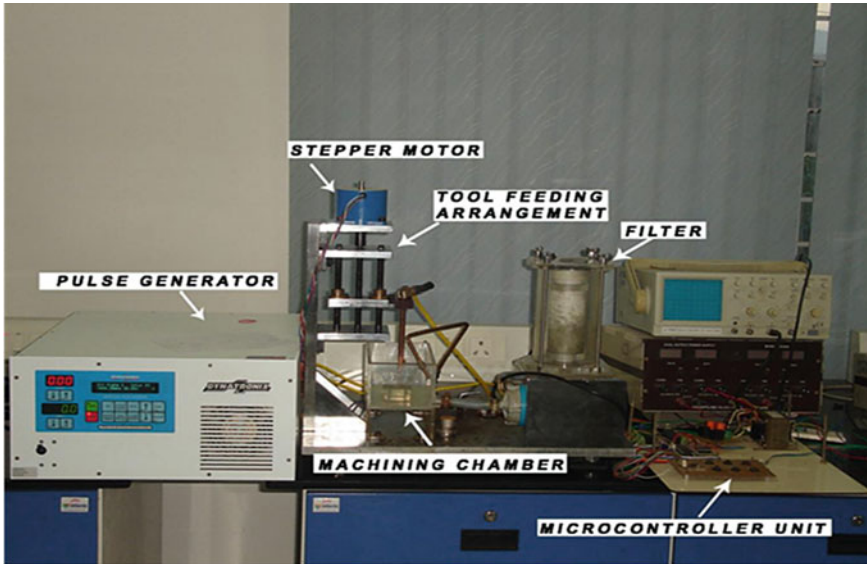


Fig. 1 Experimental setup showing sub-units

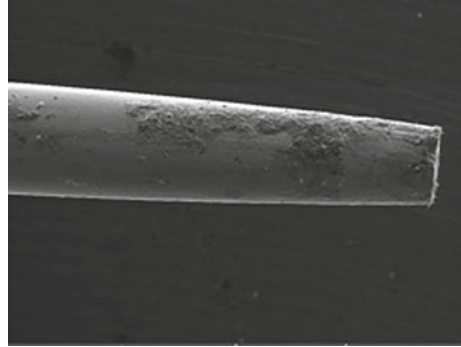
unit to supply pulsed power. It is a single axis machine with only vertical movement of the tool.

2.2 Input Factors Used for the Experiments

The work material used in this experimentation was SS-304 sheet of 45 mm × 43 mm × 200 μm size. The tool was made of tungsten with a diameter of 380 μm. The lateral surface of the tool was insulated to enable localized machining. Citric acid (C₆H₈O₇) solution which is considered as an environment friendly electrolyte was used for machining. Citric acid is normally extracted from citrus fruits (lime, lemon etc.), vegetables and plants and this organic compound belongs to the group of carboxylic acids. It is applied for metal cleaning purposes and has the potential to prevent precipitates formed during machining that are insoluble in nature and cause hindrance to the process [20]. Organic acids are generally considered as weak electrolytes with less conducting capabilities [28].

The input parameters selected for study were supply voltage (Volts), current (Ampere), pulse on-time (in milliseconds: ms) and electrolyte concentration (gram/litre: g/l). The frequency at 50 Hz and the electrode gap at 40 μm were kept as constant values. The machining rate (MR) which reveals the speed of the process and the overcut (OC) which shows the accuracy of the generated micro-hole dimensionally were taken to assess the performance. The micrograph of the micro tool is presented in Fig. 2.

Fig. 2 Tungsten micro-tool
(Diameter 380 μm)



2.2.1 Estimation of Performance Characteristics

The estimation of some important characteristics in EMM process are given below.

$$\text{Machining Rate} = \text{Thickness of workpiece } (\mu\text{m}) / \text{machining time (s)}$$

$$\text{Radial Overcut} = (\text{Hole diameter} - \text{Tool diameter}) / 2$$

$$\text{Duty cycle} = (\text{Pulse on-time} / \text{Pulse period}) \times 100$$

where Pulse period is equal to 'Pulse on-time + Pulse off-time'

For example 50 Hz denotes 50 pulses/s which means $1/50 = 20$ ms duration for each pulse. Now a duty cycle of 1:1 indicates 10 ms pulse on-time and 10 ms pulse-off-time

In pulse on-time period, the machining occurs while the pulse- off-period is utilized for flushing the by-products and other contaminants from the electrode gap by the passing electrolyte.

Preliminary trials were performed to decide the initial level of selected input parameters. When the voltage level was kept below 8 v, no dissolution of the work-piece was observed for a long time. Hence 8 V served as initial base value and other factors were set accordingly. The experimental design followed was Taguchi's L9 orthogonal array with four factors, each at three levels. The input parameters were optimized using GRA multi-objective optimization technique.

3 Optimization by GRA

The GRA technique was applied for optimization of EMM process in which the required outcome of each performance parameter may vary as higher machining rate

Table 1 Experimental inputs and results

Trail no.	Input factors				Response factors	
	Voltage (Volts) V	Current (Ampere) A	Pulse on-time (ms) T-on	Elec. conc. (g/l) EC	Machining rate (MR) ($\mu\text{m/s}$)	Overcut (OC) (μm)
1	8	1	10	15	0.0556	81.83
2	8	1.2	15	20	0.0849	63.23
3	8	1.4	17.5	25	0.0915	102.77
4	10	1	15	25	0.0906	98.11
5	10	1.2	17.5	15	0.0753	93.46
6	10	1.4	10	20	0.0457	60.9
7	12	1	17.5	20	0.0909	114.39
8	12	1.2	10	25	0.0711	65.56
9	12	1.4	15	15	0.0867	84.16

and lower overcut are preferred. GRA could convert a process having multiple objectives into a process of single base objective that gives an optimal solution to satisfy all the objectives. The technique uses a sequences of mathematical expressions to reduce the multi-objectives into common relational grade for comparing and finding the solution [29].

The input factors, their levels used in the L9 design and the outcomes attained are presented in Table 1.

3.1 Different Stages of GRA

Data processing or Normalization is the first step in this method in which the different units of the performance characteristics are made comparable by converting them to fit into a range of values between 0 and 1. Thus the original sequence of values is now converted into a comparable sequence by normalizing the values.

In accordance with targeted value designed to obtain, the expression for normalization varies as follows.

To obtain the characteristic of ‘larger the better’, the following expression is applied.

$$x_i^*(k) = \frac{x_i^o(k) - \min x_i^o(k)}{\max x_i^o(k) - \min x_i^o(k)} \quad (1)$$

where $x_i^o(k)$ is originally existing sequence, $x_i^*(k)$ is sequence obtained after the data underwent preprocessing, $\max x_i^o(k)$ implies the largest value of $x_i^o(k)$, and $\min x_i^o(k)$ implies the smallest value of $x_i^o(k)$.

For “the lower-the better”, the normalization expression is:

$$x_i^* (k) = \frac{\max x_i^o(k) - x_i^o(k)}{\max x_i^o(k) - \min x_i^o(k)} \quad (2)$$

Grey relational coefficient (GRC) is found out next. This value expresses the correlation between normalized quality characteristics of ideal and actual values. It is given by:

$$\begin{aligned} \text{GRC, } \xi_{ij} &= \frac{\min_i \min_j |x_i^o - x_{ij}| + \zeta \max_i \max_j |x_i^o - x_{ij}|}{|x_i^o - x_{ij}| + \zeta \max_i \max_j |x_i^o - x_{ij}|} \\ &= \frac{\Delta_{\min} + \zeta \Delta_{\max}}{|x_i^o - x_{ij}| + \zeta \Delta_{\max}} \end{aligned} \quad (3)$$

where x_i^o is the ideal results of normalization obtained for the i th characteristics and ζ is the distinctive coefficient, defined within the range of $0 \leq \zeta \leq 1$.

GRG (Grey relational grade): To reduce the number of GRCs requiring comparison, the sequences are converted into its mean values which are referred as GRGs. The GRGs are obtained by:

$$\text{Grey relational grade, } \alpha_j = \frac{1}{N} \sum_{i=1}^N \xi_{ij} \quad (4)$$

Here, α_j is the GRG for j th trial and N provides the number of response parameters.

3.2 GRA Results

The results obtained at various stages of GRA process for the EMM performance characteristics like Machining rate (higher-the-better) and Overcut (lower-the-better) are summarized below in Table 2. The table includes S/N ratio values, normalized values, GRC values and the GRG values obtained through the mathematical equations at different stages of the GRA calculations.

The Table 2 provides grey relational grade for all the nine EMM experiments conducted to generate micro-hole on the sheet of SS-304 utilizing tungsten tool and solution of citric acid. The grey relational grade with highest value is considered to be nearer to the ideal value. The table shows experiment number 2 as having the highest grade of 0.848 that gives the best multiple performance characteristics. The parametric combination includes 8 V (Volts), 1.2A (Ampere), 15 ms ('Pulse-on-time' period) and 20 g/l (concentration of electrolyte).

Table 2 Summary of GRA results

Trial no.	S/N Ratio		Normalization		Grey relational coefficient		GRG
	MR	OC	MR	OC	MR	OC	
1	25.099	-38.258	0.216	0.609	0.389	0.561	0.475
2	-21.422	-36.018	0.856	0.956	0.776	0.920	0.848
3	-20.772	-40.237	1.000	0.217	1.000	0.390	0.695
4	-20.857	-39.834	0.980	0.304	0.962	0.418	0.690
5	-22.464	-39.413	0.646	0.391	0.586	0.451	0.518
6	-26.802	-35.692	0.000	1.000	0.333	1.000	0.667
7	-20.829	-41.168	0.987	0.000	0.974	0.333	0.654
8	-22.963	-36.333	0.555	0.913	0.529	0.852	0.690
9	-21.240	-38.502	0.895	0.565	0.827	0.535	0.681

Table 3 Response table for means

Level	Voltage (V)	Current (A)	Pulse on-time (T-on)	Electrolyte Concentration (EC)
1	0.6727	0.6064	0.6107	0.5581
2	0.6251	0.6855	0.7397	0.7229
3	0.6750	0.6808	0.6224	0.6918
Delta	0.0499	0.0791	0.1290	0.1648
Rank	4	3	1	2

3.2.1 Analysis of Response Table for Means

The response table for means reveals the influence of each input factor on the process. The response table for means is depicted below in Table 3.

The response table values clearly reveal that pulse on-time as the most significant factor that is followed by electrolyte concentration, supply current and supply voltage in that order for their influence on the electrochemical micromachining process of SS-304 by citric acid solution.

3.2.2 Analysis of Response Plot of GRG

The average response table as well as the average response graph could provide the optimal levels of each input factor of the EMM process. The mean response plot of the GRG is presented in Fig. 3. It can graphically show the significance of each parameter on the basis of mean values. With reference to the response-table and the response-plot, the optimal set could be formed as $V_3-A_2-T-on_2-EC_2$.

The response graphs of GRG presents the corresponding variation of the response while each parameter’s level changes from 1 to 3. Based on response graph for GRG

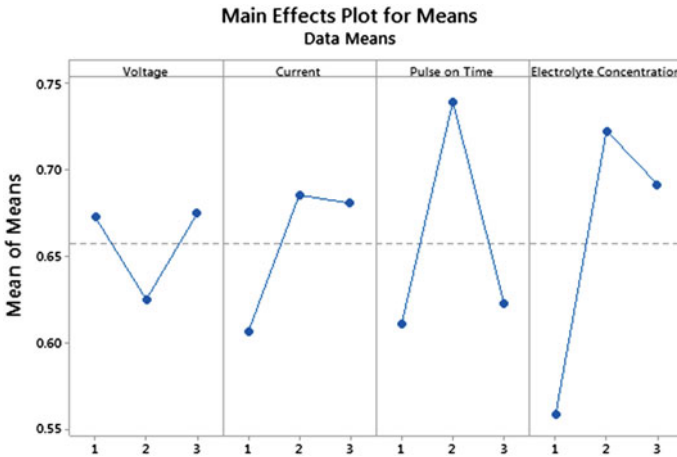


Fig. 3 Main effects plot for GRG

revealed in Fig. 3, the optimum combination of machining parameters are found to be: The voltage at level-3 (12 V), current at level-2 (1.2A), pulse-on-time at level-2 (15 ms) and concentration of electrolyte at level-2 (20 g/l).

4 Discussion

The observations made on the process of generating micro-holes on SS-304 material through electrochemical micromachining by using tungsten tool and citric acid as electrolyte have been discussed below.

4.1 Optimal Parametric Combination

The performance parameters evaluated in the process of making micro-holes by EMM are machining rate and overcut. The requirement is that of higher machining rate and lower overcut. The Grey relational analysis technique used for multi-objective optimization has produced an optimal combination comprising a voltage of 12 V, supply current of 1.2 A, pulse on-time period of 15 ms and an electrolytic concentration of 20 g/l among the different input combinations used in the experiments.

An analysis of the above combination shows that the voltage at highest level (level 3) would account for the higher machining speed of the process whereas the middle level inputs of current, pulse on-time and electrolytic concentration (all at level 2) contribute for the moderate speed of the process as well as reduction in

overcut. Past literatures on EMM process have revealed that increase in applied voltage increases machining rate but reduces the accuracy. This is because, tendency for stray machining increases at higher voltages resulting in overcut. Using a weak electrolyte like citric acid also reduces the machining speed which leads to improved process accuracy [28].

4.2 How the Input Factors Affect the EMM Process?

Bhattacharyya et al. investigated the effect of various input parameters on the performance of EMM process during the investigation to generate micro-holes on copper sheet. The report states that the input factors affect the process in such a way that improved accuracy can be achieved only along with moderate machining speed. Such an input combination include voltage at higher level, moderate level of pulse on-time (to provide enough pulse off-time to flush the sludge from the inter electrode gap) and the electrolyte at lower concentration level [30].

Higher voltage normally increases the machining rate as it causes increase in current, current density (current/area) and electric field (voltage/unit length) which increase the dissolution rate at the machining gap. But if it exceeds optimum level, tendency for the evolution of H_2 at the cathode tool increases and also these gas bubbles may get trapped in the machining gap as a result of which current density of the anode workpiece is lowered and electrolyte resistivity is increased thereby reducing the machining rate [31].

Normally the machining rate is increased for increased electrolyte concentration as more conducting ions are available for dislodging the ions from the anode work material as per the investigation of Ayyappan et al. in the machining of an alloy steel with a mixed electrolyte [32]. But there is an optimum limit up to which this increase in machining rate can happen after which the ions tend to clog the electrode gap and disrupt the machining. Ghoshal et al. employed H_2SO_4 (sulphuric acid) solution to produce micro-channels on SS-304 material and observed that electrolyte concentration of lower level as well as higher level, both result in stray machining. The study revealed that only moderate level of electrolyte concentration could serve as optimum level [33]. With higher level of electrolyte concentration, more ions are released in the solution and their mobility may be curtailed due to attraction between ions. If more ions are available in the electrolyte solution, as charge carriers their chaotic distribution around the inter electrode gap cause non-uniform electric field resulting in stray dissolution.

For rise in pulse on-time, the machining rate also gets raised. Increase in duty-cycle (i.e. pulse on-time) simultaneously decreases pulse off-time. Hence, if the pulse-off-time period is insufficient to eliminate the reaction products from the electrode gap, it may lead to short-circuit between the anode (workpiece) and the cathode (tool) causing micro sparks that produce overcut. Again if the pulse on-period is longer, the electrolyte solution at the gap may get heated up causing sparks and stray cut.

Fig. 4 Micro-hole machined at 12 V, 1A, 20 ms & 20 g/l

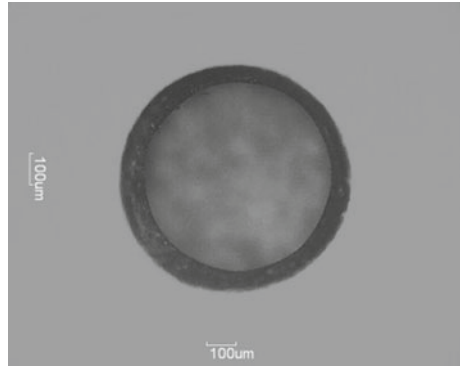
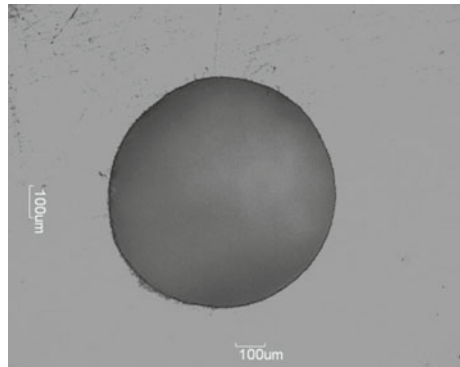


Fig. 5 Micro-hole machined at 8 V, 1A, 10 ms & 15 g/l



4.3 Micro-hole Images

The micrographs of the micro-holes machined on SS-304 sheet using citric acid solution are shown in Figs. 4 and 5. The micrographs show moderate quality of circular holes, the circumference of which have slightly rough edges. The usage of citric acid as electrolyte has resulted in the reduction of overcut considerably. Citric acid being a weak electrolyte provides a very slow machining rate compared to other inorganic electrolytes. However it produces good quality holes with less stray cut.

5 Conclusions

An experimental EMM setup was utilized to generate micro-holes on a sheet of SS-304, using a tool made of tungsten material and citric acid as electrolyte. Taguchi's design of L9 was applied to conduct the experiments and the input parameters were optimized through GRA multi-objective optimization technique. The important conclusions are noted down.

- Citric acid which is an environment friendly electrolyte can be successfully utilized in the EMM process for micromachining.
- The machining speed of citric acid is slow due to its weak acidic nature. However it improves the accuracy of the drilled holes.
- Among the input parameters studied, ‘pulse-on-time’ was found to be the most significant factor followed by electrolyte concentration, supply current and supply voltage in that order for their influence on the electrochemical micromachining process of SS-304 by citric acid solution.
- The optimum combination of machining parameters found through GRA is: The voltage at level-3 (12 V), current at level-2 (1.2A), pulse-on-time at level-2 (15 ms) and concentration of electrolyte solution at level-2 (20 g/l) for maximizing the machining rate and minimizing the overcut.

References

1. Bhattacharyya, B. (2015). *Electrochemical micromachining for nanofabrication, MEMS and nanotechnology*. UK: William Andrew Publications.
2. Mouliprasanth, B., & Hariharan, P. (2020). Scaling approach towards electrochemical micro-machining: A method to evaluate similarity. *The International Journal of Advanced Manufacturing Technology*. (Springer-Verlag London Ltd., part of Springer Nature). <https://doi.org/10.1007/s00170-020-05604-3>.
3. Schuster, R., Kirchner, V., Allongue, P., & Ertl, G. (2000). Electrochemical micromachining. *Science*, 289, 98–101.
4. Bhattacharyya, B., Doloi, B., & Sridhar, P. S. (2001). Electrochemical micro-machining: New possibilities for micro-manufacturing. *Journal of Materials Processing Technology*, 113, 301–305.
5. Mithu, M. A. H., Fantoni, G., & Ciampi, J. (2011). A step towards the in process monitoring for electrochemical microdrilling. *International Journal of Advanced Manufacturing Technology*, 57, 969–982. <https://doi.org/10.1007/s00170-011-3355-x>.
6. Ghoshal, B., & Bhattacharyya, B. (2013). Influence of vibration on micro-tool fabrication by electrochemical machining. *International Journal of Machine Tools and Manufacture*, 64, 49–59.
7. Thanigaivelan, R., & Arunachalam, R. M. (2010). Experimental study on the influence of tool electrode tip shape on electrochemical micromachining of 304 Stainless steel. *Materials and Manufacturing Processes*, 25, 1181–1185.
8. Rathod, V., Doloi, B., & Bhattacharyya, B. (2014). Sidewall insulation of microtool for electrochemical micromachining to enhance the machining accuracy. *Materials and Manufacturing Processes*, 29(3), 305–313. <https://doi.org/10.1080/10426914.2013.864407>.
9. Jain, V. K., Kalia, S., Sidpara, A., & Kulkarni, V. N. (2012). Fabrication of micro-features and micro-tools using electrochemical micromachining. *The International Journal of Advanced Manufacturing Technology*, 61(9–12), 1175–1183.
10. Wang, Q., Xiao, J., & Li, Y. (2011). Experimental study on the through-mask electrochemical micromachining (EMM) Process. *Advanced Materials Research*, 189–193, 69–692. (Trans Tech Publications, Switzerland).
11. Kumar, S., & Bhattacharyya, B. (2018). Electrochemical micromachining of micro square pattern using reusable masked tool. *Materials and manufacturing processes*. Taylor & Francis. <https://doi.org/10.1080/10426914.2018.1532582>.

12. Pooranachandran, K., Deepak, J., Hariharan, P. & Mouliprasanth, B. (2019). Effect of flushing on electrochemical micromachining of copper and inconel 718 alloy. *Advances in Manufacturing Processes, Lecture Notes, in Mechanical Engineering*. Springer Nature Singapore Pte Ltd. https://doi.org/10.1007/978-981-13-1724-8_6.
13. Geethapriyan, T., Manoj Samson, R., Thavamani, J., Arun Raj, A. C., & Pulagam, B. R. (2019). Experimental investigation of electrochemical micro-machining process parameters on stainless steel 316 using sodium chloride electrolyte. *Advances in Manufacturing Processes, Lecture Notes, in Mechanical Engineering*. Springer Nature Singapore Pte Ltd. https://doi.org/10.1007/978-981-13-1724-8_6.
14. Subburam, V., Ramesh, S., Mohan Kumar, P. N., & Srinivasan, A. (2018). Performance optimization of electrochemical micromachining of micro-holes on inconel 625 alloy. *International Journal of Precision Technology*, 8(1), 66–84.
15. Ramesh, S., & Subburam, V. (2019). Electrochemical micromachining of aluminium alloy composite. *Advances in Manufacturing Technology, Lecture notes in Mechanical Engineering*, 309–317. https://doi.org/10.1007/978-981-13-6374-0_36.
16. Hackert-Oschatzchen, M., Lehnert, N., Martin, A., & Schubert, A. (2016). Jet-electrochemical machining of particle reinforced aluminum matrix composites with different neutral electrolytes. *IOP Conference Series: Materials Science and Engineering*, 118, 012036.
17. Subburam, V., Ramesh, S., Arunachalam, R. M., & Thanigaivelan, R. (2013). Effect of acidified electrolyte on the performance of electrochemical micromachining, in Proceedings of the Second International Conference on Advances in Materials Processing and Characterisation (AMPC 2013), vol. II, pp. 799–806.
18. Tang, L., & Yang, S. (2013). Experimental investigation on the electrochemical machining of 00Cr12Ni9Mo4Cu2 material and multi-objective parameters optimization. *International Journal of Advanced Manufacturing Technology*, 67, 2909–2916.
19. Liu, J., Zhu, D., Zhao, L., & Xu, Z. (2015). Experimental investigation on electrochemical machining of γ -TiAl intermetallic, 15th machining innovations conference for aerospace industry. *Procedia CIRP*, 35, 20–24.
20. Ryu, S. H. (2009). Micro fabrication by electrochemical process in citric acid electrolyte. *Journal of Materials Processing Technology*, 209, 2831–2837. <https://doi.org/10.1016/j.jmatprotec.2008.06.044>.
21. Huaiqian, B., Jiawen, X., & Ying, L. (2008). Aviation-oriented micromachining technology—micro-ECM in pure water. *Chinese Journal of Aeronautics*, 21, 455–461.
22. Schulze, H. P., & Schatzing, W. (2013). Influences of different contaminations on the erosive and the electrochemical micro-machining, The Seventeenth CIRP Conference on Electro Physical and Chemical Machining (ISEM), *Procedia CIRP*, vol. 6, pp. 58–63.
23. Suresh, P., Venkatesan, R., Sekar, T., Elango, N., & Sathiyamoorthy, V. (2014). Optimization of intervening variables in micro EDM of SS316L using a genetic algorithm and response-surface methodology, *strojniski vestnik. Journal of Mechanical Engineering*, 60(10), 656–664. <https://doi.org/10.5545/sv-jme.2014.1665>.
24. Sathiyamoorthy, V., Sekar, T., & Elango, N. (2015). Optimization of processing parameters in ECM of die tool steel using nanofluid by multiobjective genetic algorithm, Article ID895696. <https://doi.org/10.1155/2015/895696>.
25. Sathiyamoorthy, V., Sekar, T., Suresh, P., Vijayan, R., & Elango, N. (2015). optimization of processing parameters in electrochemical machining of AISI 202 using response surface methodology. *Journal of Engineering Science and Technology*, 10(6), 780–789.
26. Krishnan, R., Duraisamy, S., Palanisamy, P., & Veeramani, A. (2018). Optimization of the machining parameters in the electrochemical micro-machining of nickel. *Materials and technology*, 52(3), 253–258.
27. Wang, M., Shang, Y., He, K., Xuefeng, X., & Chen, G. (2019). Optimization of nozzle inclination and process parameters in air-shielding electrochemical micromachining. *Micromachines*, 10, 846. <https://doi.org/10.3390/mi10120846>.

28. Leese, R., & Ivanov, A. (2018). Electrochemical micromachining: Review of factors affecting the process applicability in micro-manufacturing. *Proceedings of the Institution of Mechanical Engineers, Part B: Journal of Engineering Manufacture*, 232(2) 195–207. (sagepub.co.uk/journalsPermissions.nav). <https://doi.org/10.1177/0954405416640172>.
29. Deng, J. (1989). Introduction to grey theory. *Journal of Grey Systems*, 1(1), 1–2.
30. Bhattacharyya, B., Munda, J., & Malapati, M. (2004). Advancement in electrochemical micro-machining. *International Journal of Machine Tools and Manufacture*, 44(15), 1577–1589.
31. Bilgi, D. S., Jain, V. K., Shekhar, R., et al. (2007). Hole quality and inter electrode gap dynamics during pulse current electrochemical deep hole drilling. *The International Journal of Advanced Manufacturing Technology*, 34(1–2), 79–95.
32. Ayyappan, S., & Sivakumar, K. (2015). Investigation of electrochemical machining characteristics of 20MnCr5 alloy steel using potassium dichromate mixed aqueous NaCl electrolyte and optimization of process parameters. *Proceedings of the Institution of Mechanical Engineers, Part B: Journal of Engineering Manufacture*, 229, 1984–1996.
33. Ghoshal, B., & Bhattacharyya, B. (2013). Micro electrochemical sinking and milling method for generation of micro features. *Proceedings of the Institution of Mechanical Engineers, Part B: Journal of Engineering Manufacture*, 227(11), 1651–1663.

Artificial Fish Swarm Algorithm Driven Optimization for Copper-Nano Particles Suspended Sodium Nitrate Electrolyte Enabled ECM on Die Tool Steel



T. Sekar, V. Sathiyamoorthy, K. Muthusamy, A. Sivakumar,
and S. Balamurugan

1 Introduction

In recent days, the usage of Electrochemical Machining Process (ECM) is higher for machining of poor machinable materials such as Superalloys, High Carbon High Chromium Die Tool Steel, Titanium alloys, Duplex Stainless Steel, Molybdenum alloys, etc. due to the non-contact mechanism employed. So, the formation of machining stress, thermal stress, micro-cracks, etc. is avoided. These materials are playing key roles in Industries like Aerospace, Automobile, Gas Turbine, Medical, and Agriculture. The anodic electrochemical dissolution process of the anode-work

T. Sekar (✉)

Department of Mechanical Engineering, Government College of Technology, Coimbatore, Tamil Nadu, India

e-mail: drtsekar76@gmail.com

V. Sathiyamoorthy

Department of Mechanical Engineering, KSRM College of Engineering, Kadapa, Andhra Pradesh, India

e-mail: sathiyamoorthy01@gmail.com

K. Muthusamy

Department of Mechanical & Mechatronics Engineering, UCSI University, Kuala Lumpur, Malaysia

e-mail: kanesan@ucsiuniversity.edu.my

A. Sivakumar

Department of Mechanical Engineering, Varuvan Vadivelan Institute of Technology, Dharmapuri, Tamil Nadu, India

e-mail: sirarira@gmail.com

S. Balamurugan

Department of Mechanical Engineering, Mahendra College of Engineering, Salem, Tamil Nadu, India

e-mail: sbalmu@yahoo.com

© The Author(s), under exclusive license to Springer Nature Switzerland AG 2021

K. Palanikumar et al. (eds.), *Futuristic Trends in Intelligent Manufacturing*,

Materials Forming, Machining and Tribology,

https://doi.org/10.1007/978-3-030-70009-6_5

piece which is controlled helps to remove the excess material from the workpiece based on Faraday's laws. Generally, the electrically conductive materials are to be acted as a cathode in ECM. This study aims to examine the impact of Cu nanoparticles suspended electrolyte on the ECM of High Carbon High Chromium die tool steel (HCHCr). The chosen objectives are namely Material Removal Rate (MRR) and average surface roughness (Ra) with the independent machining parameters, flow-rate of electrolyte, voltage applied, and tool feed-rate. The 15% plain Sodium Nitrate aqua electrolyte and Copper nanoparticles suspended Sodium Nitrate aqua electrolyte were selected for machining [1]. The HCHCr die tool steel is mostly utilized in automobile industries for making dies. The measured hardness value in the Rockwell 'C' scale is 67 HRc, which is highly tedious to the machine by conventional machining process. The primary reason for using Copper nanoparticles in ECM is to penetrate the passive layer and ensures the current density at the machining zone of Inter Electrode Gap (IEG) for improving the performance of ECM. The formation of the passive layer is quite common when Nitrate based aqua solution is used for ECM and it prevents transferring energy from the cathode resulting in a reduction of machining rate, so it causes the spikes on the machined surface. The basic advantage of Nano-particles behaves differently when compared to Bulk materials if used the same composition [2, 3]. The properties of Nano-particles depend on their size, geometry, and working environment. Copper is generally preferred as cathode-tool material for ECM due to its higher electrical conductivity [4–9]. Full factorial experiments were designed to conduct 54 experiments i.e., 3 factors with three levels each, so 27 experiments with Copper nanoparticles suspended aqua electrolyte and using plain Sodium Nitrate aqua electrolyte solution. The parameters were optimized using the Artificial Fish Swarm Algorithm (AFS).

2 Copper Metal Nano-particles Analysis

The commercially purchased Copper nanoparticles size and surface morphology were analyzed by Scanning Electron Microscope (SEM) for ensuring the particles should be in nano size [10–13]. Its structural characterization was analyzed by the X-Ray Diffraction as shown in Fig. 1 [14]. The XRD results revealed that three-peak at 2θ values of 43.7, 51.1, and 73.4 degrees corresponding to (1 1 1), (2 0 0) and (2 2 0) planes of Copper. The received particles are having an FCC structure and using the Debye-Scherrer equation, the average size of the particles found to be 30 nm [15]. Besides, the size of the Copper metal Nano-particles could be ensured by 5 SEM tests with multiple magnifications as shown in Fig. 2.

The Copper nanoparticle average size is 34 nm and differed by 11.76% from XRD results. It is concluded that the average particle size of Copper nanoparticle is in the range of 30–34 nm. Based on the trial experiments, it was observed that the macro-sized particles clog the passage of the electrolyte flow results in poor performance of ECM. This research work was conducted by using Copper metal nanoparticles of 40 gm. The conductivity of electrolytes acts as a key role in getting better MRR and Ra.

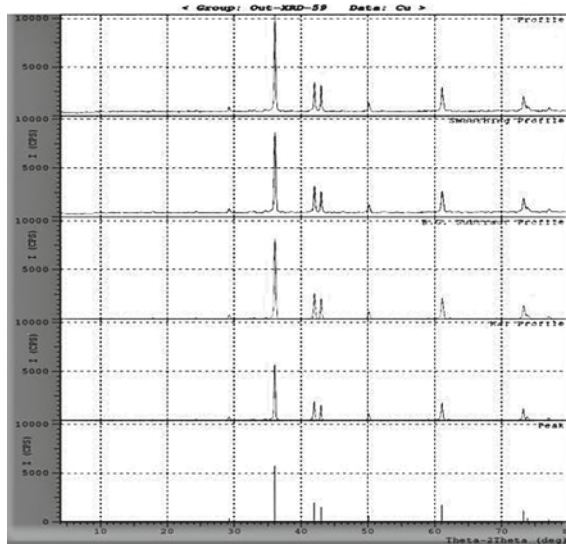


Fig. 1 Copper metal nano-particles X-ray diffraction results

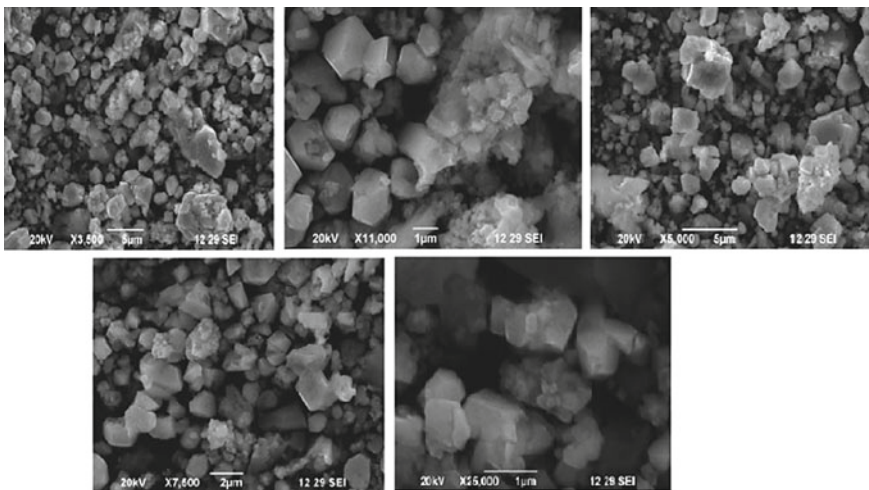


Fig. 2 SEM results with different magnifications

The uniform current density across the IEG improves the machining performance with a better surface finish [1, 16]. A Deluxe water test kit—Model 191E, as shown in Fig. 3, has been used to analyze the electrolyte properties in terms of pH value, electrical conductivity, electrolyte temperature, and total dissolved solids.

The obtained properties of plain Sodium Nitrate aqua electrolyte and Copper nanoparticles suspended Sodium Nitrate aqua electrolyte are presented in Table 1.

Fig. 3 Deluxe water test kit-model 191 E



Table 1 Properties of electrolytes

SI.No.	Electrolyte properties	Plain aqua sodium nitrate	Copper metal nano-particles suspended aqua Sodium Nitrate
1	pH	9.30	9.76
2	Electrical conductivity (mS)	17.34	18.64
3	TDS (ppt)	15.92	17.10
4	Turbidity (NTU)	0	0

3 Experimentation

3.1 Machining Setup

Figure 4 shows the complete machining setup with machining cell, epoxy coated tank, panel box for tooling control, pressure gauge, and flow meter with two-digit accuracy. D.C Servo Motor has been employed to give the vertical feed to the tool. The electrolytes were pumped by a centrifugal pump and pass through the cathode copper tool. When the control unit is ‘ON’, the ionization took place at the electrolyte and transfers the energy. The shape of the tool is generally the negative mirror image of the required shape. The anode-workpiece and cathode-tool were separated by a small gap (0.1–0.5 mm as IEG), hence the electrochemical machining was done at the IEG. The IEG was initially set at small values and the process is trying to keep it constant. The short-circuit problems are prevented if the tool feed rate is equivalent to the material dissolution rate [17]. For this experimentation, an IEG of 0.5 mm was initially set, and continuously monitoring the ampere rating values. The ampere rating abruptly varied if the dissolution rate of material not in uniform, Hence, adjust the IEG manually for obtaining better performance of ECM. France makes a Sartorius Weighing machine with 1 mg accuracy was utilized to measure



Fig. 4 Complete setup for ECM

the loss of weight of the machined specimen, the experiments were conducted for three minutes without interrupting and measured the MRR in mm^3/min . A Surf-test device was used to measure the surface roughness values at different locations of the machined workpiece. The average of three values was taken as Ra values of the workpiece machined. The tool is shown in Fig. 5.

It was made of Copper and the physical geometry is a Circular pattern with a straight jet [18, 19]. It has nine-hole each with a 1.8 mm diameter for allowing the electrolyte flow. The outer diameter of the tool is 25 mm and the sidewall thickness of 3 mm which ensures the uniform distribution of electrolyte at IEG [20].

Fig. 5 Circular pattern with straight jet tool



Table 2 HCHCr die tool steel

Element	C	Mn	SI	S	P	Cr	Fe
wt%	1.936	0.27	0.48	0.089	0.044	11.84	85.34

Table 3 Levels of machining parameters

Influencing parameters	Symbol	Levels		
		-1	0	+1
Electrolyte flow rate (lpm)	Q	8	10	12
Voltage (V)	V	12	15	18
Feed rate (mm/min)	F	0.1	0.32	0.54

3.2 Characteristics of the Selected Workpiece Material

The HCHCr die tool steel is one of the most preferred tool materials for die-making in Automobile Industries. The die-making process needs more time and cost than that of conventional machining and hence, unconventional machining i.e., an ECM is chosen for making the cavity with an approximate degree of accuracy. The final shape of dies will have been trimmed by the wire-cut EDM process [21]. The composition of chemicals in HCHCr die tool steel is shown in Table 2.

3.3 Design of Experiments

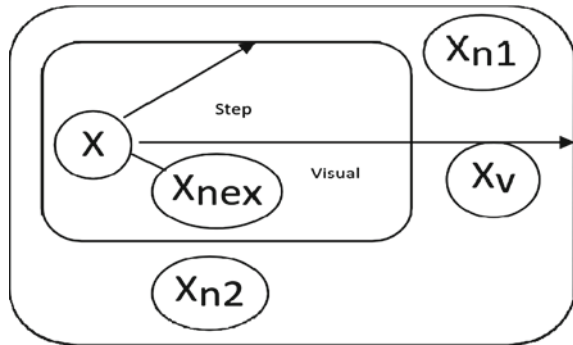
The levels of the selected machining parameters are given in Table 3 to establish the relationship between them. The parameters selected are namely flow rate of electrolyte (lpm), voltage applied (V), and feed rate of tool (mm/min).

Analysis of Variance (ANOVA) test was performed to understand the impact of the parameters selected on the MRR and Ra. Basic objective of study is to enhance the performance by achieving the maximum MRR and minimum Ra. In practically, it is highly impossible to achieve the objectives concurrently. In contradiction, the maximum MRR affects the surface finish and vice versa. So, it is aimed to achieve the objective without compromising the working conditions [22]. The data are significant if the P-values are achieved at lower values.

4 Optimization Using Artificial Fish-Swarm Algorithm

Artificial Fish-Swarm Algorithm (AFSA) is a multi-objective algorithm to optimize the ECM influencing parameters to obtained better MRR and SR [23–25]. AFSA

Fig. 6 External perception of artificial fish-swarm algorithm



performs better in getting optimum results, especially in ECM. Fish and their social behavior inspired them to develop the optimization algorithm. Fish always keep maintaining their colonies through their intelligence behaviors. Intelligent behaviors of fish can be observed while searching for foods, communication networks, responding to dangers, and prevents from dangers. Convergence speed, flexibility, and results' accuracy are the major algorithm benefits. Additionally, Artificial Fish (AF) is a fictional object of true fish that utilized to conduct the analysis and could be understood by using animal ecology knowledge. The AF recognizes external perception through its vision as shown in Fig. 6.

The algorithm is given below.

Pseudo-code of Fish Swarm Intelligent Algorithm:

Step 1: Initialize $X = (x_1, x_2, \dots, x_n)$ and $X_v = (x_{v1}, x_{v2}, \dots, x_{vn})$, subsequently this process can be stated as follows:

$$x_i^y = x_i + \text{Visual.rand}(), \quad i \in (0, n) \tag{1}$$

$$X_{\text{next}} = X + (X_v - X) / (|X_v - X|) \cdot \text{Step.rand}(). \tag{2}$$

where “xi” is the optimizing variable, “rand ()” creates random numbers between zero and 1, “n” is the number of variables and “Step” is length of the step. The AF model contains two parts such as variables and functions. The variables are: “X” represents position of the AF, while “Step” represents moving length of the step. “Visual” represents the visual distance, while “δ” represents the crowd factor ($0 < \delta < 1$).

Step 2: Random behavior: It is a behavior of fish in search of food. In general, the fish identifies the availability of food concentration in water through vision or sense and then subsequently selects the tendency. Behavior depiction state:

Let “Xi” be the AF and select a state “Xj” randomly in its visual distance,

“Y” is the food concentration, which otherwise known as value of the objective function, the greater Visual which AF easily finds the global extreme values and converges.

$$X_j = X_i + \text{Visual.rand} () \quad (3)$$

If $Y_i < Y_j$ in the maximum problem, it moves forward a step in the direction.

$$X_i^{(t+1)} = X_i^{(t)} + \left(X_j - X_i^{(t)} \right) / \left| X_j - X_i^{(t)} \right| \cdot \text{Step.rand} () \quad (4)$$

Otherwise, choose again randomly a state X_j and assess if it fulfills the forward condition. If it can't fulfill after “try_number” times, it moves randomly a step. Once the “try_number” is small in “AF_Prey”, the AF can randomly swim and subsequently it escape from the local extreme field values.

$$X_i^{(t+1)} = X_i^{(t)} + \text{Visual.rand} () \quad (5)$$

Step 3: Searching behavior: The basic living habit-fact of fishes that it assembles together while moving process in water, which assures the existence of the colony and helps to keep away from threats. Description of behavior: Let “ X_i ” be the AF, “ X_c ” be the center-position and “nf” be the companion's number in the neighborhood ($d_{ij} < \text{Visual}$), “n” is a total number of fish. $Y_c > Y_i$ and “nf” ($n < \delta$) represents the companion center has more food (higher fitness function value) and not over-crowded. Hence it moves a step forward to the center of companion, otherwise, the preying behavior.

$$X_i^{(t+1)} = X_i^{(t)} + \left(X_c - X_i^{(t)} \right) / \left| X_c - X_i^{(t)} \right| \cdot \text{Step.rand} () \quad (6)$$

The crowd-factor restricts the scale of swarms, and more only AF cluster in the best-area, that guarantees AF travels optimum in a broad-field.

Algorithm 3 (Movement along with direction)

```

input:  $x^i, l, u, d^i$ 
 $\lambda \sim U[0, 1]$ 
for  $k = 1, \dots, n$  do
  if  $d_k^i > 0$  then
     $y_k^i \leftarrow x_k^i + \lambda \frac{d_k^i}{\|d^i\|} (u_k - x_k^i)$ 
  else
     $y_k^i \leftarrow x_k^i + \lambda \frac{d_k^i}{\|d^i\|} (x_k^i - l_k)$ 
  end if
end for

```

Step 4: Swarming behavior: During the food searching process, if a single fish or school of fishes find the food, partners of the neighborhood very quickly trail to reach the food. Description of behavior: Let “ X_i ” be the AF, and it explores the companion “ X_j ” in the neighborhood ($d_{ij} < \text{Visual}$), which has the greatest “ Y_j ”. If $Y_j > Y_i$ and $n_f (n < \delta)$, it refers to companion “ X_j ” has higher food-concentration and nearby is not over-crowded, it moves forward a step to the companion “ X_j ”.

$$X_i^{(t+1)} = X_i^{(t)} + \left(X_j - X_i^{(t)} \right) / \left| X_j - X_i^{(t)} \right| \cdot \text{Step} \cdot \text{rand}() \quad (7)$$

Else, execute the test for preying behavior.

Step 5: Chasing behavior: Generally random movements carried out in water for searching food/companions in a wider range. Description of behavior: Select a random state in the vision, subsequently move towards to this state, which is the default behavior of “AF Prey”.

$$X_i^{(t+1)} = X_i^{(t)} + \text{Visual} \cdot \text{rand}() \quad (8)$$

Step 6: Leaping behavior: Fish can stop somewhere in the water when the difference in values of objective of food concentration becomes smaller within the iterations, it may fall into local extreme, so change the parameters randomly to still- state for leaping out.

Algorithm : (Leaping behavior)

input: x, l, u

$\text{rand} \sim U\{1, \dots, m\}$

for $k = 1, \dots, n$ **do**

$Y_1 \sim U[0; 1]; Y_2 \sim U[0; 1]$

if $Y_1 > 0.5$ **then**

$y_k = x^{\text{rand}}_k + Y_2 (u_k - x^{\text{rand}}_k)$

else

$y_k = x^{\text{rand}}_k - Y_2 (x^{\text{rand}}_k - l_k)$

end if

end for

5 Results and Discussion

Effect of Parameters at 12 Voltage condition

Figure 7 shows the significant effects of plain Sodium Nitrate and Copper metal Nano-

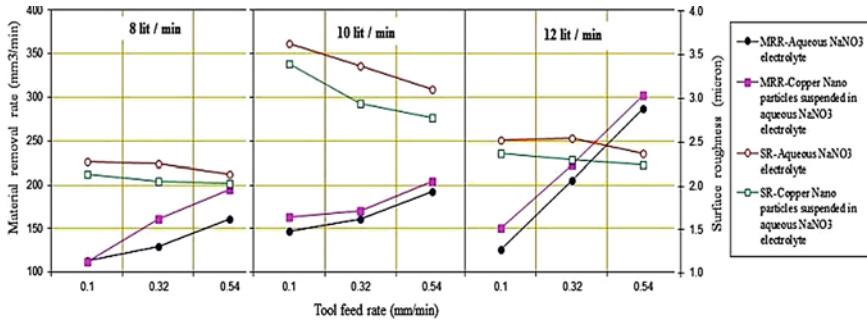


Fig. 7 Effects of copper metal nano-particles on MRR and Ra at 12 V

particles suspended Sodium Nitrate aqua electrolytes on MRR and Ra of HCHCr die tool steel with various flow rates of electrolyte.

The Copper metal Nano-particles suspended Sodium Nitrate aqua electrolyte significantly improves a better MRR and Ra, especially at 12 lpm condition with higher feed rate. The optimum flow rate could ensure the uniform current density in the machining zone results in improved performance. A higher flow rate flushes-out the residues at the IEG and provides the smooth passage for transferring energy. Lower-level discharge rates affect the MRR rather than the Ra which is identified. The higher MRR and lower Ra values were obtained at 0.54 mm/min i.e., at a higher feed rate for all discharge conditions. The MRR of 310.787 mm³/min is achieved using Copper metal Nano-particles suspended Sodium Nitrate aqua electrolyte at 0.54 mm/min feed rate and 12 lit/min electrolyte flow rate and its corresponding Ra value is 2.25 micron. This result is 10.81% higher when compared to plain Sodium Nitrate aqua electrolyte. In general, precipitated metal hydroxides from the anodic dissolution affects the machining performance, because it acts as a barrier for electrical conductivity. In another fact found at 10 lpm that the performance was worsened because of the transition phase from unstable to stable current density at the machining zone.

Effect of Parameters at 15 Voltage

The selected electrolyte effects with various levels at 15 V were presented in Fig. 8

The Fig. 8 showed the evidence for the impacts of discharge rates on the chosen objectives. The way for achieving a higher MRR at 12 lpm as compared to 8 lpm due to improving the current density across the machining gap. However, the copper metal Nano-particles helps to achieve 25% higher MRR than that of a plain electrolyte. Again, it was proved that the formation of the passive layer would have been broken in turns to ensure the uniform current density across the machining area. Even though achieved maximum MRR, but the Ra was 2 micron. The lower surface roughness was achieved as 1.65 micron at 10 lpm condition. This was 25% lower when compared to 12 lpm. So, these process parameters are interdependent and can be selected accordingly i.e., priority dependent.

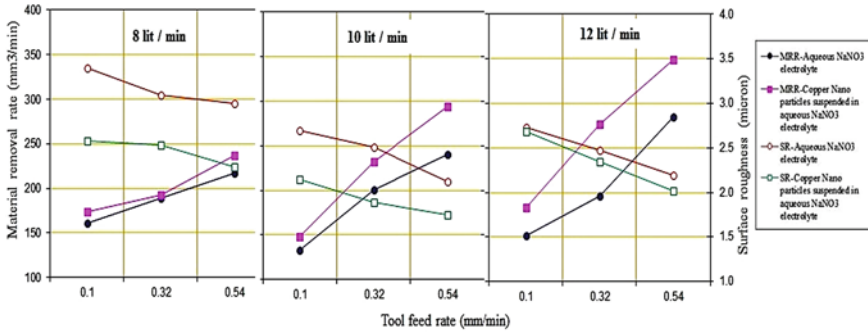


Fig. 8 Effects of copper metal nano-particles on MRR and Ra at 15 V

Effect of Parameters at 18 Voltage

In ECM, the applied voltage increases result in increasing MRR due to improved current density across the IEG. Again, it was proven that higher feed rates give better values of MRR, because the dissolution rate is mainly influenced by the tool feed rate for maintaining the IEG consistently. Gases are emanating during the electrochemical machining, the Copper metal Nano- particles suspended Sodium Nitrate aqua electrolyte avoids the gas bubbles accumulation at the IEG. This can directly avoid the formation of short-circuit in turns to form the spikes.

Figure 9 reveals that the maximum of MRR 347.876 mm³/min has been achieved using Copper metal Nano-particles suspended Sodium Nitrate aqua electrolyte at 0.54 mm/min, 18 V and 12 lpm and the corresponding Ra is 1.6 micron, it is 12% higher MRR and 50% lower surface roughness when compared to the plain electrolyte. The amazing fact was found at 12 V condition, the lower Ra is 1.2 micron and MRR is 300.112 mm³/min, which emphasizes the role of optimization. The energy requirement will get down while selecting the optimum parameters accordingly. Hence, the optimization was done using AFSA and found the optimum values of this research work.

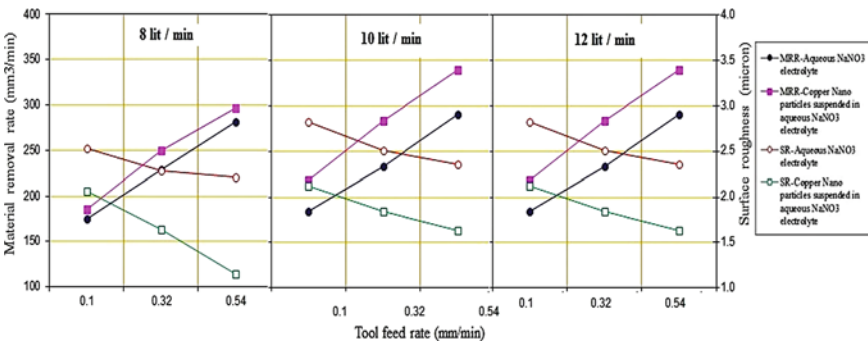


Fig. 9 Effects of copper metal nano-particles on MRR and Ra at 18 V

The AFSA results showed the optimum conditions of the chosen parameters are: 15.75 V, 0.54 mm/min, and 11 lpm in obtaining the better MRR and Ra concurrently.

The ANOVA test has been performed to analyze the significance of chosen influencing parameters for both electrolytes, The R^2 value of plain and Copper metal Nano-particles suspended Sodium Nitrate aqua electrolytes are 94.11% and 97.01% respectively which showed the results are statistically significant.

6 Validation Test

The validity experiment was done for ensuring the consistency of this research work and revealed that the deviation of the result from the AFSA values was found to be 4.8%, hence the adopted strategy for obtaining optimum parameter values is so significant and consistent.

7 Conclusion

Experiments were conducted to examine the impacts of Copper metal Nano-particles suspended Sodium Nitrate aqua electrolyte on electrochemically machined CHCr die tool steel in turn to improve the performance of ECM. The basic objectives of this work were to achieve better MRR and Ra simultaneously without compromising each other values accordingly. The conclusions listed below were drawn based on the results:

- The selected key machining factors namely flow rate of electrolyte, voltage applied, and tool feed rate are interdependent.
- The Copper metal Nano-particle size which was utilized for this research work found to be 30-34 nm by XRD and SEM.
- The Copper metal Nano-particles suspended 15% Sodium Nitrate aqua electrolyte performs better in achieving improved MRR and Ra simultaneously.
- The Copper particles effectively penetrate the generated passive layer at IEG results in improved current density across the machining zone.
- Formation of spikes prevented by ensuring the uniformity of current density by the effective removal of debris at IEG.
- The maximum MRR of 347.876 mm³/min was achieved using Copper metal Nano-particles suspended Sodium Nitrate aqua electrolyte at 0.54 mm/min, 18 V, and 12 lpm and the corresponding Ra is 1.6 micron which is 12% higher in MRR and 50% lower in surface roughness than that of plain electrolyte.
- The achieved lower Ra was 1.2 micron at 0.54 mm/min, 12 V and 12 lpm and the corresponding MRR is 300.112 mm³/min, which emphasizes the need for optimization to minimize the energy requirements as well as to obtain better objective values.

- The Artificial Fish Swarm Algorithm (AFSA) was employed to obtain the optimum values for improving the performance of ECM and the values are found to be 15.75 V, 0.54 mm/min, and 11 lpm.
- The result of the confirmatory experiment revealed that the deviation of the result from the AFSA value was found to be 2.5%, hence the adopted strategy is significant and consistent.

References

1. Shibuya, N., Ito, Y., & Natsu, W. (2012). Electrochemical machining of tungsten carbide alloy micro-pin with sodium nitrate solution. *International Journal of Precision Engineering and Manufacturing*, 13(11), 2075–2078.
2. Chandra, P., Goyal, R. N., Singh, J., Singh, A., Shim, Y. B., & Srivastava, A. (2013). Gold nanoparticles and nano composites in clinical diagnostics using electrochemical methods, hindawi publishing corporation. *Journal of Nanoparticles*, 2013(535901), 12.
3. Sekar, T., Arularasu, M., & Sathiyamoorthy, V. (2016). Investigations on the effects of Nano-fluid in ECM of die steel. Measurement. Elsevier, vol. 83, pp. 38–43.
4. Wong, K., Michael, V., & Castillo, J. (2010). Heat transfer mechanisms and clustering in nanofluids. *Hindawi Publishing Corporation Advances in Mechanical Engineering*, 2010(795478), 9.
5. Thomas, S., & Sobhan, C. B. P. (2011). A review of experimental investigations on thermal phenomena in nanofluids. *Nanoscale Research Letters*, 9(61), 377.
6. Ding, Y., Chen, H., Wang, L., Yang, C. Y., He, Y., Yang, W., et al. (2007). Heat transfer intensification using nanofluids. *KONA Powder and Particle Journal*, 25, 23–38.
7. Kanagasabapathi, N., Balamurugan, K., & Mayilsamy, K. (2012). Wear and thermal conductivity studies on nano copper particle suspended soya bean lubricant. *Journal of Scientific & Industrial Research*, 71(7), 492–495.
8. Theivasanthi, T., & Alagar, M. (2010). X-Ray diffraction studies of copper nanopowder. *Scholars Research Library Archives of Physics Research*, 1(2), 112–117.
9. Theivasanthi, T., & Alagar, M. (2011). Nanosized copper particles by electrolytic synthesis and characterizations. *International Journal of the Physical Sciences*, 6(15), 3662–3671.
10. Li, X., Zhu, D., & Wang, X. (2007). Evaluation on dispersion behavior of the aqueous copper nano-suspensions. *Journal of Colloid and Interface Science*, 310(2), 456–463.
11. Mehta, A., Tantia, D. K., Jha, N. M., & Patel, N. (2012). Heat exchanger using Nanofluid. *International Journal of Advanced Engineering Technology IJAET*, 3(4), 49–54.
12. Pirahmadian, M. H., & Ebrahimi, A. (2012). Theoretical investigation heat transfer mechanisms in nanofluids and the effects of clustering on thermal conductivity. *International Journal of Bioscience, Biochemistry & Bioinformatics*, 2(2), 90–94.
13. Ghadimi, A., Saidur, R., & Metselaar, H. S. C. (2011). A review of nanofluid stability properties and characterization in stationary conditions'. *International Journal of Heat and Mass Transfer*, 54(17–18), 4051–4068.
14. Hascalik, A., & Caydas, U. (2007). A comparative study of surface integrity of Ti-6Al-4 V alloy machined by EDM and AECG. *Journal of Materials Processing Technology*, 190(1-3), 173–180.
15. Kaviarasan, V., Venkatesan, R., & Natarajan, E. (2019). 'Prediction of surface quality and optimization of process parameters in drilling of Delrin using neural network', *Progress in Rubber, Plastics and Recycling Technology*, 35(3).
16. Hall, B. D., Zanchet, D., & Ugarte, D. (2000). Estimating nanoparticle size from diffraction measurements. *Journal of Applied Crystallography*, 33(6), 1335–1341.

17. Kozak, J., Chuchrob, M., Ruszajb, A., & Karbowski, K. (2000). The computer aided simulation of electrochemical process with universal spherical electrodes when machining sCopper lptured surfaces. *Journal of Materials Processing Technology*, 107(1–3), 283–287.
18. Sathiyamoorthy, V., & Sekar, T. (2015). Optimization of processing parameters in ECM of Die tool steel using nano fluid by multi objective genetic algorithm. *The Scientific World Journal*, 895696, 1–6.
19. Yong, L., Yunfei, Z., Guang, Y., & Liangqiang, P. (2003). Localized electrochemical micromachining with gap control. *Sensors and Actuators A*, 108(1–3), 144–148.
20. Pa, P. S. (2013). High-performance micro- electrochemical machining via optoelectronic irradiation and a graded modular tool. *International Journal of Advanced Manufacturing Technology*, 64(1–4), 179–186.
21. Liu, Y., Zhu, D., Zeng, Y., & Yu, H. (2011). Development of microelectrodes for electrochemical micromachining. *International Journal of Advanced Manufacturing Technology*, 55(1–4), 195–203.
22. Jadhav, P. V., Bilgi, D. S., & Harel, A. S. (2011). An experimental investigation into the spike profile obtained during electrochemical hole drilling of blind holes. *International Journal of Engineering Science and Technology (IJEST)*, 3(2), 1682–1692.
23. Natarajan, E., Kaviarasan, V., Lim, W. H., Tiang, S. S., Parasuraman, S., & Elango, S. (2020). Non-dominated sorting modified teaching–learning-based optimization for multi-objective machining of polytetrafluoroethylene (PTFE). *Journal of Intelligent Manufacturing*, 31(4), 911–935. <https://doi.org/10.1007/s10845-019-01486-9>.
24. Suresh, S., Elango, N., Venkatesan, K., Lim, W. H., Palanikumar, K., & Rajesh, S. (2020). Sustainable friction stir spot welding of 6061-T6 aluminium alloy using improved non-dominated sorting teaching learning algorithm. *Journal of Materials Research and Technology*, 9(5), 11650–11674. <https://doi.org/10.1016/j.jmrt.2020.08.043>.
25. Natarajan, E., Kaviarasan, V., Lim, W. H., Tiang, S. S., & Tan, T. H. (2018). Enhanced multi-objective teaching-learning-based optimization for machining of Delrin. *IEEE Access*, 6(1), 1–19.

Comparative Analysis Between Conventional Method Versus Machine Learning Method for Pipeline Condition Prediction



Firdaus Basheer, Mohamed Saleem Nazmudeen, and Fadzliwati Mohiddin

1 Introduction

The world is currently facing industrial revolution 4.0 where digitalization plays an important part in our daily lives. Businesses are racing to start using digitalization to their benefit as it is seen to improve performance and efficiency, leading to cost optimization, which in turn generates more revenues for the company to thrive in today's competitive environment. One area of interest is the application of digitalization for the efficient maintenance of equipment. The maintenance of equipment is crucial for businesses as it eliminates or reduces the number of failures that may occur during production which may disrupt the supply chain.

Maintenance and diagnosis are key to ensure equipment availability and help to optimize operating costs. This is because the total operating expenditures of the plant can exceed by 30% due to equipment maintenance, or fall within the range of 60–75% of the equipment lifecycle cost [1]. The impaired function of machinery that operates outside the design specification may disrupt production yield. On the other hand, equipment maintenance can positively increase the revenue of a company by improving the machine lifetime. With the right maintenance strategy, corrective maintenance can be reduced and maintenance costs can be further reduced through predictive and preventive maintenance strategies [2]. Predictive maintenance is favoured

F. Basheer · M. S. Nazmudeen (✉) · F. Mohiddin
UTB School of Business, Universiti Teknologi Brunei, Jalan Tungku Link, Mukim Gadong A,
BE1410 Bandar Seri Begawan, Brunei
e-mail: mohamed.saleem@utb.edu.bn

F. Basheer
e-mail: firdaus.basheer@gmail.com

F. Mohiddin
e-mail: fadzliwati.mohiddin@utb.edu.bn

due to its ability to predict failure and decrease hands-on tool time required to perform maintenance work in the field, making it an economical and cost-efficient approach.

To date, there has been an increase in the number of ageing assets requiring pipeline facilities. Pipeline maintenance can be complex especially when it involves subsea, underground, or remote locations. There is significant interest in developing fit for purpose maintenance strategy of the pipeline to minimize repair cost and downtime of equipment due to plan or unplanned activities. Pipeline maintenance in subsea, underground, or remote locations incurs high maintenance costs involving logistics arrangement. Under pressure by regulations, safety in managing pipelines is a top priority for any pipeline operator. When a leak suddenly occurs, the response time in managing this repair needs to be as short as possible to minimize impact and exposure.

Several conventional methods for pipeline condition prediction have shown promising outcomes such as reliability analysis, split system approach, standard data structure, Monte Carlo simulation method, and other types of modelling. However, these methods have limitations in terms of accuracy and effectiveness of the methods.

The machine learning algorithm method seems to be the popular choice in this era due to its ability to process real-time information and handle a big volume of data whilst giving instant results on the status of the pipeline condition. Due to this reason, several kinds of research are trying to compare the prediction accuracy of the different machine learning methods.

Most of the studies conducted on the pipeline prediction methods were primarily focusing on accuracy-either on improving the accuracy of the method in question or comparing the accuracy of various types of pipeline prediction methods. None of the work involved cost analysis to evaluate the most economical and cost-efficient pipeline predictive maintenance method. This paper is an extension to our previous publication [3] to examine the existing studies on methods of pipeline condition prediction and compares their areas of focus, the objective of prediction, the types of data collected, and the outcomes. The objective of this literature review is to screen the most effective Machine Learning Methods that currently exist which can be considered for the pipeline operator. This analysis will also be used to conduct a future study on the economic cost of these methods.

1.1 Overview of the Literature Review

In this comparative analysis, 34 articles related to pipeline prediction methods have been referred to. The overview of the pipeline prediction method is represented in Figs. 1, 2 and 3.

The full breakdown of the machine learning algorithm methods considered in this literature review is shown below.

The articles used in this comparative analysis were based on the following considerations:

Pipeline prediction method

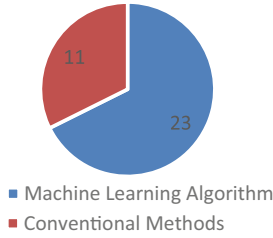


Fig. 1 Pipeline prediction method article breakdown

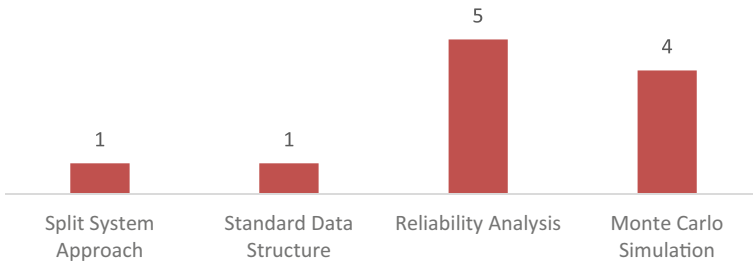


Fig. 2 Conventional methods articles breakdown

Pipeline Prediction using Machine Learning Methods

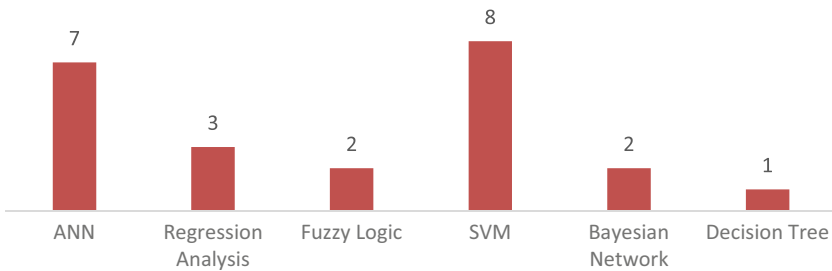


Fig. 3 Machine learning method articles breakdown

- Major above ground, an underground or subsea pipeline that has the same problems such as wall thickness loss, leaks, and etcetera. Major focus is put on subsea pipelines since many factors could affect pipeline integrity.
- Research work should be based on how the methods can be applied to existing and ageing pipelines. Future installation improvements were not included in this literature review.
- Only methods that are commonly used and giving promising results were considered.

1.2 Scope of This Comparative Analysis and Contributions

The main contributions of this paper can be summarized as follows:

Section 2 provides an overview of the motivation for the comparative analysis between conventional methods against machine learning methods. Section 3 justifies the case for predicting pipeline conditions and then outlines the different types of methods that have been developed. A full summary of the prediction methods under this comparative analysis was tabulated in Sect. 4 and Sect. 5 by addressing the problem, objectives of the studies, type of data collected for the methods used in both conventional and machine learning. Section 5 further outlines the comparison between conventional methods and machine learning methods as well as the comparison among the machine learning methods. Section 6 suggested future research challenges in these fields (Fig. 4).

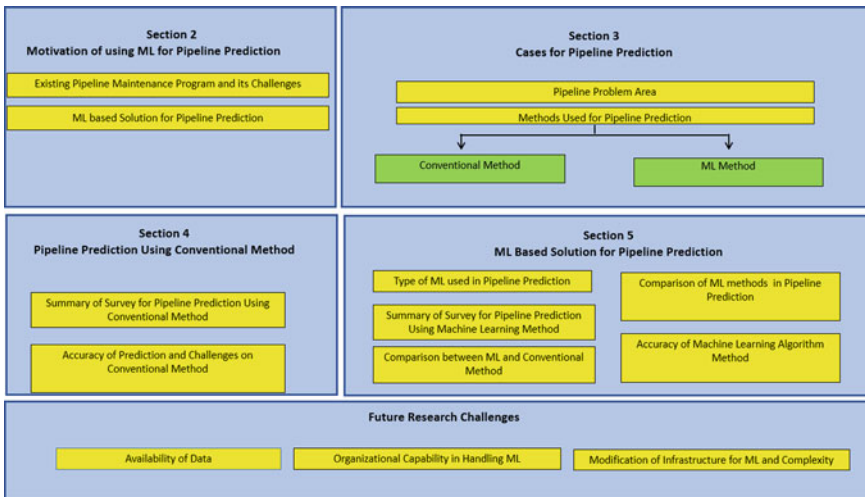


Fig. 4 Taxonomy of comparative analysis between conventional method and machine learning

2 Motivation for Using Machine Learning for Pipeline Prediction

2.1 Existing Pipeline Maintenance Program and Its Challenges

The existing pipeline maintenance program is time-based and mainly derived from reliability analysis using codes and standards published by engineering bodies or associations. The drawbacks of using this method are as follow:

- The existing pipeline maintenance program tends to be too conservative since it is a time-based approach. This increases OPEX cost and minimizes production availability especially if the pipeline involves in-line pigging.
- Most of the time, failure could happen in between the planned inspection (or maintenance) leading to unplanned shutdown and production interruption.

2.2 Machine Learning Based Solution for Pipeline Prediction

The constant push towards safer pipeline operation driven by legislative requirement has made pipeline operators extra vigilant in maintaining their pipelines. Furthermore, there is also a need for pipeline operator to maximize their revenue by optimizing their production while ensuring safe operation. The latter could potentially be solved through the deployment of machine learning by making use of past data for existing infrastructure or by installing sensors for a new set up. Machine learning could use past data or process existing signals to predict the condition of the pipeline.

3 Cases for Pipeline Prediction

3.1 Pipeline Problem Areas

Most of the problem areas widely focused on pipeline failures due to corrosion and creep [4]. Sun et al., have studied the effect of preventive maintenance (PM) on pipeline system reliability and how it could contribute to a cost-effective maintenance strategy. They emphasized that pipelines are a complex system and imperfect repairs would need to be considered since the majority of the maintenance program of the assets are time-based preventive maintenance methods (TBPM). However, it has to be noted that in their research work, they claimed that for a pipeline with different preventive maintenance actions carried out, TBPM was not suitable for effective pipeline reliability and system configuration model. They proposed that

imperfect maintenance modelling needs to use a similar method as an improvement factor method so that the changes in the pipeline reliability requires good prediction accuracy to make an optimal decision. They also highlighted the existing models/methodologies are not able to meet the industrial need to improve pipeline reliability nor does it able to consider multiple imperfect repairs on a pipeline since the result of the PM only requires sectional replacement of the pipeline. Therefore, they proposed to address this issue by considering the split system approach (SSA) method to predict pipeline reliability consisting of multiple imperfect PM actions resulting from both TBPM and RBPM strategy. They have developed a model for the effects of PM activities from pipeline repair history and inspection results using reliability function [4].

Alison et al. have conducted a study to understand the typical failure modes and mechanisms for underground infrastructure systems that are used in a municipal water system. Their research has also considered the pipe material's advantages and disadvantages as well as to understand all the parameters affecting water pipe infrastructure systems [5]. The standard data structure was established based on physical or structural parameters, operational or functional parameters, and environmental parameters to predict the remaining life of water pipes. The correlation between different pipe material types and their life cycle failure modes and mechanisms is crucial to define the key parameters affecting water pipelines [5].

Ahammed [6] has used deterministic approaches to addresses the problem of estimating the remaining strength of corroded pipelines that are free of any uncertainty. In his research, he carried out the remaining life assessment of the corroded pipeline with rapid corrosion growth. The information obtained was used to predict safe operating pressure of the pipeline at any time and hence, both an economic inspection plan as well as corrective maintenance can be scheduled effectively [6].

Hallen et al. have proposed structural reliability analysis in their research work to evaluate the integrity of in-service corroded pipelines in Mexico using high-resolution magnetic flux leakage (MFL) or ultrasonic technology-based (UT) inline inspection tool [7].

Pandey has used reliability analysis to deal with uncertainties in pipeline maintenance decision-making. He also took into account the future preventive maintenance inspection frequency and the estimated costs involved in pipeline condition assessment. The primary objective of his research was to come up with an optimal pipeline inspection frequency. The repair strategy would then be based on a quantitative probabilistic approach to secure the pipeline's reliability before reaching its end of life [8].

Mahmoodian and Li have explored the use of a reliability-based methodology and stochastic model to assess and determine key factors that can affect the residual strength of corroded steel pipes. They mentioned that a pipeline failure will occur when its residual strength is below the pipeline operating pressure. The probability of failure as a result of corrosion can be estimated using an analytical time-variant method. This will help to estimate the remaining life of the pipeline which requires maintenance action. For the pipeline with more than one corrosion pit, the assessment was done using the system reliability analysis method. The methodology has enabled the quantitative assessment of pipeline failures and this method can also be used for

other structures that are subject to localized deterioration. The verification of the results was carried out using the Monte Carlo simulation technique [9].

Shuai et al. have conducted a study to define an alternative method to predict burst capacity. The existing conservative methods for burst capacity prediction in the pipeline are costly in terms of maintenance. In their research, Shuai et al. developed a new burst prediction model with good precision for corroded pipelines. Failure probability of corroded pipeline was predicted using Monte Carlo (MC) simulation method. The parameters that have the most influence on corroded pipelines were investigated by analyzing the uncertainties from both parameter and model sensitivity [10].

Shu Xin li et al. have used the cumulative distribution function (CDF) to estimate cumulative probable failure for a pipeline, calculated using the Monte Carlo simulation technique [11].

Ossai et al. have examined the problem of failure probability estimation on corroded pipelines that have limited information. They used the pipeline corrosivity index (PCI) based on the retained pipe-wall thickness at a given time to estimate the failure probability of corroded pipelines. Based on their research, Markov modelling and Monte Carlo simulation have been used in other research for the quantification of the corrosion growth size in a pipeline. Therefore, based on this info, they have used Markov modelling and Monte Carlo simulation to predict the pipeline failure based on different corrosion wastage rates. The exposure time for the pipeline to leak was then estimated using the Weibull probability function [6, 8, 12–14]. They believed the method that they have developed in their research is useful to manage the integrity of ageing or corroded pipeline [15].

Reza et al. research was focusing on dynamic modelling for predicting pipeline performance. The motivation around their research was based on the fact that the majority of other research works were only focusing on static modelling using corrosion rates which were derived from either past inspection data and sometimes based on the subjective judgment from technical experts. Therefore, the main objective of their research work was to come up with a dynamic reliability model to predict pipeline performance. The model that they developed was based on the remaining life assessment of the pipeline by taking into account the rate of internal and external corrosion as well as other factors that can affect the system performance. Qualitative input was used in their initiatives such as experts' judgment and assumptions to fill the data gap. Hence, to overcome all of the uncertainties stated, they believed the Bayesian Network would be a suitable method for a dynamic probabilistic model. In their research, they have studied the causality of each variable that could result in the pipeline failures and the outcome was demonstrated in the network diagram that they have developed. Based on their study from the inspection records of several years, corrosion failure is a time-dependent process [16].

Amit et al. addressed the challenges of locating the internal corrosion damage in hundred miles long of oil and gas pipelines. Despite advances in inline inspection technology, the pipelines still have large uncertainties due to their pre-existing conditions, corrosion resistance, elevation data, and test measurement. They developed a method based on probabilistic methodology and using Bayesian Network to predict the damage location along the pipelines. The prediction was based on the pipeline

internal corrosion direct assessment (ICDA). The model is dependent on characteristics such as flow, corrosion rate, and past inspection data. The accuracy could also be affected as a result of uncertainties such as elevation data, pipeline geometry, and flow characteristics [17].

3.2 *Methods Used for Pipeline Prediction*

3.2.1 Conventional Method

The conventional methods for pipeline prediction are typically derived from reliability analysis, standards, and codes published by a reputable organization, risk-based approach, and other deterministic or probabilistic assessment methods. The methods developed were based on calculations from the available codes and standards. The codes were reviewed periodically and improvement is normally made based on research activity, industry experience, and technical professionals review. The conventional methods require on the spot data, either online measuring system or through inspection exercise to deduce the existing condition of the piping.

Among the conventional methods that have been considered in this literature review is the split system approach, Standard Data Structure approach, Reliability analysis approach. There are many methods developed based on reliability analysis which includes program based methods and also the traditional calculation method. Examples of program-based Reliability analysis included in this literature review are the Stochastic Method, Monte Carlo Simulation, and Bayesian Network methods.

3.2.2 Machine Learning Method

Machine learning, in essence, is an algorithm based program derived from historical data. The mathematical model is built directly from data through the theory of statistics without the need (or minimal) to have a predefined mathematical model. The developed model then study the pattern and derived inferences from the inputs introduced. Once the developed model is optimized, it can then make an accurate prediction for the future state, or to gain knowledge of the existing state, or both. There are three types of Machine Learning algorithm (MLA) namely, supervised MLA, unsupervised MLA, and semi-supervised MLA [18].

4 Pipeline Prediction Using Conventional Method

4.1 Summary of Survey for Pipeline Prediction Using Conventional Methods

See Table 1.

4.2 Accuracy of Prediction and Challenges on Conventional Method

Despite the conventional methods above have met the accuracy of the prediction, however, the methods were limited to specific parameter rather than a holistic approach. Furthermore, the methods are less flexible to changes since the prediction output is based on the predefined parameter, and hence, any changes outside the predefined parameter that is believed that could affect the pipeline condition will not be able to contribute to the prediction. This has led to the improvement in the conventional methods less impactful for pipeline predictive maintenance. As a result, the conservative factor would still need to be maintained in the calculation to ensure the risk of reducing the preventative maintenance interval of the pipeline is mitigated.

5 Machine Learning (ML) Based Solution for Pipeline Prediction

5.1 Type of ML Prediction (Classification/Regression)

The most common type of machine learning used in pipeline prediction is regression and classification methods. The output of prediction for regression is a numerical value derived from the input data set. Whereas for classification method, it uses a class value for the prediction. Both types of Machine Learning prediction above are supervised Machine Learning as it requires data sets to be fed and trained before it can analyze and predict the new input data (Table 2).

5.2 Comparison Between Machine Learning and Conventional Methods

The summary of the comparison between Machine Learning and Conventional methods were tabulated in Table 3. Based on the tabulated summary, the pipeline

Table 1 Literature review summary

Method	Paper	Problem addressed	Objective	Data collected	Outcome
Split system approach	[4]	The effect of different PM actions on the system reliability and configuration cannot be modelled using Time Based Preventive Maintenance (TBPM)	To predict the reliability of pipelines with multiple imperfect preventive maintenance actions	Pipeline repair history	The prediction model can accurately predict the pipeline condition despite multiple PM actions carried out on the pipeline
Standard data structure	[5]	Many parameters such as physical factors could affect the infrastructure of the pipeline. The effects of these parameters may lead to failure	To classify the criticality of the pipeline and identify the minimum parameter required to determine and predict the condition of the pipeline. The number of parameters used varied based on the criticality	Pipeline failure mode compilation based on literature review and pipe failure consequences	Standard data structures were developed based on 100 parameters identified which could affect the condition and performance of the water pipeline
Stochastic model and Monte Carlo simulation	[9]	Threats due to metal corrosion in ageing oil and gas pipelines	To enable quantitative assessment of pipeline failures that can also be used for other structure that is experiencing localized deterioration	Pipeline data	The effect of the operating pressure of the pipeline is more significant compared to the effect of yield strength of the pipe materials. The proposed time-variant reliability method can be used to predict the service life of the pipeline system

(continued)

Table 1 (continued)

Method	Paper	Problem addressed	Objective	Data collected	Outcome
Reliability analysis	[6]	Pipeline with live corrosion defects	To predict the remaining life of corroded pipelines at any point in time	Depth of metal loss and axial length	The calculation links the reliability index, failure variables that can affect the overall pipeline reliability
Reliability analysis	[19]	The methods used in B31G is only for the estimation of the remaining strength of the pipeline at that particular instance. The method did not forecast the future remaining strength of the pipeline	Modify the B31G method to develop a model that can predict the future remaining strength of the pipeline	Past inspection results were used along with the pipeline data	Based on the model developed, the allowable pressures of the pipeline were affected significantly by the exposure period. The values of the corrosion parameters also significantly affected the remaining strength
Structural Reliability analysis	[7]	The significant effort required to assess the corroded pipeline using data obtained from high-resolution magnetic flux leakage (MFL) or ultrasonic technology-based (UT) ILI tools also known as 'smart pigs'	To formulate operating and maintenance strategies for the safe operation of this pipeline over its targeted service life	Inspection data	The maintenance strategies developed using this method can be cost-effective. The prediction of pipeline failures is referencing on reliability level target value

(continued)

Table 1 (continued)

Method	Paper	Problem addressed	Objective	Data collected	Outcome
Monte Carlo simulation	[11]	The traditional design code is not designed to predict pipeline failure	To employ the Cumulative Distribution Function (CDF) as a probabilistic model to predict underground pipeline failure	Pipeline data	Cumulative Distribution Failure (CDF) outweight Probability Density Function (PDF) for pipeline failure prediction. However, further effort is required for more precise predictions
Monte Carlo simulation	[10]	Various models that were used to predict the burst capacity of corroded pipelines are conservative and cause unnecessary repair costs	To develop a more precise burst prediction model based on Monte Carlo (MC) simulation method	Pipeline data	The proposed model shows good precision when compared with other commonly used codes
Probabilistic method	[8]	Corrosion assessment on oil and gas underground pipelines are inaccessible for direct inspection	To determine the optimal inspection frequency of the pipelines	Inspection data	Based on the results of the prediction, the method was able to come up with an optimal inspection frequency, thus, minimizing the overall cost of pipeline maintenance

(continued)

Table 1 (continued)

Method	Paper	Problem addressed	Objective	Data collected	Outcome
Dynamic modelling using Bayesian networks	[16]	Most of the pipeline reliability studies only focused on static models based on corrosion rates, past inspection reports, or judgments from technical expertise to predict pipeline failure	To propose a preliminary dynamic reliability model for the pipeline predictive maintenance program	Operational data and inspection results	Bayesian networks were seen as effective for analyzing the corroded pipeline performance. The dynamic model produced a realistic result to predict the remaining life of the pipeline based on the current and historical pipeline data
Reliability deterministic prediction	[20]	The uncertainties present within metal-loss data reduce the accuracy of pipeline remaining life prediction	To find the capacity equation that is capable of predicting the future growth of defects by altering the DNV-RP-F101 safety equation	Metal Loss Information;	The method could improve the estimation of pipeline remaining life by anticipating future growth of corrosion defects
Markov Modelling and Monte Carlo simulation	[15]	Accuracy of failure probability estimation of corroded pipelines that have limited information	To predict pipeline failure based on Pipeline Corrosivity Index (PCI) along with Monte Carlo simulation, Markov modelling, and Weibull function	Inline inspection data of the X52 grade onshore transmission pipeline was used	The accuracy of the pipeline probability failure prediction can be improved by considering small leakage, burst, and rupture information

Table 2. Summary of survey for pipeline prediction using machine learning method

Method	Paper	Problem addressed	Objective	Data Collected	Outcome
Bayesian network	[17]	Locating internal corrosion damage in long oil and gas pipelines is challenging especially when large uncertainties exist from the pipeline	To predict the damage due to corrosion along the pipelines based on the inspection data	Pipeline Inspection data	The developed model was able to focus on locations with a high probability of damage
Artificial neural network	[21]	Unable to prioritize inspection plan for rapidly deteriorating sewer system that is 2200 miles long	To develop a pipeline condition prediction model to identify pipelines at risk of failure so that inspections can be prioritized	Sewer System Evaluation Survey	The neural network is capable of learning the deterioration trends
Artificial neural network	[22]	Most of the pipeline prediction models are developed based on the corrosion factor only	To develop a pipeline prediction model based on several factors besides corrosion	Pipeline inspection data	ANN provides better results compare to regression analysis. The model could help to ease pipeline operators to prioritize the inspection based on the assessment and prediction outcome

(continued)

Table 2 (continued)

Method	Paper	Problem addressed	Objective	Data Collected	Outcome
Artificial neural network	[23]	The deviation between the calculated corrosion rate using the internal corrosion prediction model (ICPM) and realistic corrosion rates can be large when the internal environmental parameters of the inspection segments are not considered	To develop an effective method for corrosion rate prediction on the wet gas pipeline	Pipeline detail; The internal corrosion inspection data	Based on the test results the model developed was effective with good accuracy obtained for the corrosion rate prediction against inspection data
Artificial neural network	[24]	To address the challenges in predicting corrosion rate on long natural gas pipeline	To predict the corrosion rate of the long-distance pipeline using a backpropagation neural network based on pipeline mileage, elevation difference, pipe inclination, pressure, and Reynolds number	Pipeline data	BP neural network model can be used to predict natural gas pipelines in different corrosive environments
Artificial neural network	[25]	The correlation between predicted and actual failure rates of pipeline based on regression analysis is relatively low (Righetti 2001)	To improve failure predictions by comparing the neural network method against previous modelling STPM (Shifted Time Power Model) and STEM (Shifted Time Exponential Model)	Historical data	The neural network outperforms the statistical models. However, some improvement is required due to databases that are relatively large and noisy

(continued)

Table 2 (continued)

Method	Paper	Problem addressed	Objective	Data Collected	Outcome
Artificial neural network/regression analysis	[26]	Pipeline inspection is mainly costly especially inline inspection to predict pipeline anomalies. The developed condition assessment or failure prediction models are subjective and only deal with one failure case	To develop a more objective pipeline prediction method that can predict pipeline failure using ANN and Regression model and to study the performance between the two	38 years of spillage data from CONCAWE 2010 report	The developed model using ANN and Regression analysis were validated and the results obtained were satisfactory. However, ANN outperforms the regression model
Artificial neural network and SVM	[27]	The quasi-static analysis used a pressure gauge sensor to detect the leak. The sensors do not give the required sensitivity of 0.001pa	To develop two quasi-static models by using a differential pressure sensor. It is believed the differential pressure sensor can achieve an accuracy of up to 0.001pa. The models were developed based on ANN and SVM. The results of both models were then compared	An experimental test bench was set up and data was generated through simulation using EPANET and MATLAB software	The SVM model performed better in the noisy environment compared to the ANN model. However, the model developed was only for single leak location prediction

(continued)

Table 2 (continued)

Method	Paper	Problem addressed	Objective	Data Collected	Outcome
Regression analysis/artificial neural network and Decision Tree	[28]	No robust methods present to assess the condition of unriggible pipelines	To develop unriggible pipeline prediction method to identify the critical factors affecting the condition, to design condition forecasting models, and develop expected deterioration curves	Historical inspection data divided into physical, external, and operational data	The models could be used to assess the pipeline condition efficiently. Based on the results, the Decision tree using M5 Ptree provided the most accurate forecasting models followed by ANN and Regression analysis
Regression analysis	[29]	Currently, there is no standard assessment scale to predict the condition of the pipelines and the majority of the developed models only deal with corrosion	The main objective of the study is to develop condition deterioration curves that can correlate with the age of the pipeline which is useful for prediction	Historical inspection data collected from three different pipelines in Qatar	The model developed can help in decision-making and assessing the pipeline condition so that the inspection plan can be prioritized accordingly
SVM	[30]	Reactive leakage identification (only able to detect after a leak occurred)	To set up a pre-warning system taking into account unknown event happening next to the pipeline	Data collected from vibration sensors installed along the pipeline	The system can detect and recognize abnormal events happening in the vicinity of the pipeline with a good recognition rate
SVM	[31]	Detection of a decrease in pressure as a result of Negative Pressure Wave (NPW)	Use SVM based classifier to derive NPW through pressure curve so that leak can be detected	Historical data from 1500 pressure curves containing 500 NPWs	The model can successfully detect NPW and detect leaks with little computation

(continued)

Table 2 (continued)

Method	Paper	Problem addressed	Objective	Data Collected	Outcome
SVM	[32]	The NPW has poor performance in detecting small leaks as the wave generated by small leakages is too weak to be diagnosed which could also be mistakenly interpreted as noise	Enlargement of weak signals caused by small leakage through the chaotic analysis method. The classification would be carried out using LS-SVM	Pipeline inner pressure data was measured by the sensors with a frequency of 5000 Hz	The methods proposed were able to detect small leakage with good performance outcomes
SVM	[33]	Monitoring status of pipeline structure based on the failure intensity and to determine the link between failure rates and materials properties	To estimate the failure rate for the pipeline in water distribution networks and to determine the relationship between failure rate effective factors	Failure data records from 2006-2012 (only failures in normal operating conditions have been considered)	The combination of clustering analysis and LS-SVM methods yields a good result in estimating the failure rate of the pipeline in question
SVM	[34]	Most leak detection method has limitation for a small number of samples. Though SVM had been widely used in pipeline prediction research, the hyper-parameters of SVM are determined through experience	To use Particle Swarm Optimization (PSO) to search the optimal hyper-parameter and to study the effectiveness of these methods in detecting multiple leaks in a pipeline	The data of Brunone friction transient models of pipeline	The proposed method had successfully met the objectives of detecting multiple leaks. The predicted values were closed to transient model values

(continued)

Table 2 (continued)

Method	Paper	Problem addressed	Objective	Data Collected	Outcome
SVM	[35]	Pipeline inspection happens periodically. While the cost of performing NDT is costly, it also requires an extensive amount of time from the measurement been deployed to getting the results	To deploy a permanently installed NDT system using Long Range Ultrasonic transducer (LRUT) with real-time processing capability for condition monitoring and to predict pipeline failures. The data obtained were processed using the Euclidean-SVM approach	Data collected from the LRUT simulation rig based on original Dataset (without noise) and dataset with 5/2/0.01/1/10 dB SNR	The proposed method was able to provide continuous monitoring for pipeline conditions. Euclidean-SVM approach provided good classification performance without the need to implement a combination of kernel function and parameters
SVM	[36]	Implementation of a pigging system is expensive and it measures the pipeline condition only at the instance it is deployed	To propose a continuous monitoring system using sensors strategically placed along the pipeline. The prediction will be done using SVM from the signal process by the Discrete Wavelet Transform (DWT)	Data is obtained from the ultrasonic sensor set up on the experimental rig	No correlation was made with a real situation. However, the combination of DWT and SVM was able to give good accuracy prediction on the presence of defects in a small pipe
Fuzzy logic	[37]	The semi-empirical and mechanistic model has limitations to predict pipeline failures accurately	To develop an optimal inspection plan by referring to recommended models, standards, and their own experience of the plant	Operating condition of the pipe, wall thickness, and corrosion rate	The method developed is flexible and easy to calibrate or modify. It is based on a combination of expert knowledge and other measurements that are readily available in the plant

(continued)

Table 2 (continued)

Method	Paper	Problem addressed	Objective	Data Collected	Outcome
Fuzzy logic	[38]	The majority of developed pipeline failure prediction models are subjective and not holistic	The main objectives are: (1) to identify and study the critical failure causes of oil pipelines, and (2) to design a failure type prediction model for such pipelines	Historical pipeline data	The results showed that the fuzzy model outperformed regression analysis and ANN techniques. However, the model still has some limitations, to accurately predict the natural hazard failure types

Table 3 Comparison between Machine Learning and Conventional Methods

Characteristics	Machine learning	Conventional
Capability	Can perform beyond conventional methods capability and can accommodate multiple variables Dynamic modelling capability	The conventional methods can accommodate limited variables only Heavily reliance on a static model to deduce the results of the prediction that are coming from corrosion rates, past inspection data, and pipeline expert recommendations [16]
Accuracy	High prediction accuracy can be obtained compared to conventional methods	Less accurate and results are derived based on probability assessment which can be too conservative due to high safety factor consideration [11]
Complexity	Less complex as the MLA software is readily available. Data can be trained once-off and can be updated from time to time	Can be complex to set up and costly especially when it involves a subsea or underground pipeline
Effectiveness	More effective as it uses past data to train the model and uses the model to deduce the newly feed data	Effective with less precision. The calculation is unable to detect changes in variables and the data used are based on “on the spot” measurement

prediction using the Machine Learning method would have a clear advantage over the conventional method for the pipeline operator. It is believed that the Machine Learning method could easily be deployed and operationalized with a minimum set up cost which in turn will significantly reduce the operating cost of pipeline maintenance. However, this is yet to be justified.

The comparison between Machine Learning and Conventional methods were based on 5 main characteristics that are believed could contribute to the overall performance of the pipeline prediction:

- The capability criteria are to assess to what extent the method can be used for the prediction (are there any variables that are almost impossible to obtain?).
- The accuracy criteria refer to how good or accurate the prediction would be.
- The complexity criteria refer to how easy the method can be deployed i.e. is there any additional hardware setup is required to enable the prediction? Or can it readily use the available infrastructure set up?
- The effectiveness refers to the positive results that the prediction method had achieved based on the previous research works.

Table 4 Comparison among machine learning methods used in pipeline prediction

Methods	Regression analysis	Support vector machine	Fuzzy logic
ANN	<p>ANN outperforms Regression Analysis in terms of accuracy. ANN is more popular compare to Regression analysis</p> <p>Neural network models are more flexible compared to the regression method, however, it may prone to overfitting issues [39]</p>	<p>SVM outperforms ANN and has a high accuracy rate</p> <p>The flexibility of training: The parameters of neural classifiers can be adjusted for optimization at the string level. SVM, however, can only be trained at the level of the holistic pattern [40]</p> <p>Storage and execution complexity: SVM occupies a large number of Support Vectors which takes up a lot of memory space. Neural Network, however, has fewer parameters that are easy to control [40]</p>	<p>ANN performance is very close to Fuzzy Logic. However, based on the charts ANN obtained better accuracy compared to the Fuzzy Logic ANN is easier to implement since it uses the non-linear technique. Fuzzy logic, on the other hand, is useful in interpreting data uncertainties using fuzzy rules [41]</p> <p>ANN requires large data to be trained whilst Fuzzy Logic does not [41]</p>
Regression analysis		<p>SVM outperforms Regression Analysis</p> <p>SVM tries to find the best margin that separates the classes and thus, reducing the risk of error. Logistic regression can have different decision boundaries</p> <p>SVM works well with unstructured and semi-structured data while regression is only limited to identified independent variables</p> <p>SVM is based on the geometrical properties of the data while regression is based on statistical approaches</p> <p>Regression is prone to risk in overfitting as compared to SVM [42]</p>	<p>The fuzzy logic can approximate both linear and non-linear relationships between the input and output variables, while the accuracy of regression analysis is dependent on the linearity between input and output variables</p> <p>Fuzzy logic is suitable for decision-making problem that has incomplete and uncertain information. It can be applied for both linear and non-linear relationships between independent and dependent variables [43]</p>

(continued)

Table 4 (continued)

Methods	Regression analysis	Support vector machine	Fuzzy logic
Support vector machine			SVM outperforms Fuzzy Logic Fuzzy logic can manage uncertainties inherent in complex systems Based on the statement quoted in Chen, the Fuzzy classifier was not friendly to use in high dimensions or complex problems with a lot of features SVM is known to have good generalization abilities and can perform best in high dimensional feature spaces [44]

5.3 Comparison of Machine Learning Methods in Pipeline Prediction

Table 4 compares the accuracy of the methods as gathered from the comparison. Based on the screening, only Support Vector Machine (SVM), Artificial Neural Network (ANN), Regression Analysis and Fuzzy Logics have been considered. This is because the methods mentioned had been used in pipeline prediction studies and had demonstrated good performance in accuracy prediction. When dealing with the comparison of these methods, most of the studies only outline the pros and cons of each method individually. The Table 4 aims to help the reader to understand the performance of each machine learning methods relative to others.

5.4 Accuracy of Machine Learning Algorithm Methods

A separate literature review was carried out to compare the accuracy among the Machine Learning methods. The data were collected from the reviewed articles related to medical and pipeline. Uddin et al. [45], have carried out studies to analyze the performance among different types of supervised machine learning algorithms including trending and its use for a different type of disease prediction. They tabulated the prediction accuracy of the machine learning algorithm methods obtained from various sources of research work related to disease prediction. Out of all the machine

learning comparison that was carried out in their studies, the ANN, SVM, Naive Bayes, Random Forest, and Logistic Regression (LR) methods were frequently used and had displayed promising outcome in the field of disease prediction.

Although Random Forest and Decision Tree consistently showing better accuracy among other methods with smaller sample sizes, these methods have been excluded in this comparative analysis since there is limited research work for pipeline prediction that was carried out using these methods. Based on the findings from their studies, the ANN has demonstrated good prediction accuracy among the three methods, compare to SVM and LR. SVM on the other hand outperforms the LR. The graphical representation of the accuracy can be seen in Figs. 5, 6 and 7 [45].

Based on the reviewed machine learning articles related to pipeline, most of the studies were concentrating on the use of ANN, SVM, and Logistics Regression. The data were represented in Figs. 8, 9, 10 and 11. The most common ANN method used in the pipeline studies were Back Propagation Neural Network (BPNN). The data collected for BPNN were from [22, 26, 28, 32, 34, 38]. For Logistic Regression, the data were collected from [26, 28, 29] and SVM data were collected based on the work done by [32, 34].

The results show that the PSO-SVM method could achieve up to 99.99% accuracy compared to the BPNN and Logistic Regression method. BPNN however, outperform Logistic Regression where BPNN’s highest prediction accuracy was 99.59% and 99.40% for LR.

In a study conducted by Senouci et al. [38], Fuzzy Logic Neural Network was another promising pipeline prediction method that can be considered. In their studies,

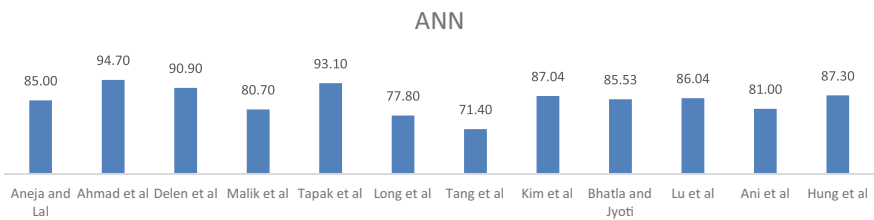


Fig. 5 ANN prediction accuracy in disease prediction

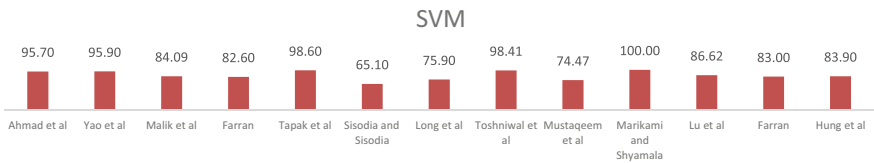


Fig. 6 SVM prediction accuracy in disease prediction

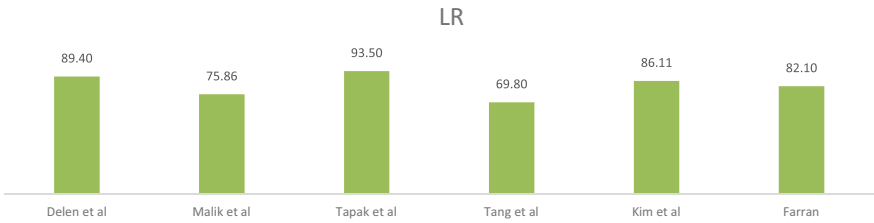


Fig. 7 Logistic regression prediction accuracy in disease prediction

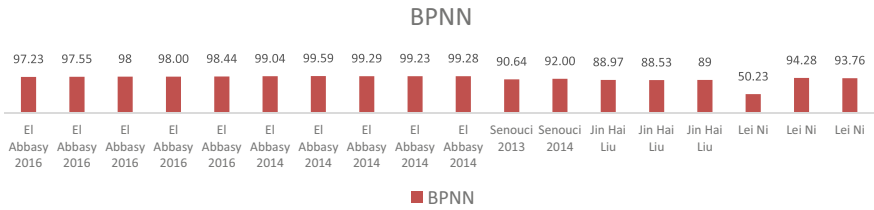


Fig. 8 BPNN accuracy for pipeline prediction

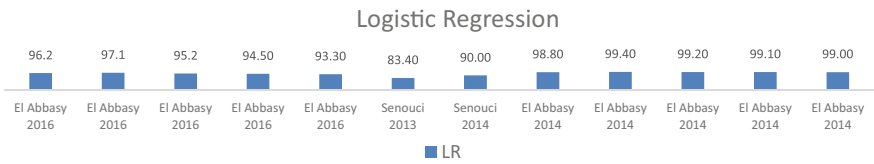


Fig. 9 Logistic regression accuracy for pipeline prediction

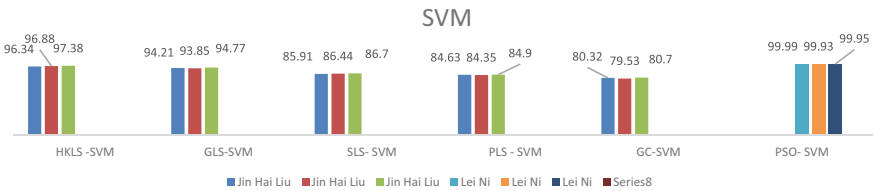


Fig. 10 SVM Pipeline prediction accuracy

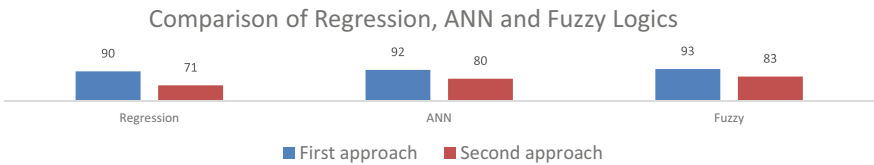


Fig. 11 Comparison of regression, ANN and fuzzy logics

the Fuzzy model was developed and compared against the previous ANN and Regression model that they have developed. The outcome of the study showed that the Fuzzy Logic method outperforms the ANN and Regression model.

Application Domain: Medical

See Figs. 5, 6 and 7.

Application Domain: Pipeline

See Figs. 8, 9, 10 and 11.

6 Future Research Challenges

6.1 Availability of Data

To come up with the most efficient and economical machine learning method for pipeline prediction, the availability of quality data is critical. For pipelines that have been operational for many years, old preventive maintenance inspection records and repair history would be beneficial to accurately determine the predictive outcome, thus will help the pipeline operator to understand the pipeline failure mode. The availability of these data is dependent on their record management shelf life and could impose a big challenge if data are no longer available.

6.2 Modification of Infrastructure for Machine Learning and Complexity

Some of the data that is required by machine learning may not be available and this requires the pipeline operator to do modification to their asset. The pipeline operator may also need to assess the technical and cost impact before considering any modification. This is to ensure the maintenance cost as a result of the machine learning method will not contribute to more maintenance cost and to avoid the increase in technical complexity in operating and interpreting the data. This may lead to an ineffective pipeline prediction program.

6.3 Organizational Capability in Handling Machine Learning

Despite the promising prospect of machine learning in pipeline predictive maintenance, another important factor to be considered is the capability of the organization

to handle the machine learning program. The existing conventional methods are using a preset program that is readily available in the market for the ease of an engineer or end-user to interpret the results of the pipeline inspection. Machine learning on the other hand would require knowledge of data science to feed or induce the right data to come up with a credible predictive outcome.

7 Conclusion

Based on the literature review, many methods can be used for the prediction of pipeline conditions and each method has its limitations. Though conventional methods have demonstrated successful outcomes, however, the accuracy is still seen as the major limitation for pipeline prediction methods. Often the conventional methods would require the deployment of inspections at that particular instant to come up with future predictions. Reliability analysis has often been used in conventional methods along with Monte Carlo Simulation. The results of the methods deployed under the conventional approach can be too conservative. As a result, this can lessen the actual benefits of reducing preventive maintenance frequency.

Machine Learning methods have been widely used for predictive maintenance. With no exceptions, machine learning methods have demonstrated good prediction accuracy for the pipeline. Based on this literature review, a few methods that are promising to be considered for pipeline condition monitoring are SVM, ANN, Regression Analysis, and Fuzzy Logics method.

Support Vector Machine (SVM) and Artificial Neural Network (ANN) are widely used for pipeline prediction and the extent of the prediction can go beyond the internal corrosion based on pipeline failure history. SVM outperforms ANN in most of the studies conducted. SVM also works well with unstructured and semi-structured data with the ability to find the best margin that separates the classes and thus, reducing the risk of error. The only major drawback for SVM is it occupies a large number of Support Vectors which takes up a lot of memory space.

The Fuzzy Logic method and Regression Analysis is also seen as the next promising methods after SVM and ANN. Fuzzy logic can outperform ANN, but it can be inaccurate if the models are not trained enough. For probabilistic analysis, Monte Carlo simulation is generally used to calculate or analyze the reliability of the pipeline.

The methods that have been identified here would be used for future works on economics assessment to determine the most viable method. This would help the pipeline operator in selecting the best methods technically and economically fit for their pipeline predictive maintenance program in the long run.

References

1. Dhillon, B. S. (2006). Maintainability, maintenance, and reliability for engineers
2. O'Donovan, P., Leahy, K., Bruton, K., & O'Sullivan, D. T. J. (2015). An industrial big data pipeline for data-driven analytics maintenance applications in large-scale smart manufacturing facilities. *Journal of Big Data*, 2, 1–26. <https://doi.org/10.1186/s40537-015-0034-z>.
3. Basheer, F., Saleem, M., & Nazmudeen, H. (2019). International Conference on Business, Management and Information Systems 1, 532–546
4. Sun, Y., Ma, L., & Morris, J. (2009). A practical approach for reliability prediction of pipeline systems. *European Journal of Operational Research*, 198, 210–214. <https://doi.org/10.1016/j.ejor.2008.07.040>.
5. St. Clair, A. M., & Sinha, S. (2014) Development of a standard data structure for predicting the remaining physical life and consequence of failure of water pipes. *Journal of Performance Constructed Facilities*, 28, 191–203. [https://doi.org/10.1061/\(ASCE\)CF.1943-5509.0000384](https://doi.org/10.1061/(ASCE)CF.1943-5509.0000384)
6. Ahammed, M. (1998). Probabilistic estimation of remaining life of a pipeline in the presence of active corrosion defects. *International Journal of Pressure Vessels and Piping*, 75, 321–329. [https://doi.org/10.1016/S0308-0161\(98\)00006-4](https://doi.org/10.1016/S0308-0161(98)00006-4).
7. Hallen, J., Caleyo, F., González, J., & Fernández-Lagos, F. (2003) Probabilistic condition assessment of corroding pipelines in Mexico. *Aaende.Org.Ar*
8. Pandey, M. D. (1998). Probabilistic models for condition assessment of oil and gas pipelines. *NDT E International*, 31, 349–358. [https://doi.org/10.1016/S0963-8695\(98\)00003-6](https://doi.org/10.1016/S0963-8695(98)00003-6).
9. Mahmoodian, M., & Li, C. Q. (2017). Failure assessment and safe life prediction of corroded oil and gas pipelines. *Journal of Petroleum Science and Engineering*, 151, 434–438. <https://doi.org/10.1016/j.petrol.2016.12.029>.
10. Shuai, Y., Shuai, J., & Xu, K. (2017). Probabilistic analysis of corroded pipelines based on a new failure pressure model. *Engineering Failure Analysis*, 81, 216–233. <https://doi.org/10.1016/j.engfailanal.2017.06.050>.
11. Li, S. X., Yu, S. R., Zeng, H. L., Li, J. H., & Liang, R. (2009). Predicting corrosion remaining life of underground pipelines with a mechanically-based probabilistic model. *Journal of Petroleum Science and Engineering*, 65, 162–166. <https://doi.org/10.1016/j.petrol.2008.12.023>.
12. Keshtegar, B., & Miri, M. (2014). Reliability analysis of corroded pipes using conjugate HL-RF algorithm based on average shear stress yield criterion. *Engineering Failure Analysis*, 46, 104–117. <https://doi.org/10.1016/j.engfailanal.2014.08.005>.
13. Breton, T., Sanchez-Gheno, J. C., Alamilla, J. L., & Alvarez-Ramirez, J. (2010). Identification of failure type in corroded pipelines: A Bayesian probabilistic approach. *Journal of Hazardous Materials*, 179, 628–634. <https://doi.org/10.1016/j.jhazmat.2010.03.049>.
14. Zhang, G., Luo, J., Zhao, X., Zhang, H., Zhang, L., & Zhang, Y. (2012). Research on probabilistic assessment method based on the corroded pipeline assessment criteria. *International Journal of Pressure Vessels and Piping*, 95, 1–6. <https://doi.org/10.1016/j.ijpvp.2011.12.001>.
15. Ossai, C. I., Boswell, B., & Davies, I. J. (2016). Application of Markov modelling and Monte Carlo simulation technique in failure probability estimation—A consideration of corrosion defects of internally corroded pipelines. *Engineering Failure Analysis*, 68, 159–171. <https://doi.org/10.1016/j.engfailanal.2016.06.004>.
16. Aulia, R., Tan, H., & Sriramula, S. (2019). Prediction of corroded pipeline performance based on dynamic reliability models. *Procedia CIRP*, 80, 518–523. <https://doi.org/10.1016/j.procir.2019.01.093>.
17. Kale, A., Thacker, B. H., Sridhar, N., & Waldhart, C. J. (2004) A probabilistic model for internal corrosion of gas pipelines. In *Proceedings of the Biennial International Pipeline Conference, IPC*, pp. 2437–2445.
18. Pentakalos, O. (2019). Introduction to machine learning. C-Impact 2019. <https://doi.org/10.4018/978-1-7998-0414-7.ch003>.
19. Ahammed, M. (1997). Prediction of remaining strength of corroded pressurised pipelines. *International Journal of Pressure Vessels and Piping*, 71, 213–217. [https://doi.org/10.1016/S0308-0161\(96\)00081-6](https://doi.org/10.1016/S0308-0161(96)00081-6).

20. Noor, N. M., Ozman, N. A. N., & Yahaya, N. (2011). Deterministic prediction of corroding pipeline remaining strength in marine environment using DNV RP -F101 (Part A). *Journal of Sustainability Science and Management*, 6, 69–78.
21. Najafi, M., & Kulandaivel, G. (2005). Copyright ASCE 2005 767 Pipelines 2005 Pipelines 2005. Pipelines 2005 Optimal Pipeline Des Operation Maintaintance Today's Economy, 767–781
22. El-Abbasy, M. S., Senouci, A., Zayed, T., Mirahadi, F., & Parvizsedghy, L. (2014). Artificial neural network models for predicting condition of offshore oil and gas pipelines. *Automation in Construction*, 45, 50–65. <https://doi.org/10.1016/j.autcon.2014.05.003>.
23. Liao, K., Yao, Q., Wu, X., & Jia, W. (2012). A numerical corrosion rate prediction method for direct assessment of wet gas gathering pipelines internal corrosion. *Energies*, 5, 3892–3907. <https://doi.org/10.3390/en5103892>.
24. Ren, C. Y., Qiao, W., Tian, X. (2012). Natural gas pipeline corrosion rate prediction model based on BP neural network. *Advances in Intelligent Soft Computing*, 147 AISC, 449–455. https://doi.org/10.1007/978-3-642-28592-9_47.
25. Achim, D., Ghotb, F., & McManus, K. J. (2007). Prediction of water pipe asset life using neural networks. *Journal of Infrastructure Systems*, 13, 26–30. [https://doi.org/10.1061/\(ASCE\)1076-0342\(2007\)13:1\(26\)](https://doi.org/10.1061/(ASCE)1076-0342(2007)13:1(26)).
26. Senouci, A., Elabbasy, M., Elwakil, E., Abdrabou, B., & Zayed, T. (2014). A model for predicting failure of oil pipelines. *Structure Infrastructure Engineering*, 10, 375–387. <https://doi.org/10.1080/15732479.2012.756918>.
27. Nasir, M. T., Mysorewala, M., Cheded, L., Siddiqui, B., & Sabih, M. (2014). Measurement error sensitivity analysis for detecting and locating leak in pipeline using ANN and SVM. In *2014 IEEE 11th International Multi-Conference Systems Signals Devices, SSD*, 7–10. <https://doi.org/10.1109/SSD.2014.6808847>
28. El-Abbasy, M. S., Senouci, A., Zayed, T., Parvizsedghy, L., & Mirahadi, F. (2016) Unpig-gable oil and gas pipeline condition forecasting models. *Journal of Performance Constructed Facilities*, 30. [https://doi.org/10.1061/\(ASCE\)CF.1943-5509.0000716](https://doi.org/10.1061/(ASCE)CF.1943-5509.0000716)
29. El-Abbasy, M.S., Senouci, A., Zayed, T., Mirahadi, F., & Parvizsedghy, L. (2014). Condition prediction models for oil and gas pipelines using regression analysis. *Journal on Construction Engineering Management*, 140. [https://doi.org/10.1061/\(ASCE\)CO.1943-7862.0000838](https://doi.org/10.1061/(ASCE)CO.1943-7862.0000838)
30. Qu, Z., Feng, H., Zeng, Z., Zhuge, J., & Jin, S. (2010). A SVM-based pipeline leakage detection and pre-warning system. *Journal of the International Measurement Confederation*, 43, 513–519. <https://doi.org/10.1016/j.measurement.2009.12.022>.
31. Chen, H., Ye, H., Lv, C., & Su, H. (2004). Application of support vector machine learning to leak detection and location in pipelines. In *Conference Rec.—IEEE International Instrumentation and Measuremt Technology Conference*, 3, 2273–2277. <https://doi.org/10.1109/IMTC.2004.1351546>.
32. Liu, J., Su, H., Ma, Y., Wang, G., Wang, Y., & Zhang, K. (2016). Chaos characteristics and least squares support vector machines based online pipeline small leakages detection. *Chaos, Solitons & Fractals*, 91, 656–669. <https://doi.org/10.1016/j.chaos.2016.09.002>.
33. Aydogdu, M., & Firat, M. (2015). Estimation of failure rate in water distribution network using fuzzy clustering and LS-SVM Methods. *Water Resource Management*, 29, 1575–1590. <https://doi.org/10.1007/s11269-014-0895-5>.
34. Ni, L., Jiang, J., & Pan, Y. (2013). Leak location of pipelines based on transient model and PSO-SVM. *Journal of Loss Prevention in the Process Industries*, 26, 1085–1093. <https://doi.org/10.1016/j.jlp.2013.04.004>.
35. Lee, L.H., Rajkumar, R., Lo, L.H., Wan, C.H., & Isa, D. (2013) Oil and gas pipeline failure prediction system using long range ultrasonic transducers and Euclidean-Support Vector Machines classification approach.
36. Isa, D., & Rajkumar, R. (2009). Pipeline defect prediction using support vector machines. *Applied Artificial Intelligence*, 23, 758–771. <https://doi.org/10.1080/08839510903210589>.
37. Singh, M., & Markeset, T. (2009). A methodology for risk-based inspection planning of oil and gas pipes based on fuzzy logic framework. *Engineering Failure Analysis*, 16, 2098–2113. <https://doi.org/10.1016/j.engfailanal.2009.02.003>.

38. Senouci, A., El-Abbasy, M. S., & Zaye, T. (2014). Fuzzy-based model for predicting failure of oil pipelines. *Journal of Infrastructure Systems*, 20, 1–11. [https://doi.org/10.1061/\(ASCE\)IS.1943-555X.0000181](https://doi.org/10.1061/(ASCE)IS.1943-555X.0000181).
39. Dreiseitl, S., & Ohno-Machado, L. (2002). Logistic regression and artificial neural network classification models: A methodology review. *Journal of Biomedical Informatics*, 35, 352–359. [https://doi.org/10.1016/S1532-0464\(03\)00034-0](https://doi.org/10.1016/S1532-0464(03)00034-0).
40. Arora, S., Bhattacharjee, D., Nasipuri, M., Malik, L., Kundu, M., & Basu, D. K. (2010). Performance Comparison of SVM and ANN for Handwritten Devnagari Character Recognition. *International Journal of Computer Science Issues*, 7, 18–26.
41. Mas'ud, A. A., Ardila-Rey, J. A., Albarracín, R., Muhammad-Sukki, F., & Bani, N. A. (2017). Comparison of the performance of artificial neural networks and Fuzzy logic for recognizing different partial discharge sources. *Energies*, 10, 1–20. <https://doi.org/10.3390/en10071060>
42. Logistic Regression Vs Support Vector Machines (SVM) | by Patricia Basse | Axum Labs | Medium, <https://medium.com/axum-labs/logistic-regression-vs-support-vector-machines-svm-c335610a3d16>.
43. Gul Polat Befrin Neval Bingol. (2013). A comparison of fuzzy logic and multiple regression analysis models in determining contingency in internal construction projects. *Construction Innovation*, 13, 445–462.
44. Chen, J., Zhang, R., & Wu, D. (2018). Equipment maintenance business model innovation for sustainable competitive advantage in the digitalization context: Connotation, types, and measuring. *Sustainability*, 10. <https://doi.org/10.3390/su10113970>
45. Uddin, S., Khan, A., Hossain, M. E., & Moni, M. A. (2019). Comparing different supervised machine learning algorithms for disease prediction. *BMC Medical Informatics and Decision Making*, 19, 1–16. <https://doi.org/10.1186/s12911-019-1004-8>.

Application of Back Propagation Algorithm in Optimization of Weave Friction Stir Welding—A Study



M. Balasubramanian, D. Jayabalakrishnan, C. Hemadri, and B. Ashwin

1 Introduction

FSW quickly gained universal industrial consideration and had been mostly concentrated on aluminum alloys all through the emergence of the FSW procedure. The ease of the FSW process to join two materials without reaching the melting point under inter-transition temperature is an add-on advantage in the FSW process. FSW technique has been most robust in AI related industries as it is a part of similar and dissimilar aluminum combinations with the workpiece thickness starting from 1-mm sheets to 75-mm thick plates. Currently, different alloy combinations, for example, magnesium ferrous, titanium, copper, nickel-based composites, have conjointly been subjected to FSW or FSP.

The adaptability of FSW to joining of unique metals (combinations of metals) in different setups has also been condensed. The fundamental standard of FSW is genuinely direct. In this technique, a rotating tool, created from a material harder than the workpiece, with a nominal shoulder diameter, and a pin, plunges into the

M. Balasubramanian (✉) · C. Hemadri

Department of Mechanical Engineering, RMK College of Engineering and Technology,
Chennai 601206, India

e-mail: manianmb@gmail.com

C. Hemadri

e-mail: Chd311@gmail.com

D. Jayabalakrishnan

Department of Mechanical Engineering, Sriram Engineering College, Chennai 602024, India

e-mail: djayabal2001@gmail.com

B. Ashwin

Department of Computer Science and Engineering, Loyola ICAM College of Engineering,
Chennai 600034, India

e-mail: ashwinblaze111@gmail.com

workpiece to a pre-decided depth. The rotating tool pin entering the workpiece produces frictional heat due to the material interaction of shoulder and workpiece. Another contribution to the heat input originates from adiabatic thermal effect made all through plastic deformation of the rotating tool. In some of the recent materials, bigger shoulder diameters are used for preventing flash and joints without defects. The FSW of dissimilar materials plates of 12.7 mm thick revealed three regions in the weld area. Initially a mechanically blended areas described by the generally evenly scattered particles of differing alloy elements. Next one was plastically deformed flow region caused by mechanical stirring comprising vortex-like lamellae of both dissimilar alloys. Further a unmixed area made out of fine equiaxed grains of the 6061Al composite was seen. They found that a firm contact between various layers, but the blending was deficient. However, bonding attained between them was better. Besides they were associated with the alternative lamellae due to the influence of threaded tool stirring action in transverse movement along the welding direction [1].

The temperature appropriation and microstructural advancement of the AA6061 Al–Cu through the FSW technique was examined [2]. The mechanically mixed region consisted of various IMCs like CuAl, CuAl₂, and Cu₉Al₄ along with α -Al and saturated solutions. This resulted in the lower dissolving of Cu in Al despite the high solubility of Al in Cu. The microstructure evolution, mechanical properties, and the presence of intermetallic components on Cu–Al dissimilar FSW joints. They achieved a better welding strength of 296 MPa under the welding conditions such as 950 rpm and 150 mm/min. They reported the existence of a mixed structure on the Al side of the SZ and the lamellar arrangement that occurred on the Cu side of the SZ [3]. The properties of similar and dissimilar joints of Al–Cu. They noticed the occurrence of some intermetallic compounds such as Al₄Cu₉, Al–Cu, Al₂Cu, and Al₂Cu₃ was studied [4].

The consequence of pin profile on the microstructure and microhardness of the Al–Cu joints was studied. They reported the tendency of plain taper pin profile (PTP) to produce maximum tensile and yield strength of 116 MPa and 101 MPa respectively [5]. The welding of dissimilar materials pure copper and pure aluminum sheets was studied. They disclosed the existence of copper particles and their dispersion throughout the aluminum matrix [6].

Al–Mg alloys to understand the generation of IMCs in the banded structure zone was studied. They also investigated the mechanical properties utilizing different tool rotational speeds. They concluded that the microstructure of the banded structure zone, quantity, and the dissemination of IMC particles changed with the rotational speed in the band morphology. Development of the quality of the banded structure zone, required less IMC particles, bands in a curved shape in the banded structure instead of a relatively short, discontinuous, and straight arrangement of bands [7]. The presence of Al/Cu content in the nugget and observed the occurrence of lamellar-like flow in the special band structure (BS) was explored. Also, with the rise of Cu content in weld nugget, the Copper piece was tending to dispense in a huge volume where the generation of the deformity was likely due to Cu with high heat input providing an intensive material flow [8]. Al/NiTi/Al composites through FSW with electrical current was developed. They reported an increase in the visco-plastic

material flow by the electric current due to the heat increase, prompting a better bonding of NiTi ribbons to the aluminium matrix. Thus a detailed study of the effect of adding reinforcements in welded portion yield improved mechanical, microstructural properties were made [9]. The multi-step FSP on aluminum and magnesium alloy composites with the addition of graphene nanoparticles was developed. They found the presence of an fine grains with an average grain size of 2.1 μm at the stir zone. They stated that the introduction of graphene particles in composites hindered and influenced Zener pinning and stimulated nucleation mechanism in the event of dynamic recrystallization [10].

This effort deals with upgrading the weld strength of joints through a unique technique for efficient stirring and correct dispersion of graphene particles. Aluminum and copper as composite structures create some unsolvable problems such as oxidation and fragmental cracks. This is an efficient welding process which helps in overcoming these problems. Linear tool movement resulted in defects like tunnel defects and voids due to improper stirring time [4]. The reinforcement of Nanoparticles is required for ensuring improved joint properties, compared with non-reinforced alloy joints [11, 12]. The rotation of the pin around its axis is normal to the weld line, and the translation of the pin along the axis would overcome the formation of the oxide layer and avoids a severe weld defect [13]. The use of sorting algorithm in optimizing the welding parameters was reported. Use of swept friction stir was discussed by [14, 15]. Importance of SiC reinforcement and importance of nano reinforcement was demonstrated by [16–18].

In previous literature, different techniques were followed for achieving better joint strength in the FSW of Al–Cu. Even though they have achieved improvement in the joint strength, they addressed problems such as voids, tunnels, cracks, and improper stirring time. To overcome this, the author of the above-mentioned problem proposed to address the novel technique, with the combined effect of eccentric weave, tool pin offset, and addition of Self-lubricated Graphene Nanoplatelets as a reinforcement material.

2 Experimental Work

A 3-axis Computer numerical controlled (CNC) 50 kN machine with the setup shown in Fig. 1 used for the study. The material under study namely copper and aluminium alloy were joined through the FSW process. For the pre-injection of graphene nanoparticles, the plates were grooved with elliptical contour at their center. The volumetric ratio of 2.06% of graphene particles was used in the weld area. This groove restricted the spilling and uniform dispersion of graphene particles during the stirring process. The graphene particles were distributed to about 4 mm. The tool path was dictated by oblique motion. Linear motion is preceded by oblique motion of the tool. Rotary motion between 800 and 1200 rpm with the feed rate between 30 and 70 mm/min was used. Based on the trials, the process parameters for each welding type were selected. Figure 2 showcases the fabricated weldments.

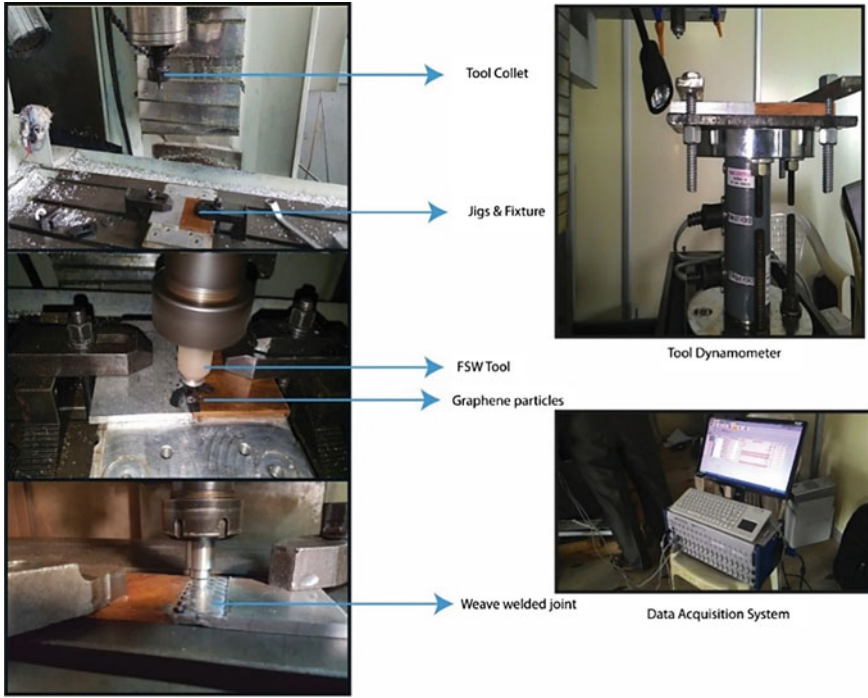


Fig. 1 Photographic view of the experimentation

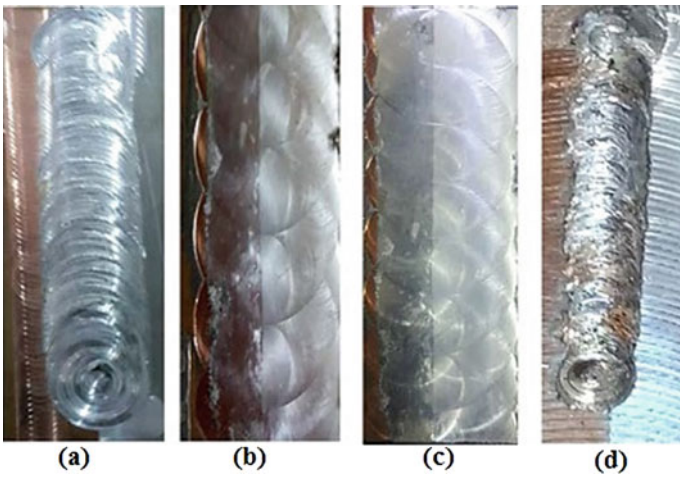


Fig. 2 Friction stir welded joints


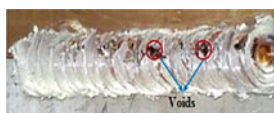
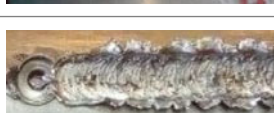
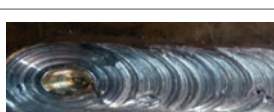
2.1 Selection of the Range of Process Parameters

The appearance of the joints is showcased in Table 1. Parameters chosen for performing experiments are presented in Table 2. The welding conditions used for the fabrication of FSW joints are given in Table 3. Rotary motion was operated between 800 and 1600 rpm for fabricating FSW joints.

In joint 1, the weld was made with a rotary speed of 1600 rpm, welding speed of 50 mm/min, and axial load of 12 kN under a linear weld without tool offset condition. It exhibited poor surface appearance with flashes and voids due to higher heat input because of higher tool rotational speed. A similar condition mentioned in the literature [19] that $\omega/2v$ ratio increased with the increase of tool rotational speed. Joint 2 was obtained using the process parameters of 1200 rpm, 50 mm/min, and axial load of 14 kN under a linear weld without tool offset condition. Cracks and voids are visible on the surface of the weld due to the increased axial force and improper mixing and compaction of the base materials. As the axial load increases, corrugations increase at the welding seam edges. Joints 3–5 underwent low heat input due to low rotational speed causing surface discontinuity defect without pin offset and unreinforced GNPs. Joint 6, made with LW-WOPO with reinforcement of GNPs under similar process conditions as joint 2, the induced defects were slightly reduced due to the addition of GNPs which act as a filler of the voids and micro-cracks. The surface appearance of the joint 6 is improved compared to Joint 1–5. Joint 7, produced with LW-WPO condition without reinforcement expelled excessive flash due to lack of compaction with a decrease of axial load. Joint 8 made with LW-WPO condition with reinforcement exhibits better appearance, minimum defects such as microvoids and cracks compared with joint 7 due to hindrance of dislocation movement resulting to increase of dislocation density. Joint 9–10 made with WW-WOPO condition without reinforcement, yield a sound joint that was free from visual defects due to excess holding time resulting in severe plastic deformation. Joint 11, produced with WW-WOPO with reinforcement resulted in proper intermixing of Cu and Al with adequate heat input condition proved to be the best. Joint 12, obtained with EWW-WPO condition without reinforcement gave a superior joint performance because of proper flow with transportation of large volume of material and homogeneous dispersion taking place. Joint 13, formed with EWW-WPO condition with reinforcement gave sound joint compared with all the other joints made with different weld and process conditions because of extensive plastic deformation that led to equiaxed grain refinement by zener pinning effect and breaking of Orowan strengthening mechanism.







Joint 14, made with WW-WOPO with GNPs showed the flash along with GNPs expelled out from the SZ because of severe plunging effect and thinning of stir zone as a result of excessive axial load. Joint 15, produced with LW-WPO without GNPs induced tunnel defect due to the effect of higher WS irrespective of the tool pin offset condition. Defects such as flashes, tunnels, or cavities resulted from abnormal stirring under improper welding circumstances [20]. In Joint 16, a defect lack of fill at the weld nugget could be observed through surface morphology due to lower heat input at tool rotational speed of 800 rpm under LW-WOPO (without GNPs). In Joint

Table 1 FSW joints surface characteristics of different welding conditions

Joints	N rpm	V, mm/min	F kN	Conditions	Joint appearance	Remarks
Joint 1	1600	50	12	LW-WOPO		Excessive flash
Joint 2	1200	50	14	LW-WOPO		Crack formation
Joint 3	1600	50	12	LW-WOPO (without GNPs)		Weld flash
Joint 4	1200	70	12	LW-WOPO (without GNPs)		Void
Joint 5	1200	50	16	LW-WOPO (without GNPs)		Flash propagation
Joint 6	1400	50	12	LW-WOPO (with GNPs)		Uniform weld
Joint 7	1200	50	14	LW-WPO (without GNPs)		Flash & thinning
Joint 8	1200	60	12	LW-WPO (with GNPs)		Defect-free Uniform striations with good weld
Joint 9	1200	60	12	WW-WOPO (with GNPs)		Defect-free weld

(continued)

Table 1 (continued)

Joints	N rpm	V, mm/min	F kN	Conditions	Joint appearance	Remarks
Joint 10	1200	50	14	WW-WOPO (with GNPs)		Defect-free weld
Joint 11	1400	50	12	WW-WOPO (with GNPs)		Defect-free weld
Joint 12	1000	50	12	EWV-WPO (without GNPs)		Minimum flash
Joint 13	1200	50	14	EWV-WPO (with GNPs)		Defect-free weld surface
Joint 14	1200	50	16	WW- WOPO (with GNPs)		GNPs flash
Joint 15	1200	70	12	LW-WPO (with GNPs)		Tunnel defect
Joint 16	800	50	12	LW-WOPO (without GNPs)		Lack of fill
Joint 17	1200	50	16	LW-WOPO (without GNPs)		cracks and pores
Joint 18	1200	30	12	LW-WPO (without GNPs)		Lack of fill

(continued)

Table 1 (continued)



Joints	N rpm	V, mm/min	F kN	Conditions	Joint appearance	Remarks
Joint 19	1200	40	12	LW-WOPO (without GNPs)		Excess thinning
Joint 20	1200	50	8	LW-WPO (without GNPs)		Voids

Table 2 Process variants

S. No	Factors	Unit	Range
1	Rotational motion of the tool (N)	RPM	800–1600
2	Speed of welding (v)	mm/min	30–70
3	Axial load (F)	kN	8–16

Table 3 Tool design

Process variants	Range
Axial load F, (kN)	12
Tool shoulder diameter D, (mm)	20
Tool tilt angle θ	0°
Plate position	Copper- advancing side (AS) Aluminum—Retreating side (RS)
Length of the pin h, (mm)	5.5
Pin diameter d, (mm)	4
Pin Profile	Cylindrical and Eccentric (e = 2 mm)
Tool material	Hardened super high-speed steel

17, a defect such as cracks and pores could be visible on the surface of the weld due to the high axial load of 16 kN under the LW-WOPO (without GNPs) condition. In Joint 18, a defect like lack of fill due to excessive softening of Al material and improper mixing at a welding speed of 30 mm/min under LW-WPO (without GNPs). In Joint 19, a defect like excess thinning of the weld nugget could be observed due to the softening of Al expelled out at high heat input developed at 40 mm/min under LW-WOPO (without GNPs). In Joint 20, a defect like voids could be observed at the weld joint due to improper material flow caused by inadequate plunge force at 8 kN under LW-WPO (without GNPs).

Figure 2a shows the LW-WOPO. Similarly, Fig. 2b shows WW-WOPO. Figure 2c shows the EWW-WPO, Similarly, Fig. 2d shows LW-WPO.

3 Optimization of Process Parameters

Feedforward neural networks with backpropagation training is utilized in optimization of process parameters.

There are of course, several studies currently under way on the output response through ANNs. The ANN simulations depicted here, however do not strive to be accurate in real time applications, however it provides with few indicators which summarises the actions of a complex system. The basic features of the network are network with their weights representing as one unit (Eq. 1). Each neuron is linked to the preceding neurons and the following layer in this network architecture; there is no connection between the neurons on the same layer.

$$O_i^\mu = f_i = \left(\sum_i W_{ij} V_j^\mu \right) = f_i \left[\sum_j W_{ij} g_j \left(\sum_k w_{jk} I_k^\mu \right) \right] \tag{1}$$

I_k^μ = inputs

w_{jk} = connection weights between input and hidden layers

W_{ij} = connection weights between hidden and output layers

V_j^μ = output of the hidden neuron

An ANN tool for small dataset analysis previously defined in the backpropagation system [21], the number of hidden neurons is low and a training-validation-test protocol is typically adopted to optimise an ANN model. In short, three subsets are created from the source of entire data set (Fig. 3). Initially, the backpropagation algorithm is applied and at the end of every repetition, the functionality of the input-output map obtained is endorsed by moving a step forward with the fixed weights by the backpropagation algorithm.

As the efficiency on the validation set starts to decrease, the iteration process is halted, even though the efficiency surges under some desired targets. The basic

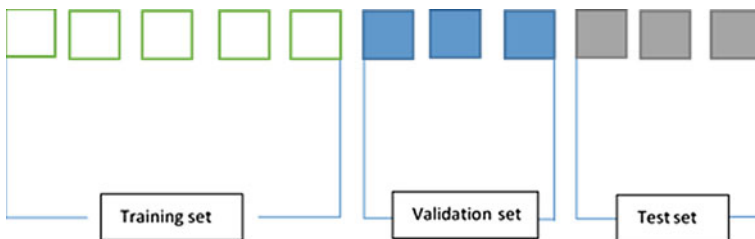


Fig. 3 Total data set is subdivided in to three subsets

concept to deal with limited datasets is to configure the requirement to extend the training by the leave-one-out cross validation technique. As shown in Fig. 4, simplified technique is presented here. In short to evaluate the co-output, the respective input-target pair is removed and each target is estimated. Figure 4 represents white squares which depicts the training set elements (input-target pairs), the blue squares represent the validation set elements, and the test set represents the grey square (one single element). At each point of the iterative preparation, validation and test cycle procedure changes. Our test set is represented by a 'hole' in the full set and moves through this total set of pairs, thus making the output values at the end. In addition, at every stage of our process, the validation set is randomly selected and the training stops when a rise in the mean square error (MSE) occurs in the validation set. This new technique certainly enables us to prevent any overfitting of data that we want to recreate by ANNs. Best results obtained through

More runs in ANNs to be taken into account for obtaining effective results by repeating every approximation shown in Fig. 4. The adjustment in initial weights permits the model to work on the cost function extensively.

On these multiple runs of the model, on an average, more stable and accurate results can be attained, since they are not governed on the variables associated with the initialization of the network and the random choice of the validation collection. After this input collection, many models characterised by different inputs can be developed, so that multiple nonlinear regressions are performed. In this way, the most important causal factors can be identified and the onset of a disease can at best be reconstructed.

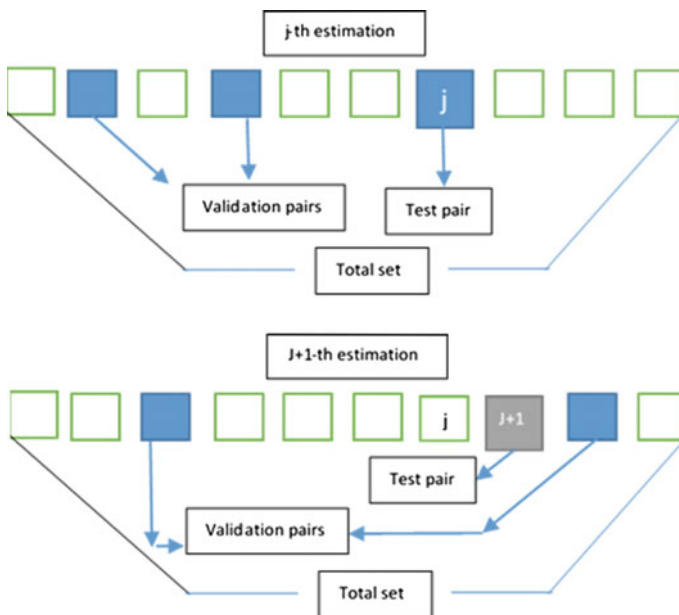


Fig. 4 Generalized leave-one-out procedure

Table 4 Best results obtained through feasible process parameters without GNP's

Type	YS (MPa)	UTS (MPa)	Elongation (%)	NTS (MPa)	Impact strength (J)	Avg. Hardness (HV)
LW-WOPO (N = 1200; v = 50; F = 12)	147	159	10.4	114	7.9	88
LW-WPO (N = 1200; v = 50; F = 12)	151	167	9	119	8.5	96
WW-WOPO (N = 1000; v = 50; F = 12)	160	180	8.1	126	9.6	104
EWV-WPO (N = 1000 v = 50; F = 12)	168	187	7.6	132	10.1	110

This fixed weighted ANN is applied to forecast the optimum process parameters of the casual input variables. The maximum best values attained with the corresponding process parameters with and without the addition of GNPs obtained by utilizing the back propagation algorithm for all the four welding conditions [LW-WOPO, LW-WPO, WW-WOPO, EWW-WPO] is presented in Tables 4 and 5 respectively.

4 Results and Discussion

4.1 Consequence of Tool Rotational Speed Without GNPs

FSW joint was fabricated using four different weld conditions namely, LW-WOPO, LW-WPO, WW-WOPO, and WW-WPO with a rotational speed of 800 to 1600 rpm range.

4.1.1 Tensile Properties

Figure 5 demonstrates generation of sufficient heat input to achieve a better weld joint in linear weld conditions at 1200 rpm. The use of pin offset in the linear weld showed a slight increase in the UTS value of 167 MPa. It was due to proper mixing and larger volume dispersion of Copper in the Al. At 1000 rpm ample heat supply in the nugget region led to a maximum UTS value of 187 MPa in weave weld Fig. 5. It could be seen

Table 5 Best results obtained through feasible process parameters with GNP's

Type	YS (MPa)	UTS (MPa)	Elongation (%)	NTS (MPa)	Impact strength (J)	Avg. Hardness (Hv)
LW-WOPO (N = 1200; v = 50; F = 12)	158	175	11	125	9.4	97
LW-WPO (N = 1200; v = 50; F = 12)	165	185	10.4	130	10.2	105
WW-WOPO (N = 1000; v = 50; F = 12)	176	205	9.2	145	11.6	118
EWV-WPO (N = 1000; v = 50; F = 12)	182	217	8.7	152	12.4	126

*N —rotational speed, rpm; v—welding speed, mm/min; F—axial load, kN

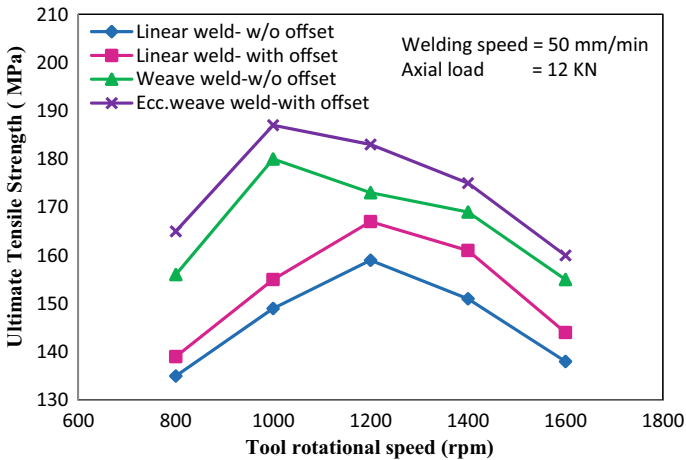


Fig. 5 Correlation of rotational speed on tensile strength

from the observed experimental results that there is no substantial improvement on UTS using pin offset. Besides, at 1600 rpm, the UTS of weld joint strength reduced to 138 MPa due to excessive heat at the SZ under LW-WOPO condition. The visual appearance of the weld joint made at 1600 rpm under LW-WOPO condition is given in Fig. 6d. The formation of thick IMCs and defects could be the reason for the reduction in the UTS, % of elongation, and YS of the welded joint. It was noticed

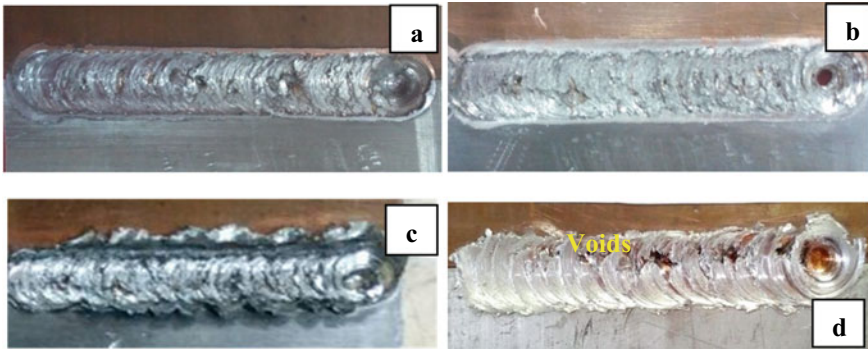


Fig. 6 Surface morphology of Al–Cu joint, **a** 1000 rpm (WW-WPO), **b** 1200 rpm (LW-WPO), **c** 800 rpm (LW-WOPO), **d** 1600 rpm (LW-WOPO)

that the heat input in the weld area gets increased corresponding to an increase of the tool rotational speed and improved the mechanical properties of the FSW weld joint. On the contrary, increasing the rotational speed beyond 1200 rpm caused a lowering of the mechanical properties. This statement was in agreement with the previous study [22].

4.1.2 Microstructure

The speed of 1000 to 1200 rpm influenced the formation of plasticized weld material created by high friction between the tool and the plate. The surface appearances of the weld produced at the above speed under WW-WPO and LW-WPO conditions respectively are shown in Fig. 6a, b respectively. Figure 6a shows a good weld surface appearance with uniform flow. However, at 800 rpm surface lines and undue flash were seen in Fig. 6c.

The increase in UTS under weave weld with pin offset was due to adequate frictional heat, material plastic deformation, forces acting on the tool, size of the stirred zone, and material flow of the FSW joints. The increased rotational speed enlarging the strained location and then the extremely strained particles were transferred to the AS from the existing RS of the joint similar to the statement in the literature [22]. Softening occurred in the HAZ, NZ, and TMAZ, as a result of the grain refinement caused by the heat input and strain during mechanical stirring which was in agreement with the previous study [23]. The rotational speed of 1000 rpm with pin offset condition tended to separate more Cu particles with smaller sizes. A unique formation of thin and uniform IMCs was noticed while using the weave weld with pin offset which improved the tensile properties of the welded joint (Fig. 7). This statement is coherent with the previous study [24].

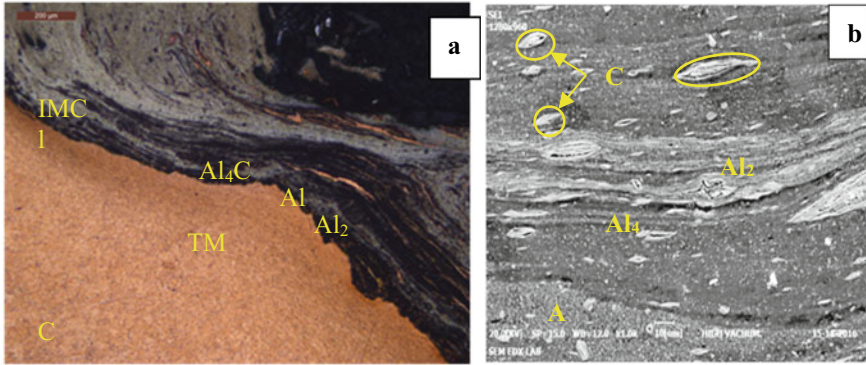


Fig. 7 IMC at the stir zone. a OM image, b SEM image

4.1.3 Microhardness

It could be noticed that the hardness in the SZ was higher than that of the base metal, and it increased with an increase in the tool rotational speed. This statement is coherent with [25]. In linear weld conditions, an active stirring of AA6061-T6 and Cu joints could not be achieved; this led to the formation of oxides in the weld zone and correspondingly reduced the hardness value 88 HV. However, the weave weld with pin offset resulted in a higher microhardness value of 110 HV. Higher rotational speed resulted in the higher heat input at the stir zone causing uniformly dispersed particles within the nugget. These uniformly dispersed particles prevented dislocation movement and thereby strengthened the weld joint. Proper mixing and larger uniform dispersion of Cu in the Al matrix were noticed using weave weld with pin offset as illustrated in Fig. 8a, b. Furthermore, under weave weld with pin offset

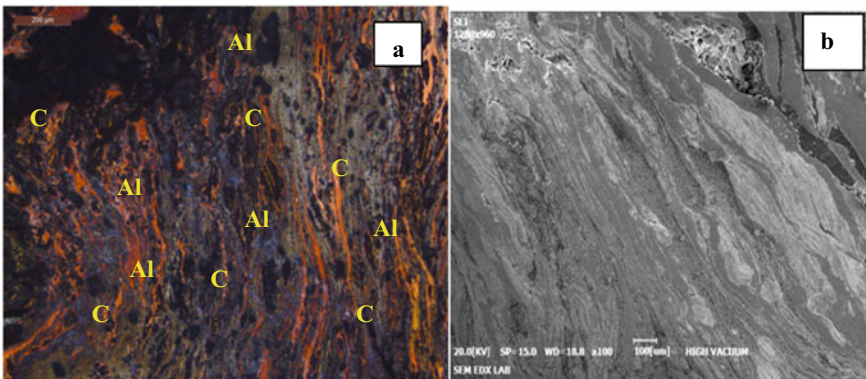


Fig. 8 Uniform dispersion of Cu particles in the aluminum matrix in the SZ. a OM image, b SEM image

condition, it hindered the dislocation density and fine grain refinement enhancing the microhardness. The presence of IMCs increased the hardness value as mentioned in the literature [26].

4.2 The Effect of Tool Rotational Speed with GNPs

It was noticed that graphene nanoplatelets increased the hardness value significantly without loss of ductility on Al–Cu in the FSW joint.

4.2.1 Tensile Properties

The eccentric weave weld with pin offset condition showed an increased UTS value of 217 MPa compared with LW-WPO and LW-WOPO produced values of 185 MPa and 175 MPa respectively. Under the weave weld, the stirring process was more efficient through stirring a larger area. So the observed results confirmed WW-WPO providing adequate heat input and thereby increasing UTS value compared with the other three welding conditions. In weave weld with tool offset condition with GNP's, the size of the stir zone increased due to the weave pattern of tool movement and subjected to intensive plastic deformation with the effect of self-lubricating nature of carbonaceous nanoplatelets [27] reported the maximum tensile strength of 158 MPa. Maximum UTS of 170 MPa [28] and [29] reported a maximum UTS of 135 MPa in FSW of dissimilar AA6061-pure Cu. In our investigation at 1000 rpm, the highest tensile strength of 217 MPa was attained in weave weld with pin offset at a nominal welding speed of 50 mm/min using GNPs.

Linear weld condition attained the NTS value of 130 MPa at 1200 rpm. The higher NTS value of 152 MPa was attained with the effect of GNPs. The higher fraction volume of stirred material was expelled out to the top surface at a rotational speed of 1600 rpm that led to the formation of defects like weld flash in the interface region as can be seen in Joint No.1 & Joint No.3 as presented in Table 1. On the other hand, the defect like lack of stirring occurred as a result of low heat input at the lower speed of 800 rpm could be seen in Joint No. 16 as presented in Table 1. The dissipation of temperature was reduced while decreasing the rotational speed that caused the decrease in the stirred region. This statement was similar to the one found in previous literature [30].

From the experiment, it was confirmed that a decrease in YS was attained when the speed increases. The tool rotational speed is a predominant operating parameter in the FSW process. When it exceeds the limit of 1200 rpm the excessive softening of plasticized weld material is formed which hinders the uniformity in the flow. The experiments revealed that the increase in heat input leading to the formation dissolution and coarsening of strengthening precipitates at the SZ [31] and the YS of the FSW joints led to reduction by lowering of dislocation density. This statement was coherent with our results [32]. In the linear weld, the maximum YS attained was

165 MPa. The addition of nanoplatelets and the active stirring effect by the tool in the weld nugget under weave weld condition increased the dispersion of nanoplatelets. These GNPs acted as fibroid particles to hold the ductile bondage in increasing the YS. This led to a maximum YS of 182 MPa. It is to be noticed that linear weld condition produced a maximum impact strength of 9.4 J with the increase of rotational speed 1200 rpm beyond which it started decreasing, whereas weave weld with pin offset covered a more substantial stirring area resulted in maximum impact strength of 12.4 J. This was relatively higher than the linear weld condition. In weave weld condition, the graphene platelets shifted in weave path through uniform dispersion in locating the particles along shear plane thereby increasing the impact strength of the weldments.

At 1000 rpm, the percentage of elongation in the FSW joint was minimum. The heat input induced at this speed had a strong influence on the percentage of elongation which can be seen in experimental results. At 1000 rpm, the tensile strength reached a maximum value, along with surge in elongation. Above 1200 rpm, the strength was reduced due to high heat resulting in grain growth leading to lower percentage of elongation of the joints. In a linear weld, the maximum percentage of elongation attained was 11% at the speed of 1200 rpm. On the other hand, weave weld with pin offset achieved a maximum percentage of elongation of 8.7% at a speed of 1000 rpm. The percentage of elongation indicated the ductility of the material. The elongation of the material depended on the maximum ductility and minimum formation of intermetallic compounds, which was restricted by the graphene platelets in preventing the formation of oxides, which resulted in defect-free joint.

4.2.2 Microhardness

In a linear weld without pin offset, the average microhardness of 97 HV was achieved, whereas weave weld with pin offset attained an average microhardness value of 126 HV. Top of the weld nugget showed hardness value of 132 HV compared with the middle and bottom layers. This is due to the grain refinement and higher dislocation density at the nugget. The high fluctuation in the hardness value within the nugget is due to the existence of corresponding IMCs. The HAZ showed the minimum hardness value of 76 HV compared with the other zones of joint as shown in Fig. 9. This is due to the development of grain coarsening [33]. In FSW dissimilar welding, the higher hardness value was recorded at the Al–Cu weld nugget because of the dynamic recrystallization. The development of rigid IMCs along with intensive plastic deformation in the SZ caused higher hardness values when compared with the aluminium and copper base materials [34]. In general, an increase in tool rotational speed increases the grain refinement strengthening which are the reasons for the increase in the hardness in SZ.

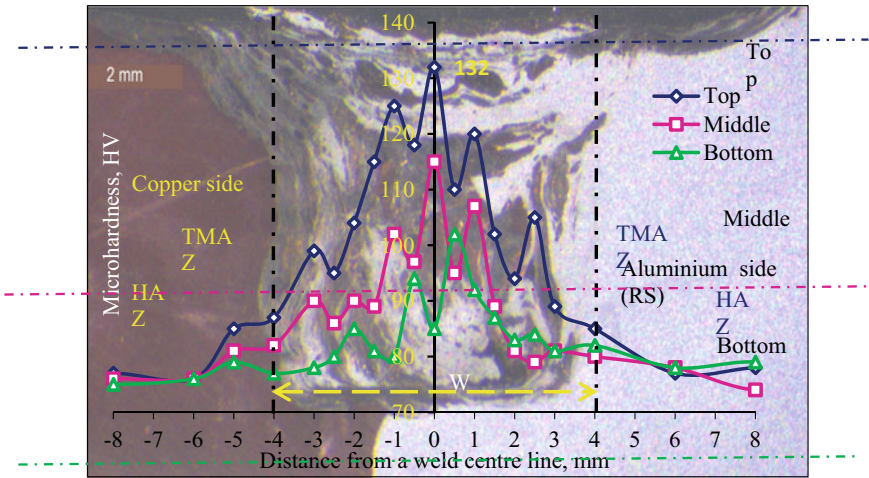


Fig. 9 Distribution of hardness along the transverse section of the weld made by WW-WPO (with GNP)s of 1000 rpm; 50 mm/min; 12 kN

4.2.3 Microstructure

The weave weld with pin offset provides defect-free weld joints (Fig. 10a). Deficient temperature contribution at low speed of 800 rpm prompting to a low quality of weld. This statement is similar to that found in the previous study [35].

Homogenous distribution of Copper in the AA 6061-T6 was attained in weave weld conditions with the use of GNP)s due to the larger stirring area and the high volume of material transportation. The increase in the hardness of 132 HV at the top of the weld nugget was due to the presence of a high amount of disintegration

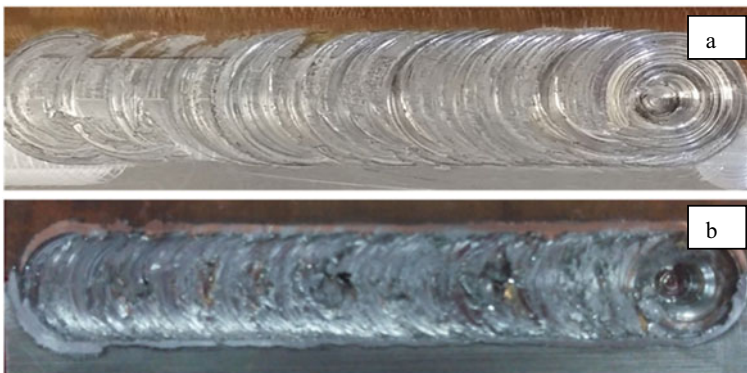


Fig. 10 Surface morphology of AL-Cu joint fabricated at 1000 rpm Under EWW-WPO (with GNP)s. **a** 1000 rpm, **b** 800 rpm

of Cu particles that might be regulated by selecting appropriate process parameters. The transverse cross-sectional characterization on the weld NZ is observed through macrostructure as shown in Fig. 11. The microstructure of base metal of AA6061 and pure copper is shown in Fig. 11a, b. The OM images justified a grain microstructure refinement in the SZ of the weld joints. The spread of copper particles in the aluminium matrix in the form of vortex flow at the top surface of the nugget could be observed through OM as shown in Fig. 11c. The formation of a long band of copper metal over the aluminium phase could be seen as shown in Fig. 11d. The onion ring formation is shown in Fig. 11e is the direct evidence for material transportation in the FSW. At 1000 rpm, the nanoplatelets are evenly dispersed throughout the weld nugget and fill the voids resulting in the absence of defects in the joint (Fig. 12).

Figure 13a justifies that the improper mixing at interface zone and intensive material clustering existing at the SZ due to improper flow of material flow. The pin aggregated the materials closer to the TMAZ due to the flow of materials downward.

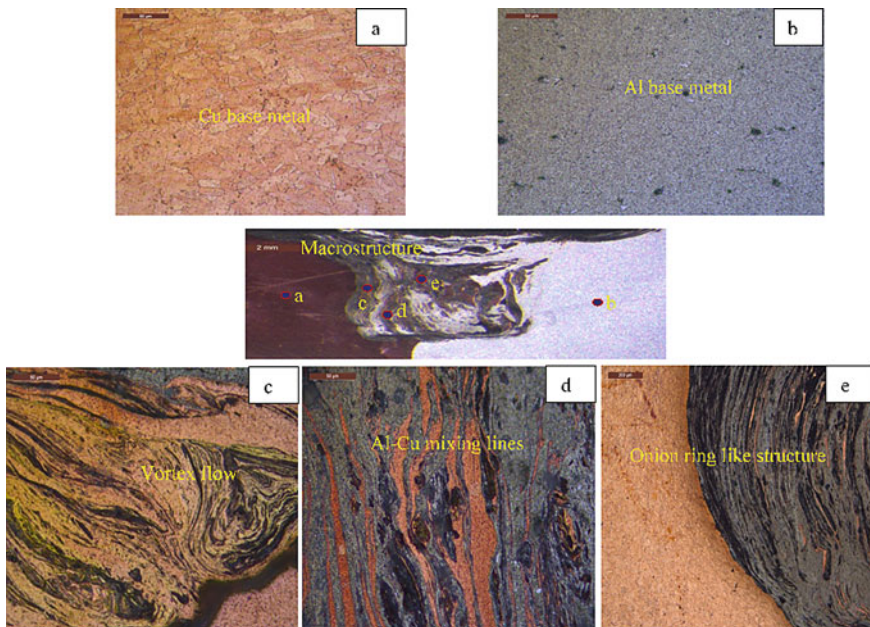


Fig. 11 Macrostructure of joint made by WW-WPO (with GNPs) of 1000 rpm **a** Cu base metal, **b** Al base metal, **c** Vortex flow like intercalated pattern, **d** lamellar like shear bands in the weld region (mixing lines) **e** Onion ring structure

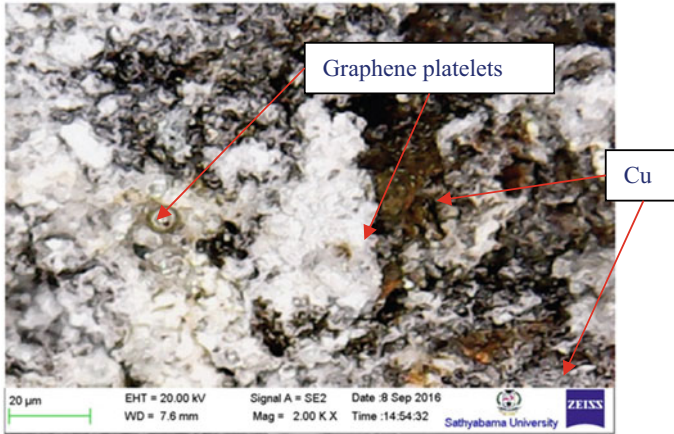


Fig. 12 Graphene existence observed through SEM at the SZ of Al–Cu joint

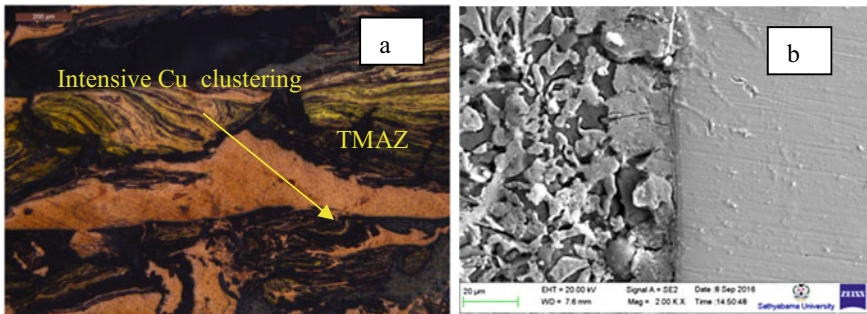


Fig. 13 a Intensive material clustering b Grain growth at stir zone

4.3 The Effect of Welding Speed Without GNPs

4.3.1 Tensile Properties

The welding speed is the critical parameter for producing a sound weld which can contribute around 33% in FSW joint strength as stated in the previous literature. Welding speed impacts the grain growth of the joints. By changing the welding speed, the temperature in the weld region can be altered. The thickness of the IMCs at the nugget area can be controlled by adjusting the same [36]. At lower welding speed, heat generation will be more in the SZ. Which experience the turbulent flow, dissimilarity in the flow stress and weaker compaction of the Al and Cu resulted in the defects generation in the SZ [37].

Linear weld without pin offset produced the UTS value of 148 MPa at 40 mm/min. As welding speed reached beyond the specified limit of 50 mm/min, the tensile

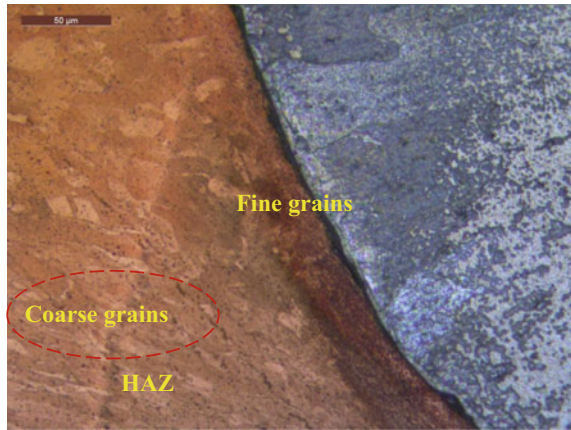
strength of the joints tends to get reduced. Surface morphology of the weld joint made under LW-WOPO condition at 40 mm/min is shown in Fig. 14a. Higher speed of 70 mm/min builds up lot of defects while lower welding speed encourages good joints [34]. When the welding speed increases, the plasticized weld metal is formed with the high frictional heat. Besides, eccentric weave weld with pin offset condition produced a UTS value of 174 MPa at 50 mm/min. Defect-free surface morphology of the weld joint made under EWW-WPO condition at 50 mm/min is shown in Fig. 14b. In a linear weld without a tool pin offset, the maximum NTS of 102 MPa was achieved at the welding speed of 40 mm/min. With an increase in welding speed to 70 mm/min, the tensile characteristics of the notched specimens tended to reduce due to the creation of more localized defects. Lower welding speed tended to enhance the material blending region and uniform IMCs development as stated in the previous study [38]. In the weave weld with the tool, pin offset the NTS value of 116 MPa was observed in the nugget at 50 mm/min.

In a linear weld, the YS of 130 MPa was noticed without pin offset. On the other side, in weave condition, a significant volume of metal transportation from front to forth under tool pin area and adequate dispersion of Al–Cu was seen with an increase in holding time which is due to both X–Y axes lead tool movement. The maximum increase in YS of 154 MPa was observed with the tool pin offset at 50 mm/min. A higher speed of 70 mm/min resulted in the lowering of the stirring rate which caused a reduction in impact strength of the welded joints. Further, the formation of oxidation and fragmental cracks resulted in a slight reduction in the impact strength. The maximum impact strength achieved in linear weld without pin offset was 6.5 J at 40 mm/min. But, in the eccentric weave weld, a better stirring of metals was attained due to the existence of a substantial welding area. The resulting value for eccentric weave pattern with pin offset was 8.9 J at 50 mm/min due to mechanical strain and heat input with proper process condition at the SZ.



Fig. 14 Surface morphology of the weld joint **a** LW-WOPO at 40 mm/min, **b** EWW-WPO at 50 mm/min

Fig. 15 Grain coarse at the HAZ



4.3.2 Microhardness

In dissimilar FSW welding, hardness was found to be higher at NZ compared with base materials. This was due to the severe plastic deformation and generation of IMCs phases in the SZ as per the Hall–Petch effect [39, 40]. When the speed of welding increased with the nominal tool rotational speed of 1200 rpm, the hardness of the material was also found to increase. In linear weld without pin offset, the microhardness value of 79 HV was achieved. On the other hand, an eccentric weave weld with a pin offset produced a maximum Vickers microhardness. The value observed was 100 HV. This was due to a large volume of plasticized material transportation and precipitation hardening effect. Higher heat input conditions resulted in formation of IMCs in SZ that increased the hardness. The HAZ exhibited a low hardness due to the occurrence of the grain coarsening effect which can be seen in Fig. 15. A similar statement had been made in the previous literature [38].

4.3.3 Microstructure

At 50 mm/min, grain size gets decreased resulting in the occurrence of dynamic recrystallization, which could be visible in both the top surface and the root of the weld nugget that is observed through OM. This reduction in grain size is due to the pinning effect of intergranular cracking of Al and Cu molecules. In FSW, the linear weld configuration resulted in a weaker joint efficiency and resulted in the defects such as improper mixing, smaller grain refinement, voids, etc. This statement was in line with the study made by [41, 42]. Formation of dendrites of micro-sized structure and spreading throughout the metallic phase of copper.

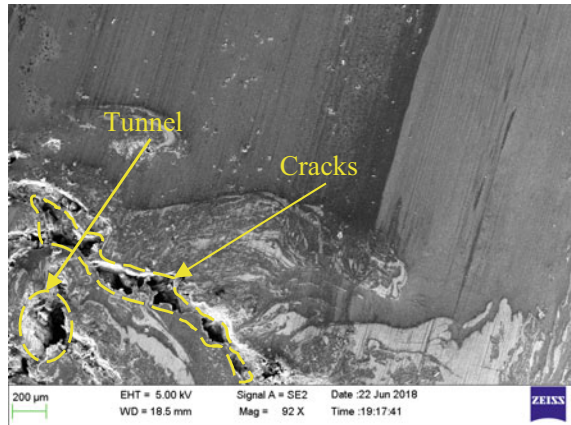
4.4 *The Effect of Welding Speed with GNPs*

4.4.1 **Tensile Properties**

The main reason for the grain growth and cluster of CuAl_2 precipitates is the slower cooling rate and higher temperature at slow speed of welding. At 40 mm/min, the UTS value of 159 MPa under linear weld without pin offset was observed. When welding speed increased, the plasticized weld metal was formed with high frictional heat. At 70 mm/min, the UTS became low to 129 MPa. Rise in viscosity in the weld zone led to high heat generation and increased extrusion intensity attributed to grains growth lowering the strength with brittle fracture behavior [43]. The parameters such as tool rotational speed and welding speed had control over the heat input in the weld region. High heat developed instigated insufficient stirring in the FSP zone at higher speed of weld with the nominal rotational speed of 1200 rpm leading to poor tensile strength [30]. The amount of material carried and extruded backward per rotation by the pin increased with the proper variables such as rotating speed and welding speed. This increased volume of material with proper mixing was attained with the help of eccentric weave weld with pin offset. Thus the strain hardening and fine grain refinement in the SZ resulted in better mechanical characteristics. Therefore, strength increase took place in the weld joint due to the incidence of strain hardening and shrinking of grains [43].

The linear weld with pin offset condition showed a UTS value of 170 MPa at 40 mm/min. Visco-plastic deformation occurred in SZ with a decrease in welding speed in the eccentric weave weld. In a previous investigation, A maximum UTS of 135 MPa was reported by [34, 44]. In our study, the eccentric weave weld pattern with tool pin offset attained maximum UTS of 195 MPa at 50 mm/min. The higher tensile strength was observed in eccentric weave weld condition compared with the liner weld as the result of uniform agglomeration of intergranular particles in the SZ. The addition of nanoplatelets also enhanced the performance of the joint by reducing voids and oxidation problems. In a linear weld without tool pin offset, the NTS value was 109 MPa attained at 40 mm/min. The tensile strength value was attained in an eccentric weave pattern without tool pin offset 129 MPa at 50 mm/min. The use of GNPs resisted the formation of oxides. At 30 mm/min, NTS of 105 MPa under tool pin offset condition was recorded. It was observed from the results obtained by [45], greater than 50 mm/min caused the tensile characteristics of the notched specimens tended to reduce with the creation of localized defects. Meanwhile, on lower welding speed, the efficient stirring on the point to point locations of the feed direction enhanced the mixture of particles, thereby increasing the strength. This statement was similar to the previous literature [46]. Study made by [47], revealed that in a linear weld without pin offset, the YS of 138 MPa was observed. In an eccentric weave pattern, the tool pin covered a larger area leading to an increase in the TMAX. Hence, maximum dynamic recrystallization took place resulting in high tensile strength. Graphene nanoplatelets were used for avoiding the voids and micro-cracks propagation problems in the weld zone. The maximum YS in eccentric weave

Fig. 16 Defect propagation under LW-WOPO at 70 mm/min



FSW with tool pin offset was 164 MPa with the addition of Graphene nanoplatelets. With the increase in welding speed beyond 50 mm/min, defects such as cracks and tunnels which deteriorated ductility resulting in a reduction in YS of the weldments as shown in Fig. 16. In a linear weld, the tool pin covered a minimum area which caused a reduction in the SZ and TMAZ and incomplete dynamic recrystallization took place which resulted in reduced impact strength. At 70 mm/min, the weld region could not be stirred efficiently leading to reduced mixing and thereby reducing the impact strength of the joints. The maximum impact strength value attained under linear weld without pin offset was 7.2 J at 40 mm/min. Besides, in weave weld with pin offset, the impact strength value was 10.2 J at constant a speed of 1200 rpm and axial load of 12 kN. This was due to the presence of graphene nanoplatelets which could avoid oxidation and fragmental cracks.

In a linear weld without pin offset, the elongation percentage was 9.6%. The use of graphene particles in nanoplatelets forms reduced the oxide formation. The maximum elongation percentage of 7.6% was attained at the eccentric weave underpin offset condition. Besides, the eccentric pin weld condition produced a higher active frictional area than other weld conditions. The joint obtained with a welding speed of 70 mm/min provided higher elongation due to high heat generation which caused the plastic flow of material with appropriate welding conditions. Greater than 70 mm/min, the elongation percentage decreased due to the reduction of avoidable grain evolution in a welded region [48]. Heat distribution dropped with a rise in welding speed and tool eccentricity [49].

4.4.2 Microhardness

The microhardness mainly depends on the welding speed. Rise in hardness resulted in as the welding speed rose at a nominal speed of 1200 rpm. The presence of uniform

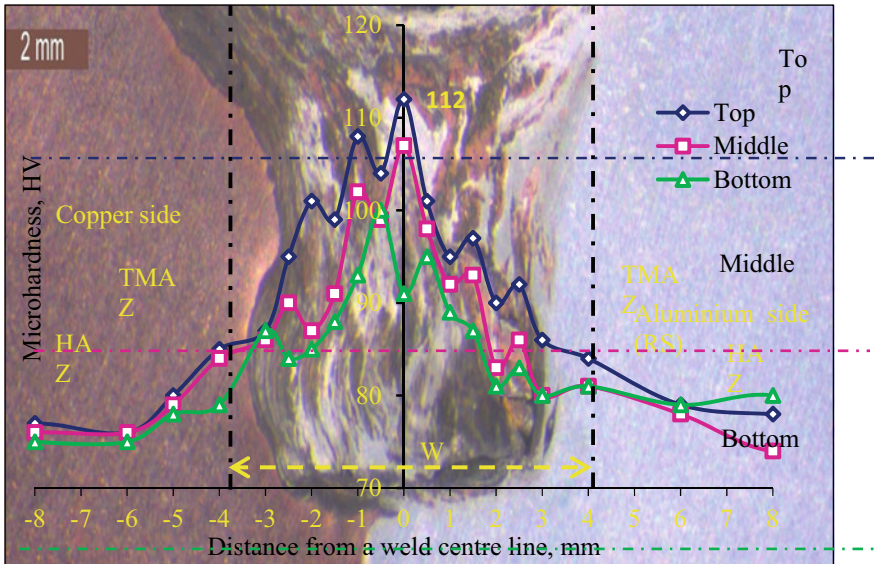


Fig. 17 Distribution of hardness along transverse cross-section of the weld made by WW-WPO (with GNPs) of 1200 rpm; 50 mm/min; 12 kN

grains at the weld nugget led to increased microhardness and mechanical properties as stated in the previous work [50].

The addition of graphene platelets has greater impact on the hardness. The average hardness of the joints increased through an increase in volume fraction. In a linear weld with pin offset, the maximum microhardness value was 92 HV at 40 mm/min. The eccentric weave weld with pin offset condition achieved the maximum microhardness value of 112 HV with a speed of 50 mm/min. Distribution along the transverse section of the weld made by EWW-WPO (with GNPs) is shown in Fig. 17. It is observed from Fig. 17 that the top region attained a maximum microhardness value of 112 HV compared with the middle and bottom of the cross-section. Small uniform grains are observed in the SZ. During the FSW process, a significant amount of heat generated in the SZ along with DRX caused by the intense shear deformation resulted in uniform grains at the SZ. This was due to the incidence of thin IMC layers at the Al–Cu intergranular area. The hardness value increased due to the fine grain refinement and the effect of mechanical twinning [51].

4.4.3 Microstructure

Joint fabricated using 50 mm/min under EWW-WPO (with GNPs) is shown in Fig. 18. The base micrographic image of base metals Cu and Al can be seen in Fig. 18a, b respectively. With the effect of welding speed, fragments of copper particles are observed in the longitudinal side of the nugget. Al₄C₃ phase is shown in Fig. 18c.

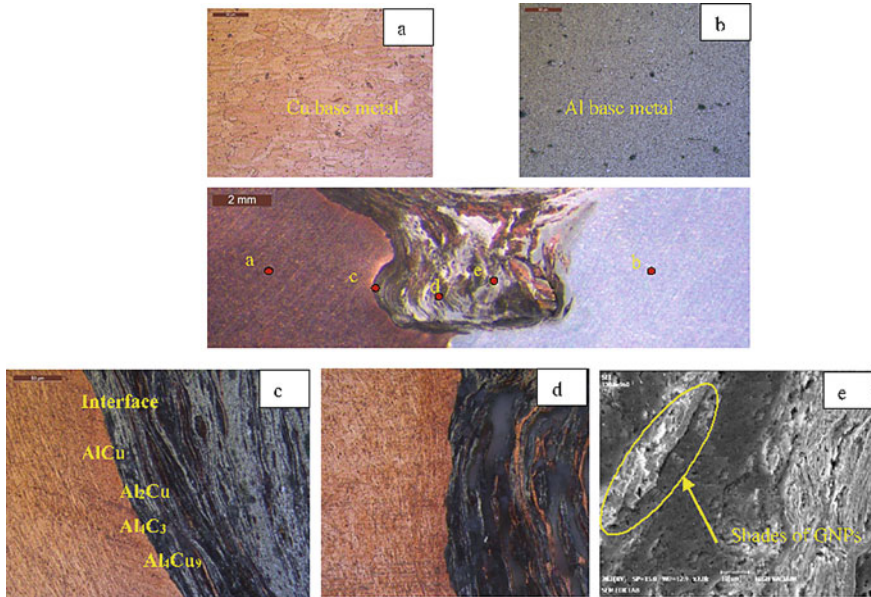


Fig. 18 Joint fabricated using 50 mm/min under EWW-WPO (with GNPs). **a** Cu base metal. **b** Fine grains with a thin layer of Cu in Al matrix. **c** interface zone at the Cu side. **d** Uniform dispersion at the weld nugget. **e** Shades of graphene particles existing inside the weld matrix

This phase is reported continuously in the Al nugget as dispersed particles. The dispersed particles at NZ is due to the stirring broke copper and dispersed them. Uniform scattering of these particles into the copper matrix occurred significantly through the adequate mixing activity offered by the FSW tool at the welding speed of 50 mm/min as can be seen in Fig. 18d. The great bonding between the copper matrix with Graphene particles caused a tendency to the formation of fewer voids in the weld joint region. This condition of an issue takes in the improvement of a perfect interface with great bonding amongst reinforcement and matrix material. Presence of graphene particles was observed and dispersed effectively on aluminium phase material which can be seen from Fig. 18e.

In the reinforced FSP matrix, significant improvement in microhardness was noticed on a par with the unreinforced matrix. An increase in tool pin eccentricity provided an increase in energy per unit length with the same welding speed as in the case of a normal pin. This could be attributed to the increase in rotational volume that required a higher force [49]. On the other hand, some limited researchers conducted research only with the use of GNPs metal matrix nanocomposites [52]. This is because of some interfacial bonding issues of MMCs and carbon base material and also problems faced in obtaining a good dispersion of GNPs within the metal matrix. The interfacial bonding between matrix and graphene nanoparticles primarily regulated the performance of physical or mechanical properties of the joint [52].

4.5 The Effect of Axial Load Without GNPs

Axial load is a more responsible for surface appearance and value of the FSW weld joints. The lower axial load led to the formation of defects such as tunnels and cracks due to the lower downforce resulting in a restriction to the vertical flow of the material in the cross-section of the weld. Besides, a further increase in axial load beyond the limit produced a significant amount of flash due to excessive thinning of the weld area [53]. On the other hand, at nominal axial load, equiaxed grains with a uniform dispersion of the precipitates were seen [48].

4.5.1 Tensile Properties

In linear weld without pin offset condition, a lower UTS value of 154 MPa was attained due to smaller heat input and plasticization that occurred in smaller volume. When the axial load exceeded the limit of 14 kN, the plastically deformed weld area was formed which led to a lower UTS value of 143 MPa. A maximum UTS of 181 MPa was achieved under eccentric weave weld with pin offset condition at the axial load of 14 kN. Some surface-oriented problems like flashes and surface lines were found reduced in eccentric weave weld with pin offset condition. A gradual increase in NTS value was observed in weave weld conditions with the axial load. In the weave weld condition, a maximum NTS value of 127 MPa was obtained. While increasing the axial load beyond 14 kN, fragmental cracks and voids were formed in the weld nugget as shown in Fig. 19. Thus resulting in a lower in the NTS value of 97 MPa at 16 kN under LW-WOPO condition.

The axial load is an important process parameter to attain a higher YS value in the weave weld condition of Al–Cu joints. In a linear weld without pin offset, a maximum YS value of 138 MPa was observed. On the other hand, weave weld with pin offset condition recorded the maximum YS value of 162 MPa with an axial load of 14 kN. With an increase in axial load, the pin plunged deep inside the material creating a high shear force that dragged the phase materials shifting towards the AS. This phenomenon increased the mechanical characterization that led to an increase in yield strength. Effective weldment with better yield strength was observed in weave

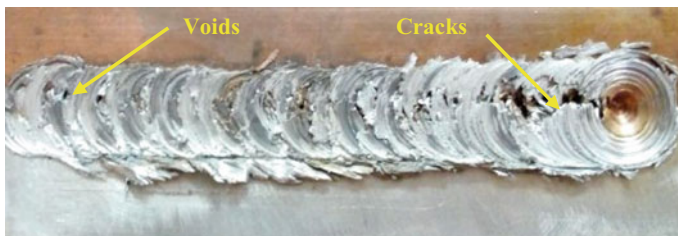


Fig. 19 Joint fabricated at 16 kN under LW-WOPO condition (Cracks and Voids at the weld nugget)

weld with pin offset condition. Whereas, the axial load was set to be higher during the penetration of the tool pin (initial plunging before the attainment of viscoplastic nature at the nugget region). Similar results were discussed in the previous literature [54]. The proper axial load should be selected for the homogeneous distribution of heat input along the traverse direction of a tool. In a linear weld without pin offset, recorded a lower impact strength of 7.2 J due to the thin weld area. When the weave weld with pin offset was used, the maximum impact strength of 9.6 J was observed with the axial load of 14 kN due to better stirring of base metals. It can be observed from the results that the weaving motion of the tool was found more effective than the linear pattern with the same axial load. In a linear weld without pin offset, the percentage of elongation obtained was 9.4% with the axial load of 16kN. Besides, weave weld achieved the maximum percentage of elongation of 7.2% accounting for the axial load of 16kN due to sufficient heat input available at the weld nugget.

4.5.2 Microhardness

Linear weld without tool pin offset reached the average microhardness value of 86 HV at 12 kN axial load, due to the inadequate stirring effect and coarsening of grains. Since more downward force is imparted by the tool, copper gains more hardness. This statement was coherent with the previous literature [27]. When the axial load increased, the material forged downward underneath the shoulder which led to an increase in the microhardness of 105HV. This was because of the presence of a higher amount of Cu particles around the tool plunge region. The fraction of Cu particles being higher at the tool plunge region resulted in the homogeneous material mixing, fine and uniform grains, and lamella structure. This statement was in agreement with the previous study [27]. Further, non-uniform hardness distribution was seen in dissimilar Al–Cu joints. A similar kind of result was reported in the previous literature [55].

4.5.3 Microstructure

The effect of an axial load of 8kN under the linear weld without pin offset led to the formation of the non-uniform phase mixing of the dissimilar metals. This was because of the generation of thick and irregular lines on the top surface of the weld nugget resulting in improper mixing of phase metals (Fig. 20a).

The fragmental cracks and pores were formed in the joints at the lower axial load of 8kN that led to inferior weld strength which can be observed through SEM image and it can also be visible in Fig. 20b. Further, an incorrect welding parameter of too small tool plunge depth generated defects like pores and cracks in the weld nugget. This statement was in agreement with the previous study [56].

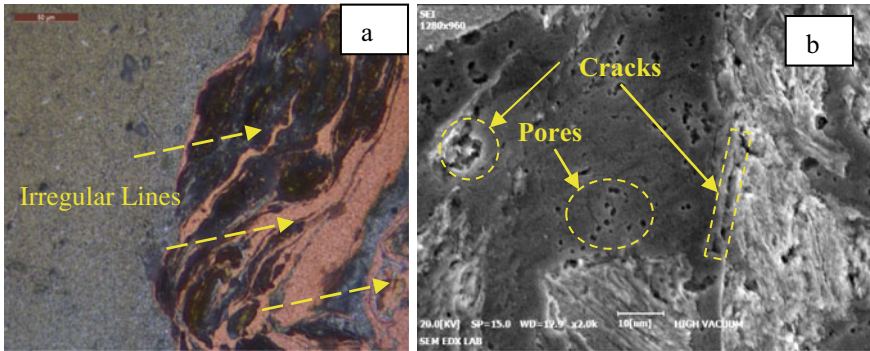


Fig. 20 Joint fabricated at 8kN under LW-WOPO condition, **a** Thick & irregular lines at the top of the weld nugget, **b** cracks and pores through SEM image at the weld nugget

4.6 The Effect of Axial Load with GNPs

4.6.1 Tensile Properties

The inference of an axial load has a considerable consequence towards tensile properties of Al–Cu welds. For all the welding conditions, the UTS increased with an increase in the axial load up to an absolute limit of 14 kN and then started decreasing. This statement is coherent with the previous study [57]. The surface morphology of the weld joint under LW-WOPO at 12 kN is shown in Fig. 21a. As the axial load increased to 14 kN, the frictional heat generation was higher at the NZ. At a lower axial load of 8 kN, peak temperature at the nugget region was low that led to incomplete dynamic recrystallization caused by coarse grain formation in the NZ which

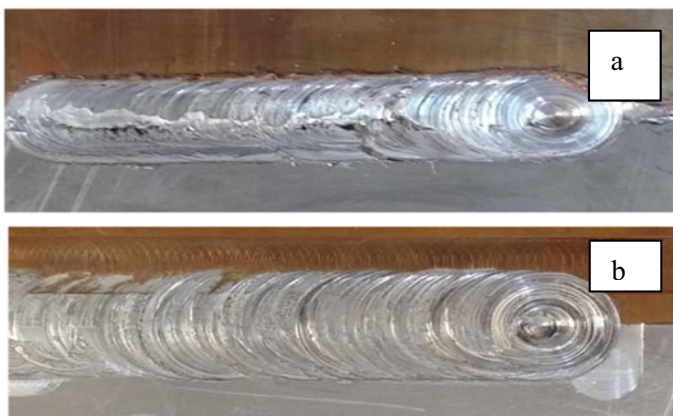


Fig. 21 Surface morphology of the weld joint, **a** at 12 kN under LW-WOPO (with GNPs), **b** at 14 kN under EWW-WPO (with GNPs)

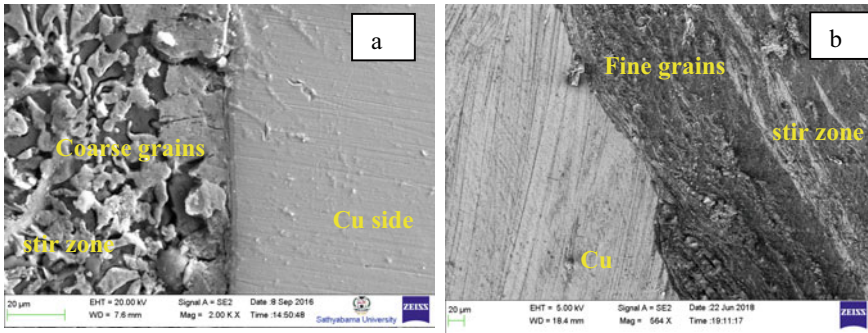


Fig. 22 a Coarse grains under LW-WOPO at 8kN, b Fine grains under EWW-WPO at 14 kN

can be seen in Fig. 22a. This caused an acceleration in the rise of fine grains as presented in Fig. 22b. This statement was in agreement with the previous literature [58]. In a linear weld without tool pin offset, a thin weld area was produced which resulted in achieving the low UTS value of 167 MPa at an axial load of 12 kN. The asymmetry of the material deformation got reduced by the axial load. This statement was coherent with the previous study [59].

As the axial load surpassed the limit of 14 kN, a plastically deformed weld area was formed which resulted in lower UTS. Eccentric weave weld made good stirring of AA 6061-T6 and pure Cu metals. In the previous literature, A maximum UTS value of 208 MPa [60]. In this study, among the four weld conditions, the maximum UTS of 212 MPa was noticed at the axial load of 14 kN in the eccentric weave weld with GNPs. The surface morphology of the weld joint fabricated under EWW-WPO (with GNPs) is presented in Fig. 22b. When the hardness value in the bead was higher than the source, at the higher axial load of 16 kN, a fracture could be formed on the parent material.

The maximum NTS value of 146 MPa was attained at the axial load of 14 kN under eccentric weave weld with pin offset (with GNPs). The weave weld with pin offset condition increased the volume of plasticized material transportation and heat input. An increase in NTS was due to the grain refinement during DRX at SZ and the robust interface between the nanoparticles and aluminium matrix led to the increasing of mechanical properties [22].

Linear weld without pin offset condition achieved the YS of 147 MPa at the axial load of 12 kN. Besides in eccentric weave weld with tool pin offset condition (with GNPs), the maximum YS of 175 MPa was observed with the axial load of 14 kN. The graphene nanoplatelets served as filler material in the voids and micro-cracks which were due to orowan strengthening and hardening effect at the interface of grain boundary and graphene platelets (Fig. 23a–b). A similar trend was followed in the previous study [61].

The significant role of the axial load acting on the tool pin at SZ during traverse motion is that it could restrict the grain growth. This was due to the occurrence of a large volume of the deformation caused by heat and strain at the nugget which

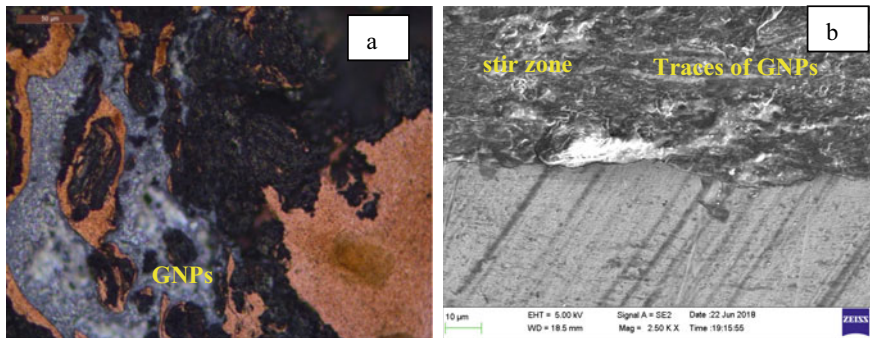


Fig. 23 Traces of GNPs at the weld nugget under EWW-WPO condition at 14 kN **a** OM image, **b** SEM image

was responsible for the hardness and impact strength. The axial load was applied to the rotating tool on the vertical axis. Proper dispersion of particles in Al matrix and uniform material flow occurred at 14 kN under weave weld with pin offset (with GNPs) resulting in better impact strength of 11.8 J. On the other hand, under linear weld without pin offset, the low impact strength of 8.5 J was attained at 12 kN. However, a further increase of axial load to 16 kN prompted surface-oriented problems and formation of defects such as fragmental cracks and pores and reduced the impact strength which can be seen in Joint No. 17 and it is presented in Table No. 1.

In a linear weld without tool pin offset, the elongation percentage of 9.8% was obtained. Besides, under eccentric weave weld condition, the axial load played an essential role in the stirring. The weave weld was found to be more effective than the linear weld due to both X–Y axes movement of the tool and higher holding time. The eccentric weave weld produced an elongation value of 7.9% at the axial load of 16kN.

4.6.2 Microhardness

In linear weld without pin offset a microhardness value of 90 HV at 12 kN was attained. The maximum microhardness value of 120 HV was achieved at the axial load of 14 kN in eccentric weave weld with pin offset (with GNPs). This was due to the grain refinement at SZ (Fig. 24a–b).

Hardness along the transverse section of EWW-WPO at 14 is shown in Fig. 25. A maximum hardness value of 124 HV was observed at the top region compared with the middle and the bottom. As per the Hall–Petch effect, the hardness value is inversely proportional to the grain size. Moreover, the presence of tiny particles of IMCs, confer to the orowan mechanism [62]. Hence, the incorporation of nanoparticles increases the hardness through microstructural refinements which are evidenced by micrographs.

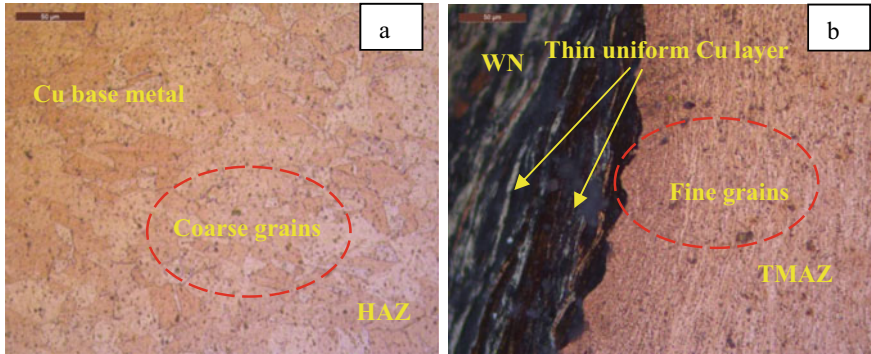


Fig. 24 a large grains at the Cu base metal, b Grain refinement under weave weld condition (with GNPs) at 14 kN

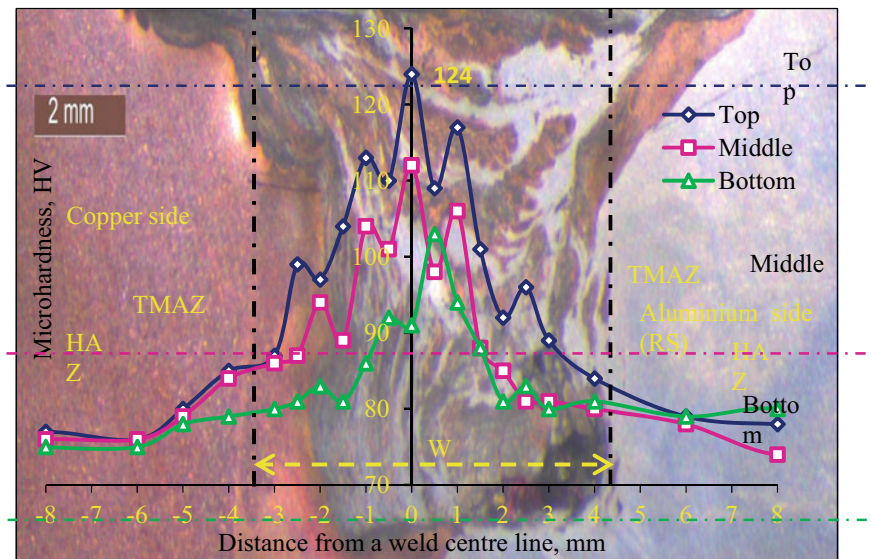


Fig. 25 Distribution of hardness along the transverse section of the weld made by WW-WPO (with GNPs) of 1200 rpm; 50 mm/min; 14 kN

4.6.3 Microstructure

The effect of a lower axial load of 8kN under the linear weld condition led to heterogeneous dispersion of Cu and GNPs particle in the Al matrix because of lower plunge force which can be seen in Fig. 26a. On the other hand, under eccentric weave weld conditions, the microstructure led to the observation of uniform dispersion of graphene platelets over the aluminium phase at the axial load of 14 kN as can be seen in Fig. 26b.

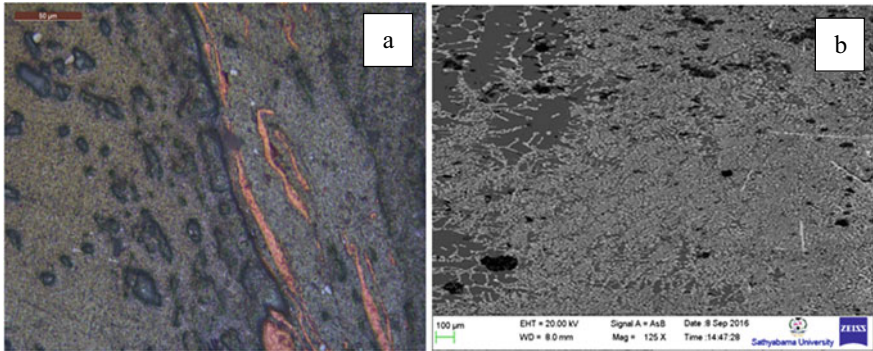


Fig. 26 **a** Heterogeneous mixing in the weld nugget under LW-WOPO, **b** Uniform dispersion at the WN under EWW-WPO

The joint fabricated under EWW-WPO at 14 kN is presented. An increase in the axial load can enhance the blending nature of layered metals in the weld nugget and subsequently build the quality of welds. The microstructure image of base metal Cu and Al is shown in Fig. 27a–e. The layer of copper measured inside the Al base is smaller as shown in Fig. 27c and witnessed by [64]. The motive behind the shape distribution behaviour is the increment in the temperature of WZ leading to softening

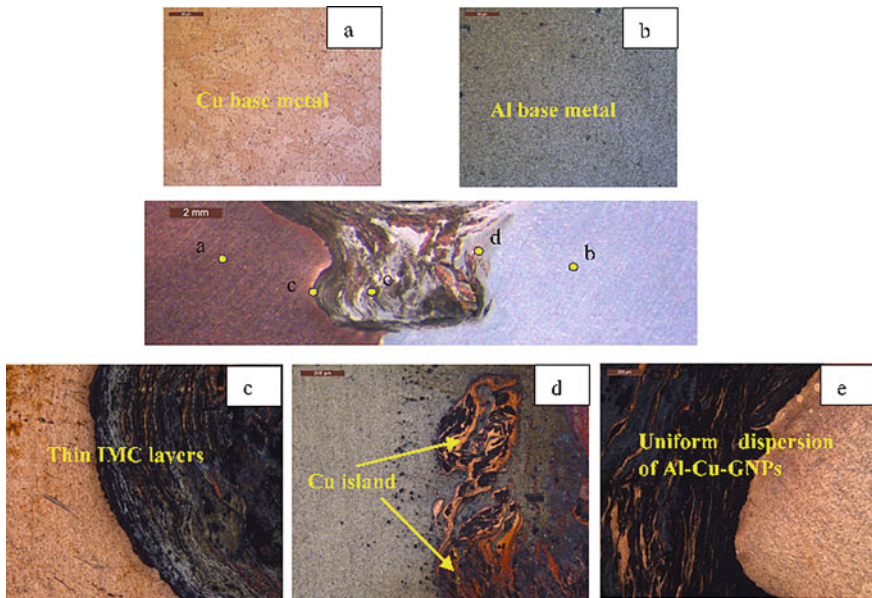


Fig. 27 Joint fabricated under EWW-WPO at 14 kN. **a** Cu base metal, **b** Al base metal, **c** Uniform IMCs layers, **d** Cu island in Al matrix, **e** Uniform dispersion of Al-Cu-GNPs particles in weld nugget

at high speeds. Nonetheless, with a more noteworthy blend limit of materials at a higher axial load of 16 kN, weak intermetallic mixes are framed, which can reduce the quality of the joints. Reinforcement of nanoparticles had a superior effect on the mechanical characteristics of the samples. This is because of Orowan strengthening mechanism [61, 62].

5 Conclusion

The following observations were made based on the experimental results under unreinforced graphene nanoparticles.

1. An UTS of 187 MPa, YS of 168, elongation of 7.6%, were achieved under the process parameters of $N = 1000$ rpm; $v = 50$ mm/min; $F = 12$ kN in eccentric weave with pin offset condition.
2. The maximum impact strength observed under the process parameters of $N = 1000$ rpm; $v = 50$ mm/min; $F = 12$ kN was 10.1 J in eccentric weave with pin offset condition.
3. The maximum NTS of 132 MPa was noticed under the process parameters of $N = 1000$ rpm; $v = 50$ mm/min; $F = 12$ kN in eccentric weave with pin offset condition.
4. The average microhardness of 110 HV was seen under the process parameters of $N = 1000$ rpm; $v = 50$ mm/min; $F = 12$ kN in eccentric weave with pin offset condition.
5. Linear weld and eccentric weave with pin offset produced the good performance of weld strength at 12 kN and 14 kN respectively. This was due to the proper downward plunging force and transportation of material under the tool causing better dispersion of Al–Cu particles. And also the uniform distribution of heat throughout the SZ.

The following observations were made based on the experimental results under reinforced graphene nanoplatelets:

1. The dissimilar joints made using eccentric weave FSW with pin offset exhibited superior mechanical properties, viz UTS of 217 MPa, YS of 182 MPa, NTS of 152 MPa, elongation of 8.7%, and impact strength of 12.4 J.
2. The best tensile strength obtained with the effect of tool rotational speed under eccentric weave weld with tool offset condition with reinforcement was 13.82% higher than the weld obtained under the same condition without reinforcement. This was 77.5% of aluminum and 96.44% of copper base material strength.
3. The effect of reinforcement of GNPs enhanced the mechanical properties of the weld joints as fibrous particles in nano levels, which in turn increased the tensile properties of joints without losing ductility based on the hall–Petch effect and Orowan strength breaking effect.

4. IMCs such as AlCu, Al₂Cu, and Al₄Cu₉ large size band layer was observed with the welding conditions LW-WOPO, whereas in a condition such as WW-WPO, EWW- WPO resulted in the formation of the thin uniform layer.
5. The formation of IMC Al₂C and Al₄C₃ (aluminum carbide) was found in the weld nugget for the joint made with the addition of GNPs.
6. The average hardness value observed at weld zone was 110 HV for weave weld made with tool pin offset (without GNPs), whereas a hardness value of 96 HV was observed for linear weld made with pin offset (without GNPs).

References

1. Ouyang, J. H., & Kovacevic, R. (2002). Material flow and microstructure in the friction stir butt welds of the same and dissimilar aluminum alloys. *Journal of Materials Engineering and Performance*, 11(1), 51–63.
2. Ouyang, J., Yarrapareddy, E., & Kovacevic, R. (2006). Microstructural evolution in the friction stir welded 6061 aluminum alloy (T6-temper condition) to copper. *Journal of Materials Processing Technology*, 172, 110–112.
3. Liu, P., Shi, Q. Y., Wang, W., Wang, X., & Zhang, Z. (2008). Microstructure and XRD analysis of FSW joints for copper T2/aluminum 5A06 dissimilar materials. *Materials Letters*, 62, 4106–4108.
4. Sinha, V. C., Kundu, S., & Chatterjee, S. (2016). Microstructure and mechanical properties of similar and dissimilar joints of aluminium alloy and pure copper by friction stir welding. *Perspectives in Science*, 8, 543–546.
5. Muthu, M. F. X., & Jayabalan, V. (2016). Effect of pin profile and process parameters on microstructure and mechanical properties of friction stir welded Al–Cu joints. *Transactions of Nonferrous Metals Society of China*, 26(4), 984–993.
6. Mubiyai, M. P., & Akinlabi, E. T. (2017). Characterization of the intermetallic compounds in aluminium and copper friction stir spot welds. *Materials Today: Proceedings*, 4, 533–540.
7. Shi, H., Chen, K., Liang, Z., Dong, F., Yu, T., Dong, X., & Shan, A. (2017). Intermetallic compounds in the banded structure and their effect on mechanical properties of Al/Mg dissimilar friction stir welding joints. *Journal of Materials Science and Technology*, 33(4), 359–366.
8. Zhang, W., Shen, Y., Yan, Y., & Guo, R. (2017). Dissimilar friction stir welding of 6061 Al to T2 pure Cu adopting tooth-shaped joint configuration: Microstructure and mechanical properties. *Materials Science and Engineering A*, 690, 355–364.
9. Oliveira, J. P., Duarte, J. F., Inacio, P., Schell, N., Miranda, R. M., & Santos, T. G. (2017). Production of Al/NiTi composites by friction stir welding assisted by electrical current. *Materials and Design*, 113, 311–318.
10. Khodabakhshi, F., Arab, S. M., Svec, P., & Gerlichd, A. P. (2017). Fabrication of a new Al-Mg/graphene nano composite by multi-pass friction-stir processing: Dispersion, microstructure, stability, and strengthening. *Materials Characterization*, 132, 92–107.
11. Lee, I. S., Hsu, C. J., Chen, C. F., Ho, N. J., & Kao, P. W. (2011). Particle-reinforced aluminum matrix composites produced from powder mixtures via friction stir processing. *Composites Science and Technology*, 71(5), 693–698.
12. Wang, W., Shi, Q. Y., Liu, P., Li, H. K., & Li, T. (2009). A novel way to produce bulk SiCp reinforced aluminum metal matrix composites by friction stir processing. *Journal of Materials Processing Technology*, 209(4), 2099–3103.
13. Cabibbo, M., Forcellese, A. M., Simoncini, M., Pieralisi, D., & Ciccarelli, . (2016). Effect of welding motion and pre-/post-annealing of friction stir welded AA5754 joints. *Materials & Design*, 93, 146–159.

14. Suresh, S., Venkatesan, K., Natarajan, E., & Rajesh, S. (2020). Performance analysis of nano silicon carbide reinforced-swept friction stir spot weld joint in AA6061-T6 alloy. *Silicon*. <https://doi.org/10.1007/s12633-020-00751-4>.
15. Suresh, S., Venkatesan, K., Natarajan, E., & Rajesh, S. (2020). Influence of tool rotational speed on the properties of friction stir spot welded AA7075-T6/Al₂O₃ composite joint. *Paper Presented at the Materials Today: Proceedings*, 27, 62–67. <https://doi.org/10.1016/j.matpr.2019.08.220>.
16. Suresh, S., Venkatesan, K., & Natarajan, E. (2018). Influence of SiC nanoparticle reinforcement on FSS welded 6061-T6 aluminum alloy. *Journal of Nanomaterials*. doi:<https://doi.org/10.1155/2018/7031867>.
17. Arun Kumar, S., Ramesh, S., Kedarvignesh, S. E., Aravind Arulchelvam, S., & Anjunath, M. S. (2019). Review of Friction stir processing of magnesium alloys. *Materials Today: Proceedings*, 16(2), 1320–1324.
18. Subramani, V., Jayavel, B., Sengottuvelu, R., & Lal Lazar, P. J. (2019). Assessment of microstructure and mechanical properties of stir zone seam of friction stir welded Magnesium AZ31B through Nano-SiC. *Materials*, 12, 1044; <https://doi.org/10.3390/ma12071044>.
19. Bisadi, H., Tavakoli, A., Tour Sangsaraki, M., & Tour Sangsaraki, K. (2013). The influences of rotational and welding speeds on microstructures and mechanical properties of friction stir welded Al5083 and commercially pure copper sheets lap joints. *Materials and Design*, 43, 80–88.
20. Chung, K., Lee, W., Kim, D., Kim, J., Chung, K. H., Kim, C., & Wagoner, R. H. (2010). Macro-performance evaluation of friction stir welded automotive tailor-welded blank sheets: Part I—Material properties. *International Journal of Solids and Structures*, 47(7–8), 1048–1062.
21. Pasini, A. (2015). Artificial neural networks for small dataset analysis. *Journal of Thoracic Disease*, 7, 953–960. <https://doi.org/10.3978/j.issn.2072-1439.2015.04.61>.
22. Liu, Q., Ke, L., Liu, F., Huang, C., & Xing, L. (2013). Microstructure and mechanical property of multi-walled carbon nano tubes reinforced aluminum matrix composites fabricated by friction stir processing. *Materials and Design*, 45, 343–348.
23. Fonda, R. W., & Bingert, J. F. (2006). Precipitation and grain refinement in a 2195 Al friction stir weld. *Metallurgical and Materials Transactions a: Physical Metallurgy and Materials Science*, 37(12), 3593–3604.
24. Fotoohi, Y., Rasaei, S., Bisadi, H., & Zahedi, M. (2014). Effect of friction stir welding parameters on the mechanical properties and microstructure of the dissimilar Al5083-copper butt joint. *Proceedings of the Institution of Mechanical Engineers, Part L: Journal of Materials: Design and Applications*, 228(4), 334–340.
25. Ko, Y.-j., Lee, K.-J., & Baik, K.-h. (2017). Effect of tool rotational speed on mechanical properties and microstructure of friction stir welding joints within Ti-6Al-4V alloy sheets. *Advances in Mechanical Engineering*, 9(8), 1–7.
26. Xue, P., Xiao, B. L., Ni, D. R., & Ma, Z. Y. (2010). Enhanced mechanical properties of friction stir welded dissimilar Al-Cu joint by intermetallic compounds. *Materials Science and Engineering a*, 527(21–22), 5723–5727.
27. Mehta, K. P., & Badheka, V. J. (2015). A review on dissimilar friction stir welding of copper to aluminum: Process, Properties, and Variants. *Materials and Manufacturing Processes*, 31(3), 233–254.
28. Al-Jarrah, J. A. (2014). Surface morphology and mechanical properties of aluminum-copper joints welded by friction stir welding. *Contemporary Engineering Sciences*, 7(5), 219–230.
29. Bhattacharya, T., Das, H., Jana, S., & Pal, T. (2017). Numerical and experimental investigation of thermal history, material flow and mechanical properties of friction stir welded aluminium alloy to DHP copper dissimilar joint. *The International Journal of Advanced Manufacturing Technology*, 88, 847–861.
30. Lee, W. B., Yeon, Y. M., & Jung, S. B. (2004). Mechanical properties related to microstructural variation of 6061 Al alloy joints by friction stir welding. *Materials Transactions*, 45(5), 1700–1705.

31. Benavides, S., Li, Y., Murr, L. E., Brown, D., & McClure, J. C. (1999). Low-temperature friction-stir welding of 2024 aluminum. *Scripta Materialia*, 41(8), 809–815.
32. Shanmuga Sundaram, N., & Murugan, N. (2010). Tensile behavior of dissimilar friction stir welded joints of aluminium alloys. *Materials and Design*, 31(9), 4184–4193.
33. Galvao, I., Leal, R. M., Loureiro, A., & Rodrigues, D. M. (2010). Material flow in heterogeneous friction stir welding of aluminium and copper thin sheets. *Science and Technology of Welding and Joining*, 15(8), 654–660.
34. Tan, C. W., Jiang, Z. G., Li, L. Q., Chen, Y. B., & Chen, X. Y. (2013). Microstructural evolution and mechanical properties of dissimilar Al–Cu joints produced by friction stir welding. *Materials and Design*, 51, 466–473.
35. Singarapu, U., Adepu, K., & Arumalle, S. R. (2015). Influence of tool material and rotational speed on mechanical properties of friction stir welded AZ31B magnesium alloy. *Journal of Magnesium and Alloys*, 3(4), 335–344.
36. Shen, J. J., Liu, H. J., & Cui, F. (2010). Effect of welding speed on microstructure and mechanical properties of friction stir welded copper. *Materials and Design*, 31(8), 3937–3942.
37. Muthu, M. F. X., & Jayabalan, V. (2015). Tool travel speed effects on the microstructure of friction stir welded aluminum-copper joints. *Journal of Materials Processing Technology*, 217, 105–113.
38. Al-Roubaiy, A. O., Nabat, S. M., & Batako, A. D. L. (2014). Experimental and theoretical analysis of friction stir welding of Al–Cu joints. *the International Journal of Advanced Manufacturing Technology*, 71(9–12), 1631–1642.
39. Akbari, M., Abdi Behnagh, R., & Davvand, A. (2012). Effect of materials position on friction stir lap welding of Al to Cu. *Science and Technology of Welding and Joining*, 17(7), 581–588.
40. Akbari, M., & Behnagh, R. A. (2012). Dissimilar friction-stir lap joining of 5083 aluminum alloy to CuZn34 brass. *Metallurgical and Materials Transactions B: Process Metallurgy and Materials Processing Science*, 43(5), 1177–1186.
41. Beygi, R., Kazeminexhad, M., & Kokabi, A. H. (2012). Butt joining of Al–Cu bilayer sheet through friction stir welding. *Transactions of Nonferrous Metals Society of China*, 22(12), 2925–2929.
42. Xue, P., Ni, D. R., Wang, D., Xiao, B. L., & Ma, Z. Y. (2011). Effect of friction stir welding parameters on the microstructure and mechanical properties of the dissimilar Al–Cu joints. *Materials Science and Engineering A*, 528(13–14), 4683–4689.
43. Ozdemir, N., Buyukarslan, S., & Sarsylmaz, F. (2007). Effect of tool profile, rotational Speed and welding speed on the mechanical behaviour of friction stir welded AA1030 aluminium alloy. *Science and Eng Journal of Firat University*, 19(4), 575–582.
44. Pande, S. V., & Badheka, V. J. (2014). Effect of tool pin offset on mechanical and metallurgical properties of dissimilar FSW joints of 6061t6 AL alloy to copper material. *Indian Welding Journal*, 47, 1–7.
45. Balasubramanian, M., & Jayabalakrishnan, D. (2019). Friction stir weave welding (FSWW) of AA6061 aluminium alloy with a novel tool path pattern. *Australian Journal of Mechanical Engineering*, 17(2), 133–144.
46. London, B. M., Mahoney, W., Bingel, M., Calabrese, R. H., Bossi, D. W. Jata, K. V., Mahoney, M. W., Ishra, R. S. Semiatin, S. L. & Lienert, T. (Eds.). (2003). *Friction Stir Welding and Processing* (p. 3). TMS: II.
47. Balasubramanian, M., & Jayabalakrishnan, S. (2018). Eccentric-weave Friction Stir Welding between Cu and AA 6061–T6 with reinforced Graphene nanoparticles. *Materials and Manufacturing Processes*, 33(3), 333–342.
48. Elangovan, K., & Balasubramanian, V. (2008). Influences of tool pin profile and welding speed on the formation of friction stir processing zone in AA2219 aluminium alloy. *Journal of Materials Processing Technology*, 200(1–3), 163–175.
49. Essa, A. R. S., Ahmed, M. M. Z., Mohamed, A. K. Y. A., & El-Nikhaily, A. E. (2016). An analytical model of heat generation for eccentric cylindrical pin in friction stir welding. *Journal of Materials Research and Technology*, 5(3), 234–240.

50. Suresh, S., Venkatesan, K., & Natarajan, E. (2018). Influence of SiC nanoparticle reinforcement on FSS welded 6061–T6 aluminum alloy. *Journal of Nanomaterials*, 2018,. <https://doi.org/10.1155/2018/7031867>.
51. Cho, H. H., Han, H. N., Hong, S. T., Park, J. H., Kwon, Y. J., Kim, S. H., & Steel, R. J. (2010). Microstructural analysis of friction stir welded ferritic stainless steel. *Materials Science and Engineering A*, 528(6), 2889–2894.
52. Nieto, A., Bisht, A., Lahiri, D., Zhang, C., & Agarwal, A. (2017). Graphene reinforced metal and ceramic matrix composites: A review. *International Materials Reviews*, 62(5), 241–302.
53. Nourani, M., Abbas, S., Milani, S., & Yannacopoulos, T. (2011). Optimization of process parameters in friction stir welding of 6061 aluminum alloy. *A Review and Case Study, Engineering*, 3, 144–155.
54. Sahu, P. K., & Pal, S. (2017). Mechanical properties of dissimilar thickness aluminium alloy weld by single/double pass FSW. *Journal of Materials Processing Technology*, 243, 442–455.
55. Saeid, T., Abdollah-zadeh, A., & Sazgari, B. (2010). Weldability and mechanical properties of dissimilar aluminum-copper lap joints made by friction stir welding. *Journal of Alloys and Compounds*, 490(1–2), 652–655.
56. Savolainen, K. (2012). Friction stir welding of copper and microstructure and properties of the welds', Ph.D. thesis. Aalto university.
57. Sevel, P., & Jaiganesh, V. (2017). Effects of axial force on the mechanical properties of AZ80A Mg alloy during friction stir welding. *Materials Today: Proceedings*, 4, 1312–1320.
58. Zhang, D., Suzuki, M., & Maruyama, K. (2005). Microstructural evolution of a heat-resistant magnesium alloy due to friction stir welding. *Scripta Materialia*, 52(9), 899–903.
59. He, X., Gu, F., & Ball, A. (2014). A review of numerical analysis of friction stir welding. *Progress in Materials Science*, 65, 1–66.
60. Akinlabi, E. T. (2012). Effect of shoulder size on weld properties of dissimilar metal friction stir welds. *Journal of Materials Engineering and Performance*, 21(7), 1514–1519.
61. Zhang, Z., & Chen, D. L. (2008). Contribution of Orowan strengthening effect in particulate-reinforced metal matrix nano composites. *Materials Science and Engineering A*, 483–484(1–2 C), 148–152.
62. Balasubramanian, M., & Jayabalakrishnan, D. (2020). Influence of pin offset and weave pattern on the performance of Al–Cu joints reinforced with graphene particles. *International Journal of Automotive and Mechanical Engineering*, 17(3), 8186–8196.

ANFIS and RSM Modelling Analysis on Surface Roughness of PB Composites in Drilling with HSS Drills



T. N. Valarmathi, K. Palanikumar, S. Sekar, and B. Latha

1 Introduction

Nowadays Particleboard (PB) is used in interior decorative applications. Particleboard panels have been fabricated using wood waste particles. As it is a low cost material it replaces wooden boards or plywood in less strength requirement applications. Wood is a natural composite also known as engineered wood are fiber-reinforced polymers. These are made by adding a little amount of adhesives and additives with wood elements such as fibers, particles, flakes, veneers and laminates. Wood composite panels are available as plain, pre-laminated, interior and exterior grades. High strength, light weight, low cost, usage of waste wood and smaller diameter trees and their flexibility in making different shaped products, free from defects and aesthetic appearance are some of the features of wood composites. Wood composite panels are widely replacing the traditional wood or steel and

T. N. Valarmathi (✉)

School of Mechanical Engineering, Sathyabama Institute of Science and Technology, Chennai 600119, India

e-mail: valarmathi.tn@gmail.com

K. Palanikumar

Department of Mechanical Engineering, Sri Sairam Institute of Technology, Chennai 600044, India

e-mail: palanikumar_k@yahoo.com

S. Sekar

Department of Mechanical Engineering, Rajalakshmi Engineering College, Chennai 602105, India

e-mail: sekarsarav@gmail.com

B. Latha

Department of Computer Science and Engineering, Sri Sairam Engineering College, Chennai 600044, India

e-mail: sivasoorya2003@yahoo.com

© The Author(s), under exclusive license to Springer Nature Switzerland AG 2021

129

K. Palanikumar et al. (eds.), *Futuristic Trends in Intelligent Manufacturing*,

Materials Forming, Machining and Tribology,

https://doi.org/10.1007/978-3-030-70009-6_8

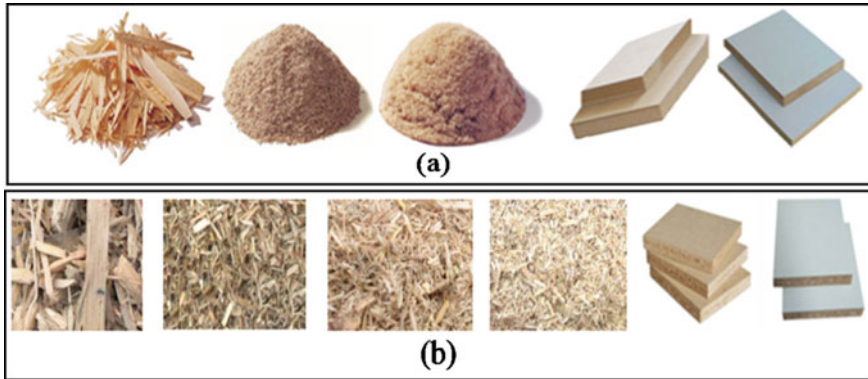


Fig. 1 Sample of wood fibers and particles used for **a** MDF and **b** PB panels

greatly reducing the demand for plywood. They are used in furniture industries, interior and exterior construction and structural applications and domestic appliances. Wood based composite products are light weight but have similar levels of strength, free from defects, uniform and aesthetic. Figure 1 is the sample of wood fibers and particles used for MDF and PB panels.

Wood composite panels are available as plain and pre-laminated MDF, plain and pre-laminated Particleboard, plain and pre-laminated Hardboard. Pre-laminated boards are available as one side or both side laminated, interior and exterior grades. MDFs are used in industries for manufacturing furniture, fixtures, modular kitchens, partitions, cabinetry, flooring, architectural millwork and moldings, doors, interiors, wood carvings, domestic appliances, toys, architectural components, etc., because of their smooth surfaces, rigid edges and superior machinability properties.

Particleboard has been a staple building material and used in the manufacturing of wall partitions, computer tables, interiors, false ceiling, wall lining, etc. Particle board is popularly used as a building material as it is cheaper, eco-friendly and available in varieties. Particle board is used as a flooring material, flooring underlayment, wall partitions, wall panels, false ceilings, ceiling tiles, core material in doors, and furniture industry (Fig. 2).

Machining is the most important process in product manufacturing industries for the removal of extra unwanted material using sawing, turning, milling, drilling, etc. Machining is carried out using traditional, computer controlled machine tools and different forms of energy to machine complex profiles, to obtain high dimensional accuracy and good surface finish, etc. Initially the composites were machined as metals and alloys leads to poor surface quality and tool wear. Hence further development is introduced in composite machining with special working conditions to obtain the optimum results.

Drilling is an extensively used machining operation in the final product assembly. Drilling produces better surface finish but milling is found to be good for economic and environmental sustainability considerations [1]. Modelling and optimization



Fig. 2 Typical applications of Particleboard

techniques are used for optimizing the machining parameters on surface roughness [2]. The parameters were optimized using regression model and Genetic algorithm in machining of hybrid composites [3]. Research works reported the consequence of machining parameters and geometry of tool on surface characteristics of wood composite panels [4–7, 15, 21] during various machining processes. ANFIS model has been successfully applied and revealed that the developed model is effective for predicting the surface roughness [5].

The impact of turning parameters and HSS drill with and without TiN coating on the characteristics of wood plastic composite has been analyzed and revealed that the sticking of particles is less in HSS than coated HSS [8, 9]. ANFIS can be effectively used for analysing the responses [10]. Process Parameters have been optimized in drilling of Delrin using Neural Network [11]. Influence of parameters are analyzed [12]. The influence of parameters on delamination in drilling is analyzed [13]. The drilling parameters have been optimized in drilling of self-healing GFRP [14]. The machining processes on the surface qualities of lumber and red pine has been reported [16, 17]. A multi-objective based optimization is applied to achieve the optimum solution in machining of Polytetrafluoroethylene [18, 19]. Feed and point angle have contribution in drilling of MDF [20].

Modelling and optimization techniques like RSM, Taguchi are used [21]. Surface roughness in drilling of MDF is analyzed using Taguchi [22]. Effect of drilling of coated composites has been analyzed [23]. Multiple-response optimization and ANOVA has been used to achieve good surface quality and metal removal rate at the same time [24]. The input parameters are optimized using Taguchi and ANOVA techniques [25]. The magnitude of torque can be determined by the drill diameter and the cutting force [26]. Taguchi and RSM methods were useful tools in predicting the effect of parameters [27–30]. The surface roughness has been analyzed in electric discharge machining of H12 tool steel and in drilling of PB [31, 32].

From literature it is asserted that the quality depends upon the surface characteristics. But the surface quality is depending on the input parameters, tool geometry, and

type of tool material. Hence the evaluation of impact of parameters during drilling is essential to improve the quality. In this work the HSS twist drills have been used to analyze the surface roughness (Ra) in drilling of PB.

2 Materials and Measurements

2.1 Plan of Experiments

The experiments are carried out on 12 mm thick particle board panels using HSS twist drills in a CNC vertical machining center (Fig. 3). Table 1 shows the parameters

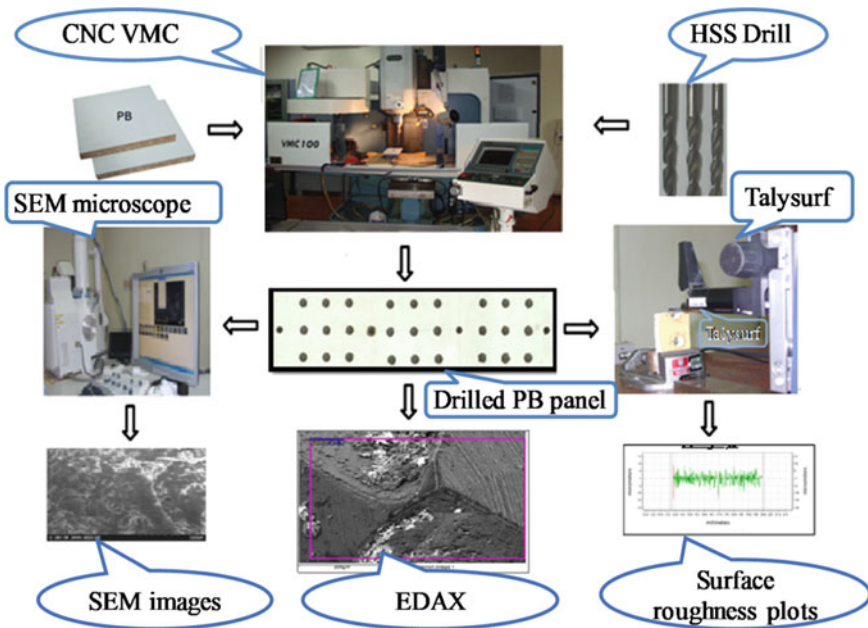


Fig. 3 Experimental arrangement

Table 1 Machining parameters used

Levels	Parameters		
	Speed (N) (rpm)	Feed (f) (mm/min)	Point angle (φ) (degrees)
1	1000	75	100
2	3000	150	118
3	5000	225	135

and levels.

2.2 Measurement of Surface Roughness

The surface roughness values (Table 2) were evaluated using Taylor Hobson meter for the analysis.

Table 2 Results and S/N ratio

Trial no.	N	f	ϕ	Ra	S/N Ratio
1.	1000	75	100	13.54	-22.6324
2.	1000	75	118	21.11	-26.4898
3.	1000	75	135	22.49	-27.0398
4.	1000	150	100	19.56	-25.8274
5.	1000	150	118	24.32	-27.7193
6.	1000	150	135	25.56	-28.1512
7.	1000	225	100	25.04	-27.9727
8.	1000	225	118	27.92	-28.9183
9.	1000	225	135	28.34	-29.048
10.	3000	75	100	11.14	-20.9377
11.	3000	75	118	16.52	-24.3602
12.	3000	75	135	17.76	-24.9889
13.	3000	150	100	12.56	-21.9798
14.	3000	150	118	21.94	-26.8247
15.	3000	150	135	24.33	-27.7228
16.	3000	225	100	25.63	-28.175
17.	3000	225	118	25.94	-28.2794
18.	3000	225	135	28.02	-28.9494
19.	5000	75	100	9.36	-19.4255
20.	5000	75	118	11.62	-21.3041
21.	5000	75	135	14.68	-23.3345
22.	5000	150	100	12.31	-21.8052
23.	5000	150	118	18.04	-25.1247
24.	5000	150	135	24.86	-27.91
25.	5000	225	100	23.11	-27.276
26.	5000	225	118	26.04	-28.3128
27.	5000	225	135	26.97	-28.6176

3 Method of Analysis

3.1 Response Surface Methodology (RSM)

RSM is a statistical method process used for developing mathematical model equation to predict the response values using experimental data. The Eq. (1) used is as

$$Y = f(X_1, X_2, \dots, X_K) \quad (1)$$

The general polynomial response equation in matrix form is given in Eq. (2) as

$$Y = X\beta + \varepsilon \quad (2)$$

3.2 Adaptive Neuro Fuzzy Inference System (ANFIS)

ANFIS combines ANN and a fuzzy logic of artificial intelligence concept to get the advantages and to eliminate the disadvantages of both techniques. In Fig. 4 ANFIS Architecture (Fig. 4) for three inputs and one output with 3 different membership functions used are presented. Training in ANFIS is performed for number of iterations containing 10, 40, 70 and 100 epochs. Three membership functions are chosen for each input to reduce the error. Generated rules are 27.

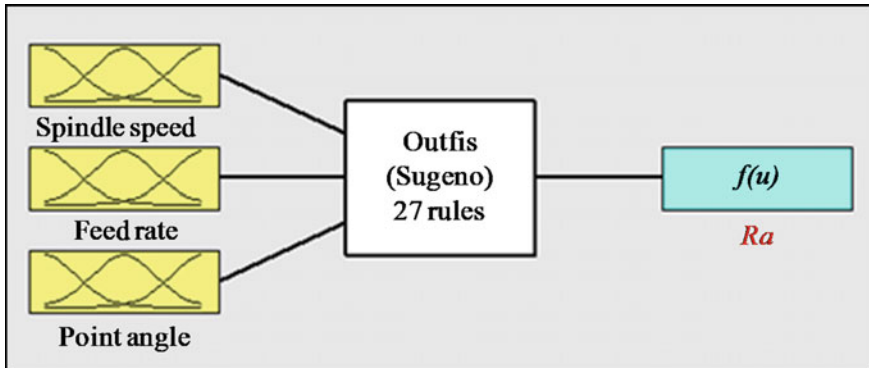


Fig. 4 Sugeno-type FIS model

4 Results and Discussion

Drilling is normally used operation in furniture industries. Drilling defects like surface roughness can be optimized by understanding the influence of input parameters. In this work, the empirical relationship between input and output variables are developed using RSM and ANFIS.

4.1 RSM Analysis

The Table 3 presents the summary of models and the ($R^2 = 0.94$) for quadratic. The quadratic model equation is given in Table 4. Results obtained presented in Table 5 for some of the experiment runs, reveals that the model has good predictive ability.

The normal probability plot and the correlation graph for predicted and actual surface roughness are presented in Figs. 5, 6 and 7. The plots indicate that the deviation is very less.

The surface plots illustrate how the response parameter relates to two input factors on the basis of mathematical model equation. Figure 7a indicates the interaction effects between point angle and spindle speed on surface roughness. It explains that low point angle and high speed is the preferred combination. The low feed and high speed combination reduces the roughness as shown in Fig. 7b. The effect of point angle and feed on the roughness is shown in Fig. 7c. For minimum surface roughness, a smaller point angle, low feed and smaller point angle combination gives better performance.

Table 3 Model summary

Source	Standard Deviation	R-Squared	Adjusted R-Squared	Predicted R-Squared	Press
Linear	2.09	0.8938	0.8799	0.8533	138.00
2FI	1.82	0.9298	0.9088	0.8741	118.50
Quadratic	1.82	0.9400	0.9082	0.8487	142.44

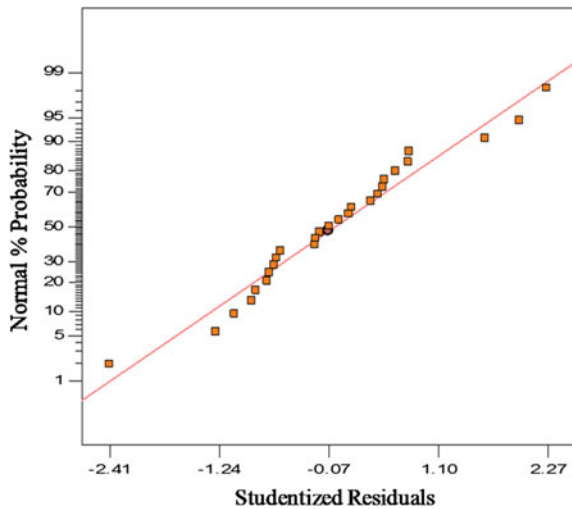
Table 4 RSM model equation

Response	Model Expression	R^2
Ra	$-62.4367 - 0.00403585 * N + 0.106691 * f + 1.12666 * \varphi + 9.98611E-08 * N^2 + 8.1679E-05 * f^2 - 0.00361365 * \varphi^2 + 9.05556E-06 * N * f + 8.01007E-06 * N * \varphi - 7.23939E-04 * f * \varphi$	94.0%

Table 5 Results of experimental, predicted values and residual error

Std order	Actual Ra	Predicted Ra	Residual	Leverage	Run order
1	25.04	24.85	0.19	0.512	7
2	11.14	10.36	0.78	0.344	10
3	24.33	23.10	1.23	0.259	15
4	27.92	28.16	-0.24	0.343	8
5	25.63	23.25	2.38	0.344	16
6	25.94	26.85	-0.91	0.259	17
7	19.56	19.30	0.26	0.344	4
8	28.02	28.10	-0.082	0.341	18
9	21.11	19.94	1.17	0.343	2
10	9.36	6.84	2.52	0.512	19

Fig. 5 Normal probability plots for residuals



4.2 Adaptive-Neuro Fuzzy Inference System (ANFIS) Analysis

The ANFIS models are developed for the output response considered. To evaluate the ability of the surface roughness model, performance factors such as coefficient of multiple determination, average training error and checking error in percentage, root mean square error (RMSE) for training data and checking data, mean absolute error (MAE) for training data, the co-efficient of determination (R²) values are determined. The error variation (variation in the errors in a set of data) can be diagnosed using MAE and RSME together. The average error in percentage is the average of the differences between actual and predicted values is also considered. The RMSE &

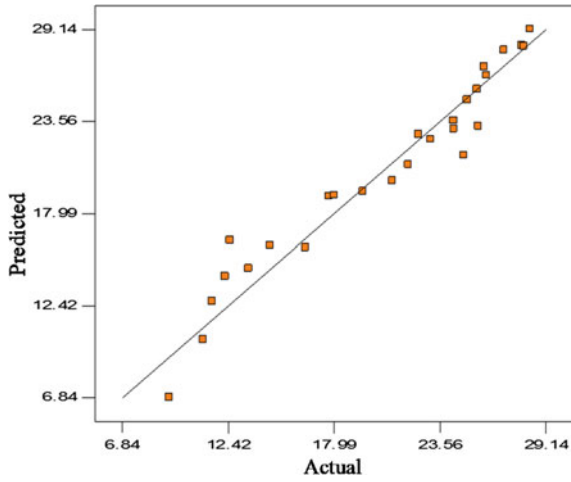


Fig. 6 Correlation graph

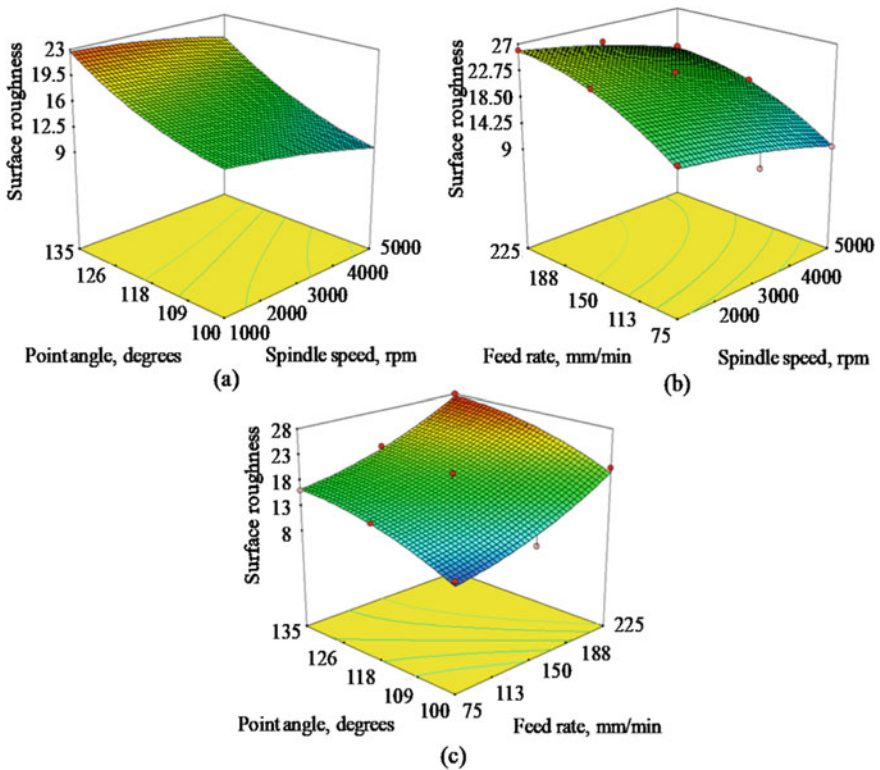


Fig. 7 Three dimensional RSM response graph for surface roughness

MAE and R2 values can be calculated by Eqs. (3), (4) and (5) as:

$$RMSE = \sqrt{\frac{\sum(x - y)^2}{n}} \tag{3}$$

$$MAE = \frac{\sum|x - y|}{n} \tag{4}$$

$$R^2 = 1 - \frac{\sum(x - y)^2}{\sum(x - \bar{y})^2} \tag{5}$$

where n-no. of patterns, x, y & \bar{y} - actual, predicted and mean of outputs.

Three types of membership functions for modelling the surface roughness of PB panels using the HSS drills are reported. The gaussmf (100 epochs) model shows smallest amount (0.067874%) of average checking error than gbellmf (0.067874%) and Gauss2mf (0.200930). ANFIS surface plots (Fig. 8) of surface roughness show the interaction effects. The required combination in getting minimum roughness is high speed, low feed and smaller point angle.

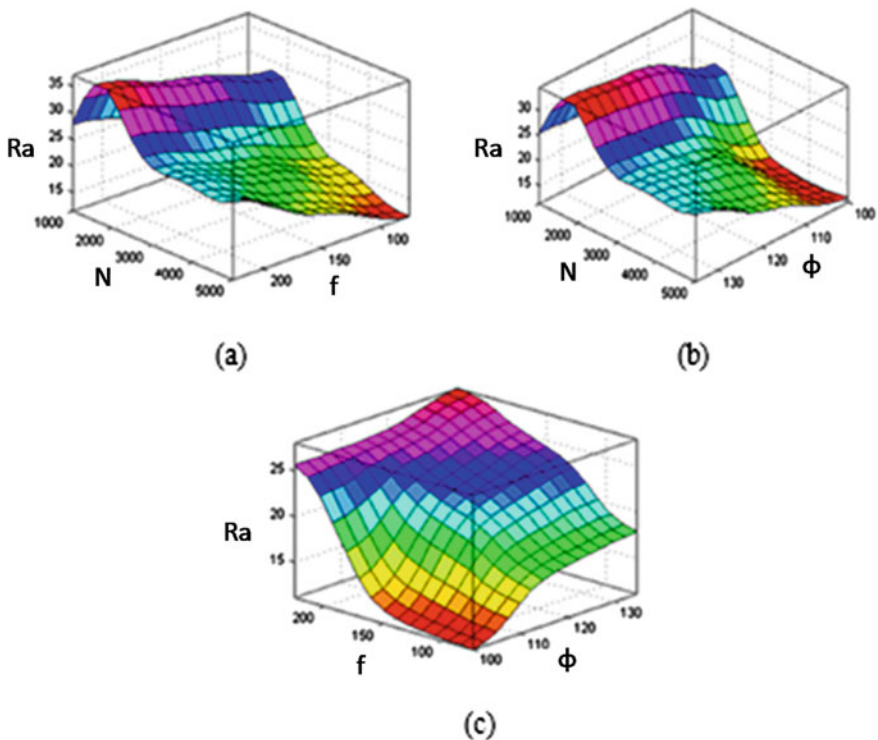


Fig. 8 ANFIS plots

Table 6 ANOVA for surface roughness with HSS drills

Source	DF	Seq SS	Adj SS	Adj MS	F	Percentage contribution
Regression Model	9	884.997	884.997	98.3330	29.580	93.9971
Spindle speed (N)	1	92.8880	93.0940	93.0940	28.000	9.86580
Feed rate (f)	1	542.192	543.908	543.908	163.60	57.5872
Point angle (φ)	1	206.436	205.099	205.099	61.690	21.9259
N * N	1	0.95700	0.95700	0.95700	0.2900	0.10164
f * f	1	1.26700	1.26700	1.26700	0.3800	0.13457
φ * φ	1	7.33400	7.33400	7.33400	2.2100	0.77896
N * f	1	22.1410	22.1410	22.1410	6.6600	2.35164
N * φ	1	0.94300	0.94300	0.94300	0.2800	0.10016
f * φ	1	10.8370	10.8370	10.8370	3.2600	1.15102
Residual Error	17	56.5180	56.5180	3.32500		6.00288
Total	26	941.515				100

4.3 ANOVA Analysis

The F-value 29.58 in ANOVA (Table 6) inferred, the model is being more effect with R2 value of 93.99 with the probability of < 0.0001 . The model expressions are satisfactory when the values of “Prob F” is less than 0.0500.

4.4 Control Factors and Their Interaction Effects

PB panels have numerous industrial applications. During the fabrication of PB panel products, the joining using drilled holes are necessary. The drilling of composite panel results in defects like poor surface characteristics, delamination, etc. In this study, for analysing the effect of factors and their interaction RSM and ANFIS modelling have been performed.

The interaction plots (Fig. 9) reveals the Ra (Fig. 9a) is small with smaller point angle and high spindle speed combinations. The increase of feed increases the Ra (Fig. 9b) and it is less for low feed and high speed combinations. The smaller point angle shows reduced surface roughness (Fig. 9c) with low feed combinations in PB panels with HSS drills. The surface roughness established in drilling being abridged with proper combination of factors.

The SEM images of PB (Fig. 10a, b) are taken with higher speed with lower feed and high feed and at low speed and HSS drill (Fig. 11) after drilling.

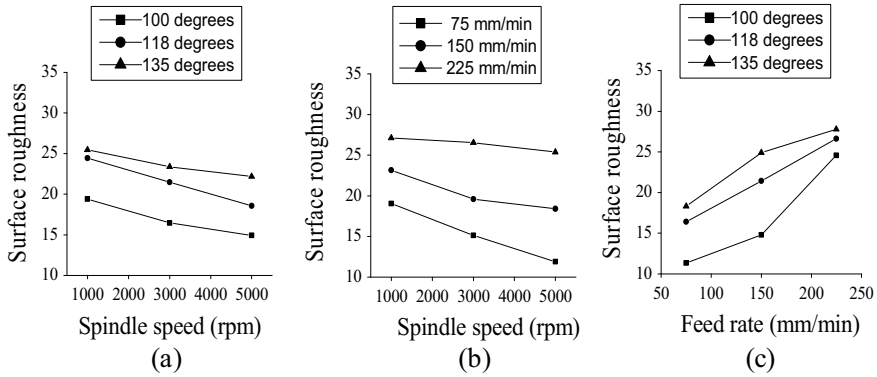


Fig. 9 Interaction effect between the parameters

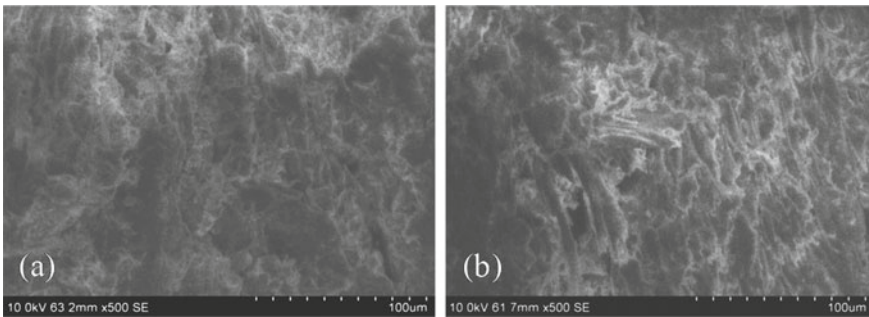


Fig. 10 SEM images at a low feed b high feed

4.5 Comparison of RSM and ANFIS Models

In the present investigation, for modelling and analysing the performances in the drilling of PB panels, two kinds of modelling technique such as RSM and ANFIS are used and compared (Table 7). The values of R2 for both models are more than 90% and hence these modelling techniques are effectively used for the different performance indicators in the drilling.

From the comparison chart (Fig. 12) shows the relationship of experimental and predicted values of used modelling techniques.

4.6 Confirmation Experiments

The results obtained for the verification tests are presented in Table 8. The test plots for confirming the predicting capability is presented in Fig. 13. The confirmation

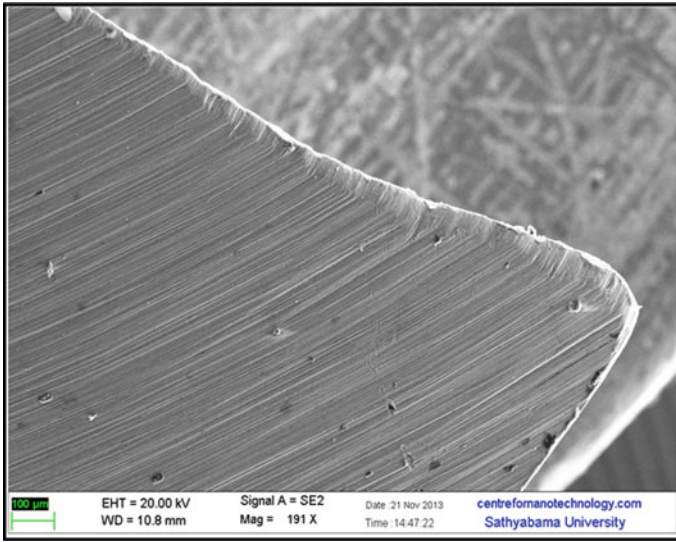


Fig. 11 SEM image HSS twist drill after drilling

Table 7 The predicted R2 values of the models

Response	R2 Value	
	RSM	ANFIS
Surface roughness	0.94	0.999

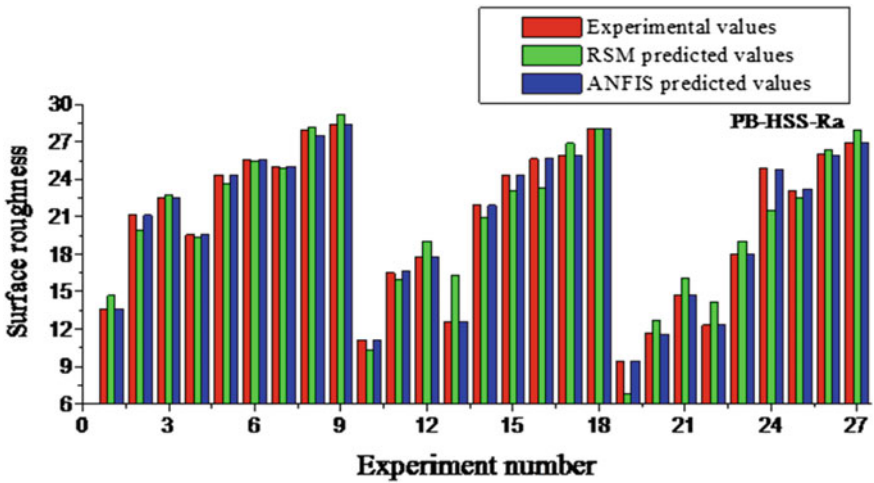
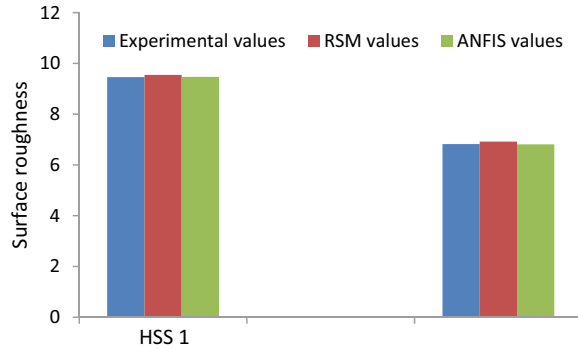


Fig. 12 Comparison plots in drilling PB using HSS Drills

Table 8 Confirmation experiments

Expt. no.	Speed	Feed rate	Point angle	Ra		
				Expt.	RSM	ANFIS
1	2000	75	100	9.46	9.55	9.47
2	4000	75	100	6.82	6.92	6.81

Fig. 13 Validation test plots

experiment test results are in close agreement and hence, the used RSM and ANFIS methods are efficient for predicting the response values in the drilling.

5 Conclusions

Drilling experiments performed on PB using twist drills made of HSS. RSM and ANFIS models are developed. The findings of the research work are

- The developed models are effective in predicting the surface roughness.
- The influence of feed and point angle interaction is more.
- The smaller point angle with low feed rate and high spindle speed combination minimizes the surface roughness in drilling of PB with HSS twist drills.

References

1. Iqbal, A., Suhaimi, H., & He, N. (2019). A sustainability comparison between drilling and milling for hole-enlargement in machining of hardened steels. *Machining Science and Technology*. <https://doi.org/10.1080/10910344.2019.1575409>.
2. Asilturk, I., & Akkuş, H. (2011). Determining the effect of cutting parameters on surface roughness in hard turning using the Taguchi method. *Measurement*, *44*, 1697–1704.

3. Baburaj, E., Mohana Sundaram, K. M., & Senthil, P. (2016). Effect of high speed turning operation on surface roughness of hybrid metal matrix (Al-SiCp-fly ash) composite. *Journal of Mechanical Science and Technology*, *30*, 89. <https://doi.org/10.1007/s12206-015-1210-y>.
4. Davim, J. P., Clemente, V. C., & Silva, S. (2009). Surface roughness aspects in milling MDF (Medium Density Fibreboard). *International Journal of Advanced Manufacturing Technology*, *40*, 49–55.
5. Beruvides, G., Castano, F., Quiza, R., & Haber, R. E. (2016). Surface roughness modeling and optimization of tungsten–copper alloys in micro-milling processes. *Measurement*, *86*, 246–252.
6. Hiziroglu, S., Jarusombuti, S., & Fueangvivat, V. (2004). Surface roughness of wood composites manufactured in Thailand. *Building and Environment*, *39*, 1359–1364.
7. Hiziroglu, S., & Kosonkorn, P. (2006). Evaluation of surface roughness of Thai medium density fiberboard (MDF). *Building and Environment*, *41*, 527–533.
8. Hutyrova, Z., Harnicarova, M., Zajac, J., Valicek, J., & Mihok, J. (2014). Experimental study of surface roughness of wood plastic composites after turning. *Advanced Materials Research*, *856*, 108–112.
9. Hutyrova, Z., Zajac, J., Michalik, P., Mita, D., Valicek, J., & Gajdos, S. (2015). Study of surface roughness of machined polymer composite material. *International Journal of Polymer Science*, Article ID 303517, 1–6.
10. Jang, J. S. R. (1993). ANFIS: Adaptive-network based fuzzy inference system. *IEEE Transactions on Systems, Man, and Cybernetics*, *1993*(23), 665–685.
11. Kaviarasan, V., Venkatesan, R., & Natarajan, E. (2019). Prediction of surface quality and optimization of process parameters in drilling of Delrin using neural network. *Progress in Rubber, Plastics and Recycling Technology*, *35*(3), 149–169.
12. Krishnamoorthy, A., rakash, S., Mercy, J.L., & Ramesh, S. (2019). Machinability studies in drilling carbon fiber reinforced Composites. *Hole-Making and Drilling Technology for Composites*. <https://doi.org/10.1016/B978-0-08-102397-6.00012-X>.
13. Latha, B., Senthilkumar, V. S., & Palanikumar, K. (2011). Modeling and optimization of process parameters for delamination in drilling glass fiber reinforced plastic (GFRP) composites. *Machining Science and Technology*, *15*(2), 172–191. <https://doi.org/10.1080/10910344.2011.579802>.
14. Lilly Mercy, J., Prakash, S., Krishnamoorthy, A., Ramesh, S., & Anand, D. A., Experimental investigation and multiresponse genetic optimization of drilling parameters for self-healing GFRP. *Journal of Mechanical Science and Technology*, *31* (8), 3777–3785.
15. Lin, R. J. T., Houts, J. V., Bhattacharyya. (2006). Machinability investigation of medium-density fibre board. *European Journal of Wood*, *60*, 76.
16. Kilic, M., Hiziroglu, S., & Burdurlu, E. (2006). Effect of machining on surface roughness of wood. *Building and Environment*, *41*(8), 074–1078. <https://doi.org/10.1016/j.buildenv.2005.05.008>.
17. Kilic, M. (2017). Determination of the surface roughness values of Turkish red pine (*Pinus brutia* (Ten.)) woods. *Bioresources*, *12*(1), 1216–1227.
18. Natarajan, E., Kaviarasan, V., Lim, W. H., Tiang, S. S., & Tan, T. H. (2018). Enhanced multi-objective teaching-learning-based optimization for machining of delrin. *IEEE Access*, *6*, 51528–51546. <https://doi.org/10.1109/ACCESS.2018.2869040>.
19. Natarajan, E., Kaviarasan, V., Lim, W. H., et al. (2020). Non-dominated sorting modified teaching-learning-based optimization for multi-objective machining of polytetrafluoroethylene (PTFE). *Journal of Intellectual Manufacturing*, *31*, 911–935. <https://doi.org/10.1007/s10845-019-01486-9>.
20. Palanikumar, K., & Valarmathi, T. N. (2016). Experimental investigation and analysis on thrust force in drilling of wood composite medium density fiberboard (MDF) panels. *Experimental Techniques*, *40*(1), 391–400.
21. Palanikumar, K. (2011). Experimental investigation and optimization in drilling of GFRP composites. *Measurement*, *44*, 2138–2148.
22. Prakash, S., Mercy, J. L., Palanikumar, K., Ramesh, S., Jamal, M. I., & Michael, A. J. (2012). Experimental Studies on Surface roughness in drilling MDF composite panels using Taguchi and Regression Analysis Method. *Journal of Applied Sciences*, *12*(10), 978–984.

23. Sangeetha, M., & Prakash, S. (2017). Experimental investigation of process parameters in drilling LM25 composites coated with multi wall carbon nano tubes using sonication process. *Archives of Metallurgy and Materials*, 62(3). <https://doi.org/10.1515/amm-2017-0268>.
24. Surinder Kumar, M., & Satsangi, P. S. (2013). Multiple-response optimization of turning machining by the Taguchi method and the utility concept using uni-directional glass fiber reinforced plastic composite and carbide (K10) cutting tool. *Journal of Mechanical Science and Technology*, 27 (9), 2829–2837.
25. Shanmughasundaram, S. (2013). Influence of graphite and machining parameters on the surface roughness of Al- fly ash/ graphite hybrid composite: a Taguchi approach. *Journal of Mechanical Science and Technology*, 2445–245.
26. Sheikh-Ahmad J. (2009). Machining of polymer composites. Springer Science Business Media, LLC, New York: Springer; <https://doi.org/10.1007/978-0-387-68619-6>, ISBN: 978-0-387-35539-9.
27. Valarmathi, T. N., Palanikumar, K., & Sekar, S. (2013). Prediction of parametric influence on thrust force in drilling of wood composite panels. *International Journal of Mining, Metallurgy & Mechanical Engineering*, 1(1), 71–74.
28. Valarmathi, T. N., Palanikumar, K., & Sekar, S. (2013a). Thrust force studies in drilling of medium density fiberboard Panels. *Advanced Materials Research*, 622–623, 1285–1299.
29. Valarmathi, T. N., Palanikumar, K. & Latha, B. (2013b). Measurement and analysis of thrust force in drilling of particleboard (PB) composite panels. *Measurement*, 46, 1220–1230.
30. Valarmathi, T. N., Palanikumar, K., & Sekar, S. (2013c). Parametric analysis on delamination in drilling of wood composite panels. *Indian Journal of Science and Technology*, 6, 4347–4356.
31. Valarmathi, T. N., Sekar, S., Antony, G., Suresh, R., & Balan, K. K. (2019). Experimental studies on surface Roughness of H12 tool steel in EDM using different tool materials: Volume 1, January 2019. https://doi.org/10.1007/978-981-13-2697-4_27.
32. Valarmathi, T. N., Palanikumar, K., Sekar, S., & Latha, B. (2020). Investigation of the effect of process parameters on surface roughness in drilling of particleboard composite panels using adaptive neuro fuzzy inference system. *Materials and Manufacturing Processes*, 469–477.

Machine Learning for Smart Manufacturing for Healthcare Applications



Nivesh Gadipudi, I. Elamvazuthi, S. Parasuraman, and Alberto Borboni

1 Introduction

The manufacturing industry has been continuously evolving since the seventeenth century to meet mass production, quality, and reliability requirements. The first generation of manufacturing industries used steam and coal-powered machines in substitution for manpower. In the very next phase of evolution, the manufacturing industry adapted the emerging energy solutions like electricity and petrochemicals [1]. Research and developments in integrated circuits and computers constituted industry 3.0. The third generation of industries involved automation and robotics using electronic controllers to enhance the mass production on shop floors. It is interesting to observe that the technological improvements in preceding generations fuelled the upcoming industrial developments. Analogically, developments on integrated circuits and computers at the time of industry 3.0 unleashed the required computational capabilities in the era of artificial intelligence and cloud computing. Advancements in technologies like artificial intelligence, cloud-based environments,

N. Gadipudi · I. Elamvazuthi (✉)

Department of Electrical and Electronic Engineering, Universiti Teknologi PETRONAS, 32610 Bandar Seri Iskandar, Malaysia
e-mail: irraivan_elamvazuthi@utp.edu.my

N. Gadipudi

e-mail: nivesh48@gmail.com

S. Parasuraman

School of Engineering, Monash University Malaysia, Bandar Sunway, 46150 Subang Jaya, Malaysia
e-mail: s.parasuraman@monash.edu

A. Borboni

Mechanical and Industrial Engineering Department, Università degli studi di Brescia, Via Branze, 38, 25123 Brescia, Italy
e-mail: alberto.borboni@unibs.it

© The Author(s), under exclusive license to Springer Nature Switzerland AG 2021

145

K. Palanikumar et al. (eds.), *Futuristic Trends in Intelligent Manufacturing*,
Materials Forming, Machining and Tribology,
https://doi.org/10.1007/978-3-030-70009-6_9

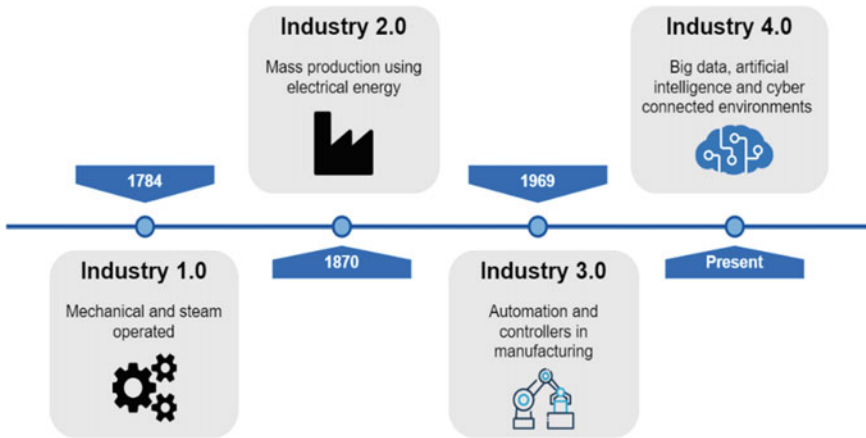


Fig. 1 Summary of the industrial revolution

and information technology infrastructure made significant changes in industry 4.0. The industrial revolution is summarised in Fig. 1.

The aim of industrial revolution 4.0 is to deliver real-time intelligent manufacturing systems aiming flexible, intelligent, and interoperable environments. The underlying layer of industry 4.0 comprises of state-of-the-art modern information technologies like cloud computing, internet of things (IoT) with the core as artificial intelligence algorithms. Artificial intelligence (AI) is the science and engineering of understanding and representing the behaviour of natural living systems in terms of software and machines to identify, extract the hidden patterns from the data [2]. AI can be considered as actively developing and researched the field of this century. It has been applied in various applications [3–7].

The base layer consists of the communication bridge between physical elements like sensors to collect data. IoT ensures the inter and intra connectivity of machines and sensors across the shop floor. This collected data is logged using cloud technologies which can be retrieved whenever needed. AI algorithms interpret meaningful insights from the data collected from physical elements. These insights can be used to predict the maintenance requirements and fault detections which maximizes the quality and ensure the continuous mass production. Besides, Virtual and augmented technologies using AI keep humans in the loop of the manufacturing process. A detailed illustration of the current generation manufacturing industry pipeline is shown in Fig. 2.

This chapter is organized as described, Sect. 2 contains the detailed classification of Machine learning algorithms, Sect. 3 explains about the smart manufacturing technologies used in industry 4.0. Section 4 covers some interesting applications of machine learning in healthcare, Sect. 5 discusses the future directions, benefits, and challenges followed by the conclusion.

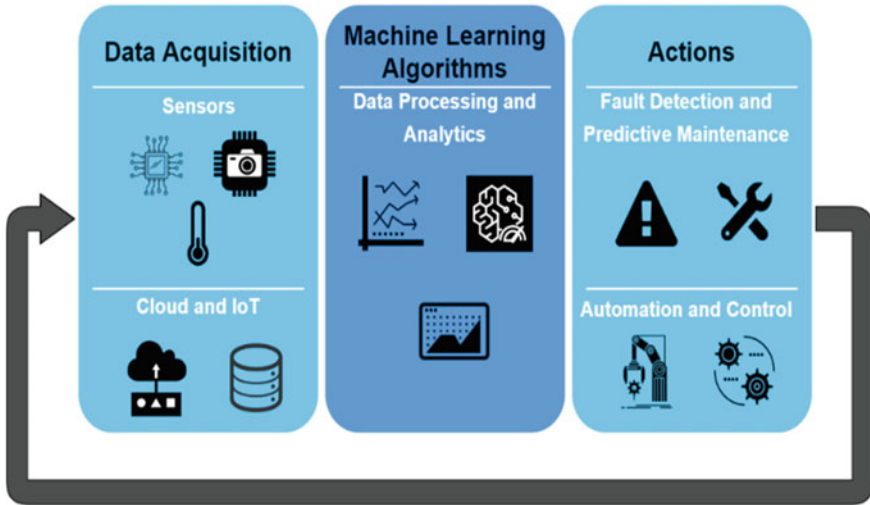


Fig. 2 The pipeline of industry 4.0 using machine learning algorithms

2 Machine Learning Algorithms

In this section, the reasons behind the rise of machine learning (ML) algorithms and various types of Machine learning algorithms are discussed. In the present era of data and connected systems, data gathering and storing has become much simpler using the latest cloud and IoT technologies. A survey conducted by Deloitte in 2018 concluded that about 63% of companies were using ML algorithms [8]. According to CISCO's report on visual index forecast global internet traffic is predicted to increase from 250 exabytes per month in 2020–400 exabytes per month in 2022 [9]. This trend can be observed from Fig. 3.

Machine Learning algorithms are a class of computational algorithms which is formulated by inspiring from the aspects of biological and human behavior. ML algorithms are a subset of AI which require enormous data to extract hidden and meaningful patterns from the data. Simultaneous development of IoT and cloud technologies in the current generation unveiled the power of ML algorithms. ML algorithms can be classified into supervised, unsupervised, and reinforcement learning. These can be further classified into regression, classification, and clustering depending upon the type of output from the algorithms. A detailed classification of ML algorithms is shown in Fig. 4.

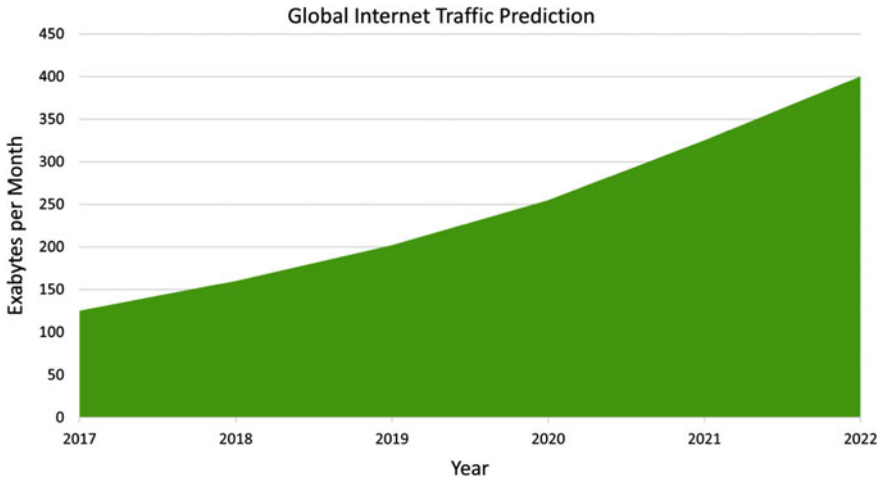


Fig. 3 Global internet traffic prediction

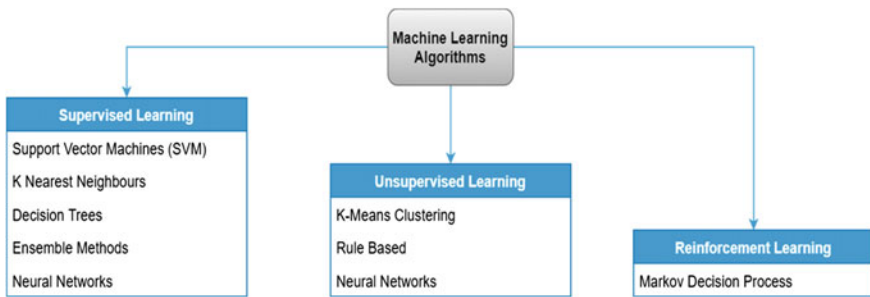


Fig. 4 Classification of machine learning algorithms

2.1 Supervised Learning Algorithms

Supervised Learning algorithms train on the data presented with input and the corresponding response or output labels. This supervised learning is further classified into classification and regression. Regression models are used to predict a continuously changing values like temperature, pressure, stock price, etc. Classification models are used to predict the discrete value associated with the input data.

2.1.1 Support Vector Machines (SVM)

It is a supervised machine learning algorithm that can be used for classification as well as regression learning. SVM performs outlier rejection by constructing a set of hyperplanes. SVM is very effective in learning from highly nonlinear or not linearly

separable data by projecting the data into higher dimensional space. Kernel functions like Radial basis functions are used to map the data from lower to higher dimensions. However, SVM is a very computationally expensive algorithm.

2.1.2 K-Nearest Neighbours

K-Nearest Neighbours (KNN) algorithms can be used for both regression and classification analysis. KNN predicts by calculating the distance between input samples and a new sample to predict the output. KNN is computationally very efficient but highly sensitive to missing data, noise.

2.1.3 Decision Trees

Decision trees are a graphical model comprising of nodes and connections and can be used for both regression and classifications analysis. Decision trees are simple, computationally fast, and easily understandable. Unlike SVM, decision trees fail to solve highly nonlinear data with high accuracies.

2.1.4 Ensemble Methods

Ensemble Methods use multiple ML algorithms to improve prediction accuracy. It works by combining the multiple prediction hypothesis from different ML algorithms. Some of the types of ensemble modelling are bootstrapping, Bayes optimal classifier, and boosting.

2.1.5 Neural Networks (Supervised)

Neural Networks are a subset of ML algorithms built based on the functionality of neurons in the human brain. Neural Networks can be used for both classification and regression at the same time can be used for supervised and unsupervised learning. In this section, only algorithms related supervised neural networks are discussed. In terms of supervised learning Mean squared error (MSE), Mean absolute error (MAE), Hinge loss, etc., are used to calculate the quantitative difference between prediction and the targets for regression analysis. For classification tasks, the probabilities of the predicted classes are converted into logarithmic values to measure the loss between predicted and targets. Training neural networks require vast data and these algorithms avoid feature engineering steps required in core ML algorithms. There are various types of neural networks for different types of input data. For instance, Convolution neural network is used for images and recurrent neural networks are used for temporal related data. The neural network proved its capabilities in terms of object detection and classification tasks. Semi-supervised learning is used in case of the small datasets.

Generative adversary networks are a type of semi supervised algorithms used to augment or generate the similar data samples.

2.2 Unsupervised Learning Algorithms

Unsupervised learning algorithms concentrate on finding the probability density rather than probability boundaries. These algorithms train on data without ground truth or target labels. Clustering is one of the main unsupervised analysis performed by ML algorithms. Clustering helps visualizing the trends in data by projecting the multidimensional data onto lower dimensions.

2.2.1 K-Means Clustering

K-means clustering partitions the input data into K clusters based on the mean, this results in Voronoi cells partitioning. Other types of K-Means are K-medians and k-medoids which minimizes the regular euclidean distance unlike squared euclidean distances in K -Means.

2.2.2 Rule-Based

Rule-Based learns to extract important information from statistical examination using if-then rules. Rule-Based learners have greater importance in unsupervised learning due to their comprehensibility [10]. These algorithms are prone to noises and overfitting due to pruning strategies.

2.2.3 Neural Networks (Unsupervised)

Unsupervised neural networks used complicated end to end architectures. These architectures reconstruct the input data and loss functions measure the deviation of reconstructed input to the actual input. Distance function like L1 and L2 are used as loss function in these types of networks. Autoencoders are a type of unsupervised neural networks used for denoising, increasing resolution, and style transfer. This field is currently open to new research, new network architectures adapted suitably for the field of study.

2.3 Reinforcement Learning

Reinforcement learning is a continuous learning algorithm utilizing dynamic programming techniques. Reinforcement learning is a continuous learning algorithm which gives an added advantage of predicting the changes in environment or data. It is modelled in the form of Markov decision process. Q-learning is a type of reinforcement learning that uses modified Markov decision process. Reinforcement learning is also referred to as a state-action mechanism. Rewards are used to award the actions taken by the software agents.

According to the discussion above, algorithms are classified according to the output type of predictions. A brief classification of ML algorithms based on supervision, classification, regression, and clustering is summarized in Table 1.

3 Smart Manufacturing

Smart manufacturing systems in industry 4.0 takes the advantage of data segregated from sensors through wired and wireless methods to improve mass production, quality while reducing costs and waste produced. Smart manufacturing systems are computer-controlled with a high level of flexibility. The high level of flexibility and efficiency in the smart manufacturing processes are achieved by using intelligent devices, connectivity, infrastructure, and processes. Different components of the smart manufacturing system are illustrated in Fig. 5.

However, the smart manufacturing paradigm can be generally broken down into three steps. First, the data is collected through different devices like sensors or manually entered by a human operator. Intelligent information technology infrastructure helps in uncomplicating the data collection process consists of various sensor nodes. Data collected will be inconsistent, noisy, and large. Using the intelligent computational processes data is filtered, compressed, and stored in the cloud for future reference or hidden patterns are extracted using artificially intelligent processes. This first step of data segregation and cleaning is very important in smart manufacturing. Secondly, the data collected is analyzed using a local or cloud-based system.

Table 1 Classification of machine learning models

Algorithm	Type	Regression	Classification	Clustering
SVM	Supervised	✓	✓	✗
KNN	Supervised	✓	✓	✗
Decision trees	Supervised	✓	✓	✗
Ensemble methods	Supervised	✓	✓	✗
Neural networks	Supervised/ Unsupervised	✓	✓	✓
K-Means	Unsupervised	✗	✗	✓

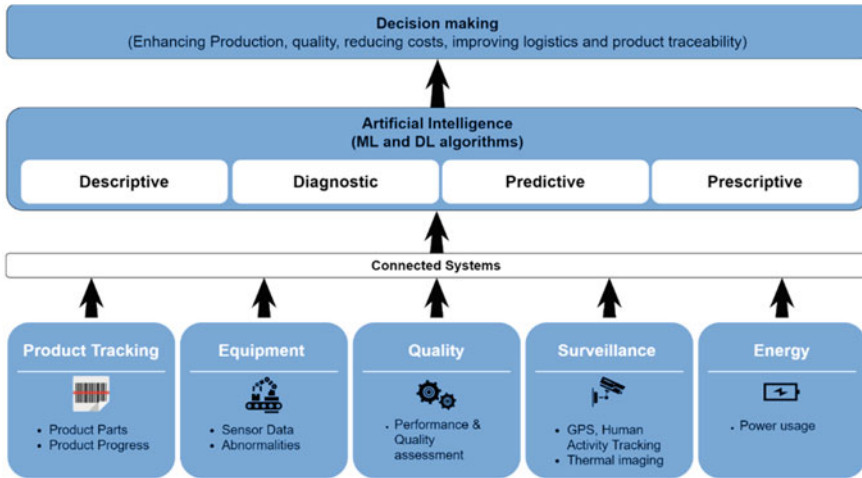


Fig. 5 Machine learning-enabled smart manufacturing layout

Depending on the type of data and the type of process different artificial algorithms are adapted as explained in Sect. 2. Analysis of data gives valuable insights into data that are descriptive, predictive, prescriptive, and diagnostic [11]. The final step of smart manufacturing involves taking necessary actions depending on the insights from intelligent algorithms. These actions include controlling a process, reducing manufacturing waste, improving the quality, improving product lifecycle, traceability, and reducing costs associated with power and manpower. The other aspect of smart manufacturing is creating efficient products using intelligent design software's. Artificial intelligence-enabled design software is used in designing microelements, aerodynamically, thermally and efficient products.

4 Applications of Machine Learning in Healthcare

In this section, recent advancements in healthcare systems using ML algorithms are discussed. The increased prevalence of the use of ML algorithms in healthcare systems increased the quality of life of patients. ML algorithms play a very important role in diagnosis, health records, drug discovering, and many more. ML algorithms are helping healthcare systems to tackle the highly complicated diseases with much greater treatment response from patients. The Healthcare industry in the unites states sums up to a revenue of 1.67 trillion dollars [12]. Analysis of data collected from trial studies is helping doctors to identify the causes of the diseases. The public healthcare expenditure as a share of GDP is increased from about 3% in 1960 to 7% in 1994 and about 10% in 2014, Sweden is the highest as shown in Fig. 6 [13].

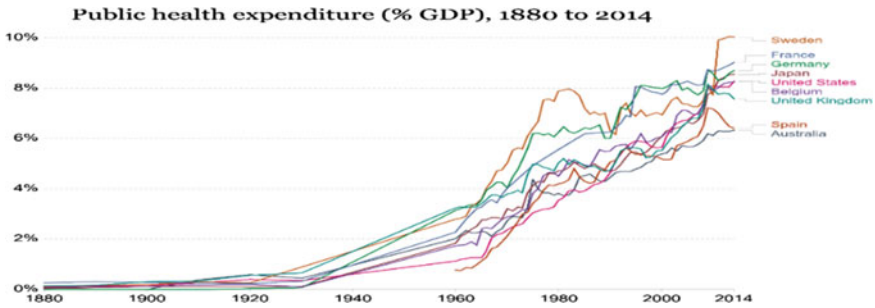


Fig. 6 Statistics of public healthcare expenditure as a share of GDP [13]

Increasingly growing data in the twenty-first century and computational capabilities allows us to make efficient use of ML algorithms for the healthcare industry. Over the past few years, ML algorithms assisted in a better quality of life for patients. The top applications of ML in healthcare are discussed below.

4.1 Disease Diagnosis and Prediction

Early diagnosis and prognosis of the disease are predominant in improving the quality of life and life expectancy of a patient. ML algorithms can be used to predict chronic progressing diseases like rheumatoid arthritis in early stages [14, 15]. The global mortality rate of cardiovascular, diabetes mellitus and Alzheimer’s are on the rise, leading to more than 20 million deaths in 2015 [16]. Accuracy of early predictions using ML algorithms more than 90% of accuracy for these diseases. The mortality rate of these diseases was tabulated in Table 2.

According to the world health organization (WHO), globally cancer is responsible for 9.6 million deaths in 2018 [17]. Diagnosis of cancer stands as one of the toughest and most painful processes by examining the changes of DNA collected from the human body. Nvidia, IBM Watson, google are working vigorously to solve this problem using the latest imaging techniques combined with ML algorithms. Early diagnosis in terms of cancer is very important to localize the tumour and to improve the 5-year life expectancy post-cancer treatment. Early diagnosis and treatment inhibit cancer from spreading to the other parts of the human body namely to

Table 2 Statistics of the mortality rate of various diseases in 1000’s

Disease	2005	2010	2015
Cardiovascular diseases	15,338	16,570	17,631
Diabetes mellitus	1133	1333	1570
Alzheimer’s	843	1147	1534

the lymph nodes, this stage is called metastasis. At this stage, it is very difficult to treat cancer and compromises the quality of life of the patient.

On the other hand, ML algorithms are also used to diagnosis mental illness. Mental illnesses like post-traumatic stress disorders (PTSD), Schizophrenia, Depression, and Autism Spectrum Disorders (ASD) were predictable by using ML algorithms considering the limitations of these algorithms for the specific disease [18]. Overall, the early diagnosis using ML algorithms are mostly non-invasive and proved their potential in diagnosing the diseases. However, this is an open and continuous research problem in the present era of artificial intelligence.

4.2 Clinical Trials and Drug Discovery

Clinical trials and drug discovery is on the verge of major developments using modern AI algorithms and data sources. This area of research using ML algorithms includes molecular compound properties and multimodal analysis to predict hidden patterns [19]. Clinical trials require a vast amount of time to draw conclusions and investment. Using ML algorithms is proven to be feasible and converge to conclusions quickly. The life cycle of clinical trials and drug discovery is interpreted clearly in Fig. 7.

Initially, RNA and DNA structures before the clinical trials are analyzed to establish a reference point. This reference point is used to analyze the trails efficiency pooling the vast data collected. Another fascinating advantage of current technologies is to gather medical records from individuals using current cloud-based technologies. Equipment like smartwatches, wearable patches, and MEMS-based pressure sensors are used to monitor the data remotely from the patients [20]. The data collected is further analyzed using intelligent ML algorithms to develop new antibiotics and personalized medicine for individuals. In conclusion, ML algorithms made huge progress over past decades contributing to drug discovery.

4.3 Outbreak Prediction

Covid-19 pandemic created huge distress in the entire world ceasing economic growth, supply chain management, and compromising mental health. This is one of the interesting areas where ML algorithms dive into predicting the outbreak. The outbreak predictions can be formulated using deterministic and stochastic studies. These insights can be used to control the outbreak and take necessary action to inhibit the spread [21]. Provided the sufficient analysis of various ML, genetic and deterministic algorithms concluding that ML algorithms provided an understanding of the number of infected patients given the country and infection rate.

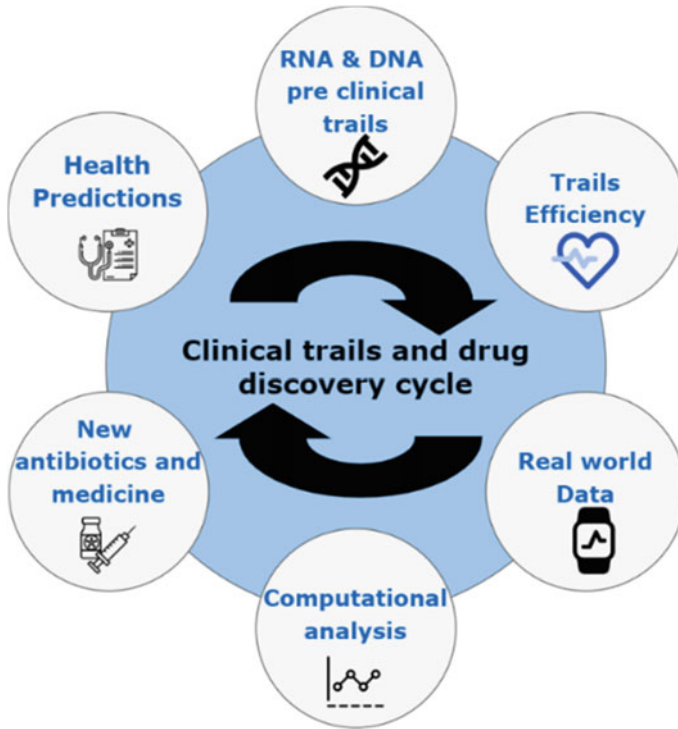


Fig. 7 The life cycle of clinal trials and drug discovery

4.4 Rehabilitation Equipment

Rehabilitation is the set of tools assisting humans in achieving optimal functioning and interaction with their surroundings. Elder people of age greater than 60 are at the risk of chronic and progressive neurological disorders. About 70% of patients are provided with neurological rehabilitation for people with stores and progressive neurological diseases. Rehabilitation includes four steps namely, assessment assignments, intervention, and evaluation [22]. The present generation sensors like electromyography (EMG), functional near-infrared spectroscopy (fNIRS), and electroencephalogram (EEG) provide the optimal response required to extract the patterns in non-invasive techniques [23]. Additionally, wearable sensors and smartphone can contribute to recording the human activity recognition required to analyze human gait [24]. Data from these sensors can be used to control the motor-assisted robotic limbs. Due to the underlying facts, there is a need for sophisticated robotic assistive systems using ML algorithms to provide intelligent robot assistive systems for disabled people.

5 Benefits, Opportunities, Challenges, and Future Direction

Smart manufacturing technologies using AI and intelligent information technological infrastructure facilitates the decision making and real-time data sharing by better connectivity of devices, low latency data transfer, and data storage. Furthermore, combining these technologies improves product design, safety while reducing the manufacturing wastes.

Due to the increasing demand for the complex and dynamic nature of present manufacturing industries for medical healthcare equipment, which is highly uncertain, ML algorithms are used. However, the error in the data collection process, noise, and missing data lead to performance downtrends. On top of it, any inaccuracies in predictions can incur negative effects and discourage the industry to adapt AI-based systems.

Generalizing and improving the ML models to work on existing and various changing environments for manufacturing healthcare equipment is expected to be the future directed of this study. In addition to this collaborating the researchers from medical, data science, and manufacturing under the same roof can also a challenging issue.

6 Conclusion

The smart manufacturing sector is the perfect stage for manufacturing healthcare applications using artificial intelligence. Even though the industry 4.0 requires massive upgrades to meet the requirements of manufacturing healthcare applications, significant benefits can be observed on the long run. From the product tracking to delivering the state-of-the-art healthcare instruments smart manufacturing is meant to induct innovative changes to process. This combination can further improve existing products making them more reliable and effective. Additionally, artificial intelligence provides advanced analytics and offers huge advantage to healthcare products in this age of industry 4.0. The effort to combine intelligent algorithms and manufacturing process for healthcare and their applications are also summarised.

Acknowledgements The authors appreciate the assistance by the Smart Assistive and Rehabilitative Technology (SMART) Research Group & Department of Electrical and Electronic Engineering, Universiti Teknologi PETRONAS, Monash University Malaysia and Università degli Studi di Brescia, Italy for their support.

References

1. Oztemel, E., & Gursev, S. (2020). Literature review of Industry 4.0 and related technologies. *Journal of Intelligent Manufacturing*, 31, 127–182.

2. Wang, L. (2019). From Intelligence Science to Intelligent Manufacturing. *Engineering*, 5(4), 615–618.
3. Truong, K. H., Nallagownden, P., Elamvazuthi, I., & Vo, D. (2020). A quasi-oppositional-chaotic symbiotic organisms search algorithm for optimal allocation of DG in radial distribution networks. *Applied Soft Computing*, 88, 106067.
4. Truong, K. H., Nallagownden, P., Elamvazuthi, I., & Dieu, V. N. (2019). An improved meta-heuristic method to maximize the penetration of distributed generation in radial distribution networks. *Neural Computing and Applications*, 32, 10159–10181.
5. Singh, K., Elamvazuthi, I., Kushaari, K., & Satyamurthy, P. (2017). Tuning of PID controller for DC servo motor using improved cuckoo search algorithm. *International Journal of Simulation: Systems, Science and Technology*.
6. Azlan, N. A., Lu, C., Elamvazuthi, I., & Tang, T. (2020). Automatic detection of masses from mammographic images via artificial intelligence techniques. *IEEE Sensors Journal*, 20, 13094–13102.
7. Ganesan, T., Vasant, P., & Elamvazuthi, I. (2016). *Advances in Metaheuristics: Applications in Engineering Systems*.
8. Davenport, T., & Kalakota, R. (2019). The potential for artificial intelligence in healthcare. *Future Healthcare Journal*, 6, 94–98.
9. Cisco. (2019). *CISCO Network Intelligent Service Provider*. <https://www.cisco.com/c/en/us/solutions/service-provider/index.html>
10. Bajic, B. (2018). *Machine Learning Techniques for Smart Manufacturing Applications and Challenges in Industry 4.0*. ResearchGate. https://www.researchgate.net/publication/328290180_Machine_Learning_Techniques_for_Smart_Manufacturing_Applications_and_Challenges_in_Industry_40
11. Wang, J. (2018). Deep learning for smart manufacturing: Methods and applications. *Journal of Manufacturing Systems*, 48, Part C, 144–156.
12. Flat World. (2020). *Top 10 Applications of Machine Learning in Healthcare*. <https://www.flatworldsolutions.com/healthcare/articles/top-10-applications-of-machine-learning-in-healthcare.php>.
13. Our World in Data. (n.d.). *Public health expenditureshare GDP*. Retrieved January 9, 2020, from <https://ourworldindata.org/grapher/public-health-expenditure-share-gdp-owid>.
14. Sharon, H., Elamvazuthi, I., Lu, C., Parasuraman, S., & Natarajan, E. (2020). Development of rheumatoid arthritis classification from electronic image sensor using ensemble method. *Sensors (Basel, Switzerland)*, 20
15. Sharon, H., Elamvazuthi, I., Lu, C., Parasuraman, S., & Natarajan, E. (2019). Classification of rheumatoid arthritis using machine learning algorithms. *IEEE Student Conference on Research and Development (SCOReD)*, 2019, 245–250.
16. Chui, K. T., Alhalabi, W., Pang, S. S. H., Pablos, P. O., Liu, R. W., & Zhao, M. (2017). Disease diagnosis in smart healthcare: innovation. *Sustainability*, 9, 2309.
17. WHO. (n.d.). *Cancer*. <https://www.who.int/news-room/fact-sheets/detail/cancer#:~:text=Cancer%20is%20the%20second%20leading,%2D%20and%20middle%2Dincome%20countries>.
18. Cho, G., Yim, J., Choi, Y., Ko, J., & Lee, S. (2019). Review of machine learning algorithms for diagnosing mental illness. *Psychiatry Investigation*, 16, 262–269.
19. Shah, P., Kendall, F., Khozin, S., Goosen, R., Hu, J., Laramie, J., et al. (2019). Artificial intelligence and machine learning in clinical development: A translational perspective. *NPJ Digital Medicine*, 2.
20. Ciuti, G., Ricotti, L., Menciasci, A., & Dario, P. (2015). MEMS sensor technologies for human centred applications in healthcare, physical activities, safety and environmental sensing: A review on research activities in Italy. *Sensors*, 15, 6441–6468.
21. Ardabili, S., Mosavi, A., Ghamisi, P., Ferdinand, F., Varkonyi-Koczy, A.R., Reuter, U., et al. (2020). COVID-19 outbreak prediction with machine learning. *MedRxiv*.
22. Oña, E.D., Cuerda, R.C., Sánchez-Herrera, P., Balaguer, C., & Jardón, A. (2018). A review of robotics in neurorehabilitation: Towards an automated process for upper limb. *Journal of Healthcare Engineering*.

23. Al-Quraishi, M.S., Elamvazuthi, I., Daud, S.A., Parasuraman, S., & Borboni, A. (2018). EEG-Based control for upper and lower limb exoskeletons and prostheses: A systematic review. *Sensors (Basel, Switzerland)*, 18.
24. Nurhanim, K., Elamvazuthi, I., Izhar, L. I., & Capi, G. (2019). Feature selection of human daily activities using ensemble method classification. *IEEE Student Conference on Research and Development (SCoReD), 2019*, 339–344.

A Comparative Analysis of Two Soft Computing Methods for Sales Forecasting in Dairy Production: A Case Study



A. Fallahpour, E. U. Olugu, K. Y. Wong, and O. C. Aja

1 Introduction

Supply chain management (SCM) is an integral part of the manufacturing industry. A supply chain is defined as a linkage connecting the manufacturing and raw materials supply processes with the end users [1]. In today's manufacturing world, supply chain resilience has become a yardstick to evaluate manufacturing performance in terms of cost reduction, production time management with focus on reducing the duration for production, shorter lead time, increase product range, waste reduction through lean stock practices, meeting customers' expectation by offering them more reliable delivery time, creating values through enhanced customer services and higher product/service quality, and employing efficient coordination in creating a bridge between demand and supply in production framework [2]. The concept of SCM has received increased attention from manufacturers, academics, consultants, and business managers [3], thus, various definitions for SCM exist from the perspectives of the users and their industries. Christopher [4] defined SCM as a management process of

A. Fallahpour · K. Y. Wong

Faculty of Mechanical Engineering, Department of Manufacturing and Industrial Engineering,
Universiti Teknologi Malaysia, 81310 UTM Skudai, Malaysia

e-mail: fallahpour.a@utm.my

K. Y. Wong

e-mail: wongky@mail.fkm.utm.my

E. U. Olugu (✉)

Faculty of Engineering, Department of Mechanical Engineering, UCSI University,
Kuala Lumpur, Malaysia

e-mail: olugu@ucsiuniversity.edu.my

O. C. Aja

Mechanical Engineering Department, Curtin University Malaysia, CDT 250, 98009 Miri,
Sarawak, Malaysia

e-mail: aja.ogboo@curtin.edu.my

© The Author(s), under exclusive license to Springer Nature Switzerland AG 2021

K. Palanikumar et al. (eds.), *Futuristic Trends in Intelligent Manufacturing*,

Materials Forming, Machining and Tribology,

https://doi.org/10.1007/978-3-030-70009-6_10

creating superior customer values at reduced cost considering all the associated value chain and developing as well as management of all-round relationships between the organization, the suppliers and customers. SCM was described by Harrison and Van Hoek [5] as a management tool for process planning and control to create relationship links between partners in the entire supply chain for a manufacturing industry with the main aim of meeting the expectations of end-customers. Global Supply Chain Management Forum (GSCMF) has identified eight processes in SCM which include, demand management, order fulfillment, supplier relationship management, manufacturing flow management, product development and commercialization, customer service management, returns management, and customer relationship management.

Various studies have been conducted to solve SCM problems using soft computing approaches. Soft computing is a set of approaches, such as fuzzy logic (FL), neural networks (NN), fuzzy neural network (FNN), genetic algorithm (GA) and genetic programming (GP), which employ existing data and create flexible information management process that can be used to solve complex problems. Soft computing techniques offer several advantages such as data imprecision tolerance, management of uncertainty, the use of partial truth (low reliable data) to achieve tractability and the ability to simulate human behavior in decision making at a low cost [6]. This paper is adopting gene expression programming (GEP) which is of the family of evolutionary programming as a new approach in soft computing for solution prediction in complex problems. The choice of GEP as a prediction computing technique is its non-requirement for cast equation for regression analyses while presenting prediction equations. ANN and GEP are the evaluation programming applied for prediction in many research studies.

Demand management is an important process of SCM. Considering that organizational strategies are founded on the vision and mission of the organization to create value for the organization and her customers/, The customers' expectation drives the quality of every organization, and as such a successful demand forecast is key to achieving the organization strategies. Soft computing can be used widely in demand management as has been employed in many surveys to achieve results in demand management and its sub-processes. From literature, sales forecasting, a sub-process of demand management indicated 80% research affinity of all researches conducted in demand management [7]. As production requires both physical and human resources, forecasting is a very vital aspect for manufacturing efficiency. For organization to remain profitable and sustainable, sales forecasting is very necessary in harmonizing the appropriate manpower demand and the required physical resources for production at various times and seasons. Sales forecasting is considered a major strategic activity and sub-process of demand management as it helps in organizational decision-making processes [7]. Studies conducted in sales forecasting show that the two different methods for sales forecasting are classical methods and artificial intelligence methods.

In the artificial intelligence methods, ANN and FNN are common powerful tools employed for forecasting and they have been utilized in sales forecasting. Kuo [8] applied the FNN in forecasting sales. The study proposed genetic algorithm (GA) which integrated fuzzy neural network (GFNN) to learn IF-THEN rules of

fuzzy for sales promotion in organization. Furthermore, the researcher integrated the results from the GFNN with forecast from ANN and observed that the results of the integration performed better than the outcome of stand-alone ANN and the results from conventional statistical methods. Pai and Lin [9] used three forecasting approaches; namely, support vector machines (SVMs), general regression neural networks (GRNN) and seasonal time series autoregressive integrated moving average (SARIMA) to model and simulate production values' forecast. The experimental results of operation showed that support vector machines (SVMs) showed better accuracy than GRNN and SARIMA. Neural network has been employed in sales forecasting in so many areas such as aggregate retail industry [10, 11], textile and apparel industry [12, 13], food products [14], glass products [15] as well as printed circuit board sales forecasting as presented by Chang et al. [16].

GEP has been used by several researchers for prediction because of its robustness. Dayik [17] employed GEP, ANN and multiple linear regression analysis for the prediction of the breaking strength of yarn. The results of this study showed that GEP, a soft computing technique indicated higher accuracy than classical statistical methods and ANN. Moghassem and Fallahpour [18] implemented GEP to predict the relationship between draw frame and spun yarn strength. In their study, an accurate equation was presented from GEP modeling and optimization using MATLAB software.

In this investigation, GEP and ANN were employed for sales forecasting in a dairy production company (ABC) which is one of the most famous brand of dairy manufacturing in Asia with enormous exports of her products around the world. Forecasting the dairy production demand is sensible and strategic, in which managers are concerned of reliance on prediction methods and its reliability and comfort ability to test and analyze it. Comparison between GEP and ANN was carried out to forecast the deal of sales based on the historical data derived from formal documents. These two soft computing approaches were applied in the forecasting of sales of the dairy products and compared their capabilities in the dairy sales forecasting.

The remaining part of this paper presented in Sects. 2, an overview of GEP, in Sect. 3, brief introduction to ANN while Sect. 4 explained the required data for this study. Furthermore, Sects. 5 and 6 involved predictions of dairy sales using GEP and ANN, respectively while Sect. 7 presented the results. Section 8 presented the conclusion.

2 Gene Expression Programming (GEP)

A genetic algorithm (GA) provides professionals with optimization solutions to constrained and unconstrained problems and has been considered one of the most important constituents of soft computing methods, thus finds application in several engineering fields [19]. Ferreira [20] invented Gene Expression Programming (GEP) as a Genetic Programming (GP) process following the proposal of Koza and Koza

[21]. The beauty of GP is that it searches solution to a problem in a problem-independent manner once the problem is clearly defined. The GP first generates chromosomes randomly with regards to the defined initial population centered on the problem. The generated chromosomes are then analyzed to appraise the fitness of each of the chromosomes in the problem thereby removing noise data. The individual chromosomes are further assigned to sets considering their properties. The processes continue in series of simulations and iterations to generate final solution.

GEP like GP can adopt genetic operators. GEP has five main components which include function set, terminal set, fitness function, control parameters and stop condition. In modeling the GEP, linear strings with specific lengths are used to encode the individuals which this linear string representation are reconfigured to non-linear entities having different sizes depending on the model. The model also has effect of shapes and the expression trees (ET) which define the object of selection in the algorithm.

Depending on the operating codes and situations that apply, a chromosome may or may not undergo modifications. The modifications in the chromosomes contribute to the learning process of the model to accept and analyze data for prediction. GEP modeling has some advantages which include: (i) Chromosomes are easy to modify/manipulate, has linear nature, relatively small and compact which gives it the ease of recombination of cluster of chromosomes or even allow transposition where necessary. (ii) The expression trees have their exclusive configurations which form the entities for selection to occur, thus may lead to reproduction of chromosomes as modified or unmodified chromosomes.

The genes of the GEP comprise the head and tail. A symbol of the head indicates that at such point, there exist functional process and terminals while a representation of the tail constitutes only the terminals. Every problem has its model and the problem determines the choice of length for the head whereas, the tail takes its length depending on the length of the head and the arguments' population. For more explanation of GEP, the reader may refer to Ferreira [20].

3 Artificial Neural Network

Artificial neural networks (ANNs) find application in several prediction modeling requirements. It can be used for feature extraction (using hidden layers). ANNs are employed in classification and uses regression (e.g., multilayer perceptron) for prediction enhancement and accuracy. To extract existing features and classify algorithms, mapping can be employed, thus forming neural network architectures for efficient (hardware) implementation [22]. In order to classify for prediction, the most widely used neural network technique is the back propagation neural network (BPNN) [1]. In the ANN modeling of the dairy sales forecast in this study, BPNN was used. For more information on modeling using ANNs, the reader may refer to Tao et al. [23] and Kaviarasan et al. [24].

4 Case Study and Data Description

In this survey, the proposed algorithm is established in the ABC dairy company. ABC dairy company was established between 1991 and 1992 in Asia. Mack was supposed to be the main/primary brand for this company's dairy products but from the inception of the company, ABC was welcome as a brand name which made ABC become the dairy company original brand [25]. The company in 1991 focused on developing strategic milk collection stations across the countries in Asia. The company expanded to industrial production of yoghurt for the first time in 1992. The expansion continued in 1993 into ice cream production when the first ice cream line was launched. Diversification in their classes of products increased as the year passes by which birthed the development of cheese production line which involved the production of different cheese flavor and specifications such as Amol white chesses, cream cheese, cumin, Lighvan and Gouda. The expansion saw the establishment of plain and flavored milk (e.g., banana milk) production line and UHT unit milk (i.e., milk with high durability in Tetrapak packaging) in 1995. The industrial dry milk production line (e.g., Whey powder) came into being in 1997 while cream cheese production line was launched in 1999.

The ABC dairy company tried to serve the customers by removing intermediaries, thus distributed their products to supermarkets directly nationwide. The company now has 23 sales and distribution branches in various provinces under the supervision of central sales organization serving more than 65,000 supermarkets, especially in main cities. In addition, by considering the company policy and diversity, new markets for the first time are directly targeted. ABC has succeeded in penetrating fast foods throughout the whole country and converted many first-degree fast foods to its permanent customers.

Table 1 shows the experimental quantities about the sold product weight. In this paper, the weight of products sold during a given month is under experiment using data for eight years. In a practical review, one hundred months have been supposed to verify the performance of business and commercial department who have the responsibility of distributing products on time, safe and secured.

The data used in this study were divided into two sets as training data and testing data such that after training, the used data for the training will not be used for the testing rather the testing data will be employed to check the performance of GEP and ANN models. Table 2 shows the selected testing data from the raw data.

5 Prediction by GEP

The used parameters for the GEP prediction process are presented in Table 3 and each parameter is defined accordingly.

The two data sets which are the training data and testing data are different sets of data, the data used for training cannot be used for testing and as such testing

Table 1 Experimental quantities of products

Month	PW	M	PW	M	PW	M	PW
1	24055	6	25910	11	26179	16	25524
2	23851	7	25646	12	22938	17	24997
3	19104	8	25569	13	23855	18	25166
4	25543	9	19126	14	19152	19	26699
5	28049	10	25716	15	23193	20	23927
21	26412	26	27051	31	25494	36	26978
22	26455	27	27259	32	24009	37	28349
23	26762	28	27978	33	26762	38	28598
24	26722	29	27881	34	26825	39	25622
25	25158	30	27800	35	27201	40	25114
41	25233	46	24513	51	26029	56	25605
42	19027	47	25909	52	18887	57	25849
43	24429	48	24955	53	26295	58	26967
44	25065	49	24910	54	25045	59	25997
45	24914	50	25944	55	25886	60	24399
61	25669	66	25483	71	24450	76	21490
62	24356	67	25993	72	22493	77	22752
63	18967	68	26006	73	18948	78	24575
64	25145	69	26957	74	18793	79	25530
65	25424	70	23541	75	21417	80	25481
81	26161	86	28740	91	21527	96	20017
82	24731	87	23041	92	18996	97	18874
83	24535	88	22582	93	20000	98	23880
84	24909	89	22457	94	18005	99	26753
85	25552	90	23118	95	18964	100	24939

Table 2 Testing data sets

Month	91	92	93	94	95	96	97	98	99	100
Product weight	21527	18996	20000	18005	18964	20017	18874	23880	26753	24939

data are reserved to evaluate the performance of the model after training. From the raw data, the selected data for the training were from 10 data set while the testing data are from 90 data set. To forecast the testing data by GEP, the GEP parameters were combined. To reduce computational time of running all the GEP parameters combinations, five combinations as shown in Table 4 were selected for testing the model using the testing data.

Table 3 GEP Parameters

Parameter acronym	Parameter definition
P1	Number of chromosomes
P2	Head size
P3	Number of gene
P4	Linking function
P5	Mutation rate
P6	One-point recombination rate
P7	Two- point recombination
P8	Gene recombination rate
P9	Gen transposition rate
P10	Number of generation
P11	Program size
P12	Function set

Table 4 The different structure of GEP for prediction

Models	P1	P2	P3	P4	P5	P6	P7	P8	P9	P10	P11	P12	R2	MSE (test)
1	30	8	2	+	0.044	0.3	0.3	0.1	0.1	2	27	+, *, /, -	0.45	1031.36
2	80	7	7	+	0.055	0.3	0.5	0.3	0.1	2	78	sin, tan, *, +	0.53	160.9
3	50	8	7	*	0.03	0.3	0.3	0.5	0.5	2	116	*, /, -, sin, tan	0.42	117.28
4	63	4	3	+	0.025	0.2	0.4	0.1	0.1	2	70	*, /, -, sin, tan	0.98	33.1
5	100	9	4	/	0.044	0.3	0.2	0.2	0.3	3	92	*, /, -, sin, tan	0.56	254.63

The simulation was supported with R-square and mean square error (MSE) analyses. The result of the analysis of the GEP as presented in Table 4 showed that the combination for Model 4 indicated best combination indicating R-square of 0.98 (98%) and mean square error of 33.10. Figure 1 shows the best result showing the predicted and real-time results. A close look at Fig. 1 shows that the real and predicted data have strong match in terms of data and trend alignment for GEP model 4 prediction.

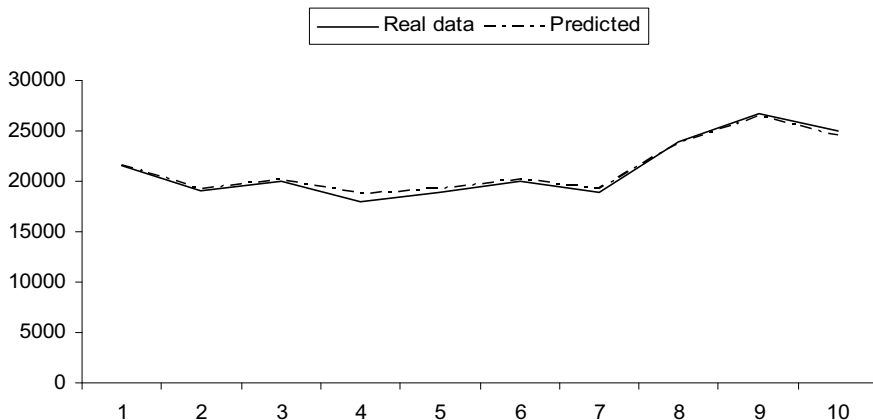


Fig. 1 Actual GEP outputs for predicting the product weight

6 Prediction by ANN

This investigation developed several different structures of ANN for training of the data and the models were also tested individually in order to obtain the best model from the trained models. These are multi-layer perceptions, generalized feed forward, Jordan/Elman, self-organization map, principal component analysis, modular network and recurrent network.

At the training level, a notable parameter that has influence in the back-propagation learning algorithm model is the learning rate. Study showed that learning rate could be accelerated by adopting large learning rate value but this choice has its drawback of creating error at the output or destabilizes the training cycle. To achieve higher accuracy and reduce error in the training output, small learning rate values offer higher convergence accuracy with low error but face the consequence of prolongs training time [10]. Hence, the use of an adaptive learning rate increases the training performance, and training was done with the back-propagation algorithm by Neuro Solutions 6. The test data described in Table 2 were also used for forecasting the dairy products. In this paper, the best trained neural network was tried for predicting future. As can be seen, the best result is 0.98 R-square and 47.65 MSE as shown in Table 5. The best test results are shown in Fig. 2.

Table 5 Results of the R-square and MSE for the testing data of the proposed GEP and the ANN

Analysis parameters	NN	GEP
R2	0.98	0.98
MSE	47.65	33.10

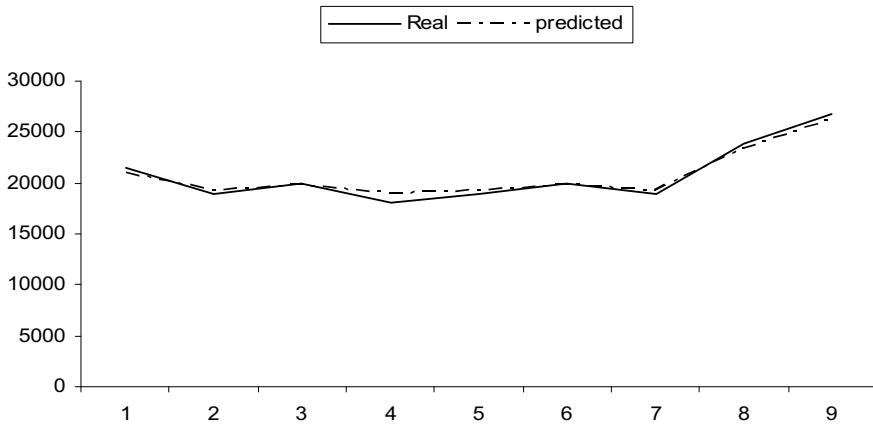


Fig. 2 Actual ANN outputs for predicting the product weight

Table 6 Results of the R-square and MSE for the training data of the proposed GEP and the ANN

Analysis Parameters	NN	GEP
R2	0.94	0.96
MSE	0.08	0.05

7 Result and Discussion

The investigations conducted forecast dairy sales using GEP and ANN models. A comparison of the two different models, GEP and ANN were conducted after the R-squares and mean square errors (MSE) were conducted for the two models. The results of GEP and ANN algorithms prediction are presented in Tables 5 and 6 for predicting the testing and training data, respectively. The results obtained for the MSE of the testing data indicates that the performance of the GEP model is better than the ANN. The MSE values of two models from the forecasting based on the testing data are 33.10 and 47.65, respectively. Table 5 shows the difference between the MSE of two models. In comparing between the GEP and ANN in training, the power of the GEP in R-square and MSE was more than the ANN. Table 6 exhibits the differences between R-square and MSE of the training data of GEP and ANN. The results of this study show that the GEP model is a better alternative for time series prediction and dairy forecasting.

8 Conclusions

In this paper, two evaluation programming have been used in forecasting in a dairy company, named ABC. This study examined the forecasting performance of the

GEP model compared with ANN. From the previous studies on sales forecasting with soft computing models, it has been shown that the soft computing models have worked better than statistical models. This study has compared the GEP and ANN models in forecasting the dairy sales of a company. In order to evaluate the power of these two evaluations programming, the study adopted the Mean Square Error (MSE) and R-square. Power of forecasting has been the same in GEP and ANN (0.98) in R-square. However, in MSE, the error rate of GEP has been less than ANN. The MSEs obtained by GEP and ANN have been 33.10 and 47.65, respectively. As a summary, the research findings have demonstrated that the GEP model has been able to perform more accurately than the ANN. Support Vector Machine (SVM) or ANFIS in forecasting the dairy products can be utilized for the future studies.

References

1. Yau, L. W., & Huang, C. C. (2006). Agent-based demand forecast in multi-echelon supply chain. *Decision Support Systems*, 42(1), 390–407.
2. Gumus, A. T., Guneri, A. F., & Keles, S. (2009). Supply chain network design using an integrated neuro-fuzzy and MILP approach: A comparative design study. *Expert Systems with Applications*, 36(10), 12570–12577.
3. Croom, S., Romano, P., & Giannakis, M. (2000). Supply chain management: An analytical framework for critical literature review. *European Journal of Purchasing & Supply Management*, 6(1), 67–83.
4. Christopher, M. (2004). *Logistics & supply chain management* (2nd ed.). Norfolk: Prentice Hall.
5. Harrison, A., van Hoek, R. (2005). *Logistics management and strategy* (3rd ed.). Prenticehall Financial Times.
6. Pal, S. K., & Ghosh, A. (2004). Soft computing data mining. *Information Sciences*, 163(1), 1–3.
7. Ko, M., Tiwari, A., & Mehnen, J. (2010). A review of soft computing applications in supply chain management. *Applied Soft Computing*, 10(3), 661–674.
8. Kuo, R. J. (2001). A sales forecasting system based on fuzzy neural network with initial weights generated by genetic algorithm. *European Journal of Operational Research*, 129(3), 496–517.
9. Pai, P.-F., & Lin, C.-S. (2005). Using support vector machines to forecast the production values of the machinery industry in Taiwan. *The International Journal of Advanced Manufacturing Technology*, 27(1), 205–210.
10. Alon, I., Qi, M., & Sadowski, R. J. (2001). Forecasting aggregate retail sales: A comparison of artificial neural networks and traditional methods. *Journal of Retailing and Consumer Services*, 8(1), 147–156.
11. Chu, C.-W., & Zhang, P. G. (2003). A comparative study of linear and nonlinear models for aggregate retail sales forecasting. *International Journal of Production Economics*, 86(3), 217–231.
12. Celia Frank, A., Garg, L., & Sztandera, A. Raheja. (2003). Forecasting women's apparel sales using mathematical modeling. *International Journal of Clothing Science and Technology*, 15(2), 107–125.
13. Thomassey, S., & Happiette, M. (2007). A neural clustering and classification system for sales forecasting of new apparel items. *Applied Soft Computing*, 7(4), 1177–1187.
14. Doganis, P., Alexandridis, A., Patrinos, P., & Sarimveis, H. (2006). Time series sales forecasting for short shelf-life food products based on artificial neural networks and evolutionary computing. *Journal of Food Engineering*, 75(1), 196–204.

15. Jeong, B., Jung, H. S., Park, N. K. (2002). A computerized causal forecasting system using genetic algorithms in supply chain management. *Journal of Systems and Software*, 60(3), 223–237.
16. Chang, P.-C., Wang, Y.-W., & Tsai, C.-Y. (2005). Evolving neural network for printed circuit board sales forecasting. *Expert Systems with Applications*, 29(1), 83–92.
17. Dayik, M. (2009). Prediction of Yarn properties using evaluation programming. *Textile Research Journal*, 79(11), 963–972.
18. Moghasssem, A. R., & Fallahpour, A. (2011). Processing parameters optimization of draw frame for rotor spun yarn strength using gene expression programming (GEP). *Fibers and Polymers*, 12(7), 970–975.
19. Majumdar, A., Mitra, A., Banerjee, D., & Majumda, P. K. (2010). Soft computing applications in fabrics and clothing: A comprehensive review. *Research Journal of Textile and Apparel*, 14(1), 1–17.
20. Ferreira, C. (2001). Gene expression programming: A new adaptive algorithm for solving problems. *Complex Systems*, 13(2), 87–129.
21. Koza, J. R., & Koza, J. R. (1992). *Genetic programming: On the programming of computers by means of natural selection*. MIT press.
22. Desheng, W. (2009). Supplier selection: A hybrid model using DEA, decision tree and neural network. *Expert Systems with Applications*, 36(1), 9105–9112.
23. Qing Tao; Jinde Cao; Meisheng Xue; Hong Qiao. (2004). A high performance neural network for solving nonlinear programming problems with hybrid constraints. *Physics Letters A*, 288, 88–94.
24. Kaviarasan, V., Venkatesan, R., & Natarajan, E. (2019). Prediction of surface quality and optimization of process parameters in drilling of Delrin using neural network. *Progress In Rubber, Plastics And Recycling Technology*, 35(3): 149–169.
25. Kalleh (2020). Kalleh Dairy Products. <http://dairy.kalleh.com/Default.aspx?alias=dairy.kalleh.com/en>. (26 Dec 2020).

AR and VR in Manufacturing



**R. Dhanalakshmi, Cherukuri Dwaraka Mai, B. Latha,
and N. Vijayaraghavan**

1 Introduction

In the current competitive scenario manufacturing industries are facing difficulties to produce the products on time with all safety measures which in most case is not happening and leading to conflict between the manufacturer and the customer. In order to bring a change to the industry the new technology which is trending and bringing the economy graphs up in the market is Augmented and Virtual reality. AR/VR technologies bring in a new environment in the workfield and create a completely new experience to the workers. Introducing AR/VR in the manufacturing sector (industry 4.0) will benefit and make the work really simple. VR creates a simulated environment where workers can modify, find, and rectify errors in the machines due to which human errors can be reduced vastly. VR allows the manufacturing sector to produce efficient quality goods for the people. Basically VR creates a separate environment when the person uses it there is no connection between the real world and the person he enters into a separate environment where he can manipulate the industrial based models according to his wish and time of redrafting can be reduced rapidly using these technologies. AR creates artificial conditions where

R. Dhanalakshmi (✉) · C. D. Mai
Department of Computer Science and Engineering, KCG College of Technology, Chennai, India
e-mail: dhanalakshmisai@gmail.com

C. D. Mai
e-mail: maidwaraka@gmail.com

B. Latha
Department of Computer Science and Engineering, Sri Sairam Engineering College, Chennai,
India

N. Vijayaraghavan
Department of Mathematics, KCG College of Technology, Chennai, India
e-mail: nvrnsb@gmail.com

the elements which are present in the real world are amplified by computational instructions.

Using these workers can keep track of the machines that are used in the manufacturing sector properly and it also allows setting markers that help in keeping track of objects. With AI technology many wonders could be done, it takes time to adapt to this new technology but once people learn the point of it then the demand is going to rise high. With the use of this AR/VR technology many unsatisfied demands of the industrial sector can be fulfilled, it can also give the sector a stress free environment by engaging workers with interesting machine related simulations. This AR/VR can completely change the economy graph of the industries upwards and bring in the industry 4.0 change. Creating pre-model simulations can help industry to prevent various accidents and advancement in machine equipment can be done easily according to the current trend with the use of AR/VR technology.

A Virtual Reality (VR) is a virtual environment generated by a computer that reflects the real world. This virtual reality connects the link between the person and the real world instead simulates a virtual environment the person needs and allow them to work in it by giving them the actual experience which will reduce most of the human errors that are caused in the industry sector. The joy of users experiencing the virtual reality environment is the success of its efficiency and performance of any VR system which may be attained via 3D position trackers and motion gestures. Few interactions can also be done using mouse, keyboard and game devices.

The virtual environment provides a platform to try out innovative designs and ideas which when incorporated excellent results can be produced since people get to know how the work has to be before itself in the virtual environment. The observer can see the simulated objects in the real world with marker location which will be really helpful in order to track any process progression. AR models are widely used nowadays by people in their mobile phones which is user friendly too so the workers need not study the entire process they can initially mess around with the interface to know about it as it does not affect the real world objects and cultivating a new type of learning experience. Using depth sensors, a virtual simulated machine is made to know where and whatever is happening in the process records. It is made to happen virtually in the environment allowing users to make changes and also to prevent accidents which are going to happen due to human error, bots can be introduced which can communicate to person through AR interface giving the user a different work experience.

2 Virtual Reality in Manufacturing Sector

It is a well known fact about virtual reality's tremendous growth in the gaming sector but it's not only for gaming any longer. Virtual reality is skating things across all industries including manufacturing sectors. Now-a-days co-bots (Collaborative Robots) and the implementation of virtual reality is emerging. From creating the design to production of every product there is a plausibility of error occurrence.

For example, in the civil industry the layout plan made and executed wrongly can be identified by the site manager only at a particular stage in-order to avoid such issues in the virtual reality technology. Due to advancement in technologies the manufacturing industries have gone through momentous changes over the years. The emergence of industry 4.0 is happening currently which mostly includes AI vision; that is virtual and augmented reality. Moreover, there is a rising demand for smart and advanced solutions to reduce the number of accidents in the manufacturing industry as this industry is prone to hazard and fatal accidents. In scenarios like this, the VR technology paves way for trying out all possible solutions virtually which provides space for industries to make headway. As discussed in the introduction section virtual reality is a virtual world generated by the computer in which a person can immerse himself as if he is in the real world. This virtual world can be explored and interacted with.

While manufacturing safety improved greatly over years, injuries and hazards graph rate has not decreased yet. Many accidents still happen due to human errors. Despite holding the title 3rd in global manufacturing, Virtual reality may help to reduce the accident rate to greater extent. With the help of VR, a virtual simulation mode is created which helps in manufacturing sector towards the production process and assembly line configurations, identifying potentially dangerous situations. From this either a dangerous hazard can be stopped or completely avoided prior to the process. Virtual reality can also be used to assess the future workplace efficiency by evaluating the task proficiency of a personnel who is performing the specific tasks in the future workplace using VR technology. By deploying this technology in the manufacturing sector better products can be produced with the help of various devices using goggles that employ cameras, depth sensors, and motion sensors which helps to visualize real working environments through simulation. A highly productive and safety environment can be experienced by professionals to assemble and automate things.

In order to manufacture goods that meet specifications, design, prototyping, testing and retesting phases must be crossed. Building full scale products for the testing phase can get very expensive. The need for a full-scale model during the testing phase can be avoided with the use of Virtual Reality. Using the VR technology, all the equipment required to build a full scale model can be identified and put together in the virtual world, before building the product in the real world. Using this approach will cut training time by 75% per person, saving millions. Application of the VR technology in the manufacturing sector can effectively bridge the skill gap between engineers and workers. VR technology can replace manuals, which are used on the traditional way of training, which is advantageous and efficient in training workers.

3 Augmented Reality in Manufacturing Sector

Augmented reality plays a vital role in the manufacturing sector similar to virtual reality, the main difference is virtual reality completely immerses the person into

a separate environment. This is where augmented reality comes into play; it uses marker location to trace the person at the correct position with this feature; many accidents that are occurring in the manufacturing sector can be reduced as dangerous locations can be marked by the AR Gadget. Augmented reality aided manufacturing (ARAM) plays a very vital role in the manufacturing sector.

AR and VR technology can prove to be extremely handy in the field of manufacturing. For instance, identifying unsafe working conditions, predicting the success rate of a product that is still under the process of manufacturing and many more. Manufacturers can also use it for tasks like presenting digital content such as displaying statistics related to a particular project or task and a worker can also find if it easy to determine the temperature of an object to know whether it is safe or unsafe to handle it with no safety gear. An employee can keep track of every action taking place around them using this marvellous piece of technology. It can even be used to accomplish complex tasks like figuring out the accurate location of coworkers, equipment that requires immediate attention and service. Using AR equals making tasks that usually are cumbersome, extremely simple. This in turn significantly increases output and reduces input.

AR helps in the sales perspective also by providing a 3D elemental model, text or video for the customer to understand the details of the product clearly and go for it, it brings transparency between the manufacturer and the customer and now advancement had been brought in such a manner that using ar customer can track and keep a record of every information, detail of their product. It serves as a learning book in a different aspect.

AR can be used for factory planning. Digital planning data can be overlaid onto views of the existing plan made in the factory. A well-grounded plan can be provided using AR technology by providing a visual representation of the prototype along with digital data. The reliable plan consequently leads to reduced time and cost. Accuracy is the most important in planning the outcome or the solution built in the AR model has to be practically applicable to implement in the sector. Another use for AR in the factory is image comparison and processing. The fundamental ideology is that, using AR overlay; comparisons can be made between the image furnished by the supplier i.e.; augmented reality overlay and the high quality image of the part under inspection. This enables technicians to rapidly get to the bottom of the issue without any problem.

3.1 Types of Virtual Reality and Augmented Reality

There are a vast of Virtual Environment systems (VE) which drives us into the imaginary immersive virtual world with the help of HMD devices. Those devices range from medium to high cost value. Some device such as Google cardboard can be experienced with smart phone to experience virtual reality. To list a few devices in VR headset, the following are

- Oculus Rift
- Google cardboard
- Haptic Gloves
- HTC Vive
- Samsung Gear VR (mobile VR).

3.1.1 Augmented Reality Can Be Grouped Such as

1. Marker-based
2. Location-based
3. Dynamic augmentation
4. Complex augmentation—marking target objects w.r.to real images.

Augmented Reality Display Technologies

An augmented Reality supports various applications with its technical features such as Computer Vision, object recognition, GPS and miniature accelerometer etc. A few technologies are described as follows.

Marker-Based AR: An image recognition technique using a camera image which has different types of visual markers like QR/2D code and the results will be sensed by the reader. Most of the applications are functioned with the use of cameras which helps to differentiate augmented images other real images. Markers applications features low processing power for reading and are easily recognizable using simple patterns. Using the information overlaid with the location of the marker, the orientation and the position can also be calculated.

Marker less AR: Marker less AR are also known as location-based, position-based or GPS based AR. It uses miniature versions of a GPS, a digital compass and a velocity meter or accelerometer, which are embedded in the device, to provide data based on the exact location and orientation of the device. Marker less AR are popular due to the existence and usage of smart phones by all everywhere which has GPS features for location tracking, mapping directions and other location based mobile applications.

Projection-Based AR: Projection-based AR is based on the technology of projecting artificial light onto real world surfaces. It also facilitates applications involving human interactions by passing light over real images. The result of the human interaction of that projected light is sensed. The difference between the two projections (expected and achieved) can be measured which helps in detecting the user's interaction. Projection-based AR also uses laser plasma technology which projects a 3D interactive hologram into mid-air to identify the human interactions.

3.2 Top Markerless Augmented Reality SDKs

Markerless Augmented Reality solutions integrates and utilizes both software and hardware. The hardware-based products includes Google Tango into software-based SDKs like Google's ARCore and Apple's ARKit. With the help of these SDKs a user can experience AR effects without any specialized equipment. ARKit and ARCore plays a vital role in making markerless AR across various smartphones and tablets. Another similar technology available in Markerless AR solution is Marxent MxT Tracking, Marxent's proprietary AR tracking SDK, MxT Tracking in combination with ARKit or ARCore provides a extremely enhanced experience to the users and MxT uses a relative tracking approach. User interactions w.r to the movements of the user is possible with the MxT. Other technologies such as Vuforia studio can integrate the CAD results and IoT data to a rich AR experience which is mostly needed for few applications. Some of the advantages include

- Increase worker productivity and satisfaction
- Reducing the cost of errors, waste and accidents
- Improving customer experiences and competitive advantage
- The Reality-Virtuality Continuum.

4 Implementing AR and VR in Manufacturing

AR and VR put together in the industry can do wonders. Firstly, into business perspectives implementing AR and VR will essentially reduce the cost that will be caused during the trial and error phase. Which ultimately increases the profits for the organization. As stated previously, AR and VR technology can be used to train personnel which also reduces the training cost. As the training is generated in the virtual world, the resources can be allocated effortlessly as per the requirement of the person undergoing training i.e.; areas that require focus according to their knowledge and expertise levels. Unquestionably, deploying and getting stuck to these technologies will take a lot of time but once people find out its advantage, it makes the working atmosphere very easy and interesting. In order to make it more interesting gaming task simulations of the actual machine can be given to the employees such that it reduces the stress and creates a different work environment. Taking a small example recently an app was released based on VR and AR where it shook the whole food industry. Basically, the app work is to scan the food and display the calories in the respective food and recommend appropriate food which user health requires and keeps a track on it. It was entirely based on AR and VR. Similarly, regarding civil and architecture an organization came up with an idea of simulating a virtual environment house where customers can view it instantly and modify it on the spot. Introducing AR and VR has made remarkable changes in the industrial sector. Ford has introduced AR and VR to its manufacturing sector and has gone to the next level in the car manufacturing sector. The benefits of this technology is not limited to only big industries. Use of

virtual magazines in the place of conventional magazines is a minimalistic change that can benefit highly as the virtual magazines are more interactive and engaging. This way, small industries/companies can make a small investment in inculcating this technology. The usage of virtual world trumps over the real world processes as it brings multiple advantages due to its diverse usability. Along with the cost benefits, VR benefits the environmental aspects as well. The energy and resources to create real world models and prototypes are almost zeroed out. VR can be used as a meeting room an exhibition stand, a workshop due to its flexibility features and almost unlimited possibilities of creating virtual spaces, Virtual reality can make manufacturing safer, quicker, more efficient and precise, and less costly.

4.1 Applications for AR in Manufacturing

1. Complex Assembly and Maintenance

The sentence that best explains “Modern manufacturing” is assembling a large number of components together in a meticulous sequence rapidly, doesn’t matter which product is being assembled. Besides being highly useful in assembly tasks, AR serves in maintenance of equipments using augmented reality for example Mitsubishi Electric.

2. Expert Support

The skills gap among the staff in the industry can be solved through telepresence. Technology solves the issue of one worker having to learn many methods of task performance. Instead of training every worker, AR technology can be used to supplement the extra knowledge that is required.

3. Quality Assurance

Nowadays the organizations that are embracing AR in manufacturing for quality assurance are experiencing a distinct degree of excellence. Before sending the assembled part to the final designing section, the AR solution helps the workers to make a comparison on how the previously assembled system will match the blueprint made initially. This manufacturing solution will not only save costs and time but also improves accuracy and allows companies to meet a high level of quality criteria. Therefore, integrating augmented reality technology into the production environment gives workers access to complete 3D models of the vehicles. Information about the manufacturing products can be directly accessed by the workers as AR in Quality Assurance is transforming reality into an interactive sphere.

4. Automation

Owing to manufacturing’s apparently inevitable trend towards increasing automation, it is natural to wonder if automation and AR are in competition with each other.

4.2 Reducing Mental Workload and Cognitive Load

Although automation fills most of the labour gap, human capabilities are still required to manage outputs. To achieve the expected output, workers face the need to be skilled with various methods and processes. In the assembly tasks, there are more than one method of assembling parts. It is a huge psychological load to be skilled at each method of assembly. These technologies serve as a 3 dimensional visual guide which are more effective than the conventional user manuals. This way, the mental load it takes to visualize the parts gets reduced. The AR prototype guides the assemblers, requiring less cognitive effort, by providing a visual guide on how to assemble a specific product. In other words, AR helps to fill the workforce skill gaps with considerably reduced mental workload. Cognitive load theory makes use of evolutionary theory to examine human perception architecture and uses that architecture to formulate unconventional, instructional procedures [1]. For instance, supplying learners with worked out samples of problems that they might come across in their respective fields will lower working memory load and aid in the moving of the required details to long-term memory. Compare this to providing students with problems to solve and only the general instructions on how to solve a problem.

Augmented reality offers the promise of providing every member of the industrial workforce with relevant, contextual and customized information and guidance from across the enterprise into their field of view in a seamless, hands-free, intuitive manner that transforms the way they work,

–Amar Dhaliwal, CEO of Atheer Inc.

The capabilities and benefits of AR-based information and instruction go beyond those of static, hard-copy instruction manuals. AR information can be delivered step-by-step in real-time and in context; it can be presented as any combination of simple 2D and complex 3D digital assets; and it can be viewed without shifting attention away from a work piece. Digital instructions can be remotely updated a single time to reflect changes in product design or new best practices and distributed widely to a remote workforce. It was learnt through some studies that the virtual environments had reduced demands for intellect. A demonstrable technique to create systems which are less intellectually demanding is by vitalizing the personnel. Therefore, imparting visual prompts are crucial to assembly tasks. In this scenario, stimulation level and the workmanship go hand in hand. Depending on the complexity of the task, the level of stimulation will vary.

4.3 AR and VR Use Cases

As mentioned in the above context AR and VR can bring up a new change in the manufacturing sector. Fundamentally a use case outlines from a user's point of view, the possible interaction between user and the system. It is generally classified into three elements: actor, system and goal. Actor is the person who is interacting with

the system. It could be a single person or a group of people. System is the process that is required to reach the goal or the end result. Goal is the final triumphant user outcome. Manufacturing is naturally tethered to the requirement of constant production and uninterrupted performance in a competitive business environment since every moment of idle time causes revenue loss. This technology's prospective to create an artificial environment of any given aspect of almost every manufacturing task makes its utilization extensive. By introducing this, better quality goods can be delivered with less production time. In Order to provide more clarity, below are some detailed examples of use cases of AR and VR in the manufacturing industry.

First use case: Remote Expert Assistance using AR

This is mainly deployed to rectify the errors in the machine when the technician is not present at the given moment. The actors in this scenario are (i) the person present in the field, next to the machine with some technical grasp (ii) the actual technician who is remotely available. The goal is to rectify the error. With the use of AR and VR technology which is the beginning of industry 4.0 the errors in the machines can be rectified remotely. In the above scenario an AR app is built which has marker functions in it when the actor in the field turns the camera towards the machine and the actual technician available remotely will be able to check what type of error it is and input it remotely to the AR application and this AR application guides with the actor in the field with the instructions that are already programmed in the application by using marker technology, so that the person can rectify the problem in the machine easily without any difficulty rather than waiting for the actual technician to arrive and rectify it which is generally a time consuming process. This method could be implemented in the manufacturing sector. These AR applications can help measure changes in the level of fluid in machines, identify unsafe working conditions for labours and visualize design components which will be helpful in order to know the working plan and progress of a particular machine. AR devices make staff mobility coherent and natural. In contemporary endeavours, manufacturing lines work around the clock and can not afford any idle time. By replicating processes and performing virtual tests of production and equipment, AR, VR technology helps spot mistakes which could likely lead to harm in the environment and rectify them before they stall operations. The above use case is advantageous in the outskirts of the city where travelling in and around the place is crucial. Since most industries are located in the outskirts of cities, in the case of emergency where the technician is not available this method, i.e.; remote expert assistance can be implemented.

Second use case: Speeding up Production

Consider an automobile manufacturing industry where it involves assembly line work, here VR glasses can be introduced for efficient production. Let us consider two different approaches to the same scenario: Assembly of car parts. First approach; the worker in the assembly line is asked to assemble the car parts in the old manner where he/she has to refer to a manual and assemble the parts. Second approach; the same person is given the Google VR glasses where all the instructions are already programmed and also has the feature of voice guidance such that the person can

assemble the parts without having to refer to an instruction manual. By the second approach, the efficiency increases by 40% and the products that are made in this manner will have no flaws as the VR technology also monitors the production process.

Third use case: AR and VR in the post production process i.e.; in transportation

AR has immense potential to benefit in every possible manner—especially in transportation. From enhancing the driving experience to avoid accidents and from providing helpful information to turn-by-turn directions, the future of the linked vehicle has never looked so astounding. With this technology the goods which are manufactured can be safely transported to the destination. This AR feature helps the driver to keep a track on goods as well drive with proper navigation to the destination. In this scenario an AR system is installed on the windshield where it displays all the necessary information on the driver screen, avoiding the distraction that would be caused if the driver has to check his phone constantly for updates.

Fourth use case: Implementing AR and VR in sorting goods according to selective criteria

This can minimize sorting errors when segregating goods that are present after manufacturing. It provides operators with visual instructions to place the appropriate product in its correct place and the AR system keeps marker on all products such that whenever there is a need of loading goods, the operator can directly access this AR system which can be connected in glasses like Google glass so that the marker displays the exact place of the product and without searching the operator can proceed and collect the required goods.

Virtual reality can be used in a manner that workers in the manufacturing industry can enjoy and learn new equipment and methods. A whole new environment can be created where workers can wear VR glasses and experience the environment. Simulation of new machines can be created in this environment.

4.4 Challenges Faced by AR and VR

Lack of proven/tested business models is one of the major obstacles to widespread adoption of the AR and VR technology. The second challenge faced by industries in adopting AR solutions is the lack of augmented reality app design and development standards. The next challenge is the potential exposure of sensitive information through wearables and cloud-based systems. Another challenge is the initial investment. Although AR and VR increases the profit rate, initial investment is little on the higher side since appropriate equipment for VR should be brought in order to apply on the field. It is essential for Augmented and virtual reality, the necessity of combining a set of regulations to create an enveloping experience generally around optic mechanical designs. But the amount of capital required to integrate optics with such high precision requires a significant volume of units to recover the investment. However, once these technologies become more prevalent in the manufacturing industry, the



Fig. 1 AR/VR market

initial investments can be retrieved. The impact that AR/VR will have on the basic gadgets that we use in our daily lives can not be turned a blind eye to. With these technologies, entirely new gadgets could come into existence which would replace the current appliances.

As proven by our reliance on devices such as the smartphone, connectivity is evidently very important. Although the global norms for 5G have not been set yet, the common expectations from it include excessive bandwidth, low latency and support for additional connected devices. If the connectivity between devices weaken, the resultant output may turn out to be incorrect or inaccurate.

As seen in Fig. 1, the graph depicts the profit market rate of AR and VR drastically increases in the long run; the only requirement is the initial investment and adoption of the 5G technology which gives enormous outcomes. Since people need to adapt to the new change in the industry it takes time to view the profit once the technology is adapted and settled the trend starts increasing drastically. If AR and VR are anticipated to be the leading technology in the staple future, lot more work is anticipated to be done in implementation of various technologies and to provide an awesome user experience, Another major drawback would be for the industries which are located in remote villages since connectivity is a major issue in villages bringing fast speed internet connection would take a long time and industries have to cope up using the slow 4G or 3G connection until then. When talking about installation of AR and VR technologies mentioning of maintenance is mandatory once the system is installed it has to be maintained properly and checked regularly if not the outcomes produced would be wrong in all aspects leading to a huge loss to the manufacturing industry.

The system must be properly maintained by the officials initially. Due to lack of knowledge on handling AR/VR products, the industry needs to bear the initial investment cost and the costs that could be caused due to product damage or breakage. Regarding order fulfillment and warehouse organization, employees must balance

between managing orders and systematic responsibilities. As we know about the responsibilities of warehouse maintenance, such as placing an order, receiving products, scan and report the data and delivery to the unit involves a lot of manual work, which can unnecessarily increase the time it takes to finish an effortless, yet mind-numbing process. AR technologies could be used in such cases to minimize the manual work and automating various activities such as recording the precise location of products and goods, increasing the speed and efficiency of the work. The necessary information is retrieved using the AR system to initiate the order. Hence it will reduce to only fetching the product and delivering it to the right place by the employees. During this process the initial marks need to be done by a human so if anything goes wrong while marking the markers then the product will be delivered from the warehouse erroneously. Another factor to be considered would be the health risks of the workers since the production process takes around 8 h per day. Workers will have to take necessary breaks from wearing these equipment constantly. Accessing user information regarding the employees and recording their performance during the usage of these technologies may raise ethical questions. There is a fine line between gathering relevant data and total surveillance. Therefore, data security can be a challenge with the use of this technology.

5 Conclusion

It is highly important to consider that the scenarios listed here are only a tiny segment of the real potential the AR and VR technology have to offer to the manufacturing industry. There will be more emerging application scenarios and challenges to implement them which are never thought possible or anticipated. By implementing AR and VR in the manufacturing sector the evolution of industry 4.0 arises. Workers and people will be benefited with various features making work easy in less time which is the requirement these days and most importantly it helps to decrease the injury rate graph in the manufacturing sector. The manufacturing resalm is being reconstructed by AR and VR. This technology is bringing a lot of eagerness in the manufacturing industry sector. This technology can lead to the improvement in safety, design function and performance, bringing mortal and machine closer.

References

1. Sweller, J. (2011). Cognitive load theory. In J. P. Mestre & B. H. Ross (Eds.), *The psychology of learning and motivation: The psychology of learning and motivation: Cognition in education* (Vol. 55, pp. 37–76). Elsevier Academic Press. <https://doi.org/10.1016/B978-0-12-387691-1.00002-8>.
2. Barandiaran, I., Paloc, C., & Grana, M. (2010). Real-time optical markerless tracking for augmented reality applications. *Journal of Real-Time Image Processing*, 5(2), 129–138.

3. Chen, R., Wang, X., & Hou, L. (2011). Augmented reality for collaborative assembly design in manufacturing sector. In N. Rao (Ed.), *Virtual technologies for business and industrial applications: Innovative and synergistic approaches* (pp. 105–117). IGI Global. <https://doi.org/10.4018/978-1-61520-631-5.ch006>.
4. Chien, S., Choo, M. A., Schnabel, W., Nakapan, M., Kim, J., & Roudavski S. (Eds.). (2016). Living systems and micro-utopias: towards continuous designing, In *Proceedings of the 21st International Conference of the Association for Computer-Aided Architectural Design Research in Asia CAADRIA 2016*, (pp. 713–722). The Association for Computer-Aided Architectural Design Research in Asia (CAADRIA), Hong Kong.
5. Cover, T., Hart, P. (1967). Nearest neighbor pattern classification. *IEEE Transactions on Information Theory*, 13(1), 21–27 (1967). (Cortes, C., & Vapnik, V. (1995). Support vector networks. *Machine Learning*, 20(3), 273–297).
6. Rish, I. (2001) An empirical study of the naive bayes classifier. In *International Joint Conference on Artificial Intelligence* (Vol. 3, no. 22, pp. 41–46).
7. Novak-Marcincin, J., Barna, J., Janak, M., & Novakova-Marcincinova, L. (2013). Augmented reality aided manufacturing. *Procedia Computer Science*, 25, 23–31. <https://doi.org/10.1016/j.procs.2013.11.004>.
8. Panchapakesan, P. (2020). Managerial challenges in VR and AR in Asia. In S. M. Loureiro (Eds.), *Managerial challenges and social impacts of virtual and augmented reality* (pp. 44–54). IGI Global. <https://doi.org/10.4018/978-1-7998-2874-7.ch003>.
9. Siltanen, S. (2012). Theory and applications of marker-based augmented reality. Espoo, VTT (p. 199 +app., p. 43). VTT Science; 3. ISBN 978-951-38-7449-0 (soft back ed.) 978-951-38-7450-6.
10. Tang, A., Owen, C., Biocca, F., & Mou, W. (2003). Comparative effectiveness of augmented reality in object assembly. In *Proceedings of the Conference on Human Factors in Computing Systems-CHI'03*. <https://doi.org/10.1145/642611.642626>.
11. Using Augmented Reality in Manufacturing to Improve Worker-PTC. Retrieved from Skills <https://www.ptc.com/en/technologies/augmented-reality/solutions-for-manufacturing>.
12. Everything You Need to Know to Build Location-Based AR App. Retrieved from <https://blog.vakoms.com/everything-you-need-to-know-to-build-location-based-ar-app/>.
13. Different Types of AR Explained: Marker-Based, Markerless & Location. Retrieved from <https://www.blippar.com/blog/2018/08/14/marker-based-markerless-or-location-based-ar-different-types-of-ar>.
14. <https://www.marxentlabs.com/what-is-markerless-augmented-reality-dead-reckoning/>.
15. Why Every Organization Needs an Augmented Reality Strategy. (2020). Retrieved from <https://hbr.org/2017/11/a-managers-guide-to-augmented-reality>.
16. AR-VR and its use in Manufacturing. (2020). Retrieved from <https://www.industr.com/en/ar-vr-and-its-use-in-manufacturing-2441777>.
17. CMTC. (2020). Retrieved from www.cmtc.com.

Industrial IoT and Intelligent Manufacturing



S. Rajarajan, S. Renukadevi, and N. Mohammed Abu Basim

1 Introduction

Making the industrial world smarter with the help of connectivity and networking through sensors, is the priority in the current scenario. Decisions are done on the global level by interconnecting users and machines. We called this phenomenal technology the Internet of Things (IoT). Its applications range from home automation, wearable, precision agriculture, smart grid infrastructure, connected transportation and intelligent manufacturing. Another derivative of IoT is Industrial IoT (IIoT) which gets widely familiarized through Industry4.0.

This is characterised by interfacing various industrial systems through their communication modules, data analytics to monitor and improving their performance to benefit the industrial sector. The systems which get connected through sensors and actuators to solve complex problems is termed as “Cyber Physical System” as shown in the Fig. 1. The performance gets bigger by combining big data with machine learning algorithms to gain deep understanding of data analytics.

Adaptability is the major concern for all the industrial systems. Current advancements are done in the industrial systems to adapt to their own environment and monitor their performance and failures. Scheduling their maintenance through

S. Rajarajan (✉)

Department of Electronics and Communication Engineering, Sri Sai Ram Institute of Technology (Autonomous), Chennai 600 044, India
e-mail: srajayaganesh@gmail.com

S. Renukadevi

Department of Mathematics, Bharathi Women’s College (Autonomous), Chennai 600 108, India
e-mail: renurajarajan24@gmail.com

N. Mohammed Abu Basim

Department of Mechanical Engineering, Velammal Institute of Technology, Chennai 601 204, India
e-mail: basim89@gmail.com

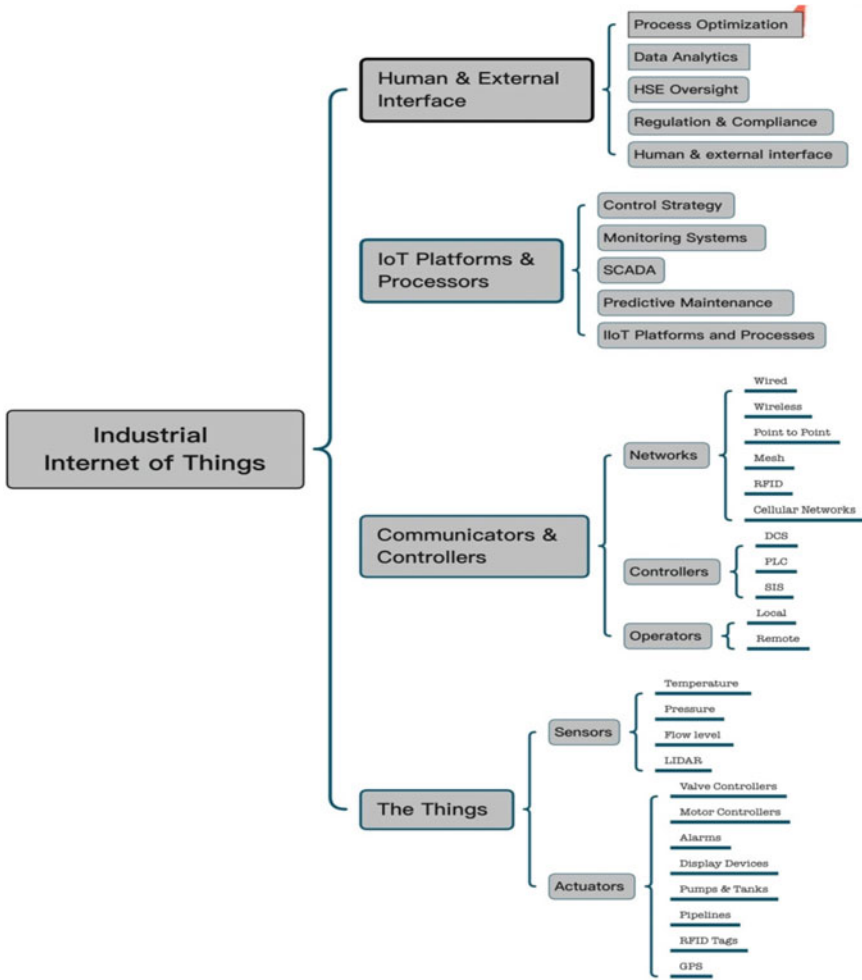


Fig. 1 IIoT framework

various control algorithms, communicating with floor counterparts and implementing auto-tracking technologies are considered as the major challenges in industry 4.0. These methodologies can be implemented, but at what cost? Sharing the data and analysing it for future decision making is considered as one of the biggest advantages of industrial IoT. For example, in the process of condition monitoring of an asset, the acquired data is analysed to prevent catastrophic failures. These data will be processed to check, when the critical error happened, loss of monetary benefits and life. These data have to be monitored continuously to take smarter decisions for smarter machines. This problem can be solved using IIoT, which was not feasible in

the previous industry era. Innovation and complexity tends to be directly proportional in the IIoT environment which the company's responsibility to optimise it.

The challenges which we had seen previously are more complex regarding the internet connectivity when compared to consumer and domestic internet. Both the categories involve various connected systems in the global level, but IIoT pertains to very constrained requirements to its networks for bandwidth connectivity. Another important aspect in IIoT is working with precision machines [1]. The failure by milli-second will give considerable loss in health and safety of the operator, machine and the most important is business. When compared to traditional design, here in this Industrial IoT- the conditions required for critical decision making are made available through standard interface and the adaptable control algorithms are designed to collect and correlate the data to enhance the efficiency and to prevent the system downtime [2].

In most end to end communication systems, the solution acts as a black box due to its restricted communication protocol. Most of the communication protocols are uniforms and can be shared easily across their defined devices. The requirement of the update and their compatibility issues makes the engineer to face many adaptability issues which may not be able to process the entire system and to create a new one. This is one of the essential reasons to implement adaptability, scalability and functionality, so that it's integration with the overall system becomes feasible. This also helps to reduce the complexity of the system without compromising the innovation [3].

An enormous system network gets processed online, so that the system can interface and communicate with other devices within an enterprise over a very long distance. Securing the systems and communication is a billion dollar questions for the assets management system. This leads to creation of smart grid architecture as a part of IIoT. The grid is designed to make the information more accessible without any security breach. Autonomous modifications and maintenance with ever changing functionality have to be incorporated within the architecture [4]. Adding more functionality and capability to the system leads to the formation of tangled web phenomena which comprises various interconnected components. This web not only shares with original designated systems, but also with all others in remote locations.

The investment done in the IIoT environment for developing and deploying the systems will be very massive in nature. In order to meet the demands of today and tomorrow, creating the grid with more flexibility is important. Creating this is not an easy task, removing the complexity of hardware interface is a major challenge. Instead, complexity and optimisation can be done in software tools to form a powerful platform that bridges the hardwares and software is the best unified approach. This scenario focuses more on innovation in application rather than hardware and software.

The platform needs to be a user friendly operating system which must be secured and configured to authenticate the users. This is very essential to integrating the systems and maximising its availability and capability. The platform must be an open operating system which makes all the global level experts take part in the developmental operations in the field of embedded and cyber security [5]. It must also possess standard Ethernet technologies to form passivity in IIoT latency and

other bandwidth requirements with the aim to inter-operable between IoT system providers and consumers using IoT.

There are various open organisations like Industrial Internet Consortium (IIC), which was formed to escalate the development by adopting the use of connecting the constituent machines, devices and other intelligent data analytics. Various testbeds were developing by IIC to simulate the real world scenario of industrial IoT solutions.

Track and Trace testbed aims in efficient usage of shop floor tools, preventing from misuse and collecting other data analytics like their performance and usage status. Bosch, Cisco, National Instruments and Tech Mahindra were responsible for developing software tools, precise location identification, interconnectivity and other application programming.

Communication and Control testbed is developed for simulating and designing power grid systems for micro grid applications. This integrates various renewable energy sources and technology like solar and wind. National instruments, Cisco and Duke Energy were responsible for creating the architecture for micro grid applications.

Asset Efficiency Testbed aims to develop various solutions regarding assets, their performance, maintenance, overhauling and replacements using data analytics collected in a real time environment. Bosch, General Electric, Intel, National Instruments, Infosys and PTC were responsible for developing the solutions.

Other testbeds like Edge Intelligence testbeds, Factory operations Visibility and Intelligence Testbeds, High speed Network Infrastructure testbeds, Industrial Digital Thread Testbed, Condition Monitoring and Predictive Maintenance Testbed and Smart Airline Baggage Management Testbed. These advancements focus more on Industrial internet solution markets, connectivity and reliability with the significance towards the pursuit of digital transformation and deployment of IoT enabled devices in the Industrial environment.

2 Methods

This IIoT technology is growing exponentially, almost one billion IIoT enabled manufacturing machines are in use, which is 400% higher than in 2015. IIoT centric ‘Smart Factory’ builds flexibility in the manufacturing process to optimize the performance and forecasting. There is an opinion among the manufacturers; the commercial landscape is being transformed by IIoT, in attracting investments towards the Industry.

The application areas of IIoT are (1) Warehousing, (2) Supply Chain management and (3) Document management

The major benefits are

- Inventory Forecasting and stock levels
- Assets, Maintenance and the extension of its lifetime

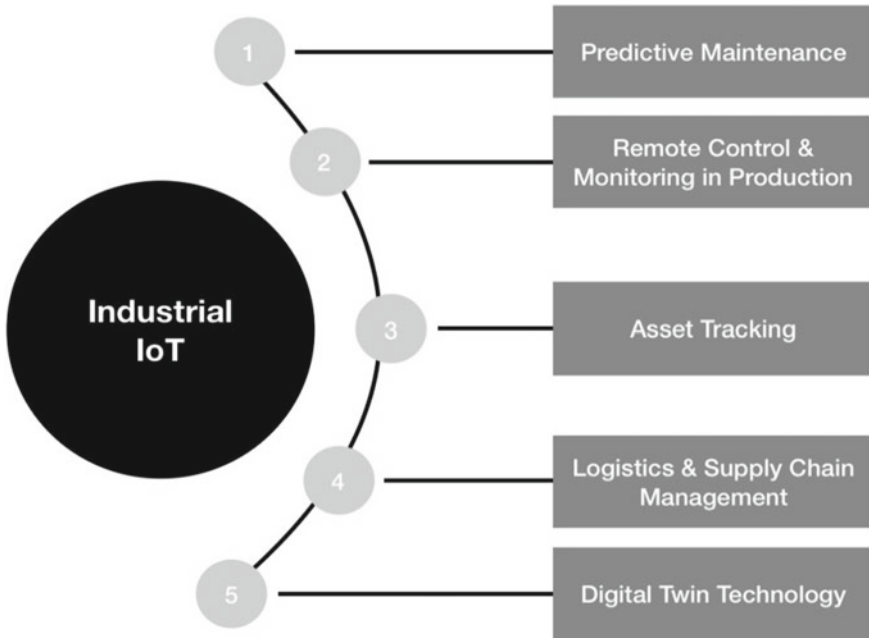


Fig. 2 Application areas of IIoT

- Increase production capacity, consistency in operations and reduced downtime of Machines
- Efficiency of the worker, reducing the human error and throughput
- Quality of materials, output and reduction in the number of defective products
- Waste reduction and overall usage of facilities
- Shorter lead times for customers

Based on the applications as shown in Fig. 2 of IIoT, this chapter is discussed under the following 5 headings, to explain the role of IoT technology in Smart manufacturing [6].

1. Predictive maintenance
2. Remote control and monitoring in production
3. Asset tracking
4. Logistics and supply chain management
5. Digital twin technology

3 Discussion

The application areas of IIoT are (1) Warehousing, (2).Supply Chain management and (3).Document management

The major benefits are

- Inventory Forecasting and stock levels
- Assets, Maintenance and the extension of its lifetime
- Increase production capacity, consistency in operations and reduced downtime of Machines
- Efficiency of the worker, reducing the human error and throughput
- Quality of materials, output and reduction in the number of defective products
- Waste reduction and overall usage of facilities
- Shorter lead times for customers

3.1 Predictive Maintenance

Unlike Periodical, planned Preventive maintenance, predictive maintenance is in practice, which depends on the condition of the asset, only when it is necessary. When there is a risk of equipment failure is predicted, the predictive maintenance is performed. Although the cost for predictive maintenance is comparatively higher than preventive maintenance, in the long run unnecessary maintenance is avoided.

As shown in Fig. 3, IIoT makes it possible to predict the health of the machinery and continuous condition-based monitoring. Incredibly easy and affordable predictive maintenance has four key trends as described in the following. When we experience all these technologies as separate applications, they are useful and valuable. But, altogether as IIoT, they flip the world of Industry [7].

1. **Wireless Connectivity:** The affordable wireless sensors make the data collection automatic and cost effective using pervasive wireless/mobile networks.
2. **Inexpensive Sensors:** With the advent of readily available, low cost. Miniaturized wireless MEMS sensors, the upfront investment on predictive maintenance becomes more affordable.

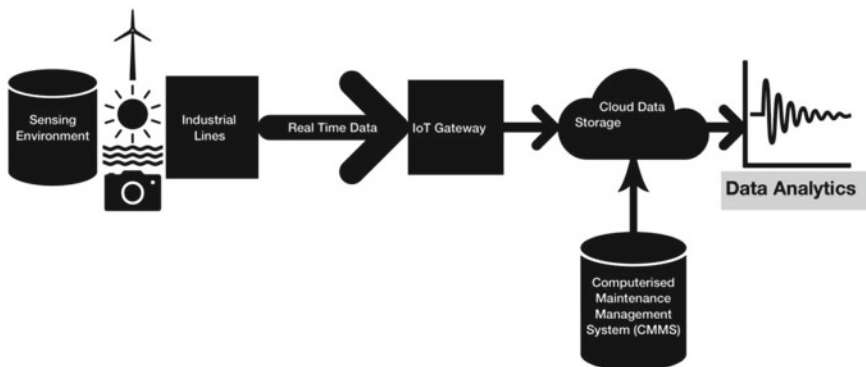


Fig. 3 Predictive maintenance infrastructure

3. **Cloud Computing:** The backbone of the IIoT is Cloud computing, which is a robust technology with higher degree of data security and can be started small and up-scale whenever there is a need.
4. **Artificial Intelligence (AI):** AI becomes an essential part of IIoT, serves as the effective digital assistant to react on sensors' data.

As per the report of PwC, the IoT enabled factories can

- *Reduce costs by 12%*
- *Improve uptime by 9%*
- *Reduce safety, health, environment, and quality risks by 14%*
- *Extend the lifetime of an aging asset by 20%*

3.1.1 Reduce Maintenance Costs

The Machineries are the functional assets of the factory, which should be maintained without failure at any point of time. In order to achieve failure-free machines, the maintenance is the key, which incurs multiple associated costs. Instead of pre-scheduled maintenance, the predictive maintenance saves a lot of money, time and manpower. The quantum of saving in maintenance depends on the population of assets, i.e., denser the machinery, larger the savings [8]. IoT technology associated with data analytics yields more accurate predictions from historical data sets about the health of the machine, expected failure of machines in a time frame. This IoT based prediction leads to proactive services, inspection, and also avoids unplanned, unnecessary downtime, and business loss.

3.1.2 Increase Asset Utilization

The profitability depends largely on costs incurred in maintenance, downtime of machines and manpower towards repair and service. As IoT based predictive maintenance, precisely predicting machine failures in a time frame, can help to fix-up the priority of service and estimation of cost to initiate the maintenance. This system provides early warnings about the health of machines/equipment which will improve the availability of machines, reliability and their performance. This will certainly increase the utilization of the asset [9].

3.1.3 Extend Asset Life

The scheduled maintenance not only costlier but changes the good spare parts of a machine unnecessarily. But, IoT sensors continuously monitor the health condition of the machines in real time, helping you to predict the failures and easily identify the parts that need replacement [10]. Therefore, predictive maintenance identifies

the events before they occur, which enables us to take necessary actions to extend the life of assets.

3.1.4 Improve Field Crew Efficiency

As the IoT based monitoring provides warnings prior, unplanned downtime of the machines, engagement of field service personnel to address the issue can be avoided. Hiring of machines, relocation of machines, purchasing the spares/components for service can be planned in advance, which avoids last minute unrest of the floor managers. As a whole, this IIoT is a boon to floor managers to maintain the production line failure-free and active always.

3.1.5 Improve Safety and Compliance

The next major advantage of having IIoT on board is Safety and Compliance of workers. Integration of human capital protocols with the IIoT environment, will give alarms whenever there is a deviation in the preset threshold values [11]. These predictive alerts protect the workers from the safety risks. The analytics on these data can identify the potential hazardous conditions for a particular industry and the compliance safety report can be generated to keep the risk levels under the threshold values in accordance with the safety regulations and statutory requirements.

3.2 Remote Control and Monitoring in Production

Industry 4.0 is the new digital face of traditional industry [12], and the production floor machines are exchanging their data with each other and these machines can be controlled remotely. There is a healthy competition between companies in adopting automation, and IoT in all domains of their business. The plant managers can easily access the plant data in their mobile phone anytime, anywhere and control the production on a single touch from their gadgets. Thanks to modern IIoT, in operating the factories 24×7 . During this COVID-19 pandemic, the industries with flexible technologies like IoT are running with minimal human intervention. Now, there is a potential demand among companies in capitalising, remotely operable technologies.

The following are the advantages of remote production control [13].

1. Prompt problem solving

The connected machines can be monitored, repaired remotely, even from other countries with the help of IoT sensors. It gives alerts about the health of the machines to the staff for instance awareness and attention. Thus, it is possible to solve the

issues immediately and avoid major problems before they happen. This will reduce the downtime of the machines, and increase the productivity.

2. Access and recovery of data

When some critical incidents happen in the production line, it is necessary to analyse the data, like a black box in a plane, to identify the root cause of the problem and to early detection of such kind of issues in future. Machine learning algorithms on historical big data can give the traceability and predict possibility of the next such occurrence. Modern production floors have programmable smart instruments, regulators and electro mechanical valves. These configurable equipment can be easily reset without much cost to factory defaults immediately after such an incident.

3. Access valuable data anywhere

The data analysis on the collected data from different plants of the same kind derives the best possible way of operating the production lines to increase the productivity with minimal cost. We need a common platform to store the huge amount of plant data, to analyse and provide the suggestions. Cloud based IIoT is the only solution to store and access the real time data anytime and anywhere. Additionally, based on the information, the comparative performance report can be generated to maximise the profitability.

4. Capacity and vision for growth

The software based effective decisions, with vision, prepare the companies globally competitive and foresee the opportunities and challenges. This will improve the operations and production processes. As a whole, this software makes the companies more autonomous and takes control over all the processes.

5. Increase efficiency

The automation enables agile, flexible and scalable processes by eliminating manual commands which are prone to human errors. The flexibility and scalability gives agility in production depending on demand. This increases the efficiency and productivity.

3.2.1 Challenges of Remote Industrial Operations

The major reasons for distributed production and outsourcing units are

1. Cost on logistics
2. Employee unions and conflicts
3. Complexity in supply chain
4. Reduction in operational costs

In distributed manufacturing facilities, remote monitoring is essential due to manufacturing and production standards, employee safety and product quality.

IIoT addresses the following limitations of the traditional industry in maintaining the distributed and outsourced manufacturing facilities [14].

1. Remote facility monitoring
2. Reliability of the equipment
3. Quality assurance of the finished products
4. Inventory management
5. Employee safety

Remote Facility Monitoring

IIoT driven, connected machines can leverage the efficient and centralised monitoring of the remote production facilities and outsourced manufacturing units. The sensors read the performance of the machines, utilization and calculate the productivity and it allows the manager to look into, second-by second operations. This will help the manager to access the data in real time, from the centralised location, about machine status, up and down time, etc.,

Reliability of the Equipment

Predictive maintenance ensures the good health of the machines and gives forecasts about the failures well in advance. This cuts the cost of a permanent, dedicated in house service team at all the production units. A common service team is sufficient to do the maintenance at all the units, based on the predictive alerts.

The predictive solution takes the inputs of different sensors and analyses the operational condition. For example, in an extruder machine, if the barrel temperature exceeds the preset threshold temperature, immediately it gives alert and activates the stopping mechanism. Suppose, the supplied power is lesser or the power factor is lesser, it will stop the machine and be intimate to the floor manager.

Quality Assurance of the Finished Products

Due to the introduction of the technologies, the quality of the end product never compromised. On the other hand, the quality practices are stringent and uniform to all distributed manufacturing units and out sourced units. IIoT network discovers the quality issues at the earliest and avoids the human error in quality assurance. The entire data of quality testing is stored in the cloud and the critical data is informed to the quality managers immediately [15]. IIoT not only reveals the quality issues but also does root cause analysis of the poor quality. An IIoT solution identifies if current equipment condition and operational parameters are likely to deter product quality, and notifies an operator.

Maintaining Optimal Inventory Levels

In the geographically distributed manufacturing facilities, the inventory management is really a challenging task. We need to balance the inventory across all the units and assure the continuous availability of raw materials for the production. None other than IIoT technology is the solution. All the inventory items are identified with its location and track their movements in the shop floor. This data will be useful in maintaining minimal inventory to facilitate all the manufacturing units smoothly run.

Employee Safety

IIoT network monitors the employees too. The health related parameters like heart rate, temperature, galvanic skin response, etc., are analysed in real time and detects the unusual patterns and reports the safety threat to prevent the employees. It also analyses the flaws in the compliance with safety standards and reports.

3.3 Asset Tracking

Tracking the valuable assets and stock is highly challenging in the manufacturing industry due to many technical and practical reasons, but it is a critical requirement in any business. IoT makes this job simple using sensors and wireless connectivity. The wireless tracking enables you to track the equipment and fleet remotely, which reduces a lot of overheads, time, waste of money and risks.

Using this IoT enabled Asset tracking we can achieve the following [16].

1. Smarter and accurate business decisions.
2. Timely refilling of Inventory to maximise the profit.
3. Reduction of negative impact among stakeholders.
4. Customer satisfaction by providing the service in time.
5. Theft prevention and recovery

3.3.1 Components of IoT Asset Tracking

Even though there are many variants in IoT enabled Asset Tracking and Management System (ATMS), the following are the more common components [17].

Tracking devices: The tracking devices are selected and deployed, depending on the objects to be tracked. Unlike one way RFIDs, straight forward tracking tags for multi functional usage, black boxes with vehicle dash cameras are in practice.

Connectivity: The backbone of asset tracking is the network which connects the trackers with the management platform. Many IIoT applications use cellular mobile networks using eSIM modules.



Fig. 4 Asset management platform

Management platform: As shown in the Fig. 4, the control station is to monitor the movements, manage the connectivity, and access the location and to process the collected data. This platform integrates all types of services related to IIoT.

Many different IoT applications, devices and platforms are in practise by replacing barcode scanners, serial number tags, etc., Nowadays, all IoT devices are identified by their IP addresses, and communicate through the internet with IoT gateways and sensors. When these connected devices share their location in terms of positional coordinates with the central intelligence platform, these are transformed into trackable devices. This digital transformation as trackable objects or assets makes it easier to monitor them remotely in real time by the asset management system, even in larger warehouses. This concept is called Smart Warehousing, in which IoT plays a major role. On the top of IoT, Data Analytics, Artificial Intelligence and Machine learning present unimaginable solutions and predictions to run the manufacturing industries more profitably.

3.3.2 Real Time Audit and Asset Tracking at in House and Vendor Location

During the health audit of assets like Jigs, Fixtures, dies, tools etc., locating the assets in the production floor or in vendor shops are painful and tiresome. The timelines fixed for such manual auditing may not be met and the collected data may not be accurate. But, the trackable objects' audits can be done on a single click of the mouse [18].

Benefits

1. Online trackable assets, reduces the time and overall cost of t asset audit.
2. It enables 24×7 monitoring and preventing the misuse of assets and in turn revenue.
3. Accurate localization of assets makes the operation of the shop floor easier and ensures securing stakeholders interest.

3.3.3 Material Handling Management Solutions

Raw Material handling, loading and unloading is another challenge in the production floor. Normally forklifts are used for this purpose but not in an effective way. In many industries, the utilization of forklifts is not optimised due to the lack of resource management. But, the optimization techniques applied in intelligent manufacturing gives a simple solution to this issue. Based on the data available about the location of materials within the production floor the forklifts paths are optimized to supply the materials for production effectively. This will largely reduce the cost of either new forklift procurement or rental [19].

Business Benefits

1. Using the historical data and its analysis the material handling and fleet usage is optimized.
2. With help of IoT Sensors, the forklifts can identify the exact location of materials available and relocate it to machines for production. This will reduce the hectic work involved in searching for material and time.

3.3.4 Inventory Tracking System

Inventories need not be maintained in a single location, but the inventory register should show the current status, in terms of numbers available and location. Using a static, software based inventory management, this issue can not be resolved. But, the Intelligent Inventory Tracking System(IITS), can give a precise, updated solution, even though the warehouses are located across the globe. Cloud based inventory servers and IoT are in place, to connect the warehouses and factories, to maximize the productivity and alert the stakeholders before the stock gets emptied [20].

3.4 Logistics and Supply Chain Management

Till the recent past, the supply chain and logistics were managed by RF technologies and infrared, involved tedious installation, and costly receivers and transmitters. But, IoT gives a lot of flexibility in asset tracking as shown in Fig. 5, with greater accuracy in location and comparably 10 times lesser cost than RF counterparts [21]. The following are the use cases of IoT applications in Logistics and supply chain management.



Fig. 5 Logistics and supply chain management

3.4.1 Track Deliveries from the Vendor to the Manufacturing Facility

Raw materials should reach the manufacturing facility in time, and is really a challenging factor in any business. It is very difficult to track the vendor vehicles, to know the exact time of delivery. In order to reduce the dispatch delays due to untracked vehicles, IoT based vehicle tracking is in practice now [22].

Benefits

- Timely supply of raw materials to the manufacturing facility.
- Productivity and operational efficiency is more.
- In case of delays, the real time dashboards will be useful to track and monitor the process.
- It improves productivity and security.

3.4.2 Track Deliveries, Materials Inside and Around Manufacturing Facilities

Truck drivers can deliver the materials with the use of IoT, precisely at the exact location. Again, the dash boards will monitor and guide the loading/unloading process and often avoid misplacement of shipments in the manufacturing facility [23]. Within the manufacturing facility or warehouses, the misplacement of materials slows down the manufacturing which leads to customer dissatisfaction.

3.4.3 Monitor Sensitive Goods to Avoid Damage or Loss

The perishable shipments require specific ambience, humidity and temperature conditions to maintain the quality. IoT applications can monitor the atmospheric conditions, shock and vibration levels even during the transit. This capability of IoT enabled supply chain management system, enables us to ship perishable products like eggs, milk, flower etc., and glass products too [24]. The vendors can be notified about the damaged shipments even before they reach the manufacturing facility, and initiate the logistics of new consignments.

3.4.4 Real-Time Fleet Management

GPS coordinates along with other telematics collected from the sensors of the vehicles are the most popular solution in the fleet management system. This telemetric data can be used to monitor the driver's compliance and behaviour [25], which ensures the safety of driver, consignments, fuel consumption and delivery schedules. Based on the driver's profile, the training programs can be arranged to the drivers to improve their professional development.

3.4.5 End-to-End Delivery Tracking

IoT powered sensors and devices, collect a huge amount of diverse data from different stages of logistics. The generation of web dashboards, integrate all these data in a single cloud based supply chain management application. Even though it is a challenging one, it gives flexible data in your fingertips to optimise the logistics. This will reduce the hectic work involved in maintaining the fleet and saves time, which in turn increases the quality of service offered by the industry [26].

3.4.6 Last-Mile Delivery Innovations

Nowadays, with the help of mobile applications, the manufactured products are being delivered on the same day itself. Especially, in the food industry the ordered foods to be delivered within an hour. Many companies are providing this service with extra premium and their customers are ready to pay extra for that. This is the most promising trend now, by using the technology which automates the end-to-end logistical operations. As soon as the backbone logistical operations are digitized, there will be even more opportunities for faster last-mile delivery by using mobile applications, predictive replenishment, smart buttons, and drones [27].

3.5 Digital Twin Technology

Gartner Inc., a leading research and advisory company, listed the Digital Twin Technology among top 10 Strategies of business trends in 2017. As shown in Fig. 6, Digital twins are virtual assets and replicas of physical machines, using sensors [28]. Even before the making of physical assets these digital duplicates can be created. The researchers create these digital twins using the historical data acquired from various sources of physical machines, equipment, and sites. The analytics softwares are much useful to collect and synthesize these operational data. With all these data and precise insights of analytics software, the digital twins are virtually modelled. The integrated AI algorithms play a major role in this virtual model to get the exact insight about the physical asset [29]. More or less the digital twins act as a live physical asset and give the optimised, best possible business solutions. Thus, digital twins are the complete digital footprint of any product from design phase to deployment phase.

These IoT based digital twins, generate data in real time, to help the businesses in a better way and predict the problems well in advance to give early warnings, prevent downtime, develop new opportunities and even plan better products for the future at lower costs by using simulations in lesser cost. Digital twins are incorporation of IoT with Big Data, AI and Machine learning, which are the main factors of Industry 4.0 [30].

Digital twin concept is a boon to the business sectors, which helps in predicting the future of physical assets by analyzing their digital counterparts. Digital twins are a new eye-opener to the organizations, to improve their products, customer service and strategic business decisions. The major application domains are addressed here [31].

- **Manufacturing:** Digital Twins changed the way of product design, prototyping, manufacturing and maintenance as well. They convert the manufacturing as intelligent manufacturing, by making high throughput with optimal resource management.

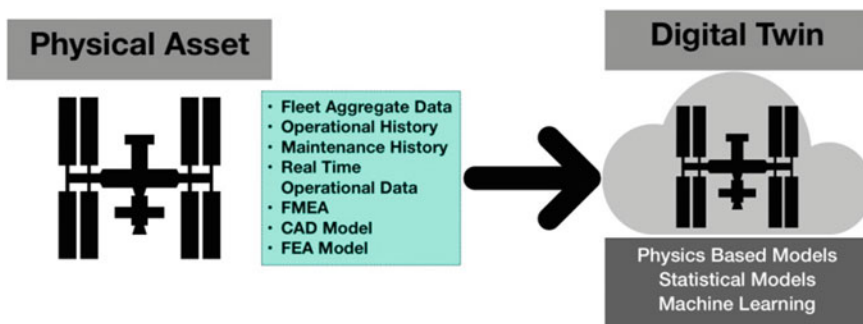


Fig. 6 Digital Twin technology framework

- **Automobile:** The main beneficiary of the Digital twin technology, is the automobile industry. The virtual twin captures the operational and critical data of the connected physical vehicle like the oil level, engine health, temperature of radiator fluid, the health of charging circuit and battery, etc., Thus it analyses the overall performance of the connected vehicle, and assures delivering a truly personalised service to the users on the ply.
- **Retail:** The virtual twins can change the experience of every customer in the retail market. This can navigate the customer towards their selected product racks, and helps in picking their choice. It helps interior planning of the retail market, security and energy management in an efficient way.
- **Healthcare:** IoT data used in digital twins hugely reduces the cost in patient monitoring, maintenance by providing personalised health care.
- **Smart Cities:** The major advantage of using digital twins is Smart cities planning and its management. These virtual models simulate the traffic and predict the challenges in handling the traffic. Digital twins are highly intelligent in revenue generation, waste management, ecological footprint, etc., It helps the city planners and policy makers to create a smart city to improve the quality of a citizen's life. The accumulated data over a period can be useful in predictive management of the smart city.
- **Industrial IoT:** Industries are now becoming smarter by the introduction of IoT and digital twins. The entire factory can be monitored, controlled and tracked remotely with the help sensors and actuators used in IoT. It collects not only operational data but also the ambience data, which are useful in predicting future operations and to remove anomalies.

3.5.1 Digital Twins in the Industry 4.0

Industry4.0 is smart and intelligent with the help of automation, IoT, AI, data exchange between connected machines. The manufacturing technologies are evolved in a better way as Digital twin centric, which brings a lot of possibilities in simulation and prototyping. The traditional approach in manufacturing has been flipped, more virtual based design processes are in practice to develop an efficient outcome. As the predictions are arrived based on the historical big data, they are more precise and accurate, by understanding critical issues, performance and unique features [32]. Any worker can be transformed as a skillful architect, using virtual digital twin training, without any trainer. Nowadays the production line machines become autonomous with the help of AI and machine learning.

In a decade from today, the factories will become fully autonomous; the autonomy of machines will reach the next level. The digital twin will be useful in evolving the autonomous industry as self-diagnosing, self-healing/repairing, self-awareness, self-optimizing, with the minimal involvement of manual operators [33]. No wonder, we can witness the machines will be speaking to each other on the production floor, by exchanging their data and health records.

4 Conclusion

IIoT is the disruptive technology, allowing industries to make data- driven decisions, to produce successful models for better productivity by using the industrial assets in an optimized way. It is proven that IIoT is the best suitable technology to transform manufacturing into intelligent manufacturing. It provides real time visibility into the remote distributed production facilities. However, rolling out an IIoT solution is not fast and easy. In order to harvest benefits, an industry should consider possible limitations and work out optimal ways to address them. In order to change the traditional practices and transform into IIoT technology, the companies have to review the operational constraints and customer engagement aspects. Definitely, the change that will go beyond anything we've seen in our lifetimes, and will demand a deep and broad transformation of the enterprise.

References

1. Online material available at, <http://dbz.164.myftpupload.com/2019/02/iiot-applications-and-examples>.
2. Online material available at, <https://breadware.com/2019/02/iiot-applications-and-examples>.
3. Online material available at, <https://iiot-world.com/industrial-iiot/connected-industry/5-challenges-of-remote-industrial-operations-solved-with-iiot>.
4. Online material available at, <https://www.thalesgroup.com/en/markets/digital-identity-and-security/iiot/inspired/smart-manufacturing>.
5. Online material available at, https://www.hitachi.com/rev/archive/2016/r2016_08/pdf/r2016_08_103.pdf.
6. Online material available at, <https://www.byteant.com/blog/5-best-use-cases-of-iiot-in-manufacturing>.
7. Industrial IIoT: How connected things are changing manufacturing|WIRED. Retrieved from [2018/07/industrial-iiot-how-connected-things-are-changing-manufacturing](https://www.wired.com/2018/07/industrial-iiot-how-connected-things-are-changing-manufacturing).
8. What is predictive maintenance and what are its benefits? Retrieved from <https://www.itconvergence.com/blog/5-benefits-iiot-based-predictive-maintenance>.
9. IIoT for predictive maintenance: essence, architecture, applications. Retrieved from <https://www.scnsoft.com/blog/iiot-predictive-maintenance-guide>.
10. Unleash the power of IIoT-based predictive maintenance. Retrieved from <https://iiot-world.com/predictive-analytics/predictive-maintenance/unleash-the-power-of-iiot-based-predictive-maintenance/>.
11. Industrial IIoT for predictive maintenance|HIOTRON. Retrieved from <https://www.hiotron.com/industrial-iiot-for-predictive-maintenance>.
12. Online material available at, <https://nexusintegra.io/advantages-remote-production-control>.
13. Online material available at, <https://calrec.com/wp-content/uploads/2018/04/Remote-Production-White-Paper-2018-v3.pdf>.
14. Online material available at, <https://www.inhandnetworks.com/solutions/remote-cnc-machine-monitoring.html>.
15. From remote to predictive maintenance: How IIoT refines a classic M2M concept. Retrieved from <https://blog.bosch-si.com/industry40/from-remote-to-predictive-maintenance-how-iiot-refines-a-classic-m2m-concept>.
16. What Is IIoT and how is it helpful in asset management?—Asset infinity. Retrieved from <https://www.assetinfinity.com/blog/what-is-iiot-and-how-is-it-helpful-in-asset-management>.

17. How IoT is transforming asset tracking. Retrieved from <https://blog.jtiot.com/iot-transforming-asset-tracking>.
18. IoT Asset Tracking Systems|Telit. Retrieved from <https://www.telit.com/industries-solutions/telematics-transport/asset-tracking/>.
19. The evolution of IoT asset tracking devices—Help Net Security. Retrieved from <https://www.helpnetsecurity.com/2020/08/25/the-evolution-of-iot-asset-tracking-devices/>.
20. 5 powerful asset tracking examples that use IoT | QuicSolv. Retrieved from <https://www.quicsolv.com/blog/internet-of-things/5-powerful-asset-tracking-examples-use-iot>.
21. The top six IoT applications in logistics|Articles|Chief Innovation Officer|Innovation Enterprise. Retrieved from <https://channels.theinnovationenterprise.com/articles/how-the-internet-of-things-will-revolutionize-the-logistics-industry>.
22. 6 Widespread Applications of IoT in logistics industry. Retrieved from <https://www.biz4intel.com/blog/6-widespread-applications-of-iot-in-logistics-industry/>.
23. How IoT in logistics revolutionizes the supply chain management. Retrieved from <https://transmetrics.eu/blog/iot-logistics-revolutionizes-supply-chain-management>.
24. 5 IoT applications in logistics & supply chain management. Retrieved from <https://www.airfinder.com/blog/iot-applications-in-logistics>.
25. Top 8 IoT applications for logistics. Retrieved from <https://www.kaaproject.org/blog/iot-applications-for-logistics>.
26. Applications of IoT in transportation and logistics business. Retrieved from <https://truckguru.co.in/blog/applications-of-iot-in-transportation-and-logistics-business/>.
27. IoT in logistics: Warehousing, fleet management & smart containers—Container xchange. Retrieved from <https://container-xchange.com/blog/iot-in-logistics>.
28. What is digital twin technology and how does it work?—TWI. Retrieved from <https://www.twi-global.com/technical-knowledge/faqs/what-is-digital-twin>.
29. What is Digital Twin Concept|Applications—Happiest minds. Retrieved from <https://www.happiestminds.com/insights/digital-twins/>.
30. Cheat sheet: What is Digital Twin? Retrieved from <https://www.ibm.com/blogs/internet-of-things/iot-cheat-sheet-digital-twin/>.
31. What is a Digital Twin|IBM. Retrieved from <https://www.ibm.com/topics/what-is-a-digital-twin>.
32. What is Digital Twin technology and what this concept means. Retrieved from <https://www.challenge.org/insights/what-is-digital-twin/>.
33. What is a Digital Twin?|GE Digital. Retrieved from <https://www.ge.com/digital/blog/what-digital-twin>.

Cyber-Physical Systems: A Pilot Adoption in Manufacturing



Srivardhini Veeraragavan, Edwin Tong Jiann, Regina Leong,
and Veera Ragavan Sampath Kumar

1 Introduction

The promise of the Fourth Industrial Revolution (IR4) or Industry 4.0, is a powerful motivation for nations and companies to accelerate their digital transformations. IR4 is no longer a futuristic concept and the COVID-19 pandemic has shown that it is closer than it originally appeared.

Many multinational organisations have laid out huge investments for digitization, expected to reach \$2.3 trillion dollars by 2023 [1] and embarking on a large-scale transformation to move up the ladder of IR4 maturity. Simplistically, adding IoT capability and migrating functionality to a network of smart embedded devices are all that is required to make the successful transition to Industry 4.0 in theory. In practice, however, there are many challenges.

S. Veeraragavan · E. T. Jiann · V. R. Sampath Kumar (✉)
School of Engineering, Monash University Malaysia, Subang Jaya, Malaysia
e-mail: veera.ragavan@monash.edu

S. Veeraragavan
e-mail: srivardhini.veera@gmail.com

E. T. Jiann
e-mail: teejaywinn@gmail.com

R. Leong
Malaysia Textile and Apparel Centre, Kuala Lumpur, Malaysia
e-mail: regina@mtma.org.my

1.1 The 4th Industrial Revolution (IR4)

IR4 is a confluence of technologies which blurs the line between the physical, digital and biological [2, 3]. Several new IR4 technologies have surfaced in the last few decades such as IoT, cyber-physical systems and data analytics that have transformed businesses. But to qualify as a true revolution, technology must have more than just an influence on society - it must behoove all people to consider the effects of their choices [2, 4].

IR4 technologies have changed the lives of not just the common man and their relationships, but have also disrupted businesses, upended economies, and changed everything to merit the term “Revolution”. Enterprises that have leveraged the IR4 technologies not only surfed the COVID-19 wave, but managed to exponential growth. Organizations that digitalized early and used data to innovate have seen exponential growth and improvement in productivity, customer experience and quality of services leading to a surge in business.

1.2 Business Needs and Economies Drive Adoption

A study by McKinsey reports that 69% of manufacturers have identified that adopting IR4 technology as their top priority, but only 41% are actually attempting pilot projects and 29% deploying at scale [4]. The reasons that prevent adoption are resource and knowledge constraints, high costs, unjustified business cases and or longer return of investments, unsuccessful and unclear pilot projects and many competing focus areas. However, these results were based on large and successful enterprises, while Small Medium Enterprises (SMEs) face major inhibition factors to embark, transform and mature towards IR4 adoption.

Another study shows that only 30% of all digital transformation projects succeed [5]. This dampens adoption by both large and small enterprises alike but poses as an especially difficult financial challenge for SMEs. However, a silver lining exists for SME's- start-ups or facilities without “past baggage” have been able to successfully create new systems of production and help bolster economies. This shows that it is possible for SMEs to adopt IR4 technologies, but successful prototype implementations are needed for SMEs to believe in the power of IR4 initiatives and motivate to invest time and effort.

In this chapter, we present one such real-life case study which address the need for a low-cost, reliable pilot that will boost IR4.0 technology adoption for SMEs in a timely manner without large investments, persuasion, or disruption to the existing operations. The presented case study shows an example of a model pilot project that demonstrated early success, with well-established needs and measured signposts (ROI, Capital Investment) that convinces the organization's management that the project is worth the investment.

1.3 Cyber-Physical Systems as a Key Technology for Digitization in Industry 4.0

Cyber-Physical Systems (CPS) play a major role in the digitization of industries in IR4.0 [6] due to its inherent ability to accommodate the dynamic conditions and requirements of industrial applications [7–9]. These requirements range from flexibility, adaptability and autonomy [7], to optimization [10], modularity and reconfigurability [11], and fault diagnosis capabilities [12]. CPS manage to accommodate these demands well and hence improve the competitiveness of businesses [13].

CPS consists of cyber and physical components integrated together to interact seamlessly [3, 14]. Cyber components such as sensors, actuators and processors are used to interact with the physical environment through perception, communication and control [15]. In the past, researchers have studied the applications of CPS and relevant technologies for enterprise adoption, such as big data for factory automation [16], real-time task and resource matching [17], real-time asset tracking [18], multi-agent systems [7], and production monitoring [19]. Other applications also include machine vision for quality inspection and assembly, semantic modelling of factories, advanced sensing, networked control systems and wireless sensor and actuator networks [20], and finally retrofitting cyber-physical production systems [21].

1.4 Retrofitting as a Solution for Digitization of SMEs

Quick successes of pilot projects will have a profound impact on an organization's belief in the power of the IR4 initiatives and motivate them to invest more towards maturity. Retrofitting is a well-known technique and has been in use since the days of semi-automatic turning machines, which were retrofitted with Numeric Kits to demonstrate viability [22].

Retrofitting in the current IR4 context refers to the process of digitizing or updating existing industry equipment to keep up with advancing Industry 4.0 technology, sustainability, and productivity. Retrofitting allows old technology to be upgraded to be used in IR4 and is attractive to SMEs for its economic benefits [21], since no or minimal new equipment needs to be purchased. Retrofitting also has a high return on investment (ROI) for legacy equipment with negligible risks [22].

In previous studies, researchers have performed retrofitting processes on milling machines [23], subsea equipment [24], Computer Numeric Control (CNC) machines [25], press brake [26] and didactic machines [27], Programmable Logic Controllers (PLCs) [28] and robotic arms [21, 25]. All the studies present different techniques with respect to the specific machine in consideration for upgrading. [21]. This can be attributed to how retrofitting is dependent on domain-specific industry equipment based on their specifications, and the lack of standardization in the meta-modelling of retrofitting.

In this study, a model pilot project is implemented in the textile industry for the automation of knitting machines that demonstrated early success and adoption for the SME involved. This study is structured as follows: Sect. 2 presents an overview of CPS concepts and characteristics, and these concepts are applied in the retrofitting of a knitting factory in a case study in Sect. 3. Finally, a discussion on the challenges and future trends for CPS is presented in Sect. 4, followed by the Conclusion.

2 Cyber Physical Systems as a Design Concept

The use of different models and architectures is inevitable in retrofitting CPS, they must be investigated before a CPS architecture is chosen based on project requirements. This section presents an overview of the technological concepts around CPS and its architectures in manufacturing.

2.1 Overview

The term CPS was coined in 2006 by the National Science Foundation [14] to refer to the next generation of engineered systems. CPS is an integration of computation and physical processes, whereby the behavior of the system is defined by both the physical and cyber aspects of the system [14] and the behavior of the physical and cyber layers affect each other [29].

Through the effects of both the physical and cyber layers on each other, an upgrade or expansion of the function of physical entity is expected to occur, so that heightened monitoring and control can occur in a safe and reliable way [30]. This implies that integrated circuits, nano and micro-electromechanical systems are also classified as CPS.

The physical and cyber aspects interact with each other through interfaces such as communication networks or intermediate components like sensors, Analog-to-Digital Converters and so on [31]. Therefore, there are the aspects of communication, control, and computation in a CPS, referred to as the 3C architecture. Through the integration and seamless collaboration between the 3Cs, services such as real-time sensing, dynamic control and intelligent services of large engineering systems [30] can take place using CPS.

2.2 Viewpoints and Definitions of CPS

CPS has numerous definitions which arise from the varying domain knowledge of the researchers who have defined CPS pertaining to the application domain. Studying the various definitions can offer better insight into the various possibilities that CPS can unlock in different domains, and to emphasize the cross-domain significance of CPS.

Lee defines CPS from an embedded systems context as “An integration of computation with physical processes whose behavior is defined by both cyber and physical parts of the system”, where the physical processes monitored are then controlled by embedded systems through feedback loops [14]. Through this definition, the system can be perceived as a breakdown of subsystems.

From a service-oriented perspective, the authors in [32] define CPS as bringing “computation and communication capabilities to physical components to create intelligence on traditionally isolated and passive devices”. In this definition, the system is broken down into independent service-oriented parts. This definition contrasts the embedded systems definition by Lee [14] in the sense that CPS is the integration of various services from a functional viewpoint.

Meanwhile, from a Mechatronics perspective, it has been argued that CPS is neither a breakdown of subsystems nor a union of functional services, but rather a combination of perspectives. The authors in [3] define CPS as “*a new breed of complex, software-intensive mechatronic systems characterized by tight integration and real-time interaction between computational, communicational and physical components and sub-systems*”.

As such, it can be said that CPS is neither a union nor an intersection of subsystems, but instead a synergy of two domains that works towards a set objective. While this may be a broad definition, it aligns with how CPS has been applied to many technological domains using a variety of models and architectures.

2.3 Existing CPS Architectures

Because of the numerous domains in which CPS can be implemented in, there are currently no universally accepted architectural frameworks. In fact, even defining the term “architecture” was a heinous task and became the motive for the development of the entire IEEE 1471 architectural standard [33]. Eventually, it was concluded that architecture was a property of the system itself rather than a thing on its own [33].

Over the years, a number of frameworks have been developed to define CPS architecture, such as the popular 3C architecture [34], 5C architecture [35] and RAMI 4.0 [36]. The 3C architecture is one of the earliest and simplest architectural models developed, and describes the three platforms that support CPS, namely communication, computation, and control.

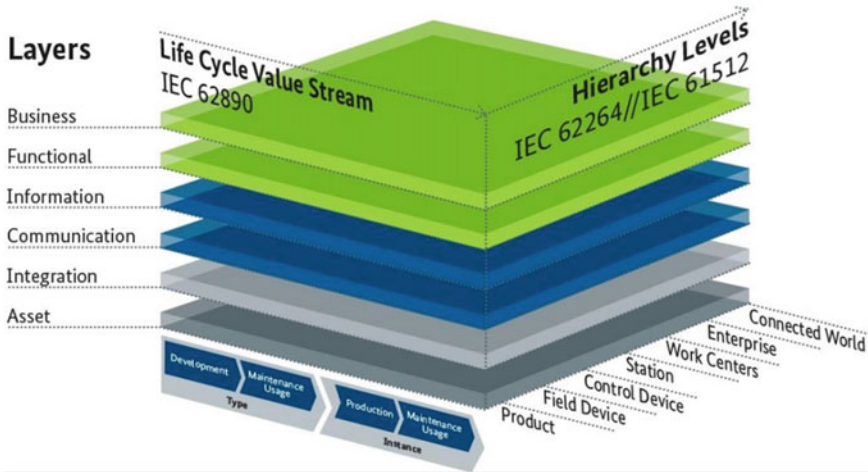


Fig. 1 RAMI 4.0 architectural model [36]

The 5C or 5-layer architecture was developed a few years after the 3C architecture and details the construction process for a CPS model from the data collection up to the analytics at the cyber level [35]. The 5C architecture consists of 5 layers, namely, (i) Smart Connection Level, (ii) Data to Information Conversion Level, (iii) Cyber Level, (iv) Cognition Level and (v) Configuration Level.

RAMI 4.0 [36] is a three-dimensional architectural model that describes the IR4 space [37]. It has six layers on the vertical axis and two on the horizontal axis, as shown in Fig. 1. The six layers are (i) Asset or Physical layer, (ii) Integration Layer, (iii) Communication Layer, (iv) Information Layer, (v) Functional Layer and (vi) Business Layer. RAMI 4.0 also describes five maturity levels of CPS applications and their functionalities. The maturity levels range from one (simple monitoring framework) to five (globally linked cooperative systems) and represent possibilities of CPS adoption at that level [36].

2.4 CPS Meta-Models

In software and system engineering, models are used to capture the physical or real-world aspects of engineering problems with different levels of abstraction [39], while meta-models are abstractions of a model that specify the structure, semantics and constraints for a family of models in a particular domain [40]. Figure 2 shows a meta-model for a CPS as described by [38], based on the CPS structure explained by Lee [14]. The components of the meta-model are the physical, communication and cyber aspects. The physical model consists of sensors, actuators and environmental components [14], and the cyber component is a combination of computational

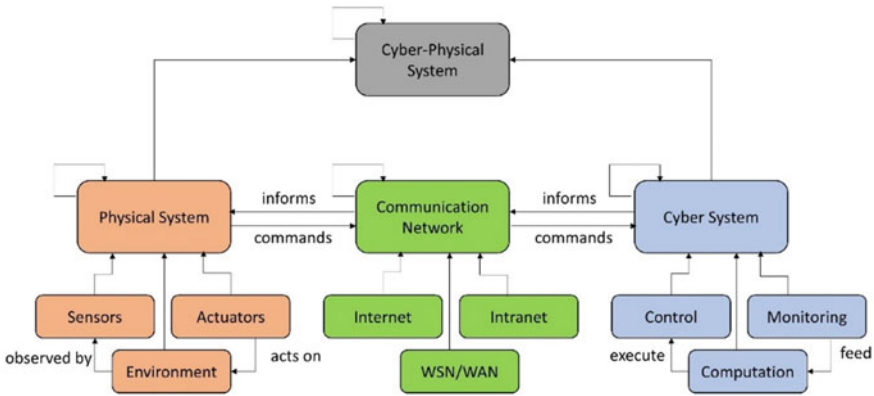


Fig. 2 CPS general meta-model based on 3C architectural framework shows the three types of meta-objects, and their relationships and self-references [38]

resources [31, 41], control algorithms [42], data storage [43] and networking [44], and decision making [45]. The communication network connects the cyber and physical components using Wireless Sensor Networks (WSN) [42], Wide Area Network (WAN), with or without the use of the internet [44].

In the subsequent section, this meta-model is adopted in a textile manufacturing context for a model pilot study involving the retrofitting of knitting machines for an SME.

3 Retrofitting Cyber-Physical Systems in Fabric Manufacturing: A Case Study

The journey towards fourth Industrial revolution begins with obtaining a consistent stream of data that can be converted to information, for analysis, and to facilitate making informed and timely decisions. Many SME's have expensive legacy equipment that are usable for many years to come (for example, the knitting machine in use in the case study). These types of equipment are ideal for digitization in a cost-effective manner without discarding them, while investing in IoT ready machines. A quick return on investment (ROI) can be expected in such cases.

The mass production of fabric in the textile industry involves long operation hours with constant material feeding into machines. The machine operators are subject to long labor hours and repetitive tasks, and these tasks (such as replacing broken threads or needles in machines) are time consuming. To address these issues in a cost-effective way that can benefit SMEs, a pilot study is conducted to retrofit the knitting machines to automate the threading and monitoring of the knitting machines. Figure 3 shows the knitting system before and after the retrofitting process of the pilot study.

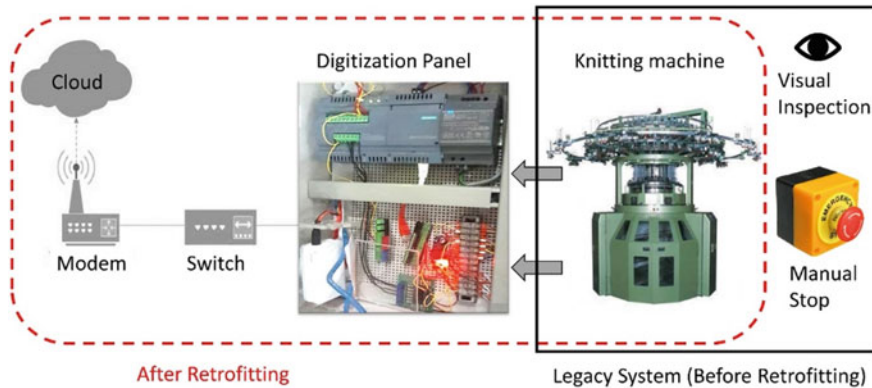


Fig. 3 Knitting Machine before and after retrofitting, where the red dotted box shows the enhanced system, and the black box shows the legacy system

3.1 Methodology

An overview of the methodology adopted in this study is presented in this section. First, a non-invasive re-engineering and development of a retrofitting plan is conducted to embed the knitting machine with required sensors, which requires an operator's help to understand machine operations and properties. Simple tabulation of the data at this stage is an important milestone, as the data can help the business owner make swift and informed decisions, even if done manually.

Then, the machines are connected to the cloud to allow transmission of sensor data and machine conditions to be stored as historical data. This data can also be transmitted to a device such as smartphone or tablet (for instant machine condition updates via push notifications). In the future, these cloud data repositories can be mined using AI algorithms to provide insights or decision-making.

To conduct this pilot study, the 5C functional architecture is chosen for its simplicity and practicality for SME use cases. The project implementation consists of 3 key steps, namely the digitization, acquisition, and analytics. During the digitization process, the knitting machine is connected to gateway devices which receive the machine status signals. The information received by the gateway devices are made accessible on the cloud from anywhere using a web browser, subject to successful data transfer over the internet. A successful digitization means that a legacy system is connected to the cyber world and ready for data acquisition.

The second step is data acquisition, where the physical devices generate and transmit data to the cloud. This data is stored in the cloud, and historic data accumulates over time. This allows updated data to be accessed at any time. However, this makes it prone to attacks as well, so we provide an additional layer of security by encoding the data at the nodes using a custom data format (determined in consultation with the plant operator team). However, the data is hexadecimal format, and therefore a simple binary conversion is used to allow the analysis software to

determine the machine states. After at least one month of data is collected, the data is batch downloaded.

The final step is the processing and analysis of the accumulated data to produce insights to machine effectiveness and manufacturing process. Collected data are imported into MATLAB (r2017b) and the machine states duration are calculated. Using the overall equipment effectiveness (OEE) formula as a guideline [46], the machine performance is calculated.

3.2 System Overview

The overall system overview is shown in Fig. 4, which illustrates the simple and non-invasive nature of the solution, the components needed and an overview of the power and signal routes from the knitting machine. An electric power point supplies 240 VAC to a voltage regulator. Then, 2 gateway devices are driven by step-down power supply units at 24 V and 5 V each. One gateway is sufficient, but the second one is provided for redundancy. The gateway devices receive signals from the knitting machine through an opto-isolator array which separates the two sides from direct physical contact for safety purposes. While this may seem trivial, this step is important safety measure that protects the organization in case the machines are still under operational or maintenance warranties.

The system hierarchy can be described in terms of the functional layers as shown in Fig. 5, consisting of the physical, network, data, computing, and application layers.

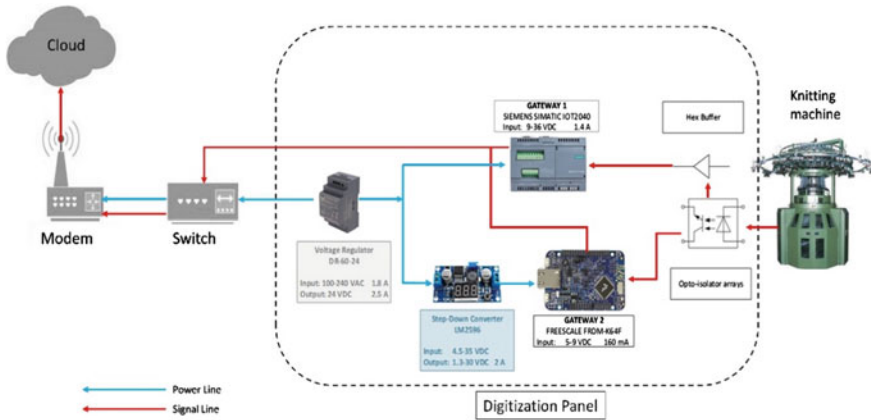


Fig. 4 System overview of the pilot implementation

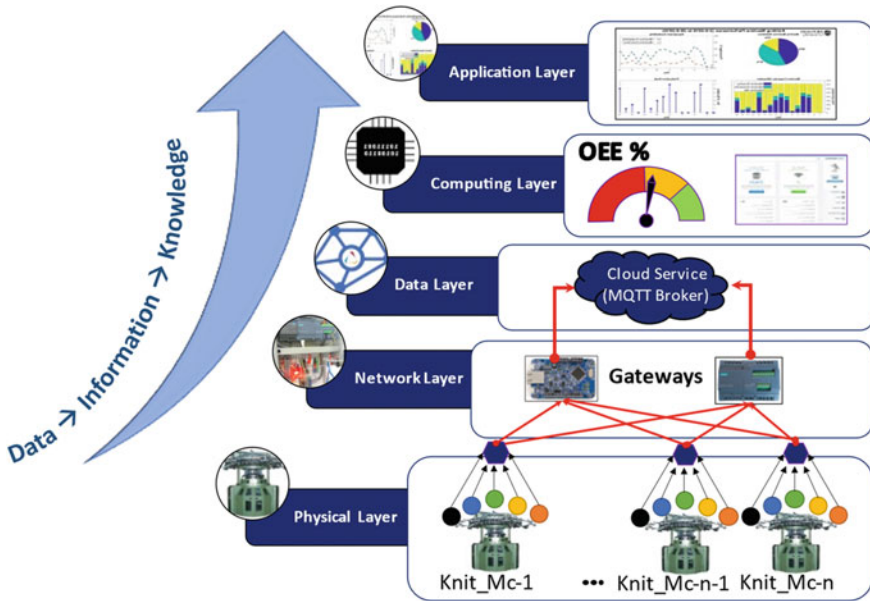


Fig. 5 System hierarchy and architectural layers

3.2.1 Physical Layer

The physical layer is the first layer, and it consists of machines, sensors, and objects that are being monitored. These components are in the physical world and made to provide information in the form of digital data. The data is fed into the gateway layer for processing and transferring to the cloud storage for remote real-time monitoring. In this system, the physical device is a circular knitting machine.

The circular knitting machine in consideration is the Fukuhara V-LPJ4B Circular Knitting Machine [47], which is a machine with 64-feeder systems fully equipped with auto controls, safety devices, fittings, and connections [47]. Each of the feeders is fitted with a sensor to detect when a thread has broken. When this happens, a signal is sent from the sensor to a control unit to halt the knitting process. The signals obtained from the machine are (i) Machine ready, (ii) Machine running (iii) Machine stopped and (iv) Machine cycle complete. These signals are non-invasively tapped from the local control panel and fed to the gateway devices. Each of these signals are represented as a binary digit as shown in Fig. 6. This simple encoding of data adds a layer of data obfuscation, optimizes data packets and provides an added security layer that will render the data useless to a hacker without the decoding.

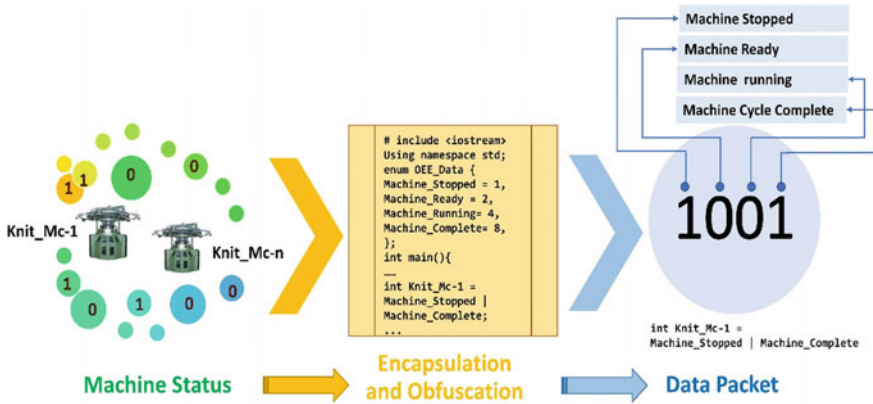


Fig. 6 Field level encoding of the knitting machine signals adds a layer of abstraction and data security

3.2.2 Network Layer

The gateway layer links the device layer with the internet. These devices have a processing power and an internet module for either wireless or wired (or both in some cases) communication. The information is processed and converted into the correct form for transport to the cloud. To enable the delivery of information across the internet, objects must be equipped with sensors connected to an internet-enabled microcontroller and a suitable application software should be used paired with a suitable protocol stack [48].

The microcontrollers can also differ greatly in terms of the price, energy consumption, functions, and software. Although the simple function of gathering data into the cloud can be done by almost any microcontrollers, it pertains that choosing the right one can lower the setup costs and installation complexity, at the same time increasing usability and effectiveness of deployment.

The gateway devices in this project are the Siemens SIMATIC IOT2040 [49] and the NXP Freedom-K64F [50]. The Siemens IOT2040 is a relatively fast industrial grade gateway device that runs on 400 MHz Intel Quark 2040 processor. It runs on the Yocto Linux operating system which is highly versatile as it can run applications written in NodeRed, Eclipse, and Arduino IDE. This device also comes with a strong and robust casing suitable for the factory environment.

On the other hand, NXP K64F is a prototyping kit with a relatively small form factor when compared to the Siemens IOT2040. This device runs on a Kinetis microcontroller unit with 120 MHz of clock speed. The processing speed is sufficient for the purpose of gathering data and publishing it on the cloud. This device runs on the Arm mBed OS. This doubles as a low-cost redundant gateway that can be used to store data and then transmit the data using other protocols (e.g. HTTP).

These two gateway devices are connected to the internet via ethernet cables and programmed to obtain machine signals and publish new machine states to the cloud

using MQTT protocol every time a change is detected. If a publish function fails (due to internet connectivity issues or other errors), the data is saved locally until the attempt to reconnect to the internet is successful. The program flowchart is shown in Fig. 7. Another functionality that has been implemented at the gateway level is payload and bandwidth optimization. By converting the 4-bit binary machine status signals into hexadecimal values the payload size is reduced thereby optimizing the data efficiency, data rates and cloud storage.

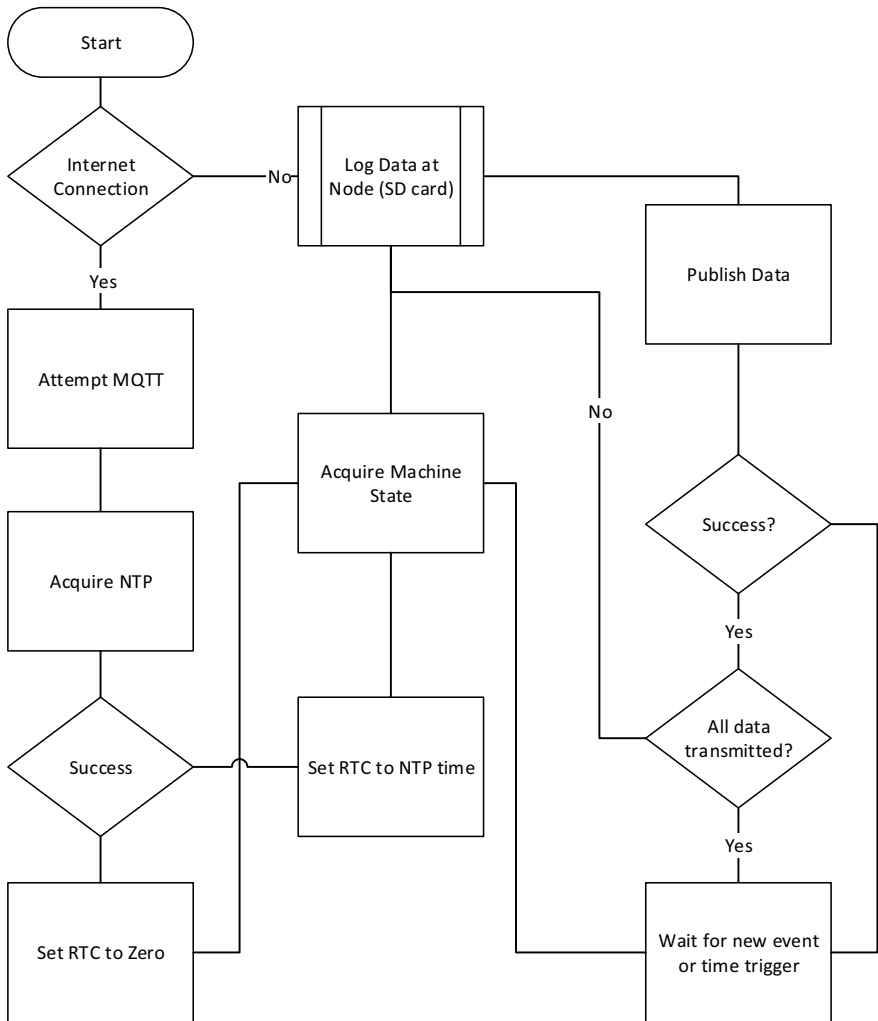


Fig. 7 Program flowchart for gateway devices connectivity

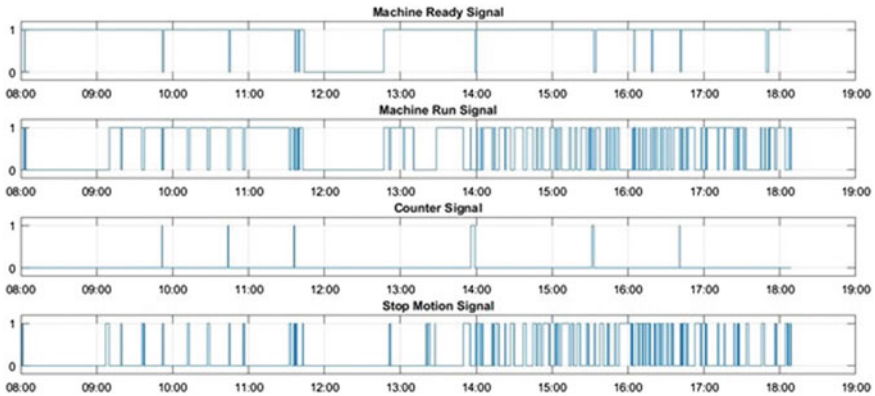


Fig. 8 Knitting machine signals batch downloaded from the IoT core platform and presented as a GUI

3.2.3 Data and Computing Layer

Altair SmartCore [51] is an IoT Core Platform as a Service (PaaS) which manages the data storage as well as offers computing capabilities, thus combining the data and computing layers into one merged layer.

The platform allows the user to gather data from deployed devices that are connected to the internet, each configured with their own identification and authentication. The data was received by the gateway devices via MQTT and was processed and reconstructed in JSON string to comply with the data streaming rules on the SmartCore IoT Platform. The platform provides user the ability to manage and view data stream in real-time. Batch historical data is downloaded from the SmartCore cloud database for analysis. The downloaded data is shown in Fig. 8, consisting of the step function of the machine signals from the knitting machines.

3.2.4 Application Layer

To let the user view and manage the data collected on the IoT platform, the data is streamed from the platform to a dashboard via MQTT over Websockets for data visualization. This is shown in Fig. 9.

3.3 Results and Outcomes

After accumulating the machine states data, the data from the cloud is batch downloaded in csv format, which is then used to analyze the machine performance for the range of dates in the batch historical data.

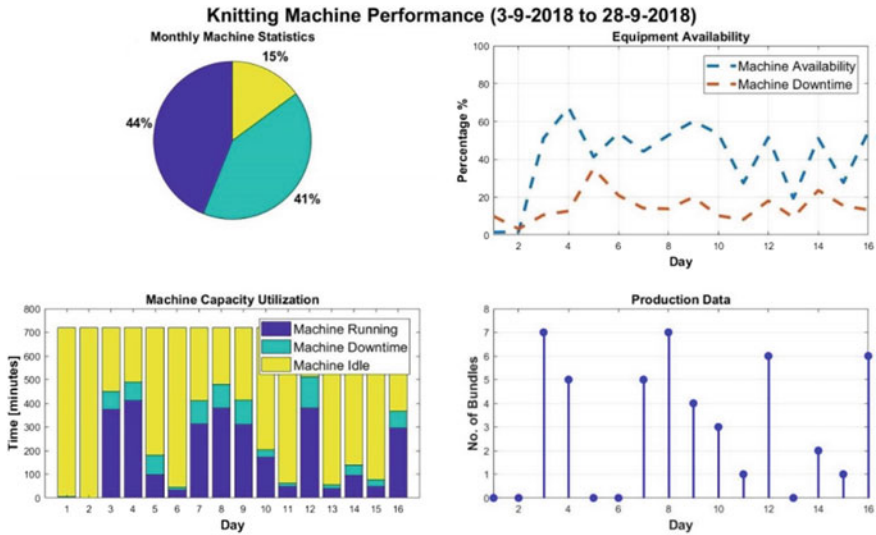


Fig. 9 Sample reports (data visualization) showing the knitting machines performance on the dashboard

3.3.1 Parsing

The large volume of historical data is sorted and analyzed using a MATLAB (r2017b) program, and individual files are created for every date. When each file contains only data collected for the day, it is easier to organize and manage the data. Because the data is in the form of hexadecimal values, they are parsed to binary values to view each of the 4-bit representation as previously depicted in Fig. 6.

3.3.2 Pre-processing

A MATLAB (r2017b) program is created to convert the trendlines into step signals and discretize the raw binary data to show timing diagrams of each of the four signals encoded in the 4-bit machine signals. This demonstrates the reliability and operational readiness to port this system as a hosted web-services and to integrate this system to other enterprise applications (ERP/MRP systems).

3.3.3 Data Analytics

The historical data can then be analyzed to understand the effectiveness of the knitting machine operations using the OEE formulae in Eqs. 1–3 [46].

$$\text{Machine Utilization (\%)} = \frac{\text{Machine Run Time}}{\text{Total Work Duration}} \quad (1)$$

$$\text{Machine Utilization (\%)} = \frac{\text{Machine Stopped}}{\text{Total Work Duration}} \quad (2)$$

$$\text{Machine Idle (\%)} = \text{Work Duration} - \text{Run Time} - \text{Stopped} \quad (3)$$

4 Challenges and Future Trends of CPS in Manufacturing Automation

CPS remain as more of a scientific concept rather than an engineering one, because with the current state of research and development there are many practical concerns associated with developing such systems. Because of the critical application scenarios of CPS, any compromise can result in serious real-world implications for the parties involved. As such, security and privacy must be key priorities in CPS design and operation [52]. For example, in the case study above, attackers can easily obtain key insider information regarding the business if the security of the system is compromised. Current research in cybersecurity of CPS aims to address and counteract these effects [52, 53] and prevent cyber-attacks. In addition, ad hoc and simple solutions are available to secure the data. For the purposes of this pilot a simple data encoding algorithm based on inputs from the machine operator was incorporated. As a result, data and the information in the cloud, even if compromised, would appear partially scrambled and hence of no value to the attackers.

Secondly, the physical layer of the CPS is considered to be the most important due to its core functionality in collecting information and interacting with the physical environment [54]. This means that the reliability and lifespan of the sensors used have a significant impact on the reliability and predictability of the entire system [55]. The limited battery capacities of sensors and actuators are not sufficient for the high-energy applications of networking, communication and control involved in CPS. To address this, studies are investigating the recent appearance of low-power RF sensors in CPS, as well as RF energy harvesting in sensor and wireless networks [55]. These are especially useful in high-power industrial applications of CPS in the manufacturing sector. The other important consideration is the regarding the warranty, and maintenance contracts that can become void due to data acquisition activities. Simple solutions can mitigate this risk, such as tapping the signals at the available levels through opto-couplers and control panels when machine interfaces are not available.

As CPS creates important business opportunities for large-scale industrial automation, there is a need for detailed scientific and engineering design methodology [56] that accommodate the inter-disciplinary and complex nature of CPS in the manufacturing context. The economic, social, and environmental implications of CPS in

IA must be accommodated in these design frameworks and pave the way for a new wave of CPS-centered manufacturing. There are many challenges in the context of IR4 adoption by SMEs. The current COVID-19 pandemic has shown that organizations that digitalized early and used data to innovate have seen exponential growth of business and improvement in productivity, customer experience and quality of services. We show how a well-planned pilot study can give perceived benefits, but also the intangible benefits the incremental success of these step-by-step method brings for all, and particularly SMEs.

As seen above, the IR4 maturity and technological innovation has several challenges- for example, seamless integration of new and legacy systems, successful pilot implementations to get management acceptance. A proven strategy is to start small, to show early returns, scale the systems to higher levels of maturity. While the early steps are to be done inhouse, the later steps such as hiring AI, data scientists, and enterprise software experts can be outsourced.

Employing AI on the retrofitted system can provide many economical and efficiency benefits, such as providing insights into productivity, efficiency of the factory, predictive maintenance and failures, and so on. In the future, Digital Twin Models of the whole Smart Factory can be used to predict the life and maintenance of the equipment to reduce losses from unexpected failures and downtimes. These areas are yet to be explored fully in the manufacturing context, and a lot of potential lies ahead for CPS the manufacturing sector.

5 Conclusion

The fourth industrial revolution has arrived and provides many opportunities for industries large and small for transformation, albeit with challenges. During the COVID-19 pandemic, early adopters of IR4 technologies have already reaped the benefits to and were able to expand their businesses greatly. In this chapter we presented an overview of the cyber-physical system architectural framework and the necessary insights to synthesize the system structure and architecture in a manufacturing context. Using the CPS architectural framework and a real-life pilot project implementation in textile manufacturing, we demonstrated the results of a successful case study. The success of the of pilot projects is an important barometer that determines the organizations resolve to invest in IR4. Using a step-by-step approach, the case study walks through a real-life implementation for fabric manufacturing in the textile industry, including the challenges faced and some practical solutions. We show how each step offers numerous benefits on its own and consolidates achievements of the previous step. The incremental improvements to the processes at a comfortable and manageable pace using the resources at their disposal results in successful adoption while quickly reaping the benefits of transition along the way.

Acknowledgements This work was supported by Monash University, Malaysian Textile and Apparel Center and MOHE grant FRGS/1/2015/TK08/MUSM/02/1.

References

1. Vacca, A., Simpson, C., & Smith, E. (2020). Worldwide digital transformation spending guide. Retrieved November 23 2020, from https://www.idc.com/getdoc.jsp?containerId=IDC_P32575.
2. MIT. (2020). The promise of the fourth industrial revolution. Retrieved November 23 2020, from <https://www.technologyreview.com/2020/11/19/1012165/the-promise-of-the-fourth-industrial-revolution/>.
3. Ragavan, S. K. V., & Shanmugavel, M. (2016). Engineering cyber-physical systems—Mechanics wine in new bottles? In *2016 IEEE International Conference on Computational Intelligence and Computing Research (ICIC)*, May 2016, pp. 1–5, <https://doi.org/10.1109/icic.2016.7919516>.
4. Garms, F., Jansen, C., Schmitz, C., Hallerstede, S., & Tschiesner, A. (2019, September). Capturing value at scale in discrete manufacturing with Industry 4.0 McKinsey. Retrieved November 23 2020, from <https://www.mckinsey.com/industries/advanced-electronics/our-insights/capturing-value-at-scale-in-discrete-manufacturing-with-industry-4-0>.
5. Forth, P., Reichert, T., de Laubier, R., & Chakraborty, S. (2020). Flipping the odds of digital transformation success! BCG. Retrieved November 23 2020, from <https://www.bcg.com/publications/2020/increasing-odds-of-success-in-digital-transformation>.
6. Karre, H., Hammer, M., Kleindienst, M., & Ramsauer, C. (2017). Transition towards an Industry 4.0 State of the LeanLab at Graz University of Technology. *Procedia Manufacturing*, *9*, 206–213. <https://doi.org/10.1016/j.promfg.2017.04.006>.
7. Leitão, P., Colombo, A. W., & Karnouskos, S. (2016). Industrial automation based on cyber-physical systems technologies: Prototype implementations and challenges. *Computers in Industry*, *81*, 11–25. <https://doi.org/10.1016/j.compind.2015.08.004>.
8. Mazzolini, M., Cavadini, F. A., Montalbano, G., & Forni, A. (2017). structured approach to the design of automation systems through IEC 61499 standard. *Procedia Manufacturing*, *11*, 905–913. <https://doi.org/10.1016/j.promfg.2017.07.194>.
9. Leitao, P., Barbosa, J., Papadopoulou, M. E. C., & Venieris, I. S. (2015). Standardization in cyber-physical systems: The ARUM case. In *Proceedings of the IEEE International Conference on Industrial Technology*, Vol. 2015-June, no. June, pp. 2988–2993, <https://doi.org/10.1109/icit.2015.7125539>.
10. Dotoli, M., Fay, A., Miśkiewicz, M., & Seatzu, C. (2017). Advanced control in factory automation: A survey. *International Journal of Production Research*, *55*(5), 1243–1259. <https://doi.org/10.1080/00207543.2016.1173259>.
11. Ladiges, J., et al. (2018). Integration of modular process units into process control systems. *IEEE Transactions on Industry Applications*, *54*(2), 1870–1880. <https://doi.org/10.1109/TIA.2017.2782679>.
12. Arroyo, E., Fay, A., Chioua, M., & Hoernicke, M. (2014). Integrating plant and process information as a basis for automated plant diagnosis tasks. In *Proceedings of the 2014 IEEE Emerging Technology and Factory Automation (ETFA)*, pp. 1–8, <https://doi.org/10.1109/etfa.2014.7005098>.
13. Wan, J., Yan, H., Suo, H., & Li, F. (2011). Advances in cyber-physical systems research. *KSII Transaction on Internet Information Systems*, *5*(11), 1891–1908. <https://doi.org/10.3837/tiis.2011.11.001>.
14. Lee, E. A., & Arunkumar Seshia, S. (2011). *Introduction to embedded systems: A cyber-physical approach* (2nd ed.). MIT Press.
15. Yu, B., Zhou, J., & Hu, S. (2020). Cyber-physical systems: An overview. In S. Hu & B. Yu (Eds.), *Big data analytics for cyber-physical systems* (pp. 1–11). Cham: Springer.
16. Zhong, R. Y., Xu, C., Chen, C., & Huang, G. Q. (2017). Big data analytics for physical Internet-based intelligent manufacturing shop floors. *International Journal of Production Research*, *55*(9), 2610–2621. <https://doi.org/10.1080/00207543.2015.1086037>.

17. Jiang, Z., Jin, Y., M. E., & Li, Q. (2018). Method of tasks and resources matching and analysis for cyber-physical production system. *Advance Mechanical Engineering*, 10(5), 168781401877782. <https://doi.org/10.1177/1687814018777828>.
18. Samir, K., Maffei, A., & Onori, M. A. (2019). Real-Time asset tracking; a starting point for digital twin implementation in manufacturing. *Procedia CIRP*, 81, 719–723. <https://doi.org/10.1016/j.procir.2019.03.182>.
19. Strang, D., & Anderl, R. (2014). Assembly process driven component data model in cyber-physical production systems.
20. Dotoli, M., Fay, A., Miśkiewicz, M., & Seatzu, C. (2019). An overview of current technologies and emerging trends in factory automation. *International Journal of Production Research*, 57(15–16), 5047–5067. <https://doi.org/10.1080/00207543.2018.1510558>.
21. Lins, T., & Oliveira, R. A. R. (2020). Cyber-physical production systems retrofitting in context of industry 4.0. *Computers & Industrial Engineering*, 139, 106193. <https://doi.org/10.1016/j.cie.2019.106193>.
22. Suh, S. H., Noh, S. K., & Choi, Y. J. (1995). A PC-based retrofitting toward CAD/CAM/CNC integration. *Computers & Industrial Engineering*, 28(1), 133–146. [https://doi.org/10.1016/0360-8352\(94\)00033-J](https://doi.org/10.1016/0360-8352(94)00033-J).
23. Stock, T., & Seliger, G. (2016). Opportunities of sustainable manufacturing in industry 4.0. *Procedia CIRP*, 40, 536–541. <https://doi.org/10.1016/j.procir.2016.01.129>.
24. Baker, J., et al. (2016). Requirements engineering for retrofittable subsea equipment. In *Proceedings—2016 IEEE 24th International Requirements Engineering Conference, RE 2016*, pp. 226–235. <https://doi.org/10.1109/re.2016.44>.
25. Arjoni, D. H., et al. (2018). Manufacture equipment retrofit to allow usage in the industry 4.0. In *Proceedings—2017 2nd International Conference on Cybernetics, Robotics and Control, CRC 2017*, Vol. 2018-January, pp. 155–161, <https://doi.org/10.1109/crc.2017.46>.
26. Ferreira, L. L. et al. (2017). A pilot for proactive maintenance in industry 4.0. <https://doi.org/10.1109/wfcs.2017.7991952>.
27. Vachalek, J., Bartalsky, L., Rovny, O., Sismisova, D., Morhac, M., & Loksik, M. (2017). The digital twin of an industrial production line within the industry 4.0 concept. In *Proceedings of the 2017 21st International Conference on Process Control, PC 2017*, pp. 258–262, <https://doi.org/10.1109/pc.2017.7976223>.
28. Langmann, R., & Rojas-Pena, L. F. (2016). A PLC as an industry 4.0 component. In *Proceedings of 2016 13th International Conference on Remote Engineering and Virtual Instrumentation, REV 2016*, pp. 10–15. <https://doi.org/10.1109/rev.2016.7444433>.
29. Lee, E. A. (2007). Computing foundations and practice for cyber-physical systems: A preliminary report. [Online]. Retrieved from <http://www2.eecs.berkeley.edu/Pubs/TechRpts/2007/EECS-2007-72.html>.
30. Liu, Y., Peng, Y., Wang, B., Yao, S., & Liu, Z. (2017). Review on cyber-physical systems. *IEEE/CAA Journal of Automatica Sinica*, 4(1), 27–40. <https://doi.org/10.1109/JAS.2017.7510349>.
31. Gunes, V., Peter, S., Givargis, T., & Vahid, F. (2014). A survey on concepts, applications, and challenges in cyber-physical systems. *KSII Transaction on Internet Information Systems*, 8(12). <https://doi.org/10.3837/tiis.2014.12.001>.
32. Lin, K., & Panahi, M. (2010). A real-time service-oriented framework to support sustainable cyber-physical systems. In *2010 8th IEEE International Conference on Industrial Informatics*, pp. 15–21, <https://doi.org/10.1109/indin.2010.5549473>.
33. Maier, M. W., Emery, D., & Hilliard, R. (2001). Software architecture: Introducing IEEE standard 1471. *Computer (Long Beach, Calif)*, 34(4), 107–109. <https://doi.org/10.1109/2.917550>.
34. Wan, K., Hughes, D., Man, K., Krilavičius, T., & Zou, S. (2010). Investigation on composition mechanisms for cyber physical systems. *International Journal of Design Analysis and Tools for Integrated Circuits and Systems*, 2.
35. Lee, J., Bagheri, B., & Kao, H. A. (2015). A cyber-physical systems architecture for industry 4.0-based manufacturing systems. *Manufacturing Letters*, 3, 18–23. <https://doi.org/10.1016/j.mfglet.2014.12.001>.

36. Schweichhart, K. Reference architectural model industrie 4.0 (RAMI 4.0).
37. Resman, M. (2019). A new architecture model for smart manufacturing: A performance analysis and comparison with the RAMI 4.0 reference model. *Journal home apem-journal.org*, 14(2), 153–165. <https://doi.org/10.14743/apem2019.2.318>.
38. Rizvi, M. A. K., & Chew, E. (2018). Towards systematic design of cyber-physical product-service systems. In *Proceedings of International Design Conference, DESIGN*, 2018, vol. 6, pp. 2961–2974, <https://doi.org/10.21278/idx.2018.0248>.
39. Clark, T., Sammut, P., & Willans, J. (2008). Applied meta modelling: A foundation for language driven development. Ceteva.
40. Fitz, T., Theiler, M., & Smarsly, K. (2019). A metamodel for cyber-physical systems. *Advance in Engineering Informatics*, 41, 100930. <https://doi.org/10.1016/j.aei.2019.100930>.
41. Cárdenas, A. A., Amin, S., & Sastry, S. (2008). Secure control: Towards survivable cyber-physical systems. In *Proceedings—International Conference on Distributed Computing Systems*, pp. 495–500. <https://doi.org/10.1109/icdcs.workshops.2008.40>.
42. Cheng, Z., Tan, Y., & Lim, Y. (2016). Design and evaluation of hybrid temperature control for cyber-physical home systems. *International Journal of Modelling, Identification and Control*, 26(3), 196–206. <https://doi.org/10.1504/IJMIC.2016.080295>.
43. Sanislav, T. (2012). Cyber-physical systems—Concept, challenges and research areas. *Control Engineering Application Informatics*, 14, 28–33.
44. Wang, L., Törngren, M., & Onori, M. (2015). Current status and advancement of cyber-physical systems in manufacturing. *Journal of Manufacturing System*, 37, 517–527. <https://doi.org/10.1016/j.jmsy.2015.04.008>.
45. Horvath, I., & Gerritsen, B. (2012). Cyber-physical systems: Concepts, technologies and implementation principles. *Proceeding on TMCE, 2012*, 19–36.
46. Vorne. (2020). What is OEE (Overall Equipment Effectiveness)? OEE. Retrieved November 16 2020, from <https://www.oee.com/>.
47. MSV Textile and Machinery. (2020). “Fukuhara V-LPJ4B 34”—Circular knitting machines (double jersey). Retrieved November 16 2020, from http://msv.com.pl/en-maszyna-3746-1335449627-fukuhara_vlpj4b.html.
48. Malche, T., & Maheshwary, P. (2015). Harnessing the Internet of Things (IoT): A review. *International Journal of Advance Research Computer Science Software Engineering*, 5.
49. SIMATIC IOT2000| SIMATIC IOT gateways| Siemens Global. Retrieved November 16 2020, from <https://new.siemens.com/global/en/products/automation/pc-based/iot-gateways/iot2000.html>.
50. FRDM-K64F Platform|Freedom Development Board|Kinetis MCUs|NXP. (2020). Retrieved November 16 2020, from <https://www.nxp.com/design/development-boards/freedom-development-boards/mcu-boards/freedom-development-platform-for-kinetis-k64-k63-and-k24-mcus:FRDM-K64F>.
51. Altair SmartWorks|smartcore overview. Retrieved November 16 2020, from <https://www.altair-smartworks.com/smartcore-overview>.
52. Fink, G. A., Edgar, T. W., Rice, T. R., MacDonald, D. G., & Crawford, C. E. (2017). Security and privacy in cyber-physical systems. In *Cyber-physical systems: Foundations, principles and applications* (pp. 129–141). Elsevier Inc.
53. Narayanan, S. N., Khanna, K., Panigrahi, B. K., & Joshi, A. (2018). Security in smart cyber-physical systems: A case study on smart grids and smart cars. In *Smart cities cybersecurity and privacy* (pp. 147–163). Elsevier.
54. Wang, L., & Haghghi, A. (2016). Combined strength of holons, agents and function blocks in cyber-physical systems. *Journal of Manufacturing Systems*, 40, 25–34. <https://doi.org/10.1016/j.jmsy.2016.05.002>.
55. Erol-Kantarci, M., Illig, D. W., Rumbaugh, L. K., & Jemison, W. D. (2017). Energy-harvesting low-power devices in cyber-physical systems. In *Cyber-physical systems: Foundations, principles and applications* (pp. 55–74). Elsevier Inc.
56. Törngren, M. et al. (2017). Characterization, analysis, and recommendations for exploiting the opportunities of cyber-physical systems. In *Cyber-physical systems: Foundations, principles and applications* (pp. 3–14). Elsevier Inc.

Intelligent Machining of Abrasive Jet on Carbon Fiber and Glass Fiber Polymeric Composites Using Modified Nozzle



M. Balasubramanian, S. Madhu, and C. Hemadri

1 Introduction

Technologically advanced manufacturing industries in the field of automobiles, aircraft, nuclear reactors, and medical applications, etc., have been demanding an alternative to metals like fiber-reinforced composites. Researchers in the area of materials and their processing are developing innovative materials with higher strength, toughness, hardness, and other properties. Polymer composites like CFRPs and GFRPs are subjected to severe delamination when the conventional machining process is used [1]. Machining by erosion results in the removal of successive surface layers of the material, thereby resulting in dissolution or melting and vaporization of the material being machined [2]. In any mechanical material removal process, mechanical energy is used for the removal of the materials using the erosion mechanism. This process is based on propelling high-velocity abrasive particles as transfer media on to the desired target. Pneumatic/hydraulic pressure is used as the energy source [3]. Machining using water as jet mostly to machine lower strength materials can be cut using stronger abrasives [2, 3].

M. Balasubramanian (✉) · C. Hemadri

Department of Mechanical Engineering, RMK College of Engineering and Technology, Chennai 601 206, India

e-mail: manianmb@gmail.com

C. Hemadri

e-mail: Chd311@gmail.com

S. Madhu

Department of Automobile Engineering, Saveetha School of Engineering, Chennai 601 205, India

e-mail: mathumarine@gmail.com

© The Author(s), under exclusive license to Springer Nature Switzerland AG 2021

225

K. Palanikumar et al. (eds.), *Futuristic Trends in Intelligent Manufacturing*,

Materials Forming, Machining and Tribology,

https://doi.org/10.1007/978-3-030-70009-6_14

1.1 Polymer Composites

The materials under discussion are very interesting in view of their low cost and flexibility in fabrication. They are valued in the aerospace industry for their stiffness, lightweight, and heat resistance. They are fabricated materials in which carbon fibers are bonded together by resins in either a sheet or a fiber wound form. Materials manufactured using polyacrylonitrile fibers, pitch resins (rayon) using the oxidation and thermal pyrolysis process [4]. The applications include aerospace, nuclear engineering and automotive manufacturing [5]. Glass fiber reinforced polymer composites, fibers are bonded with resins like epoxy and vinyl ester. Glass fibers are classified based on their geometry such as continuous fibers, discontinuous (short) fibers, E-Glass fibers, C-Glass fibers and T-Glass fibers and finds use in ships, automobiles, aerospace and automobile engine compartments [5, 6].

1.2 Abrasive Jet Machining of Polymer Composite

Machining was done on carbon fiber sheets with Al_2O_3 abrasive particles. The material removal obtained at a pressure of 8 bar, a nozzle diameter of 5 mm, and a stand-off distance of 8 mm was maximum [7]. An increase in the removal of material at a higher rate in the machining of CFRP is evidenced with high pressure and a lesser gap between nozzle and target surface. Silicon carbide and Al_2O_3 did offer good surface finish. The volume of material machined is increased while surface roughness is decreased. Reduction in roughness also resulted due to wider gap between the nozzle tip and the target [8, 9]. It was noticed that the harder aluminum oxide (Al_2O_3) abrasive particle minimize the surface roughness [10, 11]. Rise in pressure resulted in rise of kinetic energy which increased the volume of material removed and reduction in roughness. Rise in the stand-off distance resulted in reduction of roughness [12]. Enhancement of the surface quality was seen at a higher frequency and higher oscillation. When the angle of oscillation increased surface smoothness also increased [13]. The jet divergence occurred when there was an increase in the SOD and the impingement of abrasive particles per unit area decreased. Hence the surface roughness was increased [14]. Higher pressure and lower volume of stream of abrasives did result in creation of lower roughness [15, 16].

Many researchers have conducted experiments but, no work related to the nozzle effect of abrasive jet on GFRP and CFRP is available in the literature. The stimulus of factors on quality of machining FRP composites is not studied in detail minimum studies have been made on the design of the nozzle and its effect on the polymeric composites for this matter.

2 Need for Modified Nozzle

Nozzles are made of a different cross-section. It is so designed to ensure minimum pressure due to bends and friction. An increase of wear in the nozzle results in divergence of a jet stream resulting in more inaccurate machining. In an earlier investigation [17, 18] by variation in the profile of the nozzles did not reveal any flow analysis of abrasive air particle mixture inside the convergent nozzles. No detailed study has been made so far on the effect of nozzle machining performance. Hence, in this article, a modified nozzle was employed for understanding the consequence of abrasive jet on the quality of machining.

2.1 Modified Nozzle

The two-dimensional view of an existing conventional nozzle normally found in the literature is shown in Fig. 1a and the three-dimensional CAD model is shown in Fig. 1a. Design modifications were made with the available nozzle as the base model, and hereafter, the newly designed nozzle will be called the modified nozzle. The novel nozzle is depicted in Figs. 1b and 2b showcases the new nozzle. Modified nozzles were machined with different diameters (1.5, 2, 2.5, 3, 3.5 mm) using hardened steel. Figure 3 is the photograph of the fabricated modified nozzle.

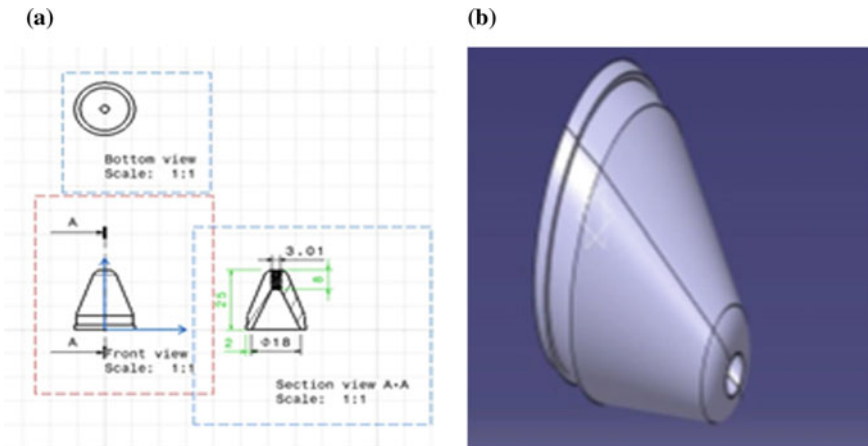


Fig. 1 a 2D view of a conventional nozzle. b CAD model of the existing nozzle

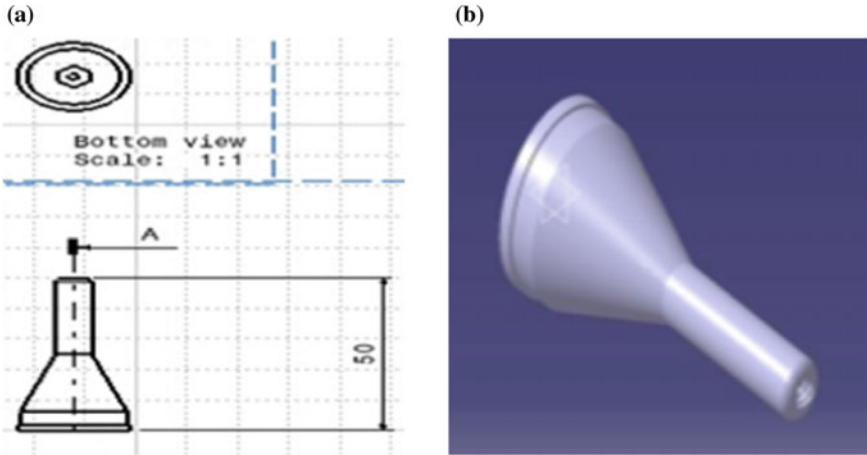


Fig. 2 a 2D drawing of a modified nozzle b CAD model of a modified nozzle



Fig. 3 Fabricated newly designed nozzle

3 Materials and Methods

Composite materials have been widely used because of their specific properties in industrial and consumer products. Nowadays, metallic materials are getting substituted by composites. Among these fibre reinforced polymer (FRP) composites, CFRP and GFRP laminates found extensive use in many engineering and domestic fields. A Review describes challenges all over the world on machining of FRP composites. In this chapter, a detailed study is done on FRP composites with a conventional and new nozzle.

Unidirectional carbon fiber composites were fabricated with a 15% fiber volume ratio. Epoxy resin was used as the binding material for these composites. The dimension of the sample is $50 \times 15 \times 3$ mm and shown in Figs. 4 and 5. Unidirectional glass fiber with a 32% fiber volume ratio was used for the study. Epoxy resin (LY

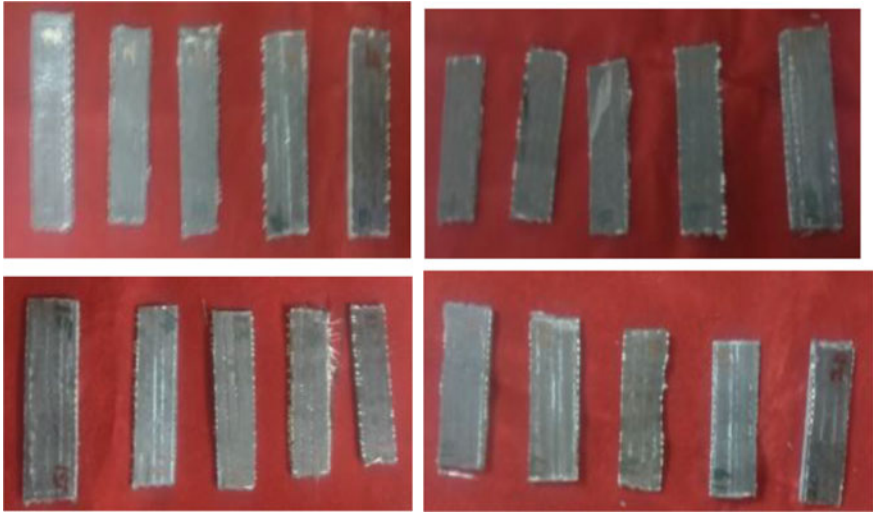


Fig. 4 CFRP samples before machining

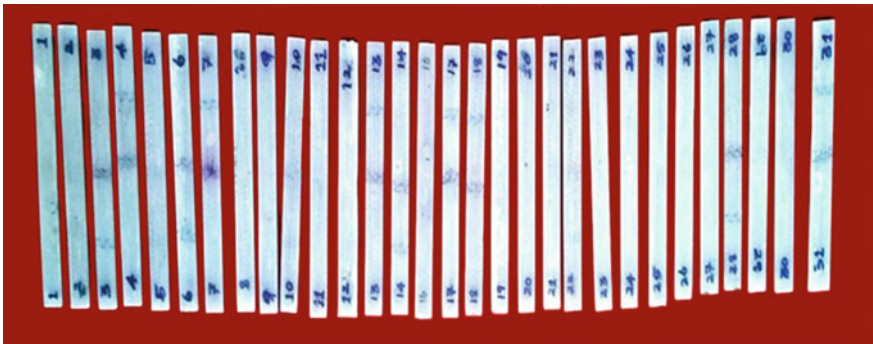


Fig. 5 GFRP samples before machining

556) was mixed with a hardener (HY 995). The resin was mixed with the hardener in a ratio of 10:1.

3.1 *Ascertaining the Essential Process Parameters*

In the earlier studies, jet pressure, stand-off distance, abrasive grain size and nozzle diameter was chosen for the study. But predominantly the factors such as pressure, stand-off distance, nozzle diameter, and abrasive size were considered to be the

Table 1 Important factors and levels

S. no.	Factor	Notation	Unit	Levels				
				(−2)	(−1)	(0)	(+1)	(+2)
1	Jet Pressure	P	MPa	0.2	0.3	0.4	0.5	0.6
2	SOD	L	mm	0.5	1	1.5	2	2.5
3	Diameter of the Nozzle	D	mm	1.5	2	2.5	3	3.5
4	Size of abrasive	S	μ	50	70	90	110	130

important factors [7, 13]. Principal factors which influences the machining characteristics are identified as Pressure (P), Stand-off distance (SOD), Nozzle diameter (D), and Abrasive size (S). The range of factors for experimentation was decided based on the above investigation. Details have been presented in Table 1.

3.2 Experimental Procedure

Fabricated specimens of the polymeric composite specimens were cleaned with a solution of distilled water and 5% Na_2CO_3 for removing the dust and any other foreign particles from the surface. Holes were made on the polymeric composite laminates using the abrasive jet machining process as per the machining conditions shown in Table 2. In this investigation, machining was conducted based on the central composite design [15, 16, 19]. 4 factors 5 levels were chosen for the experimentation. In total, 62 trials were conducted (31 using the conventional nozzle and 31 using the modified nozzle). Figure 6a and show the CFRP and GFRP samples respectively after abrasive jet machining.

4 Results and Discussion

Machining was performed on composite laminates using an orthodox and modified nozzle. The results of MRR and roughness (Ra) were depicted in Tables 3 and 4.

Table 2 Machining conditions

1	Type of machine	Mixing chamber (Vortex)
2	Abrasive particle	Silicon carbide (SiC)
3	Used medium	Air
4	Rate of flow	8 g/min
5	Type of nozzle	(i) Conventional nozzle (ii) Modified nozzle

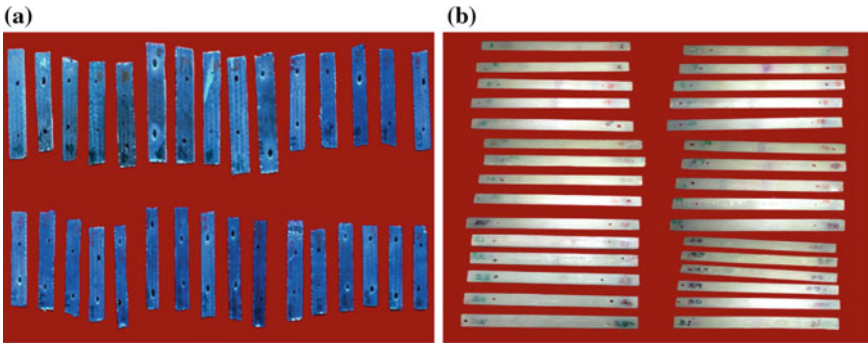


Fig. 6 a CFRP samples after machining b GFRP samples after machining

4.1 Effect of Process Parameters on CFRP Composites

Design modification was made on the existing conventional nozzle for changing the flow pattern of the abrasive medium. Conventional nozzle produces turbulent flow and, modified nozzle produced two-phase flow. Simultaneous radial and axial flow is imparted to the air abrasive mixture. The air abrasive mixture inside the nozzle progressed forward with radial and axial velocity.

4.1.1 Effect of Pressure and SOD on MRR

The investigation showed the material removal rate obtained as 0.006 g/s in the case of a modified nozzle for a minimum pressure of 0.2 MPa. At 0.6 MPa pressure, the MRR obtained was 0.1 g/s. In the case of the normal nozzle, the material removal rate was 0.003 g/s at 0.2 MPa and 0.061 g/s at 0.6 MPa pressure. In the current investigation in the case of a conventional nozzle for a minimum standoff distance of 0.5 mm, the material removal rate obtained was 0.011 g/s. 0.0157 g/s was attained when the SOD was high (2.5 mm). For the modified nozzle, 0.016 g/sec and 0.026 g/sec was attained at 0.5 mm and 2.5 mm respectively. Figure 7a, b indicate the correlation between pressure and stand-off distance on material removal rate using a conventional and modified nozzle.

Figure 7 shows a rise in the rate of machining as a result of the maximum pressure and the minimum SOD. A surge in jet pressure inside the conventional and modified nozzles gained more volume of material removal. The material removal rate achieved was maximum in a modified nozzle when compared to the conventional one. When the pressure rises, the dynamic energy of the particle is also increased, resulting in a rise of the machining rate. The clearance between the workpiece and nozzle was minimum resulting in rise of MRR. There was a decrease in the volume of machining resulting from an increase in SOD.

Table 3 Results of CFRP samples

Expt	Coded values				Conventional nozzle			Modified nozzle		
	P	L	D	S	MRR (g/s)	M _t (s)	Ra (μm)	MRR (g/s)	M _t (s)	Ra (μm)
1	-1	-1	-1	-1	0.001	27.0	3.213	0.006	22.0	1.041
2	1	-1	-1	-1	0.016	19.0	4.213	0.029	16.0	1.042
3	-1	1	-1	-1	0.002	17.0	3.654	0.016	14.0	0.904
4	1	1	-1	-1	0.015	13.0	4.654	0.003	10.0	0.797
5	-1	-1	1	-1	0.016	17.0	4.768	0.004	14.0	1.050
6	1	-1	1	-1	0.031	15.0	5.786	0.011	12.0	0.788
7	-1	1	1	-1	0.036	18.0	6.036	0.017	13.0	0.982
8	1	1	1	-1	0.024	19.0	3.543	0.019	12.0	0.852
9	-1	-1	-1	1	0.023	17.0	4.567	0.025	14.0	0.919
10	1	-1	-1	1	0.036	13	3.213	0.047	5.6	0.897
11	-1	1	-1	1	0.002	14	2.567	0.003	8.0	0.929
12	1	1	-1	1	0.015	19	2.546	0.017	15	0.799
13	-1	-1	1	1	0.004	23	1.879	0.007	19	0.727
14	1	-1	1	1	0.006	15	1.678	0.009	11.6	0.751
15	-1	1	1	1	0.002	23	1.756	0.004	5.7	0.930
16	1	1	1	1	0.005	18	1.675	0.007	14.0	0.930
17	-2	0	0	0	0.002	17	1.865	0.006	11.0	1.282
18	2	0	0	0	0.061	9	1.326	0.100	4.0	0.663
19	0	-2	0	0	0.0112	16	2.564	0.016	10.0	1.282
20	0	2	0	0	0.0157	18	1.581	0.026	11.0	0.732
21	0	0	-2	0	0.003	19	1.547	0.009	13.0	0.727
22	0	0	2	0	0.018	25	1.491	0.027	18.0	0.746
23	0	0	0	-2	0.005	13	1.721	0.010	7.0	0.726
24	0	0	0	2	0.013	12	3.102	0.024	5.6	0.852
25	0	0	0	0	0.052	12	2.561	0.069	6.1	0.927
26	0	0	0	0	0.032	14	1.987	0.041	4.5	0.726
27	0	0	0	0	0.012	14	1.876	0.021	7.0	0.775
28	0	0	0	0	0.001	11	1.654	0.010	5.0	0.726
29	0	0	0	0	0.015	12	1.765	0.018	7.0	0.726
30	0	0	0	0	0.017	16	1.678	0.027	12.0	0.726
31	0	0	0	0	0.032	13	1.786	0.064	5.7	0.801

Table 4 Results of GFRP samples

Expt	Values				Conventional nozzle			Modified nozzle		
	P	L	D	S	MRR (g/s)	M _t (sec)	Ra (μm)	MRR (g/s)	M _t (sec)	Ra (μm)
1	-1	-1	-1	-1	2.53	46	2.167	0.113	41	0.896
2	1	-1	-1	-1	1.7	32	3.123	2.460	21	1.068
3	-1	1	-1	-1	1.82	29	4.432	1.532	25	1.351
4	1	1	-1	-1	2.85	27	2.456	1.310	22	0.907
5	-1	-1	1	-1	2.82	38	3.123	2.324	32	1.512
6	1	-1	1	-1	1.62	31	2.765	2.330	25	1.423
7	-1	1	1	-1	1.24	43	3.987	7.841	37	1.546
8	1	1	1	-1	1.85	32	2.415	7.50	29	1.097
9	-1	-1	-1	1	1.82	45	3.670	4.521	39	0.967
10	1	-1	-1	1	1.35	32	3.126	7.920	25	0.943
11	-1	1	-1	1	2.07	37	2.956	3.231	31	1.021
12	1	1	-1	1	1.22	40	2.523	7.753	33	0.938
13	-1	-1	1	1	1.84	41	2.564	7.201	37	1.044
14	1	-1	1	1	1.4	38	1.987	7.790	30	0.897
15	-1	1	1	1	0.14	57	2.452	5.411	49	1.102
16	1	1	1	1	0.96	49	2.132	7.610	44	0.971
17	-2	0	0	0	1.75	56	1.886	6.731	48	0.943
18	2	0	0	0	3.91	32	1.604	7.970	19	0.802
19	0	-2	0	0	0.81	36	1.687	2.693	25	0.843
20	0	2	0	0	0.7	37	3.312	1.302	27	1.669
21	0	0	-2	0	0.84	51	1.742	2.660	28	0.871
22	0	0	2	0	0.48	57	1.932	3.232	37	0.966
23	0	0	0	-2	0.81	43	2.061	5.754	38	1.031
24	0	0	0	2	1.44	41	1.997	7.131	32	0.997
25	0	0	0	0	2.93	47	2.435	6.160	39	1.214
26	0	0	0	0	1.97	42	2.126	5.541	37	0.987
27	0	0	0	0	1.77	51	1.980	4.301	48	1.145
28	0	0	0	0	3.55	38	2.134	5.790	34	1.216
29	0	0	0	0	1.13	34	1.986	6.602	30	0.998
30	0	0	0	0	3.68	40	2.321	7.040	35	1.034
31	0	0	0	0	3.44	44	3.014	0.690	39	1.113

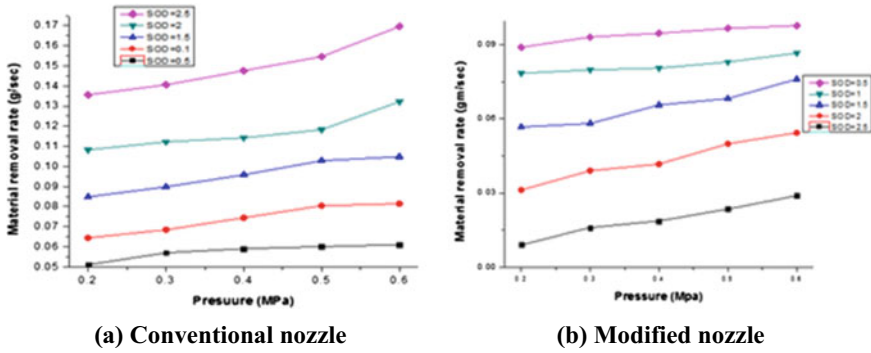


Fig. 7 Correlation between pressure and SOD on MRR in CFRP

4.1.2 Effect of Pressure and Nozzle Diameter on MRR

The MRR obtained using the modified nozzle of diameter 3.5 mm was 0.027 g/s and for the conventional nozzle, 0.018 g/s. Using a modified nozzle of 1.5 mm diameter, 0.009 g/s was obtained. It was 0.003 g/s for the conventional nozzle. Figure 8a, b submits the consequence of pressure and nozzle diameter on the material removal rate using a conventional nozzle and a modified nozzle respectively.

Figure 8 shows the maximum pressure and maximum nozzle diameter causing a surge in the MRR of CFRP samples. The highest material removal rate was obtained when the nozzle diameter was maximum. An increase in the nozzle diameter increased the stream rate which in turn increased the removal of material. In the case of the modified nozzle, increased mass flow rate accompanied by pressure and offered a relatively high MRR.

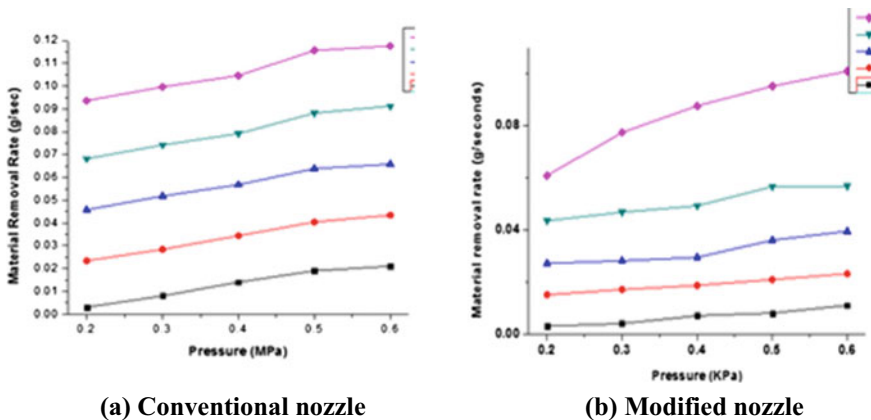


Fig. 8 Effect of pressure and nozzle diameter on MRR in CFRP

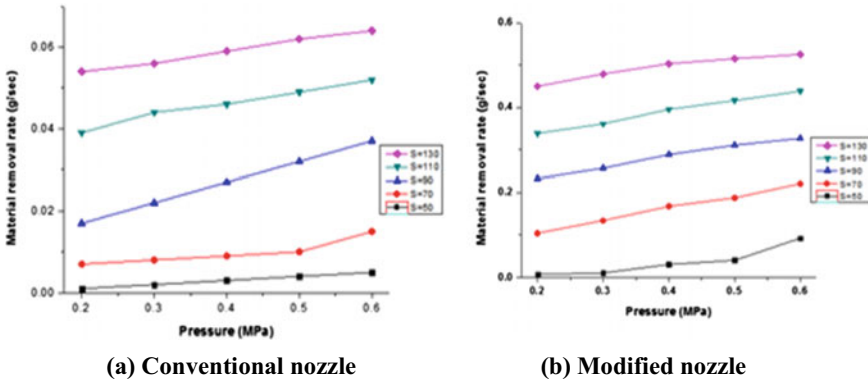


Fig. 9 Effect of pressure and size of abrasive on MRR in CFRP

4.1.3 Effect of Size of Abrasive on MRR

Abrasive particle of 50 micron flowed through the modified nozzle, resulting in a MRR of 0.01 g/s, whereas, in the conventional nozzle, the MRR obtained was 0.005 g/s. when 130 micron particles was transferred via a modified nozzle, 0.024 g/s was obtained, whereas, the MRR obtained in the conventional nozzle was 0.013 g/s. Figure 9a, b show the correlation between pressure and size of abrasive on volume of material removal in conventional and modified nozzle respectively. In previous works, 0.0657 g/s was obtained [8]. The maximum abrasive particle size surged the rate of material removal in both the nozzles. But, the rate of removal was high in the case of a modified nozzle.

Rise in removal of material with the use of improved nozzle maybe due to surge in the impetus of abrasive particles on the material generating craters of a greater depth, leading to wearing down of work material. At 6 bar pressure, 0.01 g/s was obtained [20]. The present investigation using modified nozzle showed that the maximum MRR of 0.1 g/s the possibility of obtaining which is significantly better than what is seen in a few studies made earlier in this context.

4.1.4 Consequence of of Jet Pressure and SOD on Roughness

At maximum pressure of 0.6 MPa, 1.326 μm was achieved by the conventional nozzle and 0.663 μm through modified. At 0.2 MPa, conventional nozzle achieved 2.417 μm and the modified nozzle 1.282 μm . At minimum SOD, roughness obtained was 2.564 μm . Higher SOD using a conventional nozzle achieved was 1.581 μm and through modified nozzle was 0.732 μm . Figure 10a, b explains the correlation between jet pressure and stand-off distance of CFRP samples on roughness (Ra). The particles of abrasives were cut into tiny parts, when the pressure of jet is increased. In addition, the design of the nozzle caused increased the kinetic energy of the particle

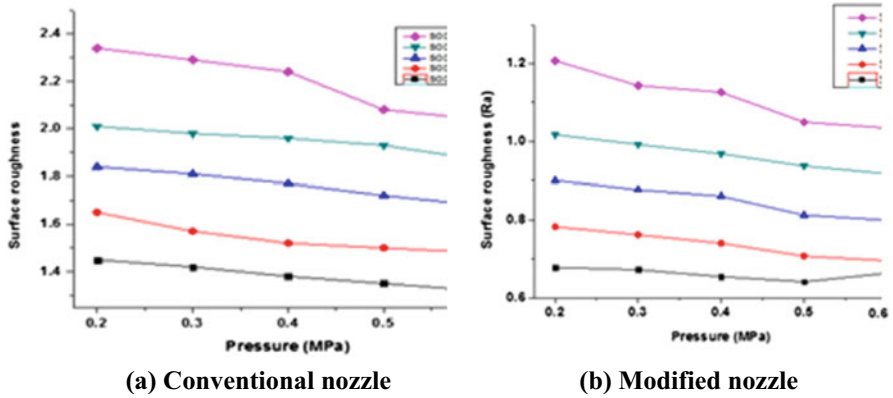


Fig. 10 Influence of pressure and SOD on roughness (Ra) in CFRP composites

and reduced the roughness of the workpiece surface. Minimum SOD reduced the surface roughness. Rise in the work nozzle clearance resulted in widening of the jet. So the kinetic energy got decreased and amplified the roughness. The roughness was minimum with the use of a modified nozzle as compared with the conventional nozzle.

4.1.5 Effect of Pressure and Diameter of the Nozzle on Roughness

The roughness assessed from a conventional nozzle of 1.5 mm diameter was 1.547 μm and with a 3.5 mm diameter it was 1.491 μm . Using a modified nozzle, the roughness achieved with 1.5 mm diameter was 0.727 μm and with 3.5 mm was 0.746 μm . Figure 11a, b indicate the correlation between jet pressure and diameter of nozzle on roughness using conventional and modified nozzles. The maximum

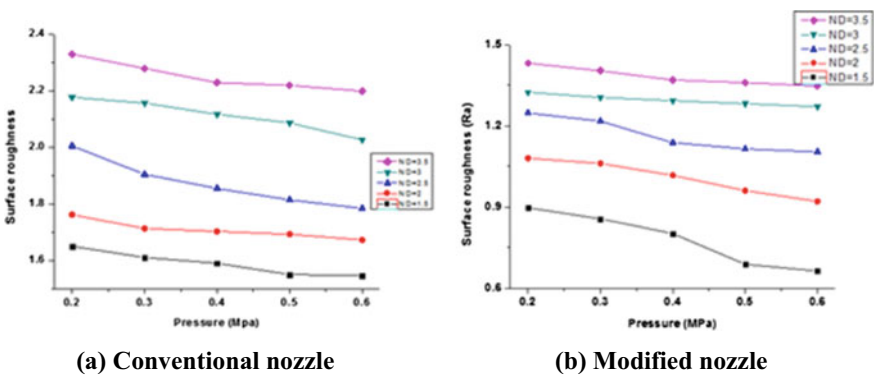


Fig. 11 Influence of pressure and nozzle diameter on roughness (Ra) in CFRP composites

pressure and minimum nozzle diameter in both the nozzles reduce roughness. The particles can lose their kinetic energy if particles come out from a nozzle of larger diameter. The flow rate was further improved by a smaller nozzle diameter, resulting in a good surface finish from a modified nozzle.

4.1.6 Consequence of Jet Pressure and Size of Abrasive on Roughness

A roughness of 3.102 μm was given by the abrasives (130 μ) blasted from the traditional nozzle. With 50-micron abrasive, roughness of 1.72 μm was obtained as against a modified nozzle which resulted in 0.726 μm . The particles of 130 μ flowing out of the modified nozzle provided a roughness value of 0.852 μm . Figures 12a, b explain the effect of pressure and size of abrasive on roughness in the CFRP samples. Fine particles with maximum jet pressure reduced the roughness in both the nozzle. The roughness value obtained was minimum in a modified nozzle. So, the minimum particle size resulted in dip of roughness. The roughness value was minimum in the modified nozzle as compared with the conventional nozzle. Higher water pressure delivered a maximum particle velocity (higher particle energy). Hence larger craters could be created on the work surface by individual impacts [13].

An increase in roughness was witnessed with a rise in stand-off distance and pressure [10]. Earlier literature showed higher values than the current investigation of 0.663 μm [18].

4.2 Effect of Process Parameters in GFRP

Samples machined using conventional and modified nozzles were investigated in abrasive jet machining.

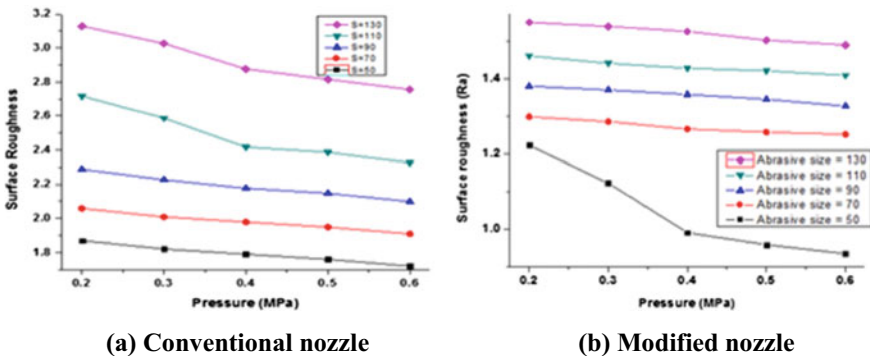


Fig. 12 Pressure and abrasive size on roughness (Ra) in CFRP

4.2.1 Consequence of Jet Pressure and SOD on MRR

The present investigation using a modified nozzle showed the material removal rate obtained as 6.731 g/s for a minimum pressure of 0.2 MPa. At 0.6 MPa pressure, 7.970 g/s was attainable. In the case of the conventional nozzle, the material removal rate was 1.75 g/s at 0.2 MPa and 3.91 g/s at 0.6 MPa pressure. 0.61 g/s was obtained in the case of a conventional nozzle for a minimum standoff distance of 0.5 mm and 0.7 g/s when the SOD was high (2.5 mm). Using a modified nozzle, at 0.5 mm SOD, 2.693 g/s and at 2.5 mm 1.302 g/s was achieved. Figure 13a brings out the consequence of jet pressure and stand-off distance on the removal of material in GFRP samples using the conventional nozzle. Figure 14b indicated the effect of pressure and SOD on the removal rate of material using a modified nozzle.

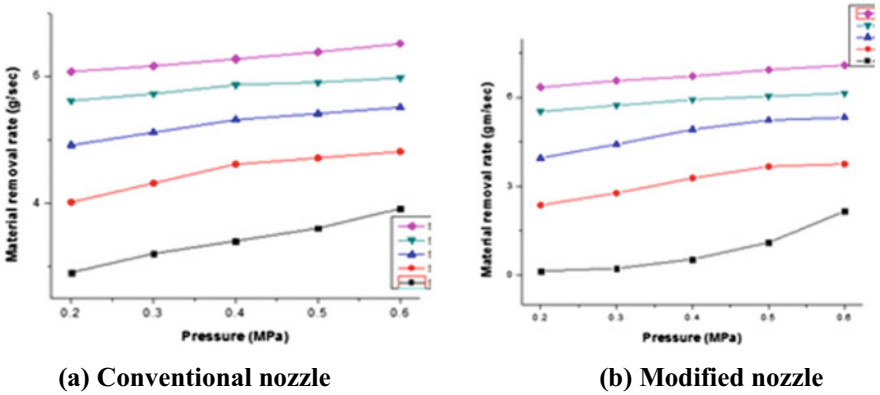


Fig. 13 Pressure and SOD on material removal rate in GFRP composite

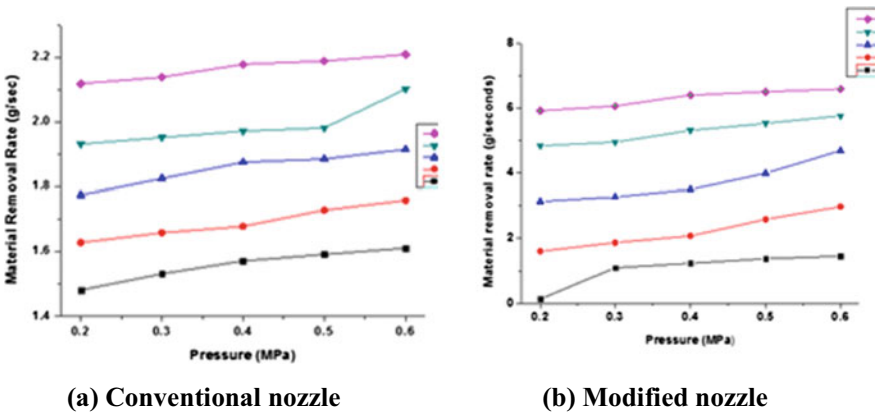


Fig. 14 Pressure and nozzle diameter on material removal rate on GFRP composites

When compared to a standard one the highest removal rate of material was achieved using the modified nozzle. The particle is energetic when the pressure has been boosted, causing an increase in the rate of material removal. When the clearance between the target and the nozzle was small, there was an improvement in MRR for both nozzles. When compared to a traditional nozzle, the highest material removal rate was achieved using a new nozzle. When the space between the nozzle tip and the target was less, the jet attacked the target with a greater velocity and area of impingement got increased, causing the higher volume of material.

4.2.2 Effect of Pressure and Nozzle Diameter on MRR

The study using the modified nozzle of diameter 3.5 mm showed 3.232 g/s of MRR. It was 1.48 g/s for the conventional nozzle. 2.660 g/s of MRR was obtained using a modified nozzle while the conventional nozzle was able to obtain 1.84 g/s. Figure 14a explains the effect of pressure and diameter of the nozzle on the material removal rate using a conventional nozzle. Figure 14b brings out the correlation between jet pressure and nozzle diameter on the material removal rate using a modified nozzle. When the nozzle diameter was maximum, the highest material removal rate was obtained in both the nozzles. MRR obtained was more in the modified nozzle compared with the conventional. The new nozzle due to its design, increased the flow rate at maximum diameter of the nozzle.

4.2.3 Effect of Pressure and Abrasive Size on MRR

When the particle of 50 μ flowed through the modified nozzle, it was 5.754 g/s, whereas, in the convergent nozzle, 2.81 g/s was attained. 130 micron abrasive was supplied through the modified nozzle, 7.131 g/s of material removal was obtained, while it was 3.44 g/s in the conventional nozzle. Figure 15a brings out the correlation between jet pressure and abrasive size using a conventional nozzle while Fig. 18b explains using a modified nozzle. The maximum particle size increased the material removal rate in both the nozzles. But, the rate of removal was high in the case of a modified nozzle. The nozzle increased the thrust of particles on the target and increased the depth of the craters on the target resulting in larger erosion and higher rate of material removal. The maximum material removal rate obtained in a modified nozzle was 7.97 g/s. But, in the conventional nozzle, the MRR obtained was 3.91 g/s. Epoxy glass fiber composites machined by using abrasive jet machining showed a maximum of 0.15 g/s [16]. In this current investigation maximum, MRR of 7.970 g/s was obtained using the modified nozzle.

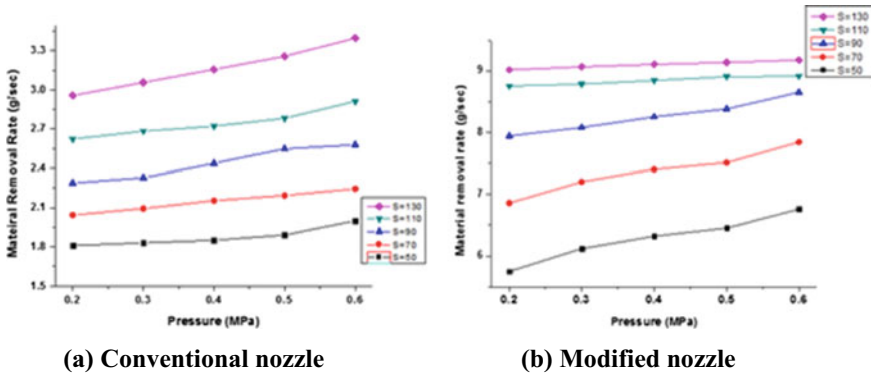


Fig. 15 Pressure and size of abrasive on MRR in GFRP composites

4.2.4 Influence of Pressure and SOD on Roughness

When the jet pressure was at 0.6 MPa, the roughness obtained using a conventional nozzle was 1.604 and 0.802 μm using new nozzle. When the pressure was minimum (0.2 MPa), conventional nozzle attained 1.886 μm and the modified nozzle was 0.943 μm . At minimum distance, roughness obtained was 1.686 μm through traditional nozzle. This value was high as compared to modified nozzle with a roughness of 0.843 μm . The roughness at higher distance with a conventional nozzle was 3.338 μm . But modified nozzle showcased 1.669 μm and showcased good finish in GFRP composite when minimum stand-off distance is chosen.

Figure 16a, b is showcasing the correlation between jet pressure and stand-off distance on roughness in GFRP composites using the conventional and the modified nozzle. Drop in roughness at maximum pressure was obtained using a modified

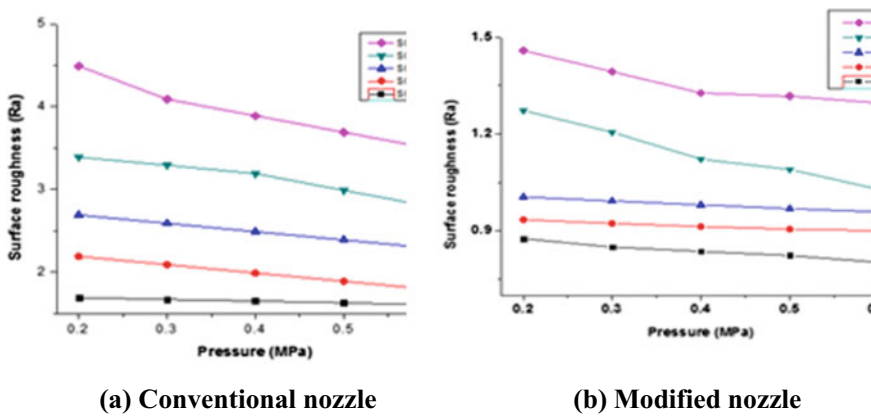


Fig. 16 Effect of pressure and SOD on roughness in GFRP samples

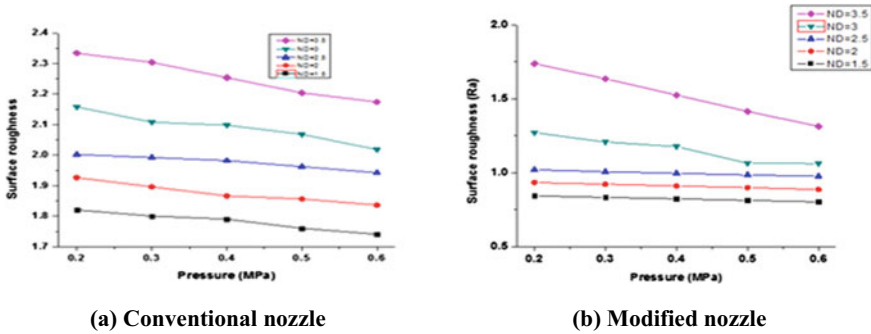


Fig. 17 Influence of pressure and nozzle diameter on roughness in GFRP

nozzle. As the abrasive jet rises, the jet becomes more energetic and the material was removed smoothly. Hence the roughness decreased for both the nozzles. As the pressure decreased, the surface roughness also increased. As the stand-off distance increased, the jet diameter also got amplified before reaching the target and reduced the kinetic energy leading to high surface roughness.

4.2.5 Effect of Pressure and Diameter of Nozzle on Roughness

A roughness value of 1.742 μm was achievable through a conventional nozzle of 1.5 mm diameter and 1.932 μm with 3.5 mm nozzle. With a modified nozzle at 1.5 mm and 3.5 mm, 0.871 μm and 0.966 μm was attained respectively. Figure 17a, b brings out the correlation between jet pressure and diameter of the nozzle on roughness in GFRP composites using the conventional and the modified nozzles. Figure 17 showcases that high pressure and reduced nozzle diameter reduces the surface roughness machining of GFRP samples using both the nozzles. The roughness value was minimum when compared with the conventional nozzles. Particles passing through the nozzles of larger diameter lost their kinetic energy before impinging the surface. Further, reduction in nozzle diameter increased the flow rate, and the velocity of the particle impinging the surface. Hence, the nozzle with a minimum diameter reduced the surface roughness value.

4.2.6 Consequence of Jet Pressure and Size of Abrasives on Roughness

130-micron particle supplied via the conventional nozzle attained 1.997 μm and with 50 μ of particle size and gave a finish of 2.061 μm . With modified nozzle roughness of 0.997 μm was obtained with 130 μ and 1.031 μm with 50 μ . Figure 18a, b brings out the influence of pressure and size of particles on roughness in GFRP composites using conventional and modified nozzles. Figure 18 shows maximum pressure and maximum particle size reducing the surface roughness in machining

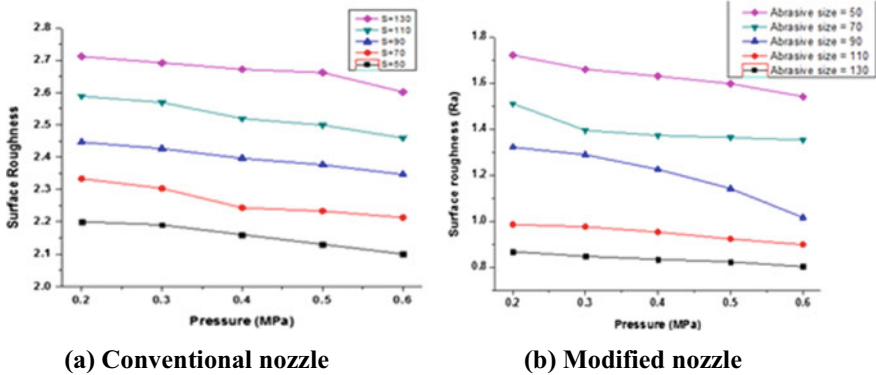


Fig. 18 Influence of pressure and abrasive particle on roughness on GFRP samples

of GFRP samples using both nozzles. The roughness value was minimum with the modified nozzle when compared to the conventional nozzle.

An abrasive particle with maximum mesh size reduced the surface roughness in both the nozzles. Further, the modified nozzle increased particle velocity. Hence, the abrasive particle with a large mesh reduced the surface roughness in the modified nozzle when compared to the conventional nozzle [11]. Surface quality was enhanced with maximum pressure [15]. Increasing stand-off distance reduced the surface roughness. When compared with earlier studies on surface roughness of GFRP, the modified nozzle produced a better surface finish in the order of 0.802 μm as against 4 μm by earlier researchers.

5 Conclusions

Modified nozzles were designed and fabricated for machining the CFRP and GFRP composites. The developed modified nozzle showed better prospects as it delivered a higher particle velocity during machining. The outcome of the trials made are presented as follows

- (a) Volume of material removal is more with the use of a modified nozzle in comparison with the conventional nozzle for both the materials under investigation.
- (b) The highest MRR of 7.97 g/s was attained at a pressure of 6 bar, stand-off distance 1.5 mm, nozzle diameter 2.5 mm, and the abrasive particle size 90 with the use of modified nozzle in the machining of GFRP, which was 50% more than obtained from the conventional nozzle. There is a substantial reduction in the machining time when the modified nozzle was used. The investigation revealed the adequacy of the minimum time of 4 s for machining the CFRP and 19 s to machine an E-glass composite of thickness 3 mm.

- (c) Modified nozzle showcased a roughness of $0.663 \mu\text{m}$ at a pressure: 0.6 MPa, stand-off distance: 1.5 mm, nozzle diameter: 2.5 mm, and abrasive size: 50 μ in CFRP.
- (d) In GFRP, $0.802 \mu\text{m}$ was obtained at a pressure of 0.6 MPa, stand-off distance: 1.5 mm, diameter of nozzle: 2.5 mm, size of abrasive: 50 micron

References

1. Abdel-Gawad, Hassan, & El-Hofy,. (2017). *Fundamentals of machining processes: Conventional and non-conventional processes* (2nd ed.). Sound Parkway: CRC Press.
2. Benedict, G. F. (1987). *Nontraditional manufacturing processes*. Sound Parkway, NW: CRC Press
3. Pandey, P. C., & Shan, H. S. (1980). *Modern machining processes*. New Delhi: TATA McGraw-Hill Publishing Company limited.
4. Martin Alberto M. (2013). *Introduction of fibre-reinforced polymers- polymers and composites: Concepts, properties and processes*. Intech Publishing Company
5. Morgan, Peter. (2005). *Carbon fibres and their composites*. Sound Parkway, NW: CRC Press.
6. Jackson, Mark J., & Paulo Davim, J. (2011). *Machining with abrasives*. New York: Springer.
7. Srikanth, D. V., & Sreenivasa Rao, M. (2014). Response surface methodology for optimization of process parameters in abrasive jet drilling of composites. *IOSR Journal of Mechanical and Civil Engineering*, 11(3), 20–26.
8. Singh, Satyendra, Shrivasa, S. P., & Dewangan, Sailesh. (2015). Analysis the machining effect of CFRP material using AJM. *Journal of Harmonized Research*, 3(4), 151–155.
9. Srikanth, D. V., Sreenivasa Rao, M., Seshu Kumar, A. (2016). Application of RSM for optimal response of process parameters on machining of CFRP composites by using AJM. In *International Conference on Electrical, Electronics, and Optimization Techniques (ICEEOT)* (pp. 1677–1681).
10. Azmir, M. A., & Ahsan, A. K. (2008). Investigation on glass/epoxy composite surfaces machined by abrasive water jet machining. *Journal of Materials Processing Technology*, 198, 122–128.
11. Azmir, M. A., & Ahsan, A. K. (2009). A study of abrasive water jet machining process on glass/epoxy composite laminate. *Journal of Materials Processing Technology*, 209, 6168–6173.
12. Azmir, M. A., Ahsan, A. K., & Rahmah, A. (2009). Effect of abrasive water jet machining parameters on aramid fibre reinforced plastics composite. *International Journal of Material Forming*, 2(1), 37–44.
13. Lemma, E., Chen, L., Siores, E., & Wang, J. (2002). Study of cutting fiber-reinforced composites by using abrasive water-jet with cutting head oscillation. *Composite Structures*, 57, 297–303.
14. Armagan, Mustafa, & Armağan Arici, A. (2016). Cutting performance of glass-vinyl ester composite by abrasive water jet. *Materials and Manufacturing Processes*, 32(15), 1715–1722.
15. Siddiqui, Tauseef Uddin, Shukla, Mukul, & Tambe, Pankaj B. (2008). Optimization of surface finish in abrasive water jet cutting of Kevlar composites using hybrid Taguchi and response surface method. *International Journal of Machining and Machinability of Materials*, 3(4), s382–402.
16. Madhu, S., & Balasubramanian, M. (2015). A review on abrasive jet machining process parameters. *Applied Mechanics and Materials*, 766–767, 629–634. <https://doi.org/10.4028/www.scientific.net/AMM.766-767.629>.
17. Madhu, S., & Balasubramanian, M. (2017). Effect of abrasive jet process parameters on machining glass fibre reinforced polymer composite. *Materialwissenschaft und Werkstofftechnik*, 48(11), 1146–1157.

18. Madhu, S., & Balasubramanian, M. (2017). Influence of nozzle design and process parameters on surface roughness of CFRP machined by abrasive jet. *Materials and Manufacturing Processes*, 32(9), 1011–1018.
19. Madhu, S., & Balasubramanian, M. (2018). Effect of swirling abrasives induced by a novel threaded nozzle in machining of CFRP composites. *International Journal of Advanced Manufacturing Technology*, 95(9–12), 4175–4189.
20. Madhu, S. (2018). Some Studies on Abrasive Jet Machining of Carbon Fibre and Glass Fibre Reinforced Polymeric Composites Using Novel Internal Threaded Nozzle, [thesis]. Anna University, <https://library.annauniv.edu/ethesis.php?subject=Mechanical%20Engineering>.

Additive Manufacturing of Nylon Parts and Implication Study on Change in Infill Densities and Structures



J. Nagarjun, S. Manimaran, and M. Krishnaprakash

1 Introduction

3D printing is gaining lot of attention all around the world with advent of various 3D printing techniques such as Fused Deposition Modelling (FDM), Powder bed and inkjet head 3D printing (3DP), Stereolithography (SLA), Selective Laser Sintering (SLS), 3D plotting/direct-write etc., [1]. However, the most preferred 3D printing technique is the FDM technology. It offers several advantages such as low cost [2], occupies less floor space, less material wastage [3], can produce complex and unique geometries with special functions [4, 5]. Lately, FDM is preferred over conventional moulding technique due to non-requirement of special tool dies which in turn reduces the initial investment considerably [6]. FDM has enabled product customization especially for small scale production with polymers still being widely used material group in the FDM process. The polymer materials such as Acrylonitrile Butadiene Styrene (ABS), Nylon (NY), Poly Lactic Acid (PLA) or even the materials reinforced using wood or metal powders are used in FDM technology [7]. 3D printers are used extensively in various applications such as orthoses, prosthesis [8], parts of unmanned aerial vehicle [9, 10], aerospace, automotive, dental and consumer markets [11].

In a study by Mohan, Senthil et al. have stressed the importance of possessing knowledge on correlation between process variables and its effect on the material properties [12]. Several researchers have printed structures in xy , yz , zx orientations

J. Nagarjun (✉) · S. Manimaran · M. Krishnaprakash
Department of Mechanical Engineering, PSG Institute of Technology and Applied Research,
Coimbatore 641 062, India
e-mail: nagarjun_jaya@outlook.com

S. Manimaran
e-mail: maniilam17@gmail.com

M. Krishnaprakash
e-mail: mkrishnaprakash24@gmail.com

and have compared experimental results. The edge orientation (yz) provides better tensile properties in comparison. This is because of alignment of fiber perpendicular to the direction of applied force [13]. Researches were also have carried out with different raster angle of print. It was concluded that the 0° raster which has material oriented along longer dimensions of the specimen showed better results in terms of properties such as tensile, compression, flexural and impact [14]. Motaparti, Taylor et al. have studied the effects of air gap on flexural strength [15] and reported that negative air gap exhibits higher yield strength. Alvarez, Kenny et al. have examined the effect of infill percentage on mechanical properties. They concluded that higher infill percentage results better strength, but at increased print time. However, the Negative air gap can reduce the quality of the part and its dimensional tolerance. Increasing infill percentage may lead to high material consumption, build time and thus increasing the cost of the part [17].

The remarkable feature of FDM is that ability to build feasible structures by optimizing the infill of the component. It is a process parameter that plays a major role in the approach towards optimal weight. It provides FDM technology the competitive edge over other Additive Manufacturing (AM) technologies. The study of mechanical properties of structures with required infill density is of great interest. The different infill structures attained via additive manufacturing provides opportunity to minimize the use of material as well as to obtain high strength to weight ratio [18]. Selection of appropriate filling pattern among various existing patterns is an key step in the sturdy production of parts [19]. Similarly, the infill density can also be selected in order to reduce the weight and time of print. The variations in infill structures provides the customer an option to print in accordance with the required function of the printed structures. But the knowledge on the strength of different infill structures is limited [20]. The 3D printed structures are anisotropic in nature because of its unique infill structures and print orientation [21]. The anisotropic behaviour of 3D printing material compels the need for more research on this area in order to understand their behaviour.

The mechanical traits of common 3D printing elements such as PLA, ABS has been experimentally validated by varying the infill structures having kept the other printing factors constant. The materials such as PLA, ABS were predominantly investigated in several studies [22–27]. However, the knowledge on the material Nylon-6 is limited. Hence the material Nylon-6 is investigated in the current study. The patterns that were considered for analysis is Honeycomb and Diamond (Rectilinear) pattern. Since, they were the common preferred patterns commercially. The mechanical behaviours such as Tensile, compression and flexural behaviour were analysed in this study.

Table 1 Properties of Nylon material [32]

Properties	Value
Density (g/cm ³)	1.12–1.14
Water Absorption-24 h (%)	1.3–1.8
T _g (°C)	48
T _m (°C)	215
Heat deflection temperature (°C)	56–80
Co efficient of thermal expansion (mm/mm/°C × 10 ⁵)	8–8.6
Tensile strength (MPa)	43–79
Elastic modulus (GPa)	2.9
Elongation (%)	20–150
Izod impact strength (J/m)	42.7–160

2 Materials and Methods

2.1 Material

The FDM specimens that were analysed in this study was Nylon which is a formulation of Nylon 6. It is a polyamide semi crystalline material [28]. It is a thermoplastic, recyclable material and hence it is widely used all around the globe [29]. It is estimated that 1,000,000 tons of Nylon is consumed in automotive industry each year [30]. Nylon has also other applications in transportation, Electrical & Electronic equipment, Sporting goods etc., One of the recent addition to the application is 3D printing. The 3D printed nylon material is suitable for prototyping, making functional parts for small manufacturing units, parts requiring secondary operations and for ruggedized packaging and Housing.

The cartridge of Nylon of standard diameter 1.75 mm was purchased from V Engineering Solutions, Erode. The cartridge includes a hydroscopic seal in order to prevent Nylon from absorbing moisture from the atmosphere. It is an engineering grade performance material. Nylon has good strength, flexibility and Durability [31]. The material is available in three colours natural, white and black. In this study, Natural nylon was used throughout. The property of the Nylon 6 material is given in the Table 1.

2.2 Model and Fabrication

The specimens were modelled using SOLIDWORKS. It is saved in .stl format in order to access the model file in the slicing software. The software package used for slicing the model is CubePro which is the prescribed software package provided

Table 2 Printing parameters used in the current study

Parameters, units	Value
Nozzle diameter, mm	0.3
Layer deposition speed, mm/s	15
Bed temperature, °C	110
Nozzle temperature, °C	240
Solid top layers	3
Solid bottom layers	3
Outer wall layers	3
Side walk layers	2
Infill pattern top/bottom	Rectilinear
Infill angle, deg	45/-45

by 3D systems. The CubePro software renders G-code which are processed by the inbuilt motherboard of the printer. The printing technique is FDM and the specimens were printed using CubePro desktop 3D printer made by 3D Systems. 3D Systems is one of the pioneers in the field of Additive Manufacturing technology. The 3D printer has a built volume of $243 \times 270 \times 230$ mm. The nozzle size of 0.3 mm diameter and with a speed of 15 mm/s was used for printing of Nylon specimens. A few parameters such as print resolution, layer height, wall thickness, speed, Orientation were adjusted according to the supplier's recommendation. The process parameters that were commonly used in this study are listed in the Table 2.

The supplier's preposition is used as baseline to produce acceptable print quality and uniformity. Just before the layer deposition, the pet sheet is applied over the bed, so that the printing failure because of non-adhesion can be prevented. The sheet is also necessary to prevent the FDM specimen from warping at high temperatures. The specimens were printed at the recommended temperature of 240 °C. The warp was prevented further by providing appropriate sidewalks. The borders were perforated for its easy removal, but it required craft blade to remove the sidewalks of nylon because of its high strength. The resolution of the material is maintained at 200 microns throughout the print. It is the resolution recommended by the companies like Cubero, Stratasys for Nylon material. The upper layer, bottom layer is maintained uniformly with three layers each. In this study, the specimens were modelled and fabricated with ASTM standards. A typical representation of cross section of tensile specimen is shown Fig. 1.

The printed specimens were later checked for accuracy of print. It was found that the thickness of the specimen was 6.6% more in comparison to the specimen model. The length and width of the specimen varied by 1.5% when compared with the model. The different Infill pattern and percentage is shown Fig. 2



Fig. 1 Layer configuration of tensile specimen

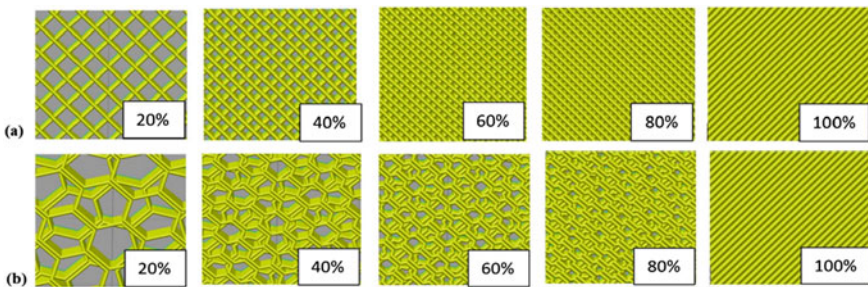


Fig. 2 Various infill densities and corresponding infill structures of a Honeycomb pattern b Diamond pattern

2.3 Experimental Study

2.3.1 UTM Test

The tensile and compressive strength of Nylon 6 material were evaluated using static and Dynamic Universal testing machine (INSTRON 8801). The tensile and compressive specimens were prepared in accordance with ASTM D638 [33] and ASTM D695 [34] respectively. Three specimens were evaluated for a particular infill structure and pattern. The tensile and compressive test were carried out with the preload of 0.1 Mpa and the test speed of 0.33 mm/s. The length of the tensile specimen between the support is 115 mm. The breadth and thickness of the tensile specimen is 13 mm and 3.2 mm respectively. The diameter and length of the compressive specimen is 10 mm and 25.4 mm respectively.

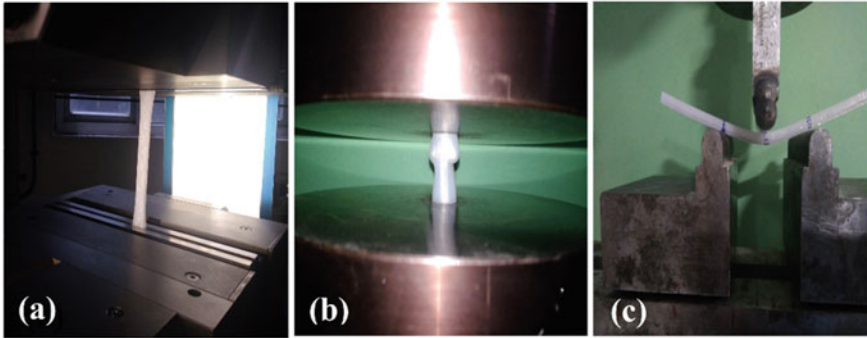


Fig. 3 Experimental evaluation a Tensile UTM Test b Compression UTM Test c 3 Point bending test

2.3.2 Three-Point Bending Test

The flexural strength of the Nylon 6 material was determined using three-point bending test. The flexural tests were conducted in accordance with ASTM D790 [35] standard. Each specimen was centered on a lower support with a support span of 51.4 mm. The width and thickness of the specimen were 12 mm and 3 mm, respectively. The steady load through the loading nose was applied and the specimen was deflected at the rate of 0.17 mm/s for a deflection of 5%. The experimental study carried out on the Tension, compression and flexural specimens are shown in the Fig. 3.

3 Results and Discussion

3.1 Influence of Infill Parameters on Tensile Strength

The Table 3 shows the influence of infill parameters such as pattern and material percentage on tensile strength of the material. The tensile strength values of Diamond and Honeycomb pattern with respect to infill percentage is shown in Fig. 4. The tensile strength increases with infill percentage non-linearly. It is normalized with 2nd degree polynomial to establish relationship between the tensile strength and infill percentage. The rectilinear structure has better tensile property over Honeycomb structure. The rectilinear also proved to have better strength to weight ratio. It may be due to the fact that more material oriented along the line of force acting over the specimen which offers better resistance to failure. On average, the Rectilinear infill offers 8.84% better tensile resistance over the Honeycomb structure for the same material weight. The SEM image of the tensile failure specimen is shown in the Fig. 5. It can be observed that the specimen suffers delayering along with the

Table 3 Data on influence of infill parameters (Pattern and infill material percentage) on Tensile strength

Specimen *(Rx/Hx)	Weight (g)	Tensile strength (Mean) (Mpa)	Strength to weight ratio (N/Kg.mm ²)
R20	5.37	17.17	3.20
H20	5.32	16.91	3.18
R40	6.51	19.60	3.01
H40	6.33	18.80	2.97
R60	7.64	23.70	3.10
H60	7.26	21.78	3.00
R80	8.78	29.64	3.37
H80	8.1	25.51	3.15
R100	9.91	41.12	4.15
H100	9.25	36.26	3.92

*Rx/Hx—'x' percentage infill material with rectilinear/Honeycomb pattern

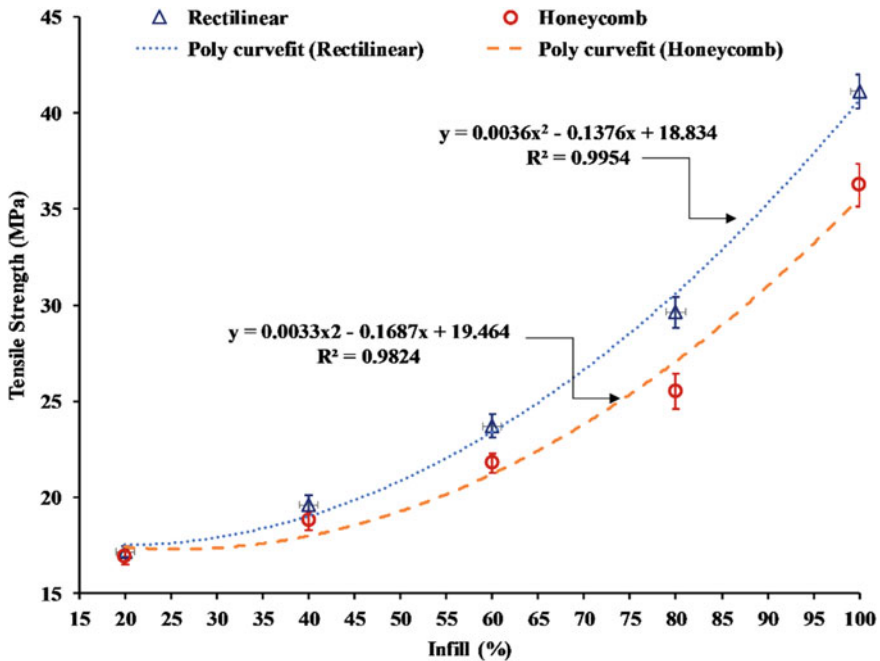


Fig. 4 Tensile strength of diamond and Honeycomb pattern for different infill densities

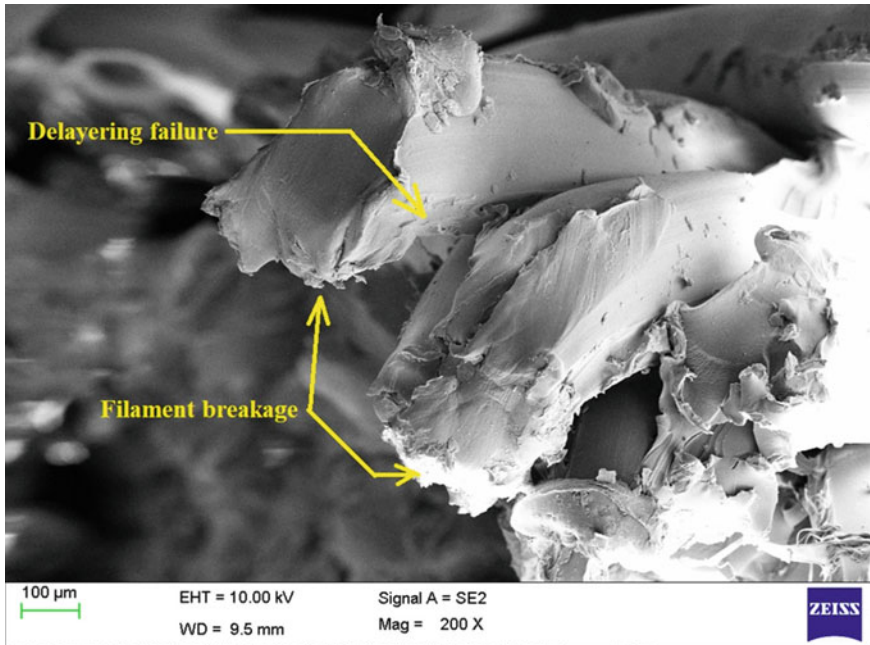


Fig. 5 SEM image of tension failure specimen

filament breakage which leads to failure of the specimen.

3.2 Influence of Infill Parameters on Compression Strength

The effect of infill parameters about the compression strength is shown in the Table 4. The compression strength values of Rectilinear and Honeycomb pattern with respect to infill percentage is shown in Fig. 6. As similar to tensile strength values, the compression strength values also increase with infill percentage non-linearly. It is normalized with 2nd degree polynomial to establish relationship between the compression strength and infill percentage. The compression strength of 3D Printed nylon varies over a wide range from 13.91 Mpa to 59.37 Mpa between 20% and 100% infill respectively. The rectilinear structure offers 11.76% more strength on average for the same material weight over honeycomb structure. This can be attributed towards more material provide more adhesion between the layers in the case of rectilinear structure. The SEM image reinstates the compression specimen fails predominantly because of adhesion failure between the layers rather than the filament failure. The compressed specimen upon close inspection through SEM shows the crack has been initiated in the adhesion layer whereas the filament layer seems to be intact (Fig. 7).

Table 4 Data on influence of Infill parameters (Pattern and Infill material percentage) on Compression strength

Specimen *(Rx/Hx)	Weight (g)	Compression strength (Mean) (Mpa)	Strength to weight ratio (N/Kg.mm ²)
R20	0.98	14.65	14.95
H20	0.98	13.91	14.20
R40	1.37	19.75	14.42
H40	1.31	18.20	13.90
R60	1.74	26.72	15.36
H60	1.65	24.66	14.95
R80	2.09	40.05	19.16
H80	1.87	34.40	18.40
R100	2.47	59.37	24.04
H100	2.22	49.39	22.25

*Rx/Hx—'x' percentage infill material with rectilinear/Honeycomb pattern

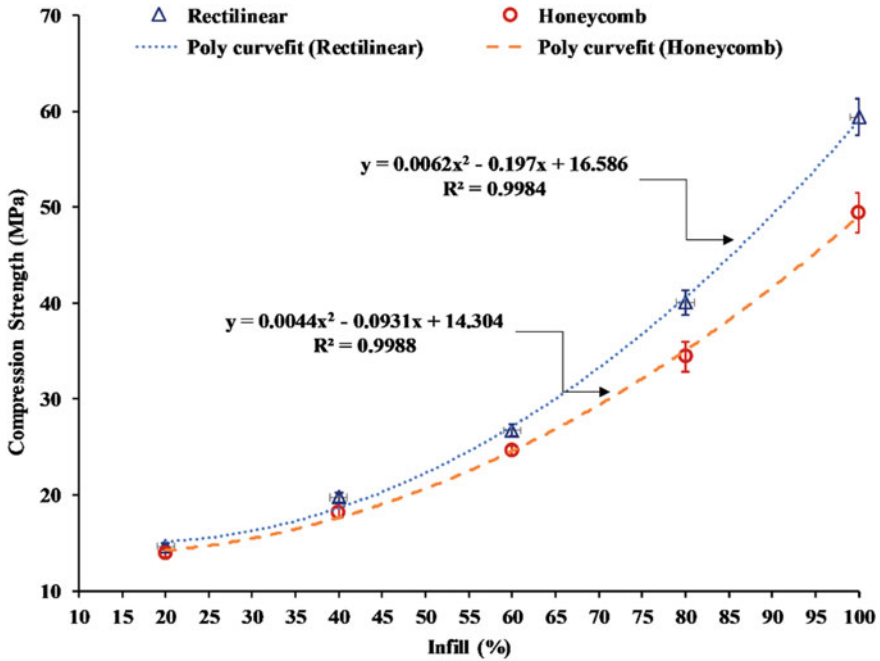


Fig. 6 Compression strength of Diamond and Honeycomb pattern for different infill densities

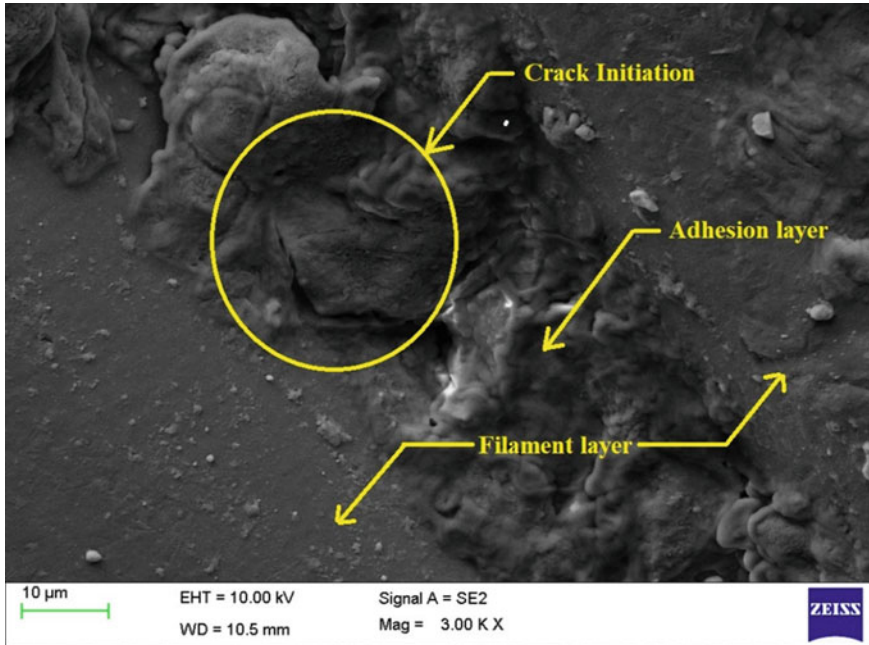


Fig. 7 SEM image of Compression failure specime

3.3 Influence of Infill Parameters on Flexural Strength

The effect of infill parameters on the flexural strength is shown in the Table 5. The flexural strength values of Diamond and Honeycomb pattern with respect to infill percentage is shown in Fig. 8. It can be observed that the flexural strength increases with infill material percentage linearly. The values can be normalized using the linear equation. The linear trendline has the R square values more than 99%. Here too, the rectilinear structure offers better strength to weight ratio when compared to honeycomb structure. There is only 50.61% increase in flexural strength on increasing infill percentage from 20% to 100%. On contrary, the tensile and compression strength increases by 109.46% and 305.25% respectively. The failure happens due to delayering and filament breakage as seen from the SEM image of flexural specimen is shown in Fig. 9.

3.4 Economic Implication

The performance of the infill structure depends on the critical area/inertia to weight ratio. The performance curves are plotted (Fig. 10) for tensile, compression and flexural strength of Diamond structure. It can be observed that excluding the 100%

Table 5 Data on influence of Infill parameters (Pattern and Infill material percentage) on Flexural strength

Specimen *(Rx/Hx)	Weight (g)	Flexural strength (Mean) (Mpa)	Strength to weight ratio (N/Kg.mm ²)
R20	1.04	24.50	23.56
H20	1.03	23.94	23.24
R40	1.09	27.10	24.86
H40	1.08	26.37	24.42
R60	1.14	29.90	26.23
H60	1.13	28.88	25.56
R80	1.2	33.10	27.58
H80	1.17	32.05	26.54
R100	1.25	36.90	29.52
H100	1.23	35.30	28.70

*Rx/Hx—'x' percentage infill material with rectilinear/Honeycomb pattern

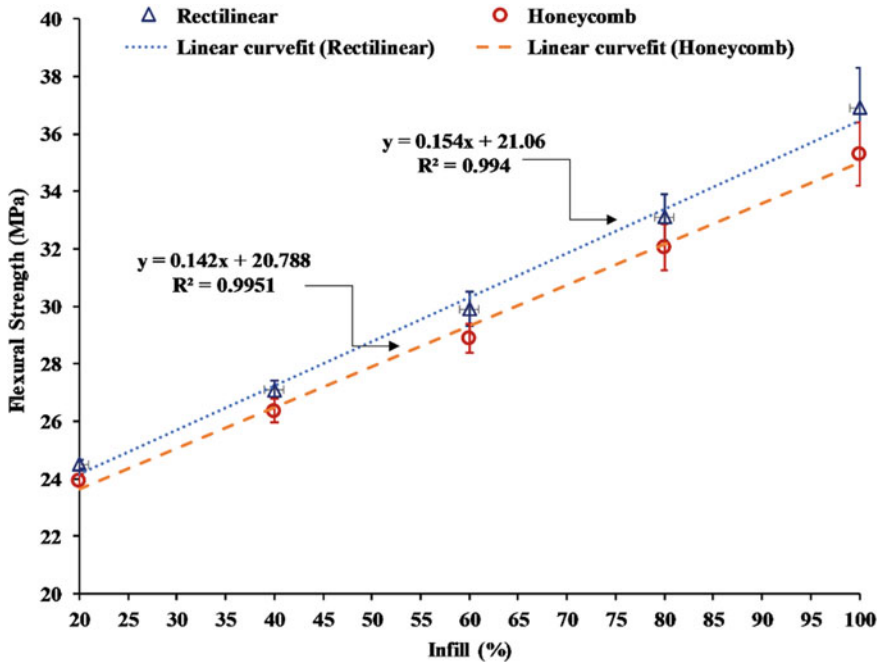


Fig. 8 Flexural strength of diamond and Honeycomb pattern for different infill densities

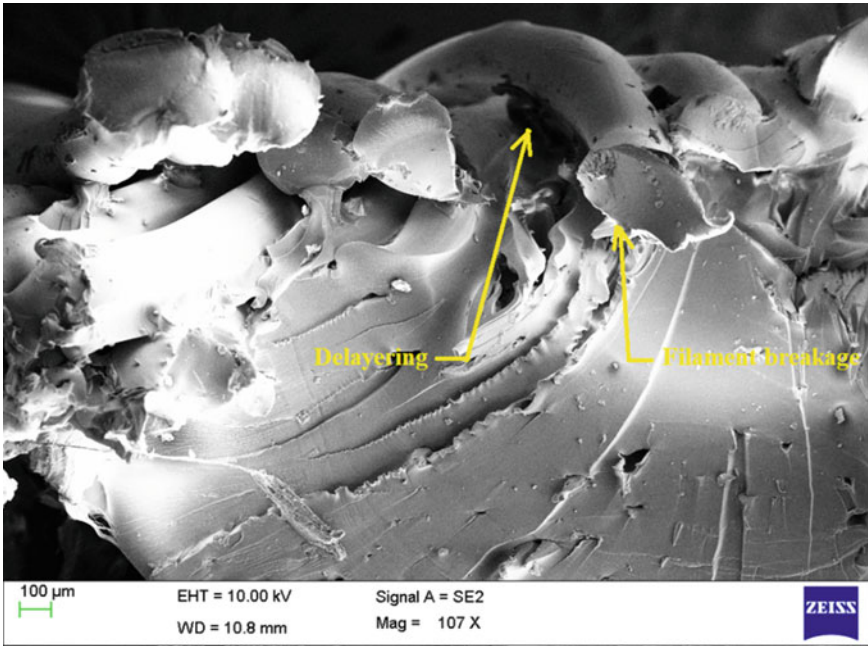


Fig. 9 SEM image of flexural failure specimen

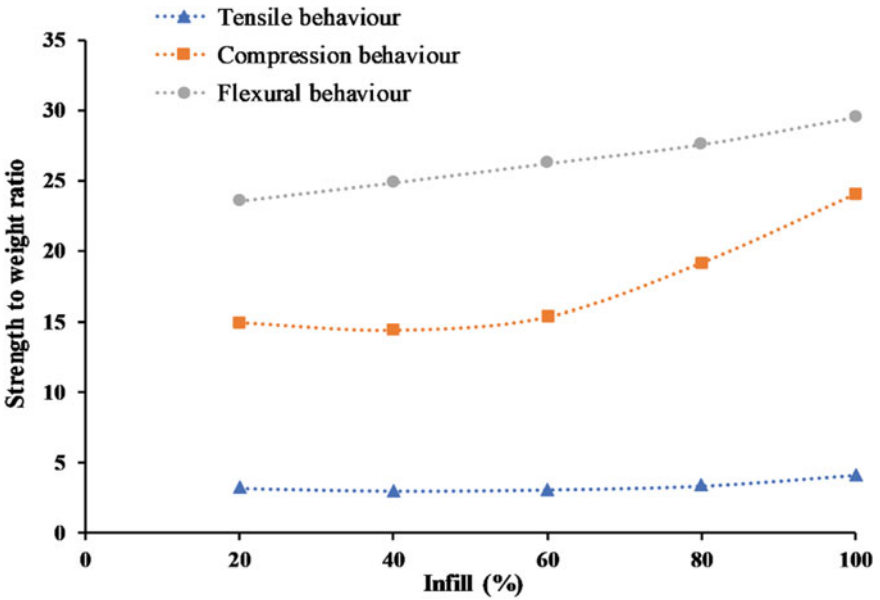


Fig. 10 Performance chart of Rectilinear structure

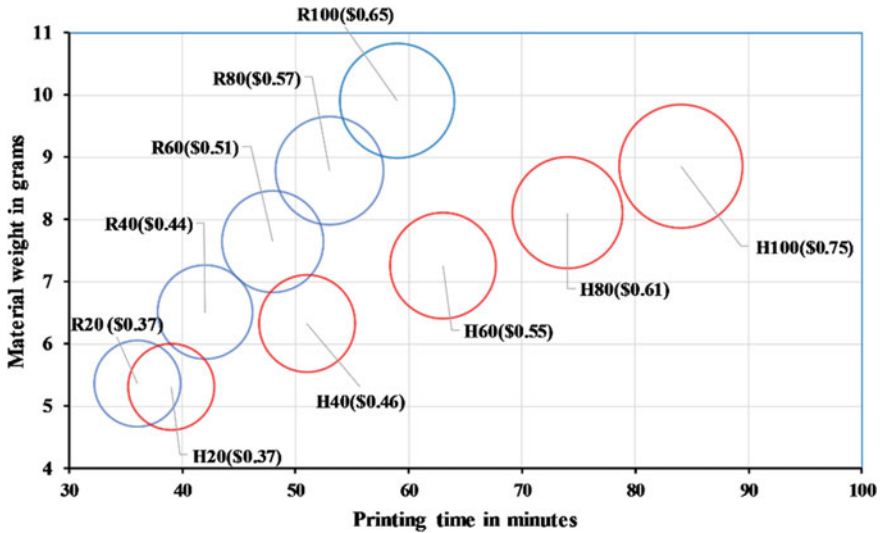


Fig. 11 Cost implication bubble chart of diamond and Honeycomb pattern

infill, the performance of 20% infill is better in terms of tensile strength. The performance drops then after 20%, it is at its lowest midway through and then increases to finally settle maximum at the 100% infill. In the case of Compression strength, the performance drops at 40% and 60% infill representing a ‘U’ curve. The performance increases linearly without any drop-in terms of flexural strength. In addition to performance the material weight and print time has to be considered for economic implication. The print time is included because the commercial 3D printing service providers primarily charge the consumer in terms of material consumption and the printing time. For understanding, the cost of printing a tensile specimen is plotted in bubble chart (Fig. 11). The abscissa and ordinate represent the printing time and material weight respectively. The size of the bubble represents the cost involved in the print. It can be observed, though the material consumption of honeycomb structure is less, it takes more time to print thereby increasing the overall cost of the fabrication.

4 Conclusion

In this study an attempt was made on investigating the mechanical behaviour of various infill densities such as 20%, 40%, 60%, 80% and 100%. The pattern Honeycomb and Rectilinear were chosen for study since they are the most preferred pattern in the AM community. The following conclusions were made based on the study.

- The tensile and compression strength of rectilinear structure was better over honeycomb structure by 8.8% and 11.76% respectively. The strength values

increase with infill density non-linearly which can be fitted with second degree polynomial having mean R square value around 99%.

- The flexural properties vary linearly with infill densities and thus can be fitted using a linear curve with mean R square value more than 99%.
- The morphological analysis revealed that tension specimen's failure was due to delayering along with filament breakage. On contrary, the compression specimens failed because of inadequate adhesion between the layers.
- The mechanical performance in terms of infill density when based on critical area/inertia and weight ratio revealed that performance of 100% infill stood best irrespective of the material property. It was followed by 20% and 80% infill in tensile, 80% and 20% in compression and the least being offered by the 60% infill in both the properties thus almost representing a U-curve.
- The overall performance of rectilinear structure is better, since it offers better resistance to the load applied when material weight is kept constant. Also, the time taken to print the honeycomb structure is 26.81% more in average when compared with rectilinear structure. Thus, the overall cost of rectilinear part is lower when compared with honeycomb

The study provides insight on the infill structure and may prove helpful while designing new infill structures in the future.

References

1. Wang, X., Jiang, M., Zhou, Z., Gou, J., & Hui, D. (2017). 3D printing of polymer matrix composites: A review and prospective. *Composites Part B Engineering*, *110*, 442–458.
2. Aumnate, C., Limpanart, S., Soathiyanon, N., & Khunton, S. (2019). PP/organoclay nanocomposites for fused filament fabrication (FFF) 3D printing. *eXPRESS Polymer Letters*, *13*(10), 898–909.
3. Askanian, H., Muranaka de Lima, D., Commereuc, S., & Verney, V. 2018. Toward a better understanding of the fused deposition modeling process: Comparison with injection molding. *3D Printing and Additive Manufacturing*, *5*(4), 319–327.
4. Liu, J., Zhao, L., Guo, Y., Zhang, H., & Zhang, Z. (2020). Multi-responsive shape memory polymer printed by fused deposition modeling technique. *Express Polymer Letters*, *14*(4).
5. Tam, K. -M. M., & Mueller, C. T. (2017). Additive manufacturing along principal stress lines. *3D Printing and Additive Manufacturing*, *4*(2), 63–81.
6. Rahim, T., Abdullah, A. M., Akil, H. M., Mohamad, D., & Rajion, Z. A. (2017). The improvement of mechanical and thermal properties of polyamide 12 3D printed parts by fused deposition modelling. *eXPRESS Polymer Letters*, *11*(12), 963–982.
7. Andrzejewska, A., Pejkowski, Ł., & Topoliński, T. (2019). Tensile and fatigue behavior of additive manufactured polylactide. *3D Printing and Additive Manufacturing*, *6*(5), 272–280.
8. Chen, R. K., Jin, Y.-A., Wensman, J., & Shih, A. (2016). Additive manufacturing of custom orthoses and prostheses—A review. *Additive Manufacturing*, *12*, 77–89.
9. Ravindrababu, S., Govdeli, Y., Wong, Z. W., & Kayacan, E. (2018). Evaluation of the influence of build and print orientations of unmanned aerial vehicle parts fabricated using fused deposition modeling process. *Journal of Manufacturing Processes*, *34*, 659–666.
10. Natarajan, E., Ang, C. T., Lim, W. H., Kosalishkwaran, G., Ang, C. K., & Parasuraman, S. (2019). Design topology optimization and kinematics of a multi-modal quadcopter and

- quadruped. In *2019 IEEE Student Conference on Research and Development (SCORED), Bandar Seri Iskandar, Malaysia* (pp. 214–218). <https://doi.org/10.1109/scored.2019.8896247>
11. Krawczak, P. (2015). Additive manufacturing of plastic and polymer composite parts: Promises and challenges of 3D-printing.
 12. Mohan, N., Senthil, P., Vinodh, S., & Jayanth, N. (2017). A review on composite materials and process parameters optimisation for the fused deposition modelling process. *Virtual and Physical Prototyping*, *12*(1), 47–59.
 13. Knoop, F., Schoepner, V., & Knoop, F. C. (2015). Mechanical and thermal properties of FDM parts manufactured with polyamide. *12*, 10–12.
 14. Ziemian, C., Sharma, M., & Ziemian, S. (2012). Anisotropic mechanical properties of ABS parts fabricated by fused deposition modelling. *Mechanical Engineering*, *23*.
 15. Motaparti, K. P., Taylor, G., Leu, M. C., Chandrashekhara, K., Castle, J., & Matlack, M. (2017). Experimental investigation of effects of build parameters on flexural properties in fused deposition modelling parts. *Virtual and Physical Prototyping*, *12*(3), 207–220.
 16. Alvarez, C., Kenny, L., Lagos, C., Rodrigo, F., & Aizpun, M. (2016). Investigating the influence of infill percentage on the mechanical properties of fused deposition modelled ABS parts. *Ingeniería e Investigación*, *36*(3), 110–116.
 17. Domingo-Espin, M., Borros, S., Agullo, N., Garcia-Granada, A.-A., & Reyes, G. (2014). Influence of building parameters on the dynamic mechanical properties of polycarbonate fused deposition modeling parts. *3D Printing and Additive Manufacturing*, *1*(2), 70–77.
 18. Schaedler, T. A., & Carter, W. B. (2016). Architected cellular materials. *Annual Review of Materials Research*, *46*, 187–210.
 19. Akhoundi, B., & Behraves, A. H. (2019). Effect of filling pattern on the tensile and flexural mechanical properties of FDM 3D printed products. *Experimental Mechanics*, *59*(6), 883–897.
 20. Forés-Garriga, A., Pérez, M. A., Gómez-Gras, G., & Reyes-Pozo, G. (2020). Role of infill parameters on the mechanical performance and weight reduction of PEI Ultem processed by FFF. *Materials & Design* 108810.
 21. Zhang, P., Liu, J., & To, A. C. (2017). Role of anisotropic properties on topology optimization of additive manufactured load bearing structures. *Scripta Materialia*, *135*, 148–152.
 22. Boros, R., Rajamani, P. K., & Kovács, J. G. (2019). Combination of 3D printing and injection molding: Overmolding and overprinting. *eXPRESS Polymer Letters*, *13*(10), 889–897.
 23. Pei, E., Melenka, G. W., Schofield, J. S., Dawson, M. R., & Carey, J. P. (2015). Evaluation of dimensional accuracy and material properties of the MakerBot 3D desktop printer. *Rapid Prototyping Journal*.
 24. Baig, S., Azizan, A. H. S., Raghavendran, H. R. B., Natarajan, E., Naveen, S., Murali, M. R., Nam, H. Y., & Kamarul, T. (2019). Effect of chitosan nanoparticle-loaded thymus serpyllum on hydrogen peroxide-induced bone marrow stromal cell damage”. *Stem Cells International*, Article ID 5142518, 12 p. <https://doi.org/10.1155/2019/5142518>.
 25. Mohan, S., Raghavendran, H.B., Karunanithi, P., Murali, M.R., Naveen, S.V., Talebian, S., Mehrali, M., Mehrali, M., Natarajan, E., Chan, C.K. and Kamarul, T. (2017). *ACS Applied Materials & Interfaces*, *9*(11), 9291–9303 <https://doi.org/10.1021/acsami.6b13422>
 26. Raghavendran, H. R. B., Natarajan, E., Mohan, S., Krishnamurthy, G., Murali, M. R., Parasuraman, S., Singh, S., & Kamarul, T. (2020). The functionalization of the electrospun PLLA fibrous scaffolds reduces the hydrogen peroxide induced cytokines secretion in vitro. *Materials Today Communications*, 101812. ISSN 2352–4928, <https://doi.org/10.1016/j.mtcomm.2020.101812>. Article in Press
 27. Yang, C., Tian, X., Liu, T., Cao, Y., & Li, D. (2017). 3D printing for continuous fiber reinforced thermoplastic composites: mechanism and performance. *Rapid Prototyping Journal*.
 28. Holbery, J., & Houston, D. (2006). Natural-fiber-reinforced polymer composites in automotive applications. *JOM Journal of the Minerals Metals and Materials Society*, *58*(11), 80–86.
 29. Huang, J. J., Keskkula, H., & Paul, D. R. (2006). Comparison of the toughening behavior of nylon 6 versus an amorphous polyamide using various maleated elastomers. *Polymer*, *47*(2), 639–651.

30. Oderkerk, J., de Schaetzen, G., Goderis, B., Hellemans, L., & Groeninckx, G. (2002). Micromechanical deformation and recovery processes of nylon-6/rubber thermoplastic vulcanizates as studied by atomic force microscopy and transmission electron microscopy. *Macromolecules*, *35*(17), 6623–6629.
31. Pan, G., Zhao, Y., Xu, H., Hou, X., & Yang, Y. (2016). Compression molded composites from discarded nylon 6/nylon 6, 6 carpets for sustainable industries. *Journal of Cleaner Production*, *117*, 212–220.
32. T. S. Srivatsan and T. S. Sudarshan, Additive manufacturing: innovations, advances, and applications. CRC Press, 2015.
33. Standard, A. (2003). Standard test method for tensile properties of plastics. *ASTM International Designation: D, 638*, 1–13.
34. Standard, A. (2015). Standard test method for compressive properties of rigid plastics.
35. International, A. (2010). Standard test methods for flexural properties of unreinforced and reinforced plastics and electrical insulating materials by four-point bending. ASTM International.

Index

A

Adaptive learning, 14, 166
Algorithms, 4, 10, 13, 15, 22, 35, 48, 52–55, 62, 68, 83, 93, 99, 101, 146–156, 162, 163, 166, 167, 185–187, 193, 200, 211, 212, 219
Aluminum alloy, 22, 91
Analysis of Variance (ANOVA), 10, 52, 58, 131, 138, 139
AR/VR, 2, 171, 172, 181
Artificial Fish-Swarm Algorithm, 52, 53, 58, 59
Artificial intelligence, 2, 5, 22, 133, 145, 146, 152, 154, 156, 160, 172, 173, 191, 196, 200, 201, 212, 220
Artificial neural network, 10, 14–17, 22, 74–77, 80, 82–87, 99–101, 133, 160–163, 166–168
Augmented, 146, 171, 173–178, 180
Automation, 2, 5, 34, 145, 177, 178, 185, 192, 193, 201, 207, 208, 219

B

Back propagation, 14, 101
Back Propagation Neural Network (BPNN), 84, 85, 162
Bayesian, 67, 68, 73, 74
Biomedical, 9
Blending, 92, 110, 122

C

Carbide tool, 10, 22
Chromosomes, 162, 165

Classification method, 69
Cloud, 145–147, 151, 154, 180, 191, 193, 194, 197, 199, 212, 214–217, 219
Coefficient, 11–13, 15, 17, 21, 29, 30, 39, 40, 136
Copper, 34, 35, 42, 48–51, 56–58, 91–93, 98, 101, 106–108, 111, 114, 115, 117, 122, 123
Corrosion, 65–68, 70–75, 77, 79, 81, 87
Cutting, 4, 9–11, 17, 131
Cutting tools, 2–4, 10
Cyber physical systems, 2, 185, 207–211, 219, 220

D

Decision models, 2
Decision trees, 77, 84, 149, 151
Die-making, 52
Digital, 2–5, 174, 175, 178, 188, 189, 191, 192, 196, 200, 201, 205, 206, 208, 214, 220
Distributed Process Planning, 2
3D printing, 245–247, 256
Drilling, 3, 9, 22, 30, 130–132, 134, 138, 140–142
Ductile, 106

E

Electrochemical, 33, 35, 40, 41, 44, 47, 50, 57, 58
Electrode, 33, 34, 36, 37, 42, 48
Electrolyte, 34–37, 39–44, 48–52, 56–59
Embedded, 2, 175, 187, 205, 209

Ensemble, 149, 151
 Epoxy resin, 228
 Euclidean, 79, 150

F

Fault diagnosis, 2, 3, 5, 207
 Feed rate, 10, 11, 22, 24, 27, 28, 30, 50, 52,
 56–58, 93, 139, 142
 Fiber-reinforced, 129, 225
 Fibre Reinforced Polymer (FRP), 226, 228
 Fibroid, 106
 Frequency, 36, 66, 72, 78, 87, 226
 Friction Stir Welding (FSW), 91–93, 95, 96,
 101, 103, 105, 106, 108, 109, 111,
 113–116, 123
 Fused Deposition Modelling (FDM), 245–
 248
 Fuzzy, 22, 23, 26, 27, 29, 30, 80, 82, 83, 86,
 136, 160, 161
 Fuzzy logic, 10, 79, 80, 82–87, 133, 160

G

Gene Expression Programming (GEP), 160–
 168
 Genetic algorithm, 10, 13–17, 22, 35, 131,
 160, 161
 Glass fiber, 226, 228, 239
 Global sustainability, 1
 Graphene, 93, 105, 106, 109, 112–115, 119,
 121, 123
 Grey Relational Analysis (GRA), 22, 35,
 37–40, 43, 44

H

Healthcare, 146, 152, 153, 156, 201
 Heterogeneous, 121, 122
 Honeycomb, 246, 249–258

I

Industry, 2, 4, 9, 21, 34, 47, 48, 52, 68, 91,
 130, 134, 145–147, 151–153, 156,
 159–161, 171–173, 176, 177, 179–
 182, 185–188, 190, 192, 194–197,
 199–202, 205, 207, 208, 211, 220,
 225, 226, 247
 Intelligent, 2, 53, 146, 151, 152, 154–156,
 185, 188, 197, 200–202, 208
 Internet of Things (IoT), 2, 146, 147, 176,
 185–189, 191, 192, 195–201, 205,
 206, 211, 217

K

K – Nearest Neighbours (KNN), 149, 151

L

Lean manufacturing, 1
 Leaping, 55
 Linear motion, 93
 Logistic regression, 82, 84, 85
 LW-WOPO, 95–99, 101–103, 105, 110, 113,
 116, 118, 119, 122, 124

M

Machine learning, 2, 5, 62–65, 68, 69, 74,
 81–84, 86, 87, 146–156, 185, 193,
 196, 200, 201
 Machine tools, 2, 3, 5, 9, 130
 Machining, 2–4, 9–11, 21, 22, 33–39, 41–
 44, 47–50, 52, 56–58, 130–133, 225–
 231, 237, 239, 241, 242
 Manufacturing, 1–3, 5, 22, 130, 145, 146,
 151, 152, 156, 159–161, 171–174,
 176–182, 185, 188, 189, 194–202,
 208, 211–213, 219, 220, 225, 226,
 246–248
 Material Removal Rate (MRR), 35, 48, 51,
 52, 56–59, 230–235, 238–240, 242
 Materials, 1, 2, 10, 21, 22, 30, 33–36, 41–
 43, 47, 48, 50, 52, 66, 70, 78, 91–93,
 95, 98, 103, 105–113, 115–117, 119,
 120, 123, 129, 130, 132, 133, 159,
 189, 190, 195, 197, 198, 211, 225,
 226, 228, 231, 234, 235, 238, 239,
 241, 242, 245–256, 258
 MATLAB, 76, 161, 213, 218
 Means clustering, 23, 150
 Mean square error values, 14
 Metaheuristic, 13
 Micro-holes, 34–36, 39, 41–43
 Micromachining, 33, 35, 40, 41, 44
 Micron, 56–59, 230, 235, 237, 239, 241, 243,
 248
 Microstructure, 92, 103, 107, 108, 111, 114,
 117, 121, 122
 Multiobjective Genetic-Algorithm
 (MOGA), 35

N

Naive Bayes, 84
 Nanoparticles, 48, 49, 57, 93, 115, 119, 120,
 123

Nanoplatelets, 93, 105, 106, 108, 112, 113, 119, 123
 Neural networks, 14, 74, 75, 82, 84, 99, 131, 149–151, 160–162, 166, 167
 Neurons, 10, 14, 99, 149
 Normalization, 38–40
 Nylon, 245–250, 252

O

Optimal cutting, 2, 4
 Optimization, 4, 10, 13, 14, 17, 22, 30, 34, 35, 37, 41, 43, 53, 58, 59, 61, 78, 82, 99, 130, 131, 161, 197, 207, 216
 Oxidation, 93, 110, 112, 113, 226

P

Particleboard, 129–131
 Pipeline, 62–87, 146, 147
 Polymers, 129, 225, 226, 245
 Polyoxymethylene, 21, 22, 30
 Prediction models, 3–5, 10, 14, 22, 67, 70, 72, 74–76, 80, 162
 Predictive, 4, 61, 62, 69, 73, 86, 87, 135, 152, 188–192, 194, 199, 201, 220
 Production, 1–5, 21, 22, 61, 65, 145, 146, 151, 159–161, 163, 172, 173, 177, 179, 180, 182, 189, 190, 192–197, 201, 202, 206, 207, 211, 245, 246

Q

Q-learning, 151
 Quadratic, 11, 135
 Quantitative, 66, 70, 149

R

Random Forest, 84
 RBPM, 66
 Recrystallization, 93, 106, 111–113, 118
 Regression, 11, 13, 16, 29, 30, 69, 74–77, 80, 82–87, 100, 131, 139, 147–149, 151, 160–162
 Rehabilitation, 155
 Reinforcement, 93, 95, 115, 123, 147, 151
 Reliability, 62, 65–68, 70, 71, 73, 87, 145, 161, 188, 191, 194, 218, 219
 Rotational speed, 92, 95, 101–106, 111, 112
 Rule-based, 150

S

Scanning Electron Microscope (SEMs), 48, 49, 58, 104, 109, 117, 118, 120, 140, 141, 250, 252, 254, 256
 Small Medium Enterprises (SMEs), 206–208, 211, 212, 220
 Smart, 2, 3, 5, 71, 146, 151, 152, 154–156, 173–176, 181, 185, 187–189, 193, 196, 199, 201, 205, 210, 212, 217
 Smart factory, 2, 188, 220
 Smart sensors, 2, 5
 Sodium Nitrate, 34, 48–50, 56–58
 Soft computing, 160, 161, 168
 Spindle speed, 22, 24, 27, 28, 135, 138, 139, 142
 Statistical, 75, 82, 133, 150, 161, 168
 Superalloys, 47
 Supervised, 68, 69, 83, 147–151
 Surface finish, 4, 33, 49, 52, 130, 226, 237, 242
 Sustainability, 1, 5, 130, 207

T

Taguchi, 35, 37, 43, 131
 Temperature, 49, 91, 92, 105, 107, 109, 112, 118, 122, 148, 174, 194, 195, 199, 201, 247, 248
 Tensile strength, 102, 105, 106, 110, 112, 247, 250–252, 256
 Time-Based Preventive Maintenance methods (TBPm), 65, 66, 70
 Titanium alloys, 9–11, 17, 47
 TLBO, 22
 Tool point angle, 22, 24, 27
 Tool Wear Rate (TWR), 35
 Training, 5, 10, 14, 16, 82, 99, 100, 133, 136, 138, 149, 163, 164, 166, 167, 173, 176, 177, 199, 201
 Turning, 3, 9–11, 13–15, 17, 22, 130, 131, 207

U

Unconventional, 52, 178
 Unsupervised, 68, 147, 149–151

V

Validation, 5, 14, 16, 17, 58, 99, 100, 142

W

Wastages, 1, 5, 67, 245

Weave weld, 101, 103–107, 110–114, 116,
117, 119–121, 123, 124

Welding, 22, 92, 93, 95, 96, 98, 101, 102,
105, 106, 109–115, 117, 118, 124